BioMed Research International

Cancer Diagnostic and Predictive Biomarkers 2015

Guest Editors: Franco M. Buonaguro, C. David Pauza, Maria Lina Tornesello, Pierre Hainaut, and Renato Franco

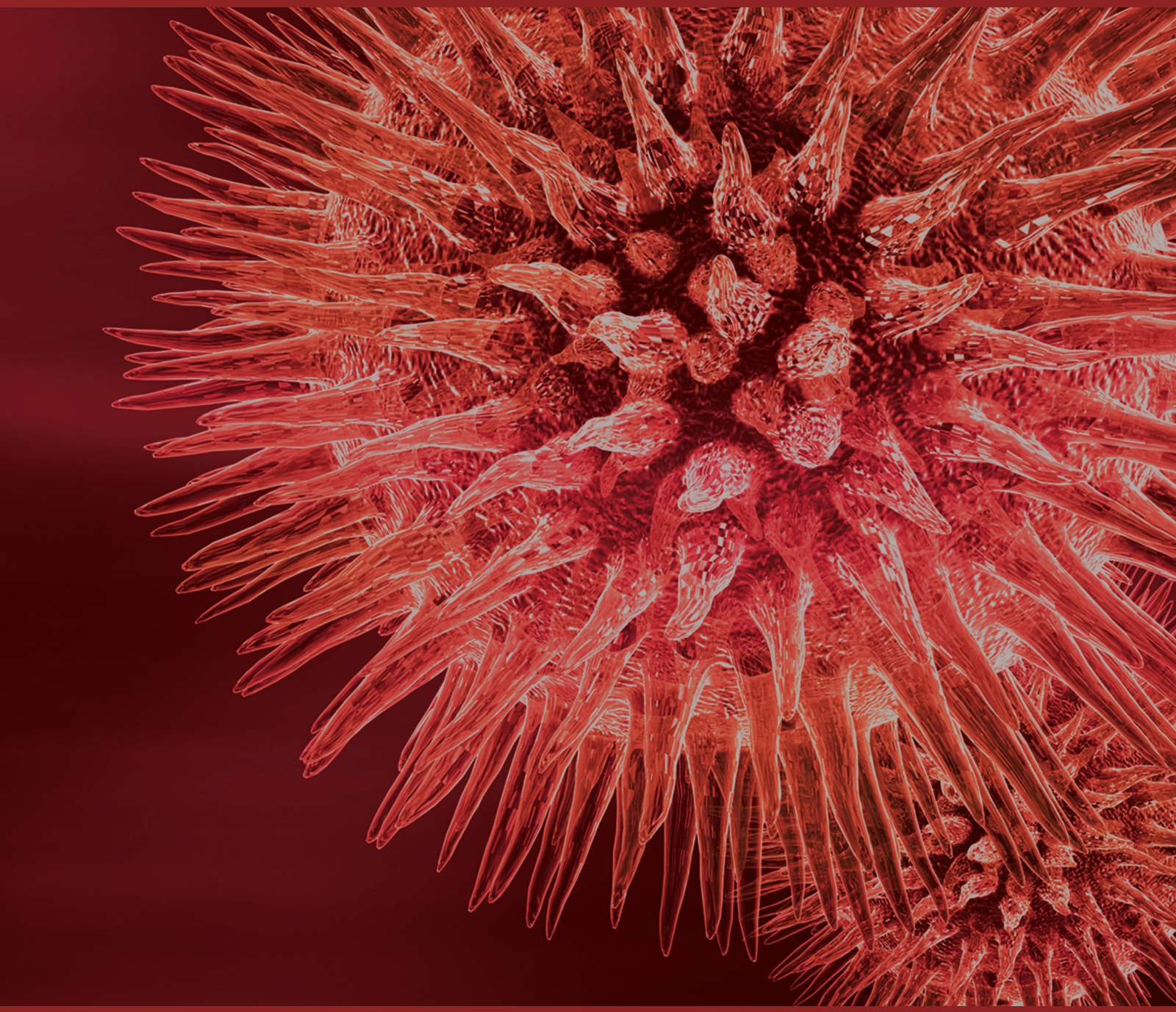

Cancer Diagnostic and Predictive Biomarkers 2015

BioMed Research International

Cancer Diagnostic and Predictive Biomarkers 2015

Guest Editors: Franco M. Buonaguro, C. David Pauza,
Maria Lina Tornesello, Pierre Hainaut, and Renato Franco

Contents

Hindawi Publishing Corporation
BioMed Research International
Volume 2015, Article ID 235985, 1 page
http://dx.doi.org/10.1155/2015/235985

Editorial

Cancer Diagnostic and Predictive Biomarkers 2015

Franco M. Buonaguro,[1] C. David Pauza,[2] Maria Lina Tornesello,[1] Pierre Hainaut,[3] and Renato Franco[4]

[1] *Unit of Molecular Biology and Viral Oncology, Department of Experimental Oncology, Istituto Nazionale Tumori IRCCS Fondazione Pascale, 80131 Napoli, Italy*
[2] *Department of Microbiology and Immunology, Institute of Human Virology, Baltimore, MD 21201, USA*
[3] *Department of Research, International Prevention Research Institute, 69006 Lyon, France*
[4] *Department of Pathology, Istituto Nazionale Tumori IRCCS Fondazione Pascale, 80131 Napoli, Italy*

Correspondence should be addressed to Franco M. Buonaguro; irccsvir@unina.it

Received 30 August 2015; Accepted 31 August 2015

Early cancer diagnosis and prediction of responsivity to treatments are crucial elements for favorable prognosis and increased effectiveness of therapies in cancer patients. This special issue compiles relevant articles focused on the development of innovative cancer biomarkers and their validation.

Availability of advanced molecular biology tools, including deep-sequencing and RNA-seq, allowed the identification of new unique biomarkers for more sensitive and specific diagnosis and the possibility to select new candidate therapeutic targets for personalized medicine.

The negative prognostic role of stem cell markers, with higher progression rate, has been reported by G. Chene et al. in preinvasive tubal lesions of ovarian carcinoma, F. Collina et al. in triple negative breast cancers, and S. H. Kim et al. in prostate cancer patients, where high level of GAPDH mRNA is a significant predictor of recurrence. The negative prognostic value, particularly for head and neck cancers, of cell-to-cell internalization was reported by M. Schwegler et al., and inverse correlation with expression levels of iNOS was reported by L. Yang et al.

Different biomarkers have been analyzed for early diagnosis and follow-up monitoring spanning within serum detection of glycosylated biomarkers (described by A. Kirwan et al.), serum levels of 15-F2t-isoprostane in non-melanoma skin cancer (B. Freitas et al.), and methylation levels of GALR1 promoter in endometrial lesions by pyrosequencing analysis (C. Kottaridi et al.). Early diagnosis of liver metastasis by CT perfusion has been reported by Y. Wang et al.

Predictive therapeutic biomarkers have been described to chemoradiation in locally advanced rectal cancer by R. Conde-Muíño et al. and to radiotherapy in localized prostate cancer by A. Wilkins et al.

The role of miRNAs in cancers and their prognostics relevance has been analyzed by A. Min et al. in oral carcinogenesis. J. Long et al. have focused on miRNA 193b in human breast cancer, and S. Wu et al. on miRNA 125b in gastric cancer.

Finally identification of HHV-8 sequences in conjunctival neoplasia of Uganda patients offers the possibility to unveil a further cancer association to such herpesvirus and highlights the need to look for indirect role of virus with low-modest oncogenic potential in immunodeficient patients (including low risk HPVs in HIV-positive patients).

By compiling these papers, we hope to enrich our readers and researchers with respect to the current wide range of cancer biomarkers, actively pursued by several worldwide research groups.

Franco M. Buonaguro
C. David Pauza
Maria Lina Tornesello
Pierre Hainaut
Renato Franco

Hindawi Publishing Corporation
BioMed Research International
Volume 2015, Article ID 373574, 9 pages
http://dx.doi.org/10.1155/2015/373574

Research Article

miR-193b Modulates Resistance to Doxorubicin in Human Breast Cancer Cells by Downregulating MCL-1

Jingpei Long,[1] Zhiwei Ji,[2] Kai Jiang,[3] Zhaoyang Wang,[4] and Guanmin Meng[3]

[1]*Department of Surgery, The Women's Hospital, School of Medicine, Zhejiang University, Hangzhou 310006, China*
[2]*School of Electronics and Information Engineering, Tongji University, Shanghai 201804, China*
[3]*Department of Clinical Laboratory, Tongde Hospital of Zhejiang Province, 234 Gucui Road, Hangzhou 310012, China*
[4]*Department of Ophthalmology, Xinhua Hospital, School of Medicine, Jiaotong University, Shanghai 200092, China*

Correspondence should be addressed to Guanmin Meng; amonggreat@hotmail.com

Received 24 March 2015; Revised 14 May 2015; Accepted 24 May 2015

Academic Editor: Franco M. Buonaguro

MicroRNAs (miRNAs) family, which is involved in cancer development, proliferation, apoptosis, and drug resistance, is a group of noncoding RNAs that modulate the expression of oncogenes and antioncogenes. Doxorubicin is an active cytotoxic agent for breast cancer treatment, but the acquisition of doxorubicin resistance is a common and critical limitation to cancer therapy. The aim of this study was to investigate whether miR-193b mediated the resistance of breast cancer cells to doxorubicin by targeting myeloid cell leukemia-1 (MCL-1). In this study, we found that miR-193b levels were significantly lower in doxorubicin-resistant MCF-7 (MCF-7/DOXR) cells than in the parental MCF-7 cells. We observed that exogenous miR-193b significantly suppressed the ability of MCF-7/DOXR cells to resist doxorubicin. It demonstrated that miR-193b directly targeted MCL-1 3′-UTR (3′-Untranslated Regions). Further studies indicated that miR-193b sensitized MCF-7/DOXR cells to doxorubicin through a mechanism involving the downregulation of MCL-1. Together, our findings provide evidence that the modulation of miR-193b may represent a novel therapeutic target for the treatment of breast cancer.

1. Introduction

Breast cancer is the most common cancer in women worldwide, which is expected to account for 29% of all new cancer cases in 2012 [1]. Surgery combined with chemotherapy is the most effective strategy for breast cancer therapy currently. However, most of the treatments are unsuccessful due to the secondary recurrence, metastasis, and drug resistance [2]. For patients who especially suffered from advanced unresectable breast cancer, systemic therapy with chemotherapy drugs is a standard treatment strategy, although the problem of drug resistance has become serious [3]. Doxorubicin (DOX), an anthracycline drug, is widely used against a wide range of cancers, such as hematological malignancies, lung cancer, and breast cancer by directly intercalating the double-strand DNA and inhibiting DNA topoisomerase II [4, 5]. However, the major problems with doxorubicin treatment are cardiotoxicity and the induction of multidrug resistance [6, 7]. Therefore, enhanced anticancer therapy through the reversal of inducible DOX resistance would be desirable.

MicroRNAs (miRNAs) are small noncoding RNAs that negatively modulate gene expression via RNA binding at imperfect complementary sequences within the 3′UTR of the target mRNA, resulting in degradation or translational inhibition [8]. Recent studies indicate that miRNAs regulate cell growth, differentiation, and apoptosis [9]. Interestingly, some studies suggest that miRNAs are involved in tumor cell resistance to chemotherapeutic agents, such as doxorubicin [10]. However, the role of miR-193b in drug resistance of breast cancer cells remains unknown. We therefore compared the expression levels of miR-193b in the drug-resistant human breast cancer cell line MCF-7/DOXR, which was established by continuous exposure to doxorubicin, with its parental MCF-7 cell line. Furthermore, we investigated whether overexpression of miR-193b could increase the DOX sensitivity

and determined the potential role of MCL-1 in miR-193b-mediated regulation of DOX resistance in human breast cancer cells.

2. Materials and Methods

2.1. Reagents. Antibodies against MCL-1 and β-actin were purchased from cell signaling (USA). Doxorubicin (DOX), 3-(4,5-dimethylthiazol-2-yl)-3,5-diphenyltetrazolium bromide (MTT), and Annexin V-FITC Apoptosis Detection Kit were obtained from Sigma-Aldrich (USA). miR-193b mimic and negative control oligonucleotide (NCO) were purchased from Genepharma Company (China). The sequences were as follows: miR-193b mimic, AACUGGCCCUCAAAGUCCCGCU; NCO, GCUCCCAACCCUUGGCCCAAGU.

2.2. Cell Lines and Culture. MCF-7 cells were obtained from American Type Culture Collection (ATCC, USA) and cultured in DMEM basic medium (Gibco, USA) with 10% fetal bovine serum (FBS, Gibco, USA) at 37°C in a humidified 5% CO_2 incubator. MCF-7/DOXR (doxorubicin-resistant MCF-7) cell line was established by stepwise exposure of MCF-7 cells to increasing concentrations of doxorubicin. The cells were initially treated with doxorubicin at 0.2 μg/mL for 2 months, and then the concentrations of doxorubicin were increased by 0.03 μg/mL every month up to a final concentration of 0.5 μg/mL. The MCF-7/DOXR cells were exposed to doxorubicin over a time period of 12 months. Doxorubicin was removed from medium 3 days before any experiments were run.

2.3. Quantitative Real-Time Polymerase Chain Reaction (RT-qPCR). Total RNA from the MCF-7 or MCF-7/DOXR cells was extracted with Trizol reagent (Invitrogen, USA). The expression of miR-193b was assayed using stem-loop reverse transcription (RT) (Chen et al. [11]) followed by real-time PCR analysis. The RT-primer sequences are as follows: 5′-CTCAACTGGTGTCGTGGAGTCGGCAATTCAGTTGAGAGCGGGAC-3′, and the cDNA was synthesized using M-MLV Reverse Transcriptase (Invitrogen, USA). The qPCR primers were used as follows: MCL-1 forward 5′-CCAATGGGCAGGTCTGG-3′, MCL-1 reverse 5′-TACGCCGTCGCTGAAAA-3′; GAPDH forward 5′-GCATCCTGGGCTACACTG-3′, GAPDH reverse 5′-TGGTCGTTGAGGGCAAT-3′. qPCR was performed using a standard protocol from the SYBR Green PCR kit (Toyobo, Japan) on the Applied Biosystems 9700 system (USA). U6 or GAPDH was used as the internal control, and the relative level of miR-363 or MCL-1 expression was determined with the $2^{-\Delta\Delta CT}$ method to calculate the fold change of the RNA expression [12].

2.4. Recombinant Plasmid Construction. The 3′-UTR sequences of MCL-1 (GenBank accession number: NM_001197320) containing the putative miR-193b binding site were amplified by PCR using the cDNA from MCF-7/DOXR cells as a template. Primers for MCL-1 3′-UTR were as follows: forward, 5′-TACTGTAAGTGCAATAGT-3′; reverse, 5′-TACCATCTTCACTAAATCT-3′. PCR products were cloned into the pMIR-REPORT miRNA Expression Reporter Vector System (pMIR, Life Technologies, USA). The mutant plasmid was created by mutating the seed regions of the miR-193b binding sites using site-directed mutagenesis kit (Takara, Japan). MCL-1 expression vector was established for the "rescue" experiment, where the open reading frame of MCL-1 was cloned into pcDNA3.1 (Invitrogen, USA). The recombinant plasmid was named pcDNA3.1-MCL-1.

2.5. Transient Transfection. Human miR-193b (50 nM), NCO (50 nM), pcDNA3.1 (2 μg/mL), pMIR reporter plasmid (2 μg/mL), and control Renilla luciferase pRL-TK vector (100 ng/mL, Promega, USA) were transfected into MCF-7/DOXR cells using Lipofectamine 2000 (Invitrogen, USA) when the cells were covered at approximately 80% confluence of the plate.

2.6. Luciferase Assay. MCF-7/DOXR cells were transfected with the MCL-1 3′UTR pMIR firefly luciferase reporter vector, control Renilla luciferase pRL-TK vector, and miR-193b mimic or NCO using Lipofectamine 2000 reagent. After 48 h transfection, cells were lysed, and assays were performed using the Dual-Luciferase Reporter Assay System kit (Promega, USA) according to the manufacturer's instructions. Results were represented as the ratio between the treatment groups and the negative control groups.

2.7. Drug Sensitivity Assay. Cells were seeded onto 96-well plates with 5×10^3 per well in growth medium and incubated for 12 h and then treated with doxorubicin at concentrations that ranged from 0.05 to 1.2 μg/mL for MCF-7 and from 0.8 to 16 μg/mL for MCF-7/DOXR, respectively. 48 h after doxorubicin treatment, MTT (20 mL, 5 mg/mL) was added to each well and incubated for 4 h. Medium was then aspirated and 100 μL DMSO was added. Absorbance was read at OD 570/655 nm using 680 Microplate Reader (Bio-Rad, USA). Doxorubicin concentrations leading to 50% cell death (IC_{50}) were determined by a MTT-dependent cell viability assay.

2.8. Western Blot Analysis. Cells were lysed in RIPA lysis buffer (Cell Signaling, USA). Protein concentrations were measured using a BCA Protein Assay kit (Pierce, USA) according to the manufacturer's instructions. Following electrophoresis on 12.5% SDS-PAGE, protein samples were transferred to a PVDF membrane (Millipore, USA). After incubating with anti-MCL-1 and anti-β-actin primary antibodies, the membranes were then incubated with horseradish peroxidase-conjugated secondary antibodies (Cell Signaling, USA). The protein levels were analyzed by enhanced chemiluminescence detection kit (Pierce, USA). β-actin was used as loading control.

2.9. Assessment of Apoptosis. Cells were transfected with mentioned RNA/DNA. After 24 h incubation, doxorubicin was then added to the cell medium at a concentration of 1.2 μg/mL. After another 24 h incubation, cells were collected

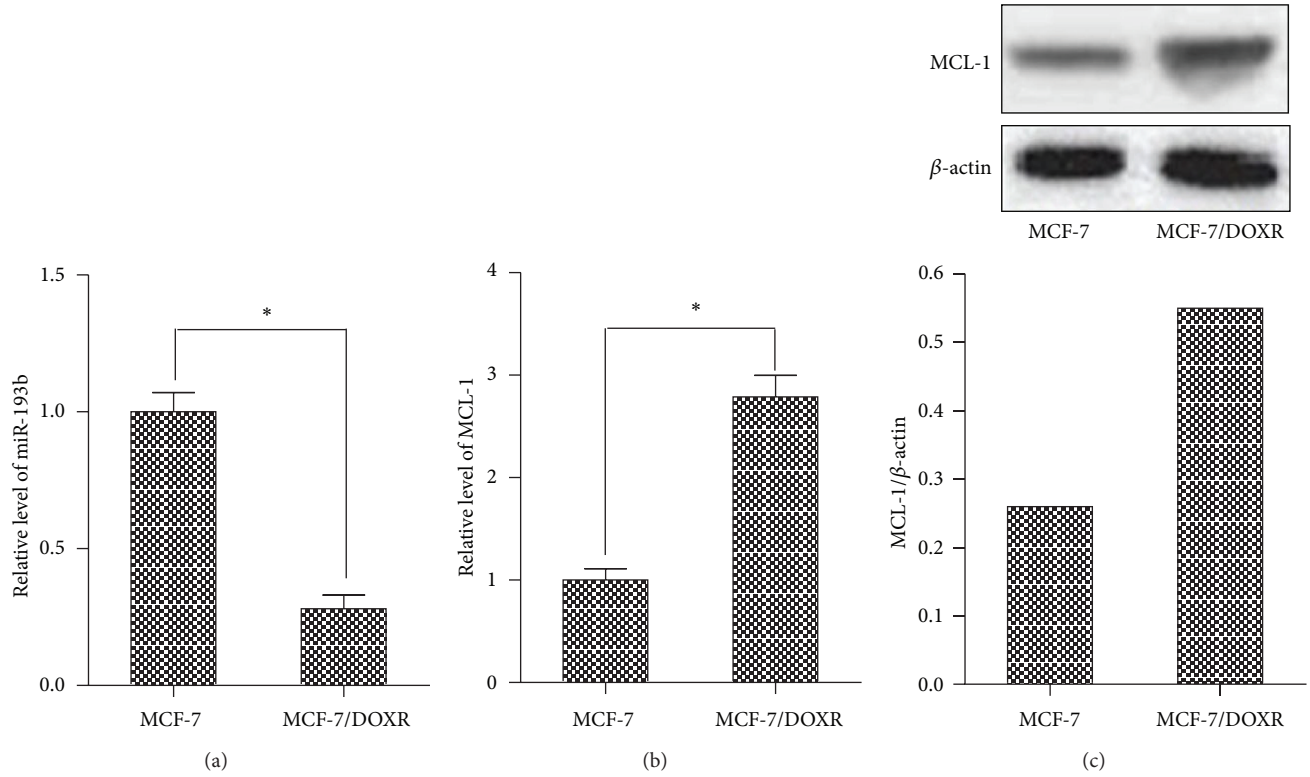

Figure 1: Downregulation of miR-193b and overexpression of MCL-1 in MCF-7/DOXR cells. (a) The miR-193b expression in MCF-7 and MCF-7/DOXR cells was detected by qPCR. $^{*}p < 0.05$. (b) qPCR analysis for MCL-1 mRNA expression levels in MCF-7 and MCF-7/DOXR cells. $^{*}p < 0.05$. (c) Western blot analysis for MCL-1 protein levels in MCF-7 and MCF-7/DOXR cells.

and assayed with an Annexin V-FITC Apoptosis Detection Kit on the flow cytometry (Becton Dickinson, USA).

2.10. Statistical Analysis. In all the experiments, data are expressed as mean ± SE and derived from at least three independent experiments. All the statistical analyses were performed using SPSS12.0 software (USA). The difference between mean values was analyzed with Student's t-test. p values of <0.05 were considered to be statistically significant.

3. Results

3.1. Downregulation of miR-193b and Upregulation of MCL-1 in Breast Doxorubicin-Resistant Cells. To investigate the relationship between miR-193b expression and doxorubicin resistance, we established a doxorubicin-resistant MCF-7 cell line (MCF-7/DOXR) by continuous exposure of MCF-7 cells to doxorubicin. As shown in Figure 1(a), the levels of miR-193b were significantly lower in MCF-7/DOXR cell line than in its parental MCF-7 cell line. We then subsequently performed qPCR and western blot to detect the expression of MCL-1. As expected, both the mRNA and protein expression levels of MCL-1 in MCF-7/DOXR cells were higher than that in its parental MCF-7 cells (Figures 1(b) and 1(c)). These data indicate that the downregulation of miR-193b and upregulation of MCL-1 may be related to doxorubicin resistance.

3.2. Transfection of miR-193b Sensitized MCF-7/DOXR Cells to Doxorubicin. Doxorubicin markedly inhibited the viability of MCF-7 in a dose-dependent manner. However, we found approximately 17.0-fold increase of IC_{50} for the MCF-7/DOXR cells in the presence of doxorubicin (IC_{50} = 6.56 μg/mL), as compared to the parental MCF-7 cells (IC_{50} = 0.39 μg/mL), indicating that the MCF-7/DOXR cells were resistant to doxorubicin (Figure 2(a)). To investigate whether miR-193b modulated chemosensitivity in breast cancer, we transfected 50 nM miR-193b mimic or NCO into MCF-7/DOXR cells. Figure 2(b) showed that miR-193b levels were effectively elevated by transfection with the mimics in the MCF-7/DOXR cells. We observed that the MCF-7/DOXR cells transfected with miR-193b exhibited significantly enhanced sensitivity to doxorubicin comparing with those transfected with NCO, with IC_{50} values of 2.180 ± 0.602 and 7.840 ± 0.901 μg/mL, respectively (Figure 2(c)). To further investigate the apoptosis-inducing effect of doxorubicin plus miR-193b in MCF-7/DOXR cells, Annexin V/PI staining for apoptosis was performed. As shown in Figure 2(d), miR-193b enhanced apoptosis in MCF-7/DOXR cells during the doxorubicin treatment. These results suggest that miR-193b increases the sensitivity of breast cancer cells to doxorubicin.

3.3. miR-193b Directly Targets MCL-1 and Suppresses Its Expression in MCF-7/DOXR Cells. MCL-1 has been reported as a potential target gene of miR-193b [13]. To further

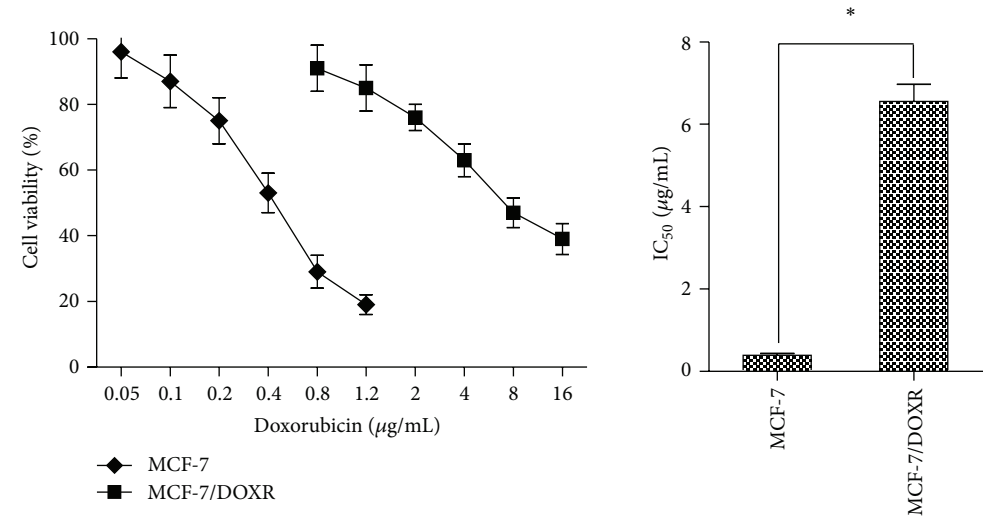

(a)

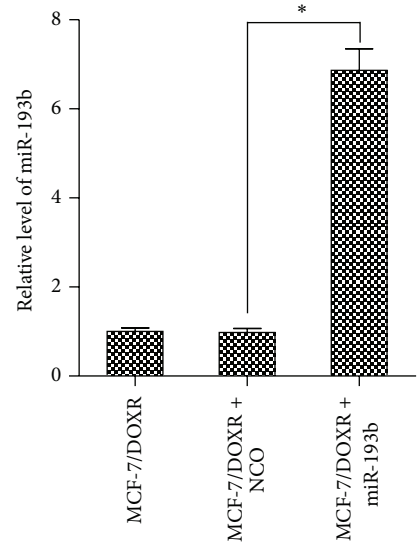

(b)

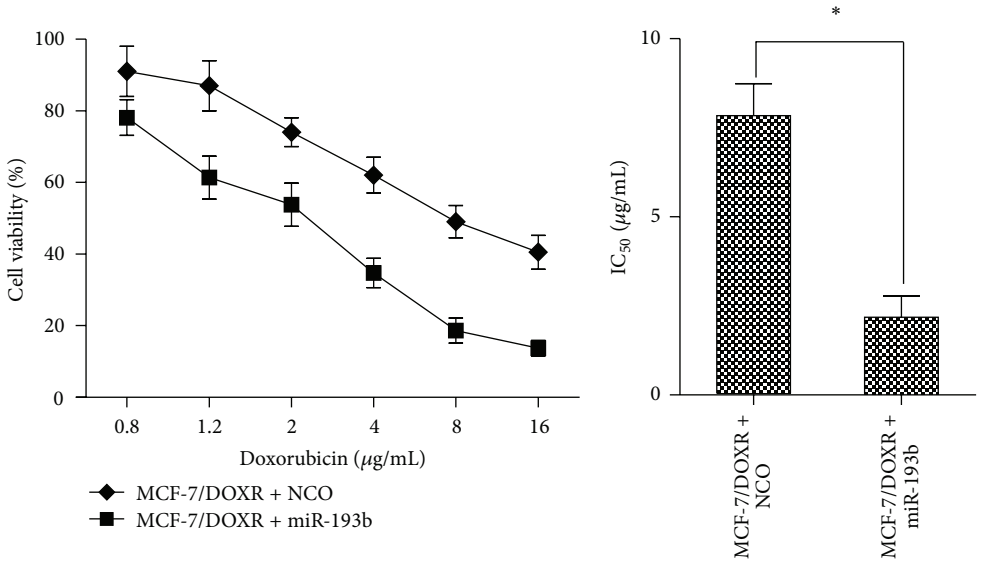

(c)

Figure 2: Continued.

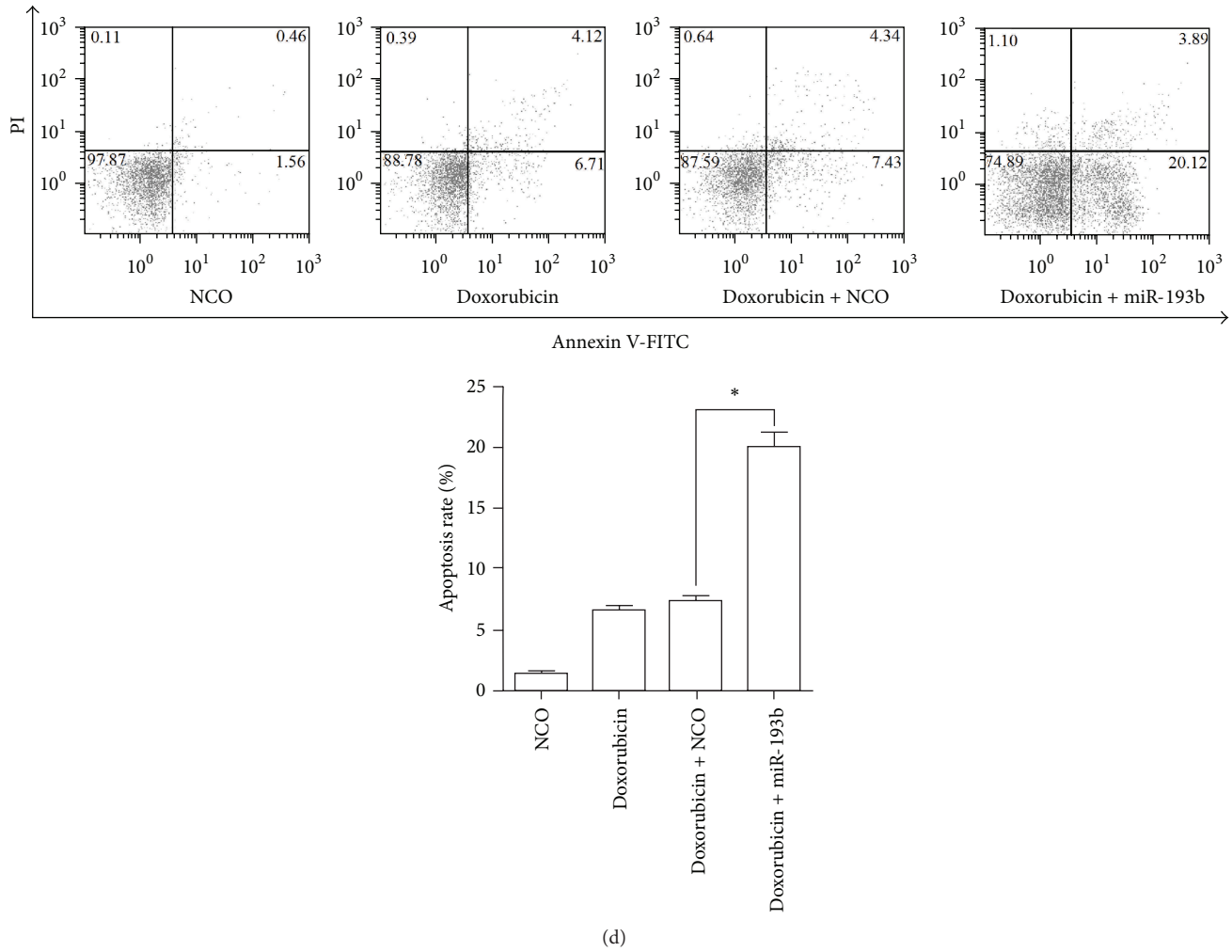

Figure 2: Transfection of miR-193b sensitized MCF-7/DOXR cells to doxorubicin. (a) MCF-7 and MCF-7/DOXR cells were treated with different concentrations of doxorubicin, and cell viability was assayed by using MTT. The IC_{50} was determined according to the survival curves, which showed the MCF-7/DOXR cell line got a 17.0-fold acquired resistance to doxorubicin compared to the MCF-7 cell line (6.560 ± 0.412 versus 0.386 ± 0.051 μg/mL, $^{*}p < 0.05$). (b) MCF-7/DOXR cells were seeded in 6-well plates and transfected with miR-193b mimic or NCO, and the miR-193b expression level was assayed by qPCR. $^{*}p < 0.05$ versus NCO group. (c) MCF-7/DOXR cells were treated with different concentrations of doxorubicin plus miR-193b or NCO, and cell viability was assayed by using MTT. The IC_{50} was significantly lower in MCF-7/DOXR cells transfected with miR-193b as compared to the cells transfected with NCO, $^{*}p < 0.05$. (d) MCF-7/DOXR cells were treated with 1.2 μg/mL doxorubicin plus miR-193b or NCO, and cell apoptosis was detected by Annexin V/PI staining. Data are expressed as the means ± SE ($n = 3$). $^{*}p < 0.05$.

explore the downstream mechanism through which miR-193b modulates doxorubicin resistance, we transfected the MCF-7/DOXR cells with miR-193b mimic or NCO. After 24 h incubation, a significant decrease in both mRNA and protein expression levels of MCL-1 was observed in MCF-7/DOXR cells transfected with miR-193b (Figure 3(a)). Furthermore, we cotransfected miR-193b mimic or NCO together with the pMIR-reporter luciferase plasmid containing 3′UTR of MCL-1 into the MCF-7/DOXR cells. As shown in Figure 3(b), miR-193b significantly suppressed the luciferase activity of the pMIR reporter with wild-type 3′-UTR of MCL-1, whereas the mutant MCL-1 3′UTR or empty pMIR-luciferase activity remained unchanged in cells transfected with miR-193b. These results indicate that MCL-1 is negatively regulated by miR-193b as its direct target gene in MCF-7/DOXR cells.

3.4. miR-193b Sensitized MCF-7/DOXR Cells to Doxorubicin through the Downregulation of MCL-1. To investigate the role of MCL-1 in miR-193b regulated doxorubicin resistance, we rescued the doxorubicin- and miR-193b-treated MCF-7/DOXR cells with MCL-1 expression vector. We observed that the transfection of pcDNA3.1-MCL-1 totally reversed the downregulation of MCL-1 by miR-193b (Figure 4(a)). More importantly, the overexpression of MCL-1 significantly reversed the viability of the MCF-7/DOXR cells treated

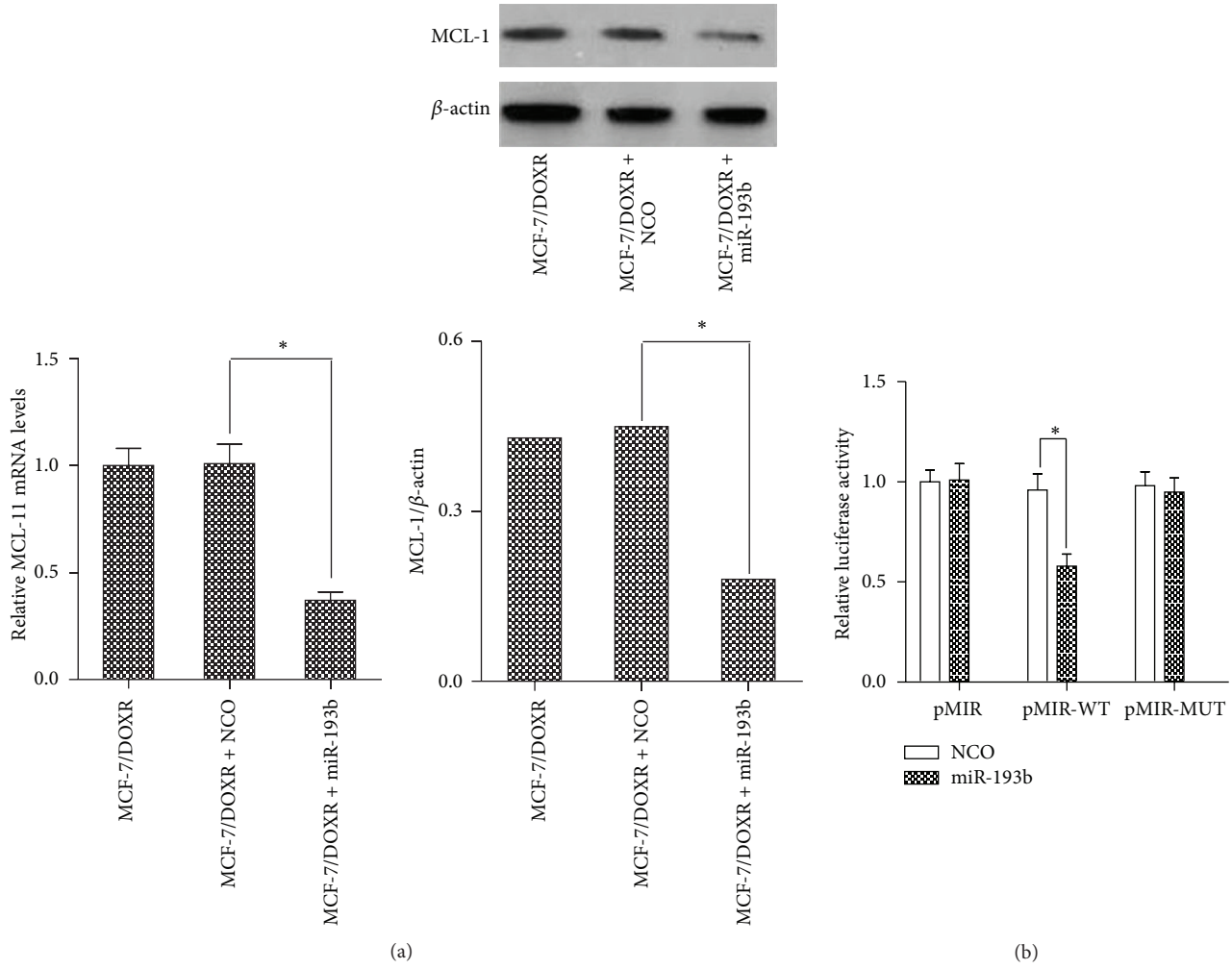

Figure 3: miR-193b directly targets MCL-1 and suppresses its expression in MCF-7/DOXR cells. (a) MCF-7/DOXR cells were transfected with miR-193b mimic or NCO incubating for 24 h, and then the mRNA expression and protein expression of MCL-1 were detected by qPCR analysis and western blot, respectively, $^{*}P < 0.05$. (b) Effect of miR-193b on MCL-1 was assessed with the dual-luciferase reporter system. The miR-193b mimic, pRL-TK, and pMIR reporter containing wild- or mutant-type 3′-UTR of MCL-1 gene were cotransfected into the MCF-7/DOXR cells, $^{*}P < 0.05$.

with miR-193b and doxorubicin (Figure 4(b)). Furthermore, we also examined the effect of MCL-1 overexpression on apoptotic cell death in MCF-7/DOXR cells treated with doxorubicin and miR-193b. The flow cytometry analysis showed that the number of apoptotic cells in pcDNA3.1-MCL-1 group was dramatically less than that in the empty pcDNA3.1 group (Figure 4(c)). Taken together, MCL-1 is a potential target through which miR-193b modulates doxorubicin resistance in human breast cancer.

4. Discussion

Although advances in both diagnosis and treatment for malignancy have contributed to the improvement of prognosis [14, 15], current available therapeutic options are very limited for patients with advanced breast cancer while the tumor tissues have developed beyond curative surgery. Chemotherapy plays an important role in the treatment of advanced breast cancer. However, acquired chemoresistance is becoming a major challenge for the patients [16]. In our study, the MCF-7/DOXR cell line was proximately 17.0 times more resistant to doxorubicin as compared with its parental MCF-7 cell line, suggesting that the continuous exposition to doxorubicin enabled breast cancer cells to acquire drug resistance. Therefore, there is an urgent need to identify the key molecules involved in breast cancer chemoresistance in order to develop novel strategies for breast cancer.

Recent studies have shown that some specific miRNAs can modulate drug resistance. Recent studies demonstrate that miR-30c, one of the well-known tumor suppressor miRNAs that promote cell death and inhibit tumor invasion, plays an important role in reversing chemotherapy resistance by regulating TWF1 and interleukin-11 [17, 18]. miR-200c expression is reported to be downregulated in multidrug-resistant MCF-7 cells as compared to the parental MCF-7 cells, while upregulation of miR-200c by its mimics could

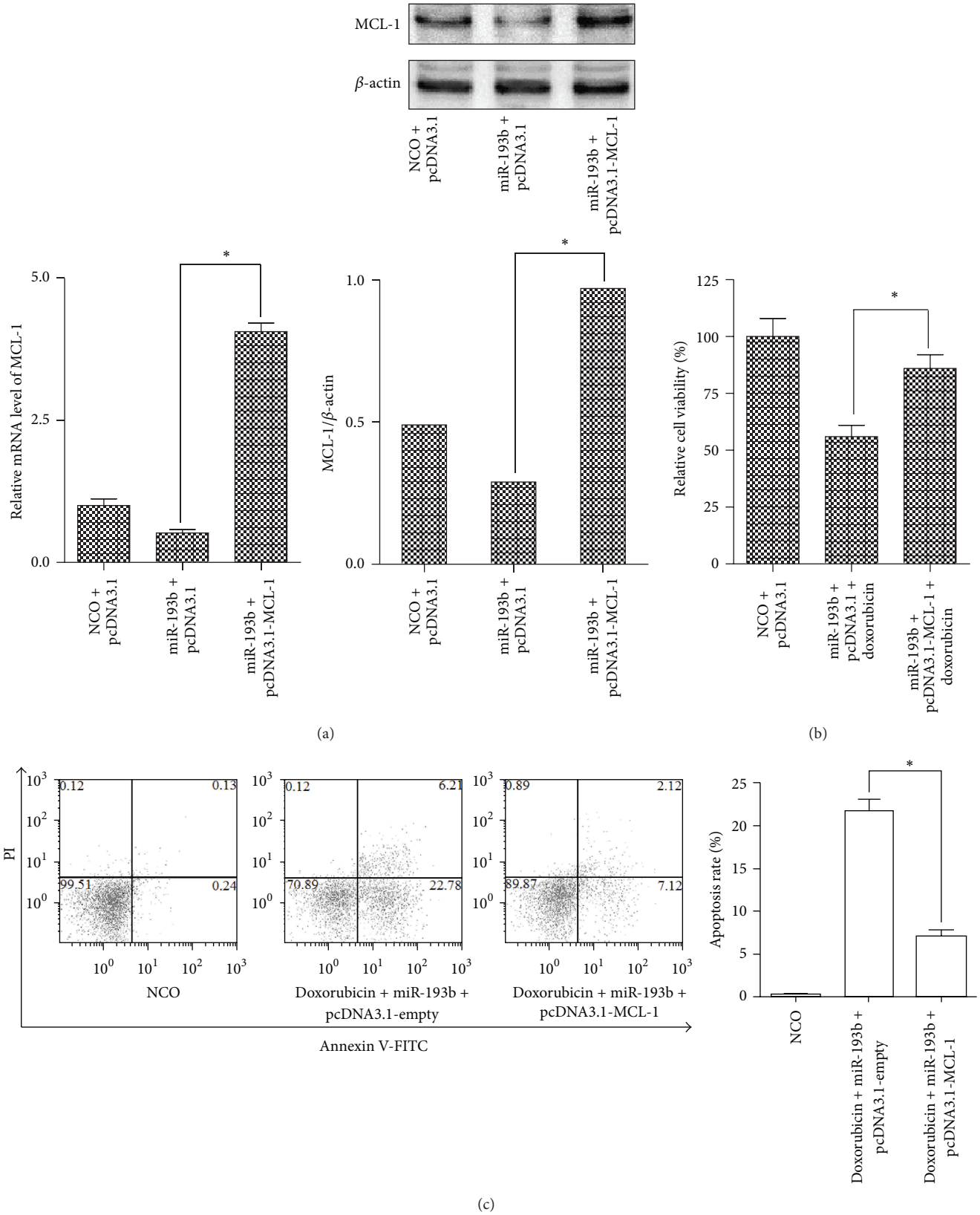

Figure 4: miR-193b sensitized MCF-7/DOXR cells to doxorubicin depending on the downregulation of MCL-1. (a) MCF-7/DOXR cells were cotransfected with miR-193b or NCO plus empty pcDNA3.1 or pcDNA3.1-MCL-1. MCL-1 mRNA and protein expression levels were assayed by qPCR and western blot, respectively, $^{*}p < 0.05$. (b) MCL-1 expression vector rescued the MCF-7/DOXR cells treated with doxorubicin (1.2 μg/mL) plus miR-193b (50 nM), suggesting miR-193b modulates doxorubicin resistance through targeting MCL-1. (c) Enforced expression of MCL-1 decreased the apoptosis induced by doxorubicin plus miR-193b. Apoptosis was measured using Annexin V/PI staining by flow cytometry. Data are expressed as the means ± SE ($n = 3$). $^{*}p < 0.05$.

enhance the chemosensitivity to epirubicin in breast cancer cells [19]. Similar to the aforementioned findings, in the present study, we found that the expression of miR-193b was lower in MCF-7/DOXR cells comparing with its parental MCF-7 cells. More importantly, transfection of MCF-7/DOXR cells with the exogenous miR-193b significantly decreased doxorubicin resistance. Furthermore, our study provided new insight into the molecular basis of doxorubicin resistance; that is, miR-193b sensitizes breast cancer cells to doxorubicin by targeting myeloid cell leukemia-1 (MCL-1).

MCL-1 is an important member of antiapoptotic BCL-2 family proteins, which is overexpressed in many human cancer cells associated with poor prognosis [20, 21]. MCL-1 is known as a tumor survival factor via suppressing the apoptosis by inhibiting the normal function of proapoptotic Bcl-2 family proteins such as Noxa [22]. Moreover, MCL-1 is reported to mediate chemotherapy resistance in multiple cancers [23, 24]. In this study, we found that MCL-1 was significantly overexpressed in MCF-7/DOXR cells, suggesting that the MCL-1 might be essential for doxorubicin resistance in breast cancer. Further results showed that MCL-1 was directly regulated by miR-193b, which is in accordance with the prior finding in melanoma [13]. Interestingly there was a negative correlation between the expression levels of miR-193b and MCL-1 in MCF-7/DOXR cells. More importantly, we found doxorubicin-induced apoptosis was inhibited in MCF-7/DOXR cells cotransfected with MCL-1 expression vector and miR-193b mimic, indicating that MCL-1 plays a pivotal role in mediating miR-193b-modulated doxorubicin resistance in human breast cancer.

5. Conclusion

We conclude that the miR-193b modulates resistance to doxorubicin in human breast cancer cells by downregulating MCL-1. Aberrant regulation of apoptosis commonly plays a key role in acquired chemotherapy resistance for cancer cells, which is largely mediated by the Bcl-2 family proteins [25]. So the present study may provide a novel individualized treatment strategy for chemotherapy-resistant tumors by miR-193b-MCL-1-apoptosis pathway.

Conflict of Interests

The authors declare that they have no conflict of interests regarding the publication of this paper.

Authors' Contribution

Jingpei Long and Zhiwei Ji contributed equally to this work.

Acknowledgments

This work was supported by Science Foundation from the Natural Science Foundation of Zhejiang Province (no. LQ14H290002) and Zhejiang Provincial Administration of Traditional Chinese Medicine (no. 2014ZB012).

References

[1] R. Siegel, D. Naishadham, and A. Jemal, "Cancer statistics for Hispanics/Latinos, 2012," *CA Cancer Journal for Clinicians*, vol. 62, no. 5, pp. 283–298, 2012.

[2] J. W. Antoon, M. D. White, E. M. Slaughter et al., "Targeting NFκB mediated breast cancer chemoresistance through selective inhibition of sphingosine kinase-2," *Cancer Biology & Therapy*, vol. 11, no. 7, pp. 678–689, 2011.

[3] G. Del Conte, C. Sessa, R. von Moos et al., "Phase I study of olaparib in combination with liposomal doxorubicin in patients with advanced solid tumours," *British Journal of Cancer*, vol. 111, no. 4, pp. 651–659, 2014.

[4] S. M. Attia and S. A. Bakheet, "Effect of dihydrokainate on the capacity of repair of DNA damage and apoptosis induced by doxorubicin," *Mutagenesis*, vol. 28, no. 3, pp. 257–261, 2013.

[5] G. Minotti, P. Menna, E. Salvatorelli, G. Cairo, and L. Gianni, "Anthracyclines: molecular advances and pharmacologic developments in antitumor activity and cardiotoxicity," *Pharmacological Reviews*, vol. 56, no. 2, pp. 185–229, 2004.

[6] K. Effenberger-Neidnicht and R. Schobert, "Combinatorial effects of thymoquinone on the anti-cancer activity of doxorubicin," *Cancer Chemotherapy and Pharmacology*, vol. 67, no. 4, pp. 867–874, 2011.

[7] D. Pramanik, N. R. Campbell, S. Das et al., "A composite polymer nanoparticle overcomes multidrug resistance and ameliorates doxorubicin-associated cardiomyopathy," *Oncotarget*, vol. 3, no. 6, pp. 640–650, 2012.

[8] J. Krützfeldt, M. N. Poy, and M. Stoffel, "Strategies to determine the biological function of microRNAs," *Nature Genetics*, vol. 38, no. 1, pp. S14–S19, 2006.

[9] A. M. Cheng, M. W. Byrom, J. Shelton, and L. P. Ford, "Antisense inhibition of human miRNAs and indications for an involvement of miRNA in cell growth and apoptosis," *Nucleic Acids Research*, vol. 33, no. 4, pp. 1290–1297, 2005.

[10] Y. Fang, H. Shen, Y. Cao et al., "Involvement of miR-30c in resistance to doxorubicin by regulating YWHAZ in breast cancer cells," *Brazilian Journal of Medical and Biological Research*, vol. 47, no. 1, pp. 60–69, 2014.

[11] C. Chen, D. A. Ridzon, A. J. Broomer et al., "Real-time quantification of microRNAs by stem-loop RT-PCR," *Nucleic Acids Research*, vol. 33, no. 20, article e179, 2005.

[12] K. J. Livak and T. D. Schmittgen, "Analysis of relative gene expression data using real-time quantitative PCR and the $2^{-\Delta\Delta CT}$ method," *Methods*, vol. 25, no. 4, pp. 402–408, 2001.

[13] J. Chen, X. Zhang, C. Lentz et al., "MiR-193b regulates Mcl-1 in melanoma," *The American Journal of Pathology*, vol. 179, no. 5, pp. 2162–2168, 2011.

[14] E. Rivera and H. Gomez, "Chemotherapy resistance in metastatic breast cancer: the evolving role of ixabepilone," *Breast Cancer Research*, vol. 12, no. 2, article S2, 2010.

[15] S. Dawood, L. Austin, and M. Cristofanilli, "Cancer stem cells: implications for cancer therapy," *Oncology*, vol. 28, pp. 1101–1107, 2014.

[16] A. H. Nwabo Kamdje, P. F. Seke Etet, L. Vecchio et al., "New targeted therapies for breast cancer: a focus on tumor microenvironmental signals and chemoresistant breast cancers," *World Journal of Clinical Cases*, vol. 2, pp. 769–786, 2014.

[17] J. Bockhorn, R. Dalton, C. Nwachukwu et al., "MicroRNA-30c inhibits human breast tumour chemotherapy resistance by regulating TWF1 and IL-11," *Nature Communications*, vol. 4, article 1393, 2013.

[18] J. Bockhorn, K. Yee, Y. F. Chang et al., "MicroRNA-30c targets cytoskeleton genes involved in breast cancer cell invasion," *Breast Cancer Research and Treatment*, vol. 137, no. 2, pp. 373–382, 2013.

[19] J. Chen, W. Tian, H. Cai, H. He, and Y. Deng, "Down-regulation of microRNA-200c is associated with drug resistance in human breast cancer," *Medical Oncology*, vol. 29, no. 4, pp. 2527–2534, 2012.

[20] L. Luo, T. Zhang, H. Liu et al., "MiR-101 and Mcl-1 in non-small-cell lung cancer: expression profile and clinical significance," *Medical Oncology*, vol. 29, no. 3, pp. 1681–1686, 2012.

[21] T. Zhang, C. Zhao, L. Luo, H. Zhao, J. Cheng, and F. Xu, "The expression of Mcl-1 in human cervical cancer and its clinical significance," *Medical Oncology*, vol. 29, no. 3, pp. 1985–1991, 2012.

[22] P. Geserick, J. Wang, M. Feoktistova, and M. Leverkus, "The ratio of Mcl-1 and Noxa determines ABT737 resistance in squamous cell carcinoma of the skin," *Cell Death and Disease*, vol. 5, no. 9, Article ID e1412, 2014.

[23] H. Karami, B. Baradaran, A. Esfehani, M. Sakhinia, and E. Sakhinia, "Down-regulation of Mcl-1 by small interference RNA induces apoptosis and sensitizes HL-60 leukemia cells to etoposide," *Asian Pacific Journal of Cancer Prevention*, vol. 15, no. 2, pp. 629–635, 2014.

[24] R. Zhang, Y. Li, X. Dong, L. Peng, and X. Nie, "MiR-363 sensitizes cisplatin-induced apoptosis targeting in Mcl-1 in breast cancer," *Medical Oncology*, vol. 31, no. 12, p. 347, 2014.

[25] S. Setia, B. Nehru, and S. N. Sanyal, "Celecoxib prevents colitis associated colon carcinogenesis: an upregulation of apoptosis," *Pharmacological Reports*, vol. 66, no. 6, pp. 1083–1091, 2014.

Hindawi Publishing Corporation
BioMed Research International
Volume 2015, Article ID 292454, 7 pages
http://dx.doi.org/10.1155/2015/292454

Research Article

The Quantified Level of Circulating Prostate Stem Cell Antigen mRNA relative to GAPDH Level Is a Clinically Significant Indictor for Predicting Biochemical Recurrence in Prostate Cancer Patients after Radical Prostatectomy

Sung Han Kim,[1] Weon Seo Park,[2] Sang Jin Lee,[3] Moon Kyung Choi,[4] Seung Min Yeon,[5] Jeong Nam Joo,[5] Ara Ko,[3] Eun Sik Lee,[6] Jae Young Joung,[1] Ho Kyung Seo,[1] Jinsoo Chung,[1] and Kang Hyun Lee[1]

[1]*Department of Urology, Center for Prostate Cancer, Research Institute and Hospital of National Cancer Center, Goyang 410-769, Republic of Korea*
[2]*Department of Pathology, Center for Prostate Cancer, Research Institute and Hospital of National Cancer Center, Goyang 410-769, Republic of Korea*
[3]*Genitourinary Cancer Branch, Center for Prostate Cancer, Research Institute and Hospital of National Cancer Center, Goyang 410-769, Republic of Korea*
[4]*Division of Specific Organ Cancer, Center for Prostate Cancer, Research Institute and Hospital of National Cancer Center, Goyang 410-769, Republic of Korea*
[5]*Biometric Research Branch, National Cancer Center, Goyang 410-769, Republic of Korea*
[6]*Department of Urology, Seoul National University Hospital of Medicine, Seoul 110-744, Republic of Korea*

Correspondence should be addressed to Kang Hyun Lee; uroonco@ncc.re.kr

Received 10 February 2015; Revised 9 May 2015; Accepted 13 May 2015

Academic Editor: Franco M. Buonaguro

The study quantified the relative absolute PSCA level in relation to the glyceraldehyde 3-phosphate dehydrogenase (GAPDH) level in the peripheral blood of 478 hormone-naive prostate cancer (PC) patients who underwent radical prostatectomy from 2005 to 2012 and evaluated its prognostic significance as a risk factor for predicting biochemical recurrence (BCR), compared to known parameters. Nested real-time polymerase chain reaction (RT-PCR) and gel electrophoresis detected PSCA levels and measured the PSCA/GAPDH ratio. Clinicopathological data from the institutional database were examined to determine the adequate cut-off level to predict postoperative BCR. A total of 110 patients had a positive PSCA result (23.0%) via RT-PCR (mean blood ratio 1.1 ± 0.4). The BCR was significantly higher in the PSCA-positive detection group ($p = 0.009$). A multivariate model was created to show that a PSCA/GAPDH ratio between 1.0 and 1.5 (HR 12.722), clinical T2c stage (HR 0.104), preoperative PSA (HR 1.225), extraprostatic capsule extension (HR 0.006), lymph node dissection (HR 16.437), and positive resection margin (HR 27.453) were significant predictive factors for BCR ($p < 0.05$). The study showed successful quantification of PSCA with its significance for BCR-related risk factor; however, further studies are needed to confirm its clinical predictive value.

1. Introduction

Prostate cancer (PC) has become the most frequent malignancy in men and causes the second highest number of cancer-related deaths. Half of all patients have metastatic disease at the initial diagnosis, and nearly half of the remainder who present with an initially localized disease will develop subsequent metastasis despite appropriate treatments [1]. To date, there have been no completely accurate diagnostic tools for controlling advanced disease states or predicting the

early progression of PC during follow-ups; therefore, many clinicians are searching for new tumor markers or other methods to improve their detection rate.

Recent research has emphasized circulating tumor cells (CTCs), detected in the blood or lymphatic fluid from the primary PC lesion, as a potentially predictive micrometastatic tumor cell. This type of cell may metastasize to other organ sites when adequate conditions for survival are met in the secondary site. The CTC count is thus considered important for predicting PC progression, determining likely treatment outcomes, and choosing early preventive measures.

In particular, prostate stem cell antigen (PSCA) has recently come under scrutiny as a potential CTC marker. The antigen is found at low expression levels in the normal state but increases when the prostate's condition becomes malignant and during progression from an early to an advanced PC state [2, 3]. The reverse transcriptase polymerase chain reaction (RT-PCR) has successfully quantified PSCA [4], prompting many other researchers to evaluate the benefits of PSCA as a diagnostic tool and explore its use in the treatment and prevention of PC in clinical and animal models [5–7].

Although this basic nested RT-PCR method for quantification of PSCA has not proven to be particularly precise upon repeated studies [8], a group from China recently used the RT-PCR method to show that circulating levels of PSCA correlated with androgen-independent progression in advanced PC [9]. Joung et al., from our institution, also showed the objective utility of using nested RT-PCR to quantify peripheral blood levels of PSCA mRNA to find several important genotypes and to predict the likelihood of biochemical recurrence (BCR) [10, 11].

Therefore, this study aimed to quantify absolute PSCA level in the peripheral blood of PC patients who underwent radical prostatectomy and relate it to a GADPH reference level (PSCA/GAPDH ratio) using RT-PCR. The study further aimed to determine PSCA's reliability as a tumor biomarker in comparison with other known clinicopathological prognostic parameters of BCR.

2. Materials and Methods

This study was approved by the Institutional Review Board (IRB number NCCNCS 05-049) with written consent from the participants. It was conducted according to the principles expressed in the Declaration of Helsinki.

2.1. Patient Selection and Blood Samples. From February 2005 to December 2012, 478 PC patients who underwent radical prostatectomy and standard pelvic lymph node dissection at the Center for Prostate Cancer, National Cancer Center, were prospectively selected for screening and possible inclusion into the study with a mean follow-up time of 42.1 ± 25.30 months. All cases were pathologically confirmed as adenocarcinomas, based on current World Health Organization criteria and Gleason grade by a single experienced uropathologist (Professor WSP, MD, PhD). Other clinicopathologic data were prospectively recorded in the Prostate Cancer Center database. No postoperative adjuvant hormonal or radiotherapies were performed until biochemical recurrence (BCR) developed, defined as a postoperative serum PSA elevation of >0.2 ng/mL assessed on two occasions, following a prior decrease to nondetectable levels. The first PSA value of 0.2 ng/mL or greater was used to define the time of recurrence.

Researchers collected preoperative blood samples and performed RT-PCR to detect PSCA. A total of 135 (28.2%) cases tested positive for PSCA. Exclusion criteria included refusal to participate in the study; missing preoperative clinicopathological data; inadequate volume of PSCA cDNA for RT-PCR; previous history of hormone therapy or chemotherapy or radiation therapy; history of invasive prostate treatment; postoperative loss to follow-up; or short follow-up less than 1 year. After excluding 25 patients based on these criteria, 110 (23.0%) patients with PSCA-positive preoperative blood samples were ultimately enrolled.

2.2. Prospectively Collected mRNA and cDNA Extraction and Reverse Transcription. Blood samples of 20 mL were obtained from patients just before the RP operation. Samples were delivered to the laboratory within an hour and nucleated cell fractions were isolated from 5 mL whole blood samples using Percoll Gradient Centrifugation (Amersham Biosciences, Uppsala, Sweden). Then, total RNA, extracted from nucleated cells, was converted to cDNA by reverse transcriptase and analyzed by PCR and nested PCR, as described in previous reports [10, 11]. After RT-PCR assay sensitivity in cultured LNCaP cells was completed, assay products were evaluated to determine PSCA positivity. A 2% agarose gel was used for electrophoresis, and an ultraviolet transilluminator (UV-T) was used for visualization. All 110 PSCA-positive samples were collected and stored at −70°C.

2.3. PSCA Quantification. The mRNA obtained from 110 PSCA-positive samples was converted to cDNA, and PCR/nested PCR reactions from the prepared cDNA were utilized to calculate the amount of PSCA mRNA. The PSCA transcript quantities were normalized with an internal glyceraldehyde 3-phosphate dehydrogenase (GAPDH) mRNA control.

The PCR-reaction mixture for quantified analysis included 5 L of cDNA, 10 μL of buffer (Go Taq), 0.25 μL of DNA Polymerase (Promega Go Taq, Promega, WI), 4 μL of dNTP 2.5 mM mixture (TaKaRa, Japan), ≤50 μL of distilled water, and 1 μL of each primer.

All primers used in this study were synthesized by Bioneer (Daejeon, Korea). The primers specific for human PSCA were 5′-CCC TGC AGC CAG GCA CT-3′ and 5′-AGG CCA ACT GCG CG AT-5′. Primers for human GAPDH were 5′-TGG TCA CCA GGG CTG CTT TTA-3′ and 5′-TCC TGG AAG ATG GTG ATG GGA TTT-3′. For nested PCR for PSCA detection, primers were 5′-CAC TGC CCT GCT GTG CTA CT-3′ and 5′-CGC GGT CCA GCA CTG CTC CC-3′. For the internal control to assess RNA integrity, GAPDH was amplified. PCR reactions were performed in a total volume of 50 μL containing 1 μL of RT product, 5 μL of 10x PCR-reaction buffer (200 mmol/L Tris HCl, pH 8.4, 500 mmol/L KCl), 0.1 μmol/L sense and 0.1 μmol/L antisense primer, 0.2 mmol/L of each dNTP, and 1 U Taq-DNA polymerase.

Amplification of 5 μL cDNA was performed using a Tube Controlled Thermal Cycler (MJ Research, Waltham, MN, USA) with the following reaction profile: 2 min of initial denaturation at 95°C followed by single cycle of denaturation at 95°C for 30 s; 30 s of annealing at 55°C followed by 35 cycles at 94°C for 30 s, 55°C for 1 min, and 72°C for 1 min; and a final extension at 72°C for 5 min. For nested PCR, 5 μL of PCR product was amplified with the same reagents and with nested primers for an additional 35 cycles. LNCaP cells were cultured, and RT-PCR assay sensitivity was determined, as described in a previous report [10, 11]. The sensitivity of LNCaP cells and other markers were all analyzed to confirm the amount of PSCA transcripts using GADPH as a reference.

Quantification was performed on 1% agarose gel treated with 0.5 μg/mL ethidium bromide stain. Then, the UV-T was used to visualize the fluorescent expression of PSCA and GAPDH, and the relative amount of PSCA transcripts was determined.

2.4. Statistical Analysis. The chi-squared and Fisher's exact tests were used to evaluate the correlation of PSCA titer and PSCA/GAPDH ratio with clinicopathological factors. Student's t-test was used to compare differences in BCR. In this study, disease progression was defined as BCR after prostatectomy. Multivariate survival analysis was evaluated using Cox's proportional hazard models to identify independent prognostic factors of BCR. Two-sided p values < 0.05 using STATA (release 9.2, STATA Inc., TX, USA) were considered statistically significant.

3. Results

The clinicopathologic characteristics and demographics of the 110 positive PSCA patients are described in Table 1. Using nested RT-PCR, a mean PSCA titer of 9531.2 ± 4272.5 was detected, and a relative mean PSCA/GADPH ratio of 1.1 ± 0.4 was detected via gel electrophoresis and UV-T (Table 1, Figure 1).

The correlation analysis of PSCA titers and known clinicopathologic prognostic parameters showed that clinical (odds ratio [OR] 15.049) and pathologic T stage presence (OR 8.431), a positive resection margin (OR 9.545), and apical tumor involvement (OR 13.291) were significantly correlated with PSCA titer, and BCR (OR 8.091) and perineural invasion (OR 8.233) were significantly correlated with the PSCA/GAPDH ratio ($p < 0.05$, Table 2). The BCR-free survival curve showed that PSCA-positive group had higher incidence of BCR than the negative group ($p = 0.009$, Figure 2).

To determine the PSCA/GAPDH ratio as a predictive prognostic factor for BCR, univariate and multivariate analyses were performed. The univariate analysis showed that the preoperative PSA, PSCA absolute titer, PSCA/GAPDH ratio, pathologic Gleason score sum, clinical T stage, positive resection margin, lymphovascular invasion, perineural invasion, extraprostatic capsule extension, seminal vesicle invasion, lymph nodal dissection, and pathologic T stage were significantly different ($p < 0.05$, data not shown). The multivariate Cox regression model showed that a PSCA/GAPDH ratio of 1.0–1.5 (HR 12.722, 95% CI 1.737–843.933), a clinical T2c stage (HR 0.104, 95% CI 0.018–0.621), preoperative PSA levels (HR 1.225, 95% CI 1.068–1.406), extraprostatic capsule extension (HR 0.006, 95% CI 0.001–0.271), lymph node dissection (HR 16.437, 95% CI 1.024–263.859), and positive resection margin (HR 27.453, 95% CI 3.5–215.318) remained significant risk factors for BCR ($p < 0.05$, Table 3).

Table 1: Patients' clinicopathologic characteristics ($N = 110$).

Parameters	N (%) or mean ± SD
Preoperative PSA (ng/mL)	11.7 ± 10.3
Prostate volume (mL)	35.5 ± 16.1
PSCA absolute titer	9531.2 ± 4272.5
>15,000	9 (8.2)
10,1001–1,5000	38 (34.5)
5001–10,000	51 (46.4)
<5000	12 (10.9)
PSCA/GAPDH ratio	1.1 ± 0.4
>1.5	11 (10.0)
1.1–1.5	56 (50.9)
0.5–1.0	35 (31.8)
>0.5	8 (7.3)
Gleason score sum	6.6 ± 0.8
Clinical stage T1	36 (32.7)
T2	56 (50.9)
T3	16 (14.6)
N1	2 (1.8)
Pathologic Gleason score sum	7.0 ± 0.9
Pathologic prostate volume (mL)	33.8 ± 15.2
Pathologic stage ≤T2b	63 (57.3)
≥T2c	47 (42.7)
N (+)	1 (0.9)
M1	4 (3.6)
Biochemical recurrence	24 (21.8)
Median time to biochemical recurrence (months)	7.0 (3–46)
Median follow-up duration (months)	42.1 ± 25.0

4. Discussion

A blood-based examination of PSA has historically been the most popular diagnostic screening tool for predicting PC risk and outcome; however, it is difficult to accurately predict the progression of advanced and localized PC even after adequate treatment based solely on PSA results, because the hormone's values can fluctuate up to 20–30% based on biological and environmental factors [12]. Therefore, many clinicians and researchers have suggested alternative prognostic measurements and markers such as derivatives of PSA kinetics, other imaging modalities, or novel tumor biomarkers to supplement or fully replace PSA and better predict PC prognosis and progression [13].

Recently, focus has shifted to micrometastatic CTC biomarkers in peripheral blood [13–15]. In particular, PSCA has

Table 2: Correlation of prostate stem cell antigen titer with known clinicopathological prognostic parameters ($B = 110$).

Parameters	Correlation with PSCA absolute titer (p value)	Correlation with PSCA/GAPDH (p value)
Age (years)	0.601	0.685
Preoperative PSA (ng/mL)	0.457	0.639
Preoperative-free PSA (ng/DL)	0.357	0.458
Prostate size (mL)	0.458	0.385
Gleason score sum at biopsy	0.508	0.741
Clinical T stage (T1, T2, ≥T3)	0.010 (OR 15.049)	0.485
Positive resection margin	0.018 (OR 9.545)	0.125
Pathologic Gleason score sum	0.630	0.571
Pathologic T stage (≤T2b or ≥T2c)	0.033 (OR 8.431)	0.187
Pathologic N or M stage	0.234	0.259
Apex involvement	0.003 (OR 13.291)	0.643
Lymphovascular invasion	0.643	0.053 (OR 7.934)
Perineural invasion	0.059 (OR 7.419)	0.039 (OR 8.233)
Extracapsular extension	0.051 (OR 7.658)	0.108
Seminal vesicle invasion	0.810	0.950
Biochemical recurrence	0.681	0.032 (OR 8.091)

OR: odds ratio; HGPIN: high grade prostatic intraepithelial neoplasm; PSA: prostatic specific antigen.

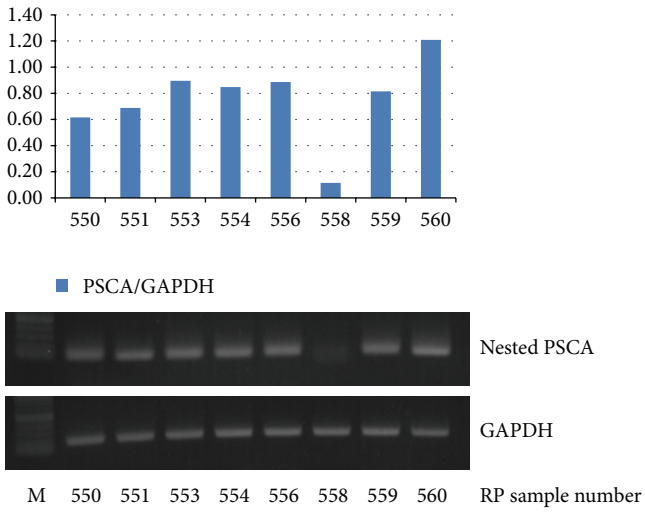

Figure 1: Detection of PSCA and GAPDH positivity using gel electrophoresis with ultraviolet transilluminator.

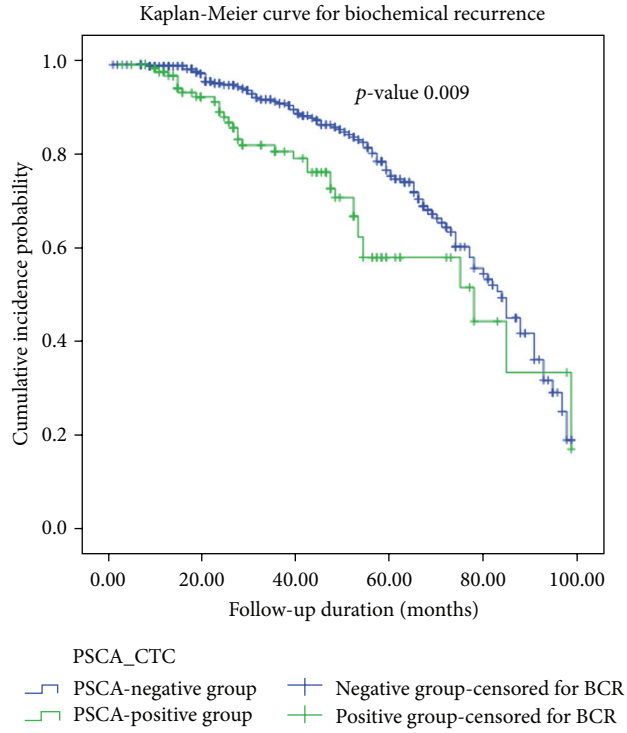

Figure 2: Kaplan-Meier curve for biochemical recurrence-free survival between PSCA-negative and PSCA-positive groups.

received recent scrutiny as a biomarker because it can accurately define the correlations between PC prognosis, diagnosis, and preventive measures [16, 17]. Highly overexpressed in human PC but with only limited expression in normal tissues, PSCA is a cell-surface antigen that belongs to the Ly-6/Thy-1 family of glycosylphosphatidylinositol-anchored proteins. The function of PSCA in normal and tumor contexts is not perfectly known; however, the Thy-1 family is known to play a role in T cell activation, proliferation, stem cell survival, and cytokine and growth factor responses. Furthermore, PSCA has already been proven to play a specific role in and have a strong relationship with PC development, because the Ly-6 family is associated with carcinogenesis, cellular activation, and cell adhesion of tumor cells [2, 18, 19].

Table 3: Multivariate analysis of BCR-related risk factors using stratified PSCA/GAPDH ratio into three subgroups.

	p value	Hazard ratio	95.0% confidence interval	
			Lower limit	Upper limit
Lymphovascular invasion	0.072	0.059	0.003	1.293
Perineural invasion	0.721	0.612	0.042	9.024
Extraprostatic capsule extension	0.008	0.006	0.001	0.271
Seminal vesicle invasion	0.589	1.464	0.367	5.838
Lymph node dissection	0.048	16.437	1.024	263.859
Resection margin negative	0.002	27.453	3.500	215.318
Neurovascular saving	0.110	4.217	0.723	24.603
Clinical T1	0.006			
cT2a, T2b	0.165	0.077	0.002	2.864
cT2c	0.013	0.104	0.018	0.621
≥cT3	0.083	14.700	0.706	306.063
Pathologic Gleason score	0.801	1.256	0.213	7.397
PSCA/GAPDH >1.5	0.052			
1.0–1.5	0.016	12.722	1.598	101.286
<1.0	0.135	5.403	0.590	49.499
Preoperative PSA	0.004	1.225	1.068	1.406
Pathologic ≤T2b	0.494	0.403	0.030	5.468

Our institution has been conducting prospective studies to find potential tumor biomarkers in the peripheral blood of Korean PC patients since 2005, and we have further reinforced the potential of PSCA as a potential PC tumor biomarker [10, 11]. The marker has already been proven to have a significant correlation with prognostic parameters of BCR, and the genetic specificity of haplotype increased the risk of PC prevalence. As our previous studies qualitatively defined PSCA as a potential PC biomarker after radical prostatectomy, we conducted this study to definitively quantify the clinical usefulness of PSCA titer in blood samples by more accurately defining the PSCA/GAPDH ratio as a significant prognostic tumor biomarker for BCR.

In this study, 28.2% ($N = 135$) of peripheral blood samples from 478 patients' blood samples were positive for PSCA, and 23.0% ($N = 110$) of samples were ultimately include. The included patients had significantly lower rates of BCR-free survival compared to others in the Kaplan-Meier plot, assessed via the log rank test ($p = 0.009$, Figure 2). The quantified PSCA/GAPDH ratio was analyzed in both correlation and multivariate models to determine its potential predictive risk factor for BCR (Tables 2 and 3). The analyses showed that the PSCA/GAPDH ratio was related to BCR and its stratified value of 1.0–1.5 (HR 12.722) was found significant for predicting BCR after radical prostatectomy ($p < 0.05$) with other significant clinical T2c stage (HR 0.104), lymph node dissection (HR 16.437), positive resection margin (HR 27.453), extraprostatic capsule extension (HR 0.006), and preoperative PSA (HR 1.225), which have been already shown in previous studies ($p < 0.05$, Table 3) [20–22].

Background analyses were performed to find an appropriate discriminating cut-off value and its clinical value in predicting the BCR. An arbitrary cut-off value of 1.2 around a median value between 1.0 and 1.5 showed a statistical discriminating power of BCR-free survival curve in the Kaplan-Meier curve with log rank test ($p = 0.034$, not shown in figure). However, this value was not finally proven to be valid for determining the statistical significance because external validation could not be performed and internal validation failed due to the limited number. Although this study has limited generalizability in defining a specific value of PSCA/GAPDH ratio due to the limited number of samples and lack of internal and external validations, this study is clinically significant because, for the first time, a study successfully suggested that quantified PSCA with a significant range value could be a potential prognostic factor for BCR and an alternative follow-up biomarker to PSA after radical prostatectomy.

Most previous PSCA studies have been based on Western patients or animal modeling studies, and only a few Asian studies have reported PSCA as a tumor biomarker strongly associated with clinicopathological parameters such as the Gleason score, pathologic stage, seminal vesicle invasion, extraprostatic capsule extension, and metastasis [4, 9, 23]. Their findings of PSCA correlation to disease invasiveness and progression were similar to our findings (Table 2). Unfortunately, however, none of those previous studies were prospectively designed, involved large numbers of samples from PC patients underwent radical prostatectomy, or involved long-term follow-up and they did not investigate PSCA's genetic, qualitative, and quantitative aspects, as was done in the present study and our previous studies [10, 11]. Thus, no definitive conclusions can yet be made, although results remain encouraging. Additionally, the subanalytic correlation study of stratified PSA, Gleason score, and pathologic T stage showed that none of the significant stratified groups of PSA, Gleason score, and pathologic T stage were significantly

related to the PSCA/GAPDH ratio ($p > 0.05$, data not shown). The PSCA/GAPDH ratio would thereby be an independent biomarker for these three markers.

The limitations of this study included the retrospective nature of the quantitative analysis, the inaccuracy of nested RT-PCR using UV-T for quantification of PSCA positivity, and no internal and external validation of our arbitrary PSCA/GAPDH cut-off value. Further larger analyses with more sensitive and accurate modalities to detect the quantified PSCA in blood samples, such as recently introduced detection equipment using nanotechnologies, are required. Additionally, longer-term follow-up is necessary to fully evaluate the prognostic value of PSCA including overall survival and progression-free survival to hormone refractory state in PC.

5. Conclusion

The study showed that a patient's quantified PSCA ratio to GAPDH (PSCA/GAPDH ratio) was significantly correlated with BCR and if its value was between 1.0 and 1.5, it was a significant risk factor for BCR. This suggested the possibilities of using PSCA/GAPDH ratio as an alternative tool for prognosis prediction than what has been examined to date. Further studies with more accurate analytic methods should be considered to detect the titers of PSCA in the peripheral blood of PC patients as an alternative to current PSA tests.

Abbreviations

cDNA: Complementary DNA
dNTP: Deoxynucleotide triphosphate
LNCaP: Oncological cell line
mRNA: Messenger RNA.

Conflict of Interests

The authors declare that there is no conflict of interests regarding the publication of this paper.

Acknowledgments

Ms. Jung Eun Kim from the Prostate Cancer Department contributed to the database management. This work was supported by a grant from the National Cancer Center (NCC-1210110 and NCC-1510170), Republic of Korea.

References

[1] R. Siegel, D. Naishadham, and A. Jemal, "Cancer statistics, 2013," *CA: Cancer Journal for Clinicians*, vol. 63, no. 1, pp. 11–30, 2013.

[2] R. E. Reiter, Z. Gu, T. Watabe et al., "Prostate stem cell antigen: a cell surface marker overexpressed in prostate cancer," *Proceedings of the National Academy of Sciences of the United States of America*, vol. 95, no. 4, pp. 1735–1740, 1998.

[3] A. C. Cunha, B. Weigle, A. Kiessling, M. Bachmann, and E. P. Rieber, "Tissue-specificity of prostate specific antigens: comparative analysis of transcript levels in prostate and non-prostatic tissues," *Cancer Letters*, vol. 236, no. 2, pp. 229–238, 2006.

[4] N. Hara, T. Kasahara, T. Kawasaki et al., "Reverse transcription-polymerase chain reaction detection of prostate-specific antigen, prostate-specific membrane antigen, and prostate stem cell antigen in one milliliter of peripheral blood: value for the staging of prostate cancer," *Clinical Cancer Research*, vol. 8, no. 6, pp. 1794–1799, 2002.

[5] M. L. Moore, M. A. Teitell, Y. Kim et al., "Deletion of PSCA increases metastasis of TRAMP-induced prostate tumors without altering primary tumor formation," *The Prostate*, vol. 68, no. 2, pp. 139–151, 2008.

[6] J. S. Lam, J. Yamashiro, I. P. Shintaku et al., "Prostate stem cell antigen is overexpressed in prostate cancer metastases," *Clinical Cancer Research*, vol. 11, no. 7, pp. 2591–2596, 2005.

[7] K.-R. Han, D. B. Seligson, X. Liu et al., "Prostate stem cell antigen expression is associated with gleason score, seminal vesicle invasion and capsular invasion in prostate cancer," *The Journal of Urology*, vol. 171, no. 3, pp. 1117–1121, 2004.

[8] D. Schamhart, J. Swinnen, K.-H. Kurth et al., "Numeric definition of the clinical performance of the nested reverse transcription-PCR for detection of hematogenous epithelial cells and correction for specific mRNA of non-target cell origin as evaluated for prostate cancer cells," *Clinical Chemistry*, vol. 49, no. 9, pp. 1458–1466, 2003.

[9] Z. Zhao, G. Zeng, W. Ma, L. Ou, and Y. Liang, "Peripheral blood reverse transcription PCR assay for prostate stem cell antigen correlates with androgen-independent progression in advanced prostate cancer," *International Journal of Cancer*, vol. 131, no. 4, pp. 902–910, 2012.

[10] J. Y. Joung, K. S. Cho, J. E. Kim et al., "Prostate stem cell antigen mRNA in peripheral blood as a potential predictor of biochemical recurrence in high-risk prostate cancer," *Journal of Surgical Oncology*, vol. 101, no. 2, pp. 145–148, 2010.

[11] J. Y. Joung, S. O. Yang, I. G. Jeong et al., "Reverse transcriptase-polymerase chain reaction and immunohistochemical studies for detection of prostate stem cell antigen expression in prostate cancer: potential value in molecular staging of prostate cancer," *International Journal of Urology*, vol. 14, no. 7, pp. 635–643, 2007.

[12] G. Sölétormos, A. Semjonow, P. E. C. Sibley et al., "Biological variation of total prostate-specific antigen: a survey of published estimates and consequences for clinical practice," *Clinical Chemistry*, vol. 51, no. 8, pp. 1342–1351, 2005.

[13] C. Stephan, H. Cammann, H.-A. Meyer, M. Lein, and K. Jung, "PSA and new biomarkers within multivariate models to improve early detection of prostate cancer," *Cancer Letters*, vol. 249, no. 1, pp. 18–29, 2007.

[14] S. F. Shariat, J. A. Karam, and C. G. Roehrborn, "Blood biomarkers for prostate cancer detection and prognosis," *Future Oncology*, vol. 3, no. 4, pp. 449–461, 2007.

[15] G. Sardana and E. P. Diamandis, "Biomarkers for the diagnosis of new and recurrent prostate cancer," *Biomarkers in Medicine*, vol. 6, no. 5, pp. 587–596, 2012.

[16] S. Ross, S. D. Spencer, I. Holcomb et al., "Prostate stem cell antigen as therapy target: tissue expression and in vivo efficacy of an immunoconjugate," *Cancer Research*, vol. 62, no. 9, pp. 2546–2553, 2002.

[17] A. B. Raff, A. Gray, and W. M. Kast, "Prostate stem cell antigen: a prospective therapeutic and diagnostic target," *Cancer Letters*, vol. 277, no. 2, pp. 126–132, 2009.

[18] I. P. Witz, "Differential expression of genes by tumor cells of a low or a high malignancy phenotype: the case of murine and human Ly-6 proteins," *Journal of Cellular Biochemistry. Supplement*, vol. 77, no. 34, pp. 61–66, 2000.

[19] T. A. Rege and J. S. Hagood, "Thy-1, a versatile modulator of signaling affecting cellular adhesion, proliferation, survival, and cytokine/growth factor responses," *Biochimica et Biophysica Acta*, vol. 1763, no. 10, pp. 991–999, 2006.

[20] T. Koie, K. Mitsuzuka, T. Yoneyama et al., "Prostate-specific antigen density predicts extracapsular extension and increased risk of biochemical recurrence in patients with high-risk prostate cancer who underwent radical prostatectomy," *International Journal of Clinical Oncology*, vol. 20, no. 1, pp. 176–181, 2015.

[21] O. Yossepowitch, A. Briganti, J. A. Eastham et al., "Positive surgical margins after radical prostatectomy: a systematic review and contemporary update," *European Urology*, vol. 65, no. 2, pp. 303–313, 2014.

[22] S. Punnen, M. R. Cooperberg, A. V. D'Amico et al., "Management of biochemical recurrence after primary treatment of prostate cancer: a systematic review of the literature," *European Urology*, vol. 64, no. 6, pp. 905–915, 2013.

[23] Z. Zhigang and S. Wenlu, "The association of prostate stem cell antigen (PSCA) mRNA expression and subsequent prostate cancer risk in men with benign prostatic hyperplasia following transurethral resection of the prostate," *The Prostate*, vol. 68, no. 2, pp. 190–199, 2008.

Hindawi Publishing Corporation
BioMed Research International
Volume 2015, Article ID 637853, 8 pages
http://dx.doi.org/10.1155/2015/637853

Research Article

The Expression and Correlation of iNOS and p53 in Oral Squamous Cell Carcinoma

Lan Yang,[1,2] Youyuan Wang,[3] Lvhua Guo,[2] Liping Wang,[2] Weiliang Chen,[3] and Bin Shi[1]

[1] *The State Key Laboratory Breeding Base of Basic Science of Stomatology (Hubei-MOST) and Key Laboratory of Oral Biomedicine Ministry of Education, School and Hospital of Stomatology, Wuhan University, 237 Luoyu Road, Wuhan 430079, China*
[2] *Key Laboratory of Oral Medicine, Guangzhou Institute of Oral Disease, Stomatology Hospital of Guangzhou Medical University, Guangzhou 510140, China*
[3] *The Sun Yat-sen Memorial Hospital of Sun Yat-sen University, Guangzhou, Guangdong 510120, China*

Correspondence should be addressed to Bin Shi; shibwh@163.com

Received 27 November 2014; Revised 22 January 2015; Accepted 22 January 2015

Academic Editor: Maria Lina Tornesello

Oral squamous cell carcinoma (OSCC) is the most prevalent form of oral cancer. Inducible nitric oxide synthase (iNOS) and p53 are associated with a variety of human cancers, but their expression and interaction in OSCC have not been fully explored. In this study, we investigated the expression of iNOS and p53 in OSCC and their correlation with tumor development and prognosis. In addition, we explored the interaction of iNOS and p53 in OSCC. The expression of iNOS and p53 in OSCC was investigated using immunohistochemical method and their interaction was studied using RNAi technique. Our results showed that the expression of both iNOS and p53 was significantly correlated with tumor stages and pathological grade of OSCC ($P < 0.05$). In contrast, there was no correlation between iNOS and p53 expression and lymph node metastasis ($P < 0.05$). The OSCC survival rate was negatively associated with iNOS expression, but not with p53. A significant increase in the expression of the p53 was observed when iNOS expression was knocked down. The immunoexpression of iNOS is correlated with tumorigenesis and prognosis of OSCC and may serve as a prognostic marker.

1. Introduction

Nitric oxide (NO) is a small gas molecule involved in a variety of biological processes including neurotransmitter, vasodilation, and immune responses [1]. NO is believed to play roles in multiple stages of various cancers. It is involved in both promoting and inhibiting the etiology of cancer depending on tumor type, NO concentration, and tumor cell sensitivity to NO [2, 3].

Endogenous NO is synthesized from L-arginine by isoforms of nitric oxide synthase (NOS). Among the three isoforms of NOS, specifically, endothelial (eNOS), neuronal (nNOS), and inducible (iNOS), iNOS produces the greatest amount of NO and is the synthase isoform most commonly associated with malignant disease [4]. iNOS expression has been detected in both normal mammalian tissues and a wide range of human cancers such as neuroblastoma, colon adenocarcinoma, ovarian cancer, stomach cancer, liver cancer, breast cancer, and head and neck cancer [5–9]. Recently, iNOS overexpression was observed in oral squamous cell carcinoma (OSCC) [10]. However, the correlation between iNOS levels and tumor stages, differentiation grade, and survival rate has not been well explored in OSCC. Sappayatosok et al. reported that iNOS shows correlation with cervical lymph node metastasis and tumor staging in OSCC [11]. A positive correlation between iNOS mRNA n and neck lymph node metastasis was also reported in squamous cell carcinoma of tongue [12].

p53 is a product of TP53 gene and has been called "the guardian of the genome." It was reported that p53 has a number of roles, in particular regulating cell cycle by halting the G1/S regulation point if DNA damage is present [13]. p53 is associated with a variety of human cancers [14]. In its wild-type form, p53 is a major tumor suppressor whose function is critical for protection against cancer [15]. In contrast, the mutant p53 protein (mt-p53) loses its original

tumor suppressor and becomes a tumor-promoting factor and promotes the process of tumor [16–18]. High frequency of mutation in TP53 gene has been shown in a variety of human tumors such as breast, brain, rectum, colon, esophagus, and lung cancers and OSCC [19]. However, the relationship between p53 expression in OSCC and tumor stages has not been well studied.

The interactions between iNOS and p53 are complicated and still unclear. As the two genes most closely associated with the tumor, the expression of iNOS and p53 and the relationship in the process of tumor development has been the focus of attention. The majority of previous studies about iNOS and p53 focused on the expression and mutation of p53 [20]. The relation between iNOS and p53 has not been studied by decreasing iNOS expression using siRNA technique.

In this study, we first investigated the expression of iNOS and p53 in 16 cases of normal oral mucosa and 72 cases of OSCC. We then evaluated the correlation between their expression levels and tumor stages, differentiation grade, and survival rate. Furthermore, the expression of iNOS was knocked down using siRNA transfection. The role of iNOS on p53 expression and tumor cell growth was then investigated.

2. Material and Methods

2.1. Tissue Preparation. A total of 88 cases of surgical biopsies specimens were obtained from Sun Yat-sen University, China, which include 16 cases of normal oral mucosa and 72 cases of oral squamous cell carcinoma. Histologically, 50 cases were well differentiated, while 10 cases were of moderate differentiation and 12 cases of poor differentiation. There are 56 cases of OSCC in early I-II stage, 16 cases in III-IV stage, and 23 cases associated with regional lymph node metastasis. All of the patients did not receive any radiation treatment. The specimens were cut into 4 μm thick serial sections, fixed in 10% formalin, and embedded in paraffin.

2.2. Reagents. Mouse anti-human iNOS monoclonal antibody and mouse anti-human p53 monoclonal antibody DO-7 were purchased from NeoMarkers (USA). Immunohistochemical detection kit was purchased from Dako (Denmark). Anti-rabbit-IgG-HRP and anti-mouse-IgG-HRP were purchased from Cell Signaling Technology (CST, USA).

2.3. Immunohistochemical Assay for Tissues. The streptavidin-biotin standard protocol was performed. Briefly, the tissue sections were deparaffinized in xylene and rehydrated in graded alcohol. Antigen retrieval was performed in citrate buffer using microwave method followed by incubation in 3% H_2O_2 at room temperature for 10 minutes to quench endogenous peroxidase. The sections were then incubated in blocking solution (3% bovine serum albumin) for 1 hour at room temperature, followed by incubation with iNOS and p53 primary antibodies overnight at 4°C. The secondary antibody was added in the next day. The tissues were then incubated for 30 min at room temperature and washed with PBS. Prior to microscopic examination, the sections were developed in DAB Chromogen and counterstained in Mayer's hematoxylin. The number of positive cells on each slice was counted based on 10 fields of view at ×200. The positive rate was calculated as the proportion of the total number of cells in the visual field. The results were divided into four levels according to the positive rate: <10% of positive cells were marked as negative (−); 10%–40% were weakly positive (+) and >50% were strongly positive (++).

2.4. Survival Analysis. The hospital visit and follow-up records were checked. The survival curves were plotted by Kaplan-Meier method and the survival rate was calculated by univariate analysis.

2.5. Tca8113 Cell in Culture. The Tca8113 cell lines were purchased from the Ninth People's Hospital of Shanghai, China. The Tca8113 cells of OSCC carry TP53 mutation. The cells were routinely cultured in DMEM low glucose medium containing 10% fetal bovine serum (FBS) and maintained in a 5% CO_2 thermostatic cell incubator at 37°C.

2.6. iNOS Gene Silencing with siRNA. The siRNA-iNOS and negative controls were synthesized and purchased from Invitrogen, China. The iNOS gene sequences are iNOS siRNA1: 5′-ACAACAGGAACCUACCAGCTT-3′; 5′-GCUGGUAGGUUCCUGUUGUTT-3′; iNOS siRNA2: 5′-ACACAAGGCCAAUACCGACTT-3′; 5′-GCGUGUAUUGGCCUGUGUUTT′-3′; negative control siRNA: 5′-ACCAUAGGAUCCUACACGCTT-3′; 5′-GCGGCUAGCUUCCUUGUGUTT′-3′. siRNA was used at a concentration of 30 nM using Lipofectamine 2000 liposomes (Invitrogen) as transfection agent (0.02%). After 24 h, Tca8113 cells were transfected with siRNA according to the manufacture's protocol. The transfection of each group of cells was observed under a fluorescence microscope.

2.7. qRT-PCR Analysis. Gene expression was analyzed by quantitative real-time PCR (qRT-PCR) using SYBR Green PCR Master Mix. The following genes were evaluated: iNOS gene (forward primer: 5′-CAGCGGGATGACTTTCCAAG-3′; reverse primer: 5′-AGGCAAGATTTGGACCTGCA-3′); p53 gene (upstream primer: 5′-ACGGTGACACGCTTCCCTGGATTGG-3′, downstream primer: 5′-CTGTCAGTGGGGAACAAGAAGTGGAGA-3′). GAPDH gene (upstream primer 5′′-CCTGGACCACCCAGCCAGCAA-3′, downstream primer: 5′-TGTTATGGGGTCTGGGATA-3′). Four groups were set up including si-1, si-2, Si-NC (negative control), and MOCK (blank control). GAPDH was used as the loading control. The experiment was repeated four times.

2.8. Western Blot Analysis. The total protein was extracted using BCA method. Western blot analysis of iNOS and p53 protein expression was performed using primary antibodies including anti-iNOS (of NOS2) and p53 antibody and the corresponding secondary antibodies. GAPDH was used as the internal reference. The specific bands were detected using West Pico Chemiluminescent Substrate (Pierce, USA) and the blots were exposed onto the Hyperfilms. The band

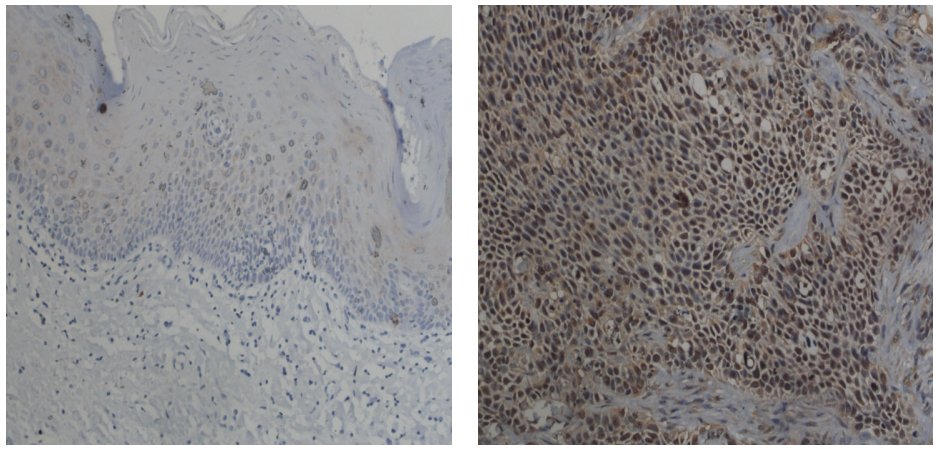

(a) (b)

Figure 1: The expression of iNOS in normal and OSCC tissues. (a) Normal control and (b) OSCC tissues. Magnification: ×200.

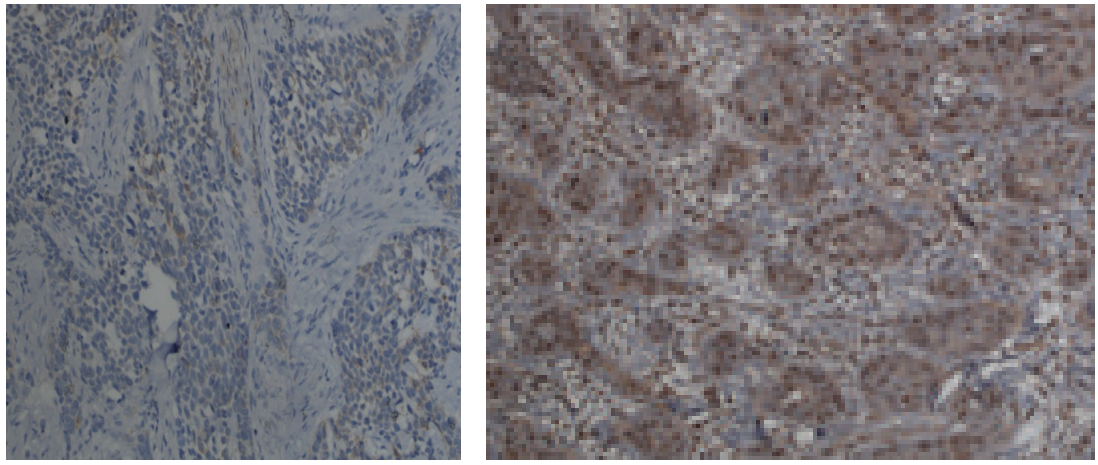

(a) (b)

Figure 2: The expression of p53 protein in normal and OSCC tissues. (a) Normal control and (b) OSCC tissues. Magnification: ×200.

intensity was quantified by the AlphaImager 2200 software. The experiment was repeated 4 times.

2.9. Cell Viability Analysis. Cell viability analysis was performed using Cell Counting Kit-8 (CCK-8) according to the manufacture's protocol. Briefly, the transfected cells' suspension (100 μL/well) was inoculated into a 96-well plate and preincubated in a humidified incubator (37°C, 5% CO_2). When the cell density reached 50%, siRNA-iNOS was transfected into the cells. At 48 h, after transfection, the medium was removed from the wells and 10 μL of CCK8 solution was added to each well. The plate was incubated for another 2 hours. The absorbance was measured at 450 nm using a microplate reader. Triplicates were set up for each group.

2.10. Statistics Analysis. SPSS16.0 software was used for statistical analysis ($\alpha = 0.05$). The expression of iNOS and p53 and the correlation were analyzed by Pearson correlation analysis. The survival curves were plotted by Kaplan-Meier method and the survival rate was calculated by univariate analysis.

3. Results

3.1. The Distribution and Expression of iNOS and p53 Protein in Normal Oral Epithelium and OSCC. As shown in Figure 1, iNOS is mainly localized in the cytoplasm with brownish yellow as positive expression. p53 was clearly observed in the cytoplasm and the nucleus. The brown particles indicated the positive expression of p53 (Figure 2). The expression of iNOS and p53 in normal oral epithelium and OSCC was significantly different. Two cases out of 16 normal oral epithelium samples have positive iNOS expression. In contrast, iNOS showed positive expression in 42 out of 72 OSCC samples (Table 1). Similarly, positive p53 expression was only observed in 3 out of 16 normal oral epithelium samples compared to 42

Table 1: iNOS and p53 expression in different tissues.

Groups	Case number (n)	iNOS		P	p53		P
		−	+ (%)		−	+ (%)	
Normal	16	14	2 (12.5%)	<0.05	13	3 (18.75%)	<0.05
OSCC	72	30	42 (58.33%)		27	45 (62.50%)	

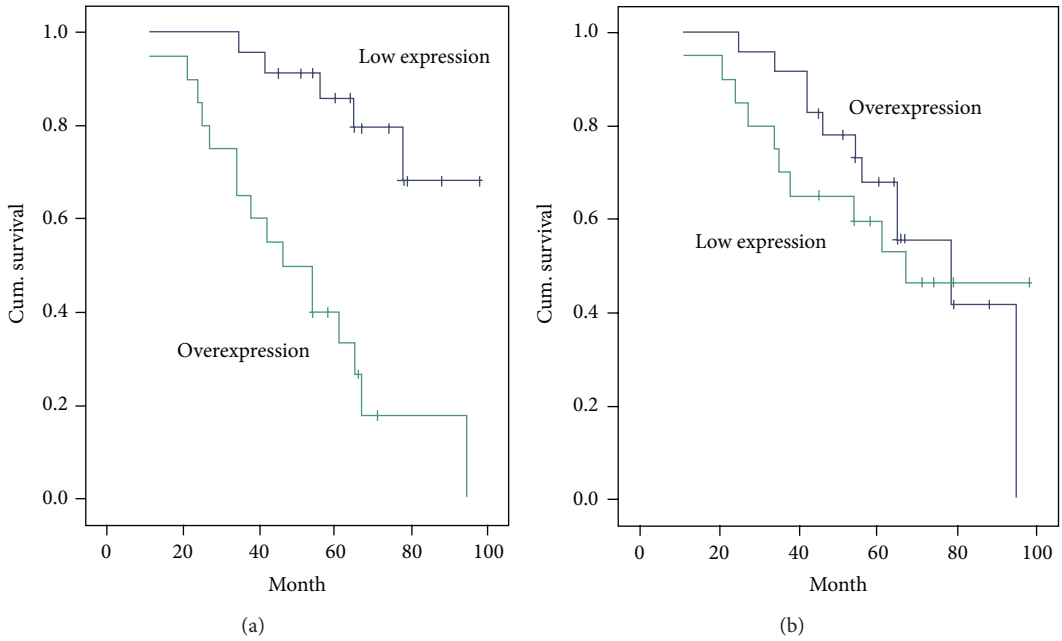

Figure 3: Survival analysis based on the expression of iNOS (a) and p53 (b).

out of 72 in OSCC samples. In addition, both proteins showed significant higher expression in oral squamous cell carcinoma than that in normal control groups ($P < 0.05$).

3.2. Correlation between iNOS and p53 Expressions in OSCC. Four-two cases (58.33%) of OSCC showed the positive expression of iNOS and 45 cases (62.50%) of OSCC have positive p53 expression (Table 2). The immunohistochemical expression of iNOS and p53 was positively correlated ($P < 0.01$).

3.3. The Immunoexpression of iNOS and p53 Was Associated with OSCC Stages and Pathologic Grade. OSCC was divided into four stages (I–IV) based on tumor size and nodal involvement. The prognosis of OSCC was also evaluated using histologic grade including moderate and poor differentiation. Our results showed that the expression of iNOS and p53 correlated significantly with the stages of OSCC ($P_{iNOS} < 0.05$, $P_{p53} < 0.05$) and pathologic differentiation grade ($P_{iNOS} < 0.05$, $P_{p53} < 0.05$). However, there was no correlation between lymph node metastasis and the immunoexpression of both iNOS and p53 ($P_{iNOS} > 0.05$, $P_{p53} > 0.05$) (Table 3). In addition, the pathological characteristics were not associated with the combined expression of both iNOS and p53 ($P_{iNOS+p53} > 0.05$).

Table 2: The correlation between iNOS and p53 expressions in OSCC.

		p53		Total (%)
		−	+	
iNOS	−	25	5	30
	+	2	40	42 (58.33%)
	Total (%)	27	45 (62.5%)	
		$\chi^2 = 54.10$	$P < 0.01$	

3.4. Survival Analysis. Figure 3 showed the Kaplan-Meier survival estimates based on the expression of iNOS and p53. The overall survival of patients with positive iNOS expression at 5 years was 38.8%, whereas the overall survival of patients with negative iNOS expression was 80.1% ($P < 0.01$) (Figure 3(a)). However, there was no statistical difference in the survival rate between positive and negative p53 expression groups ($P > 0.05$).

Table 3: The correlation between iNOS and p53 protein expressions and pathologic grade.

Groups/classification	Case number (n)	iNOS		P value	p53		P value
		−	+ (%)		−	+	
Tumor stage							
I~II stage	56	27	29 (51.79%)	$P < 0.05$	26	30 (53.18%)	$P < 0.05$
III~IV stage	16	3	13 (81.25%)		1	15 (93.75%)	
Pathologic differentiation grade							
Moderate	60	28	32 (53.33%)	$P < 0.05$	26	34 (56.67%)	$P < 0.05$
Poor	12	2	10 (83.33%)		2	12 (91.67%)	
Lymph node metastasis							
Have	23	10	13 (56.52%)	$P > 0.05$	9	14 (60.87%)	$P > 0.05$
No	49	20	29 (59.18%)		18	31 (63.27%)	

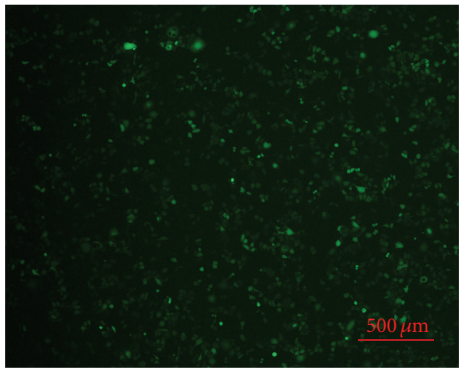

Figure 4: Tca8113 cells transfected with siRNA-INOS (si-1).

3.5. The Interaction between iNOS and p53 Expressions. To further investigate the correlation between iNOS and p53 expressions in OSCC, we knocked down the expression of iNOS in OSCC Tca8113 cells through siRNA transfection.

Two siRNA sequences (si-1 and si-2) and a negative control (si-NC) of siRNA-iNOS were transfected into Tca8113 cells (Figure 4). The expression of iNOS and p53 after iNOS silencing was investigated using RT-PCR and western blot. The results showed that the expression of iNOS was effectively knocked down in si-1 and si-2 transfection groups (Figures 5(a) and 5(b)). However, the expression of p53 was significantly enhanced in response to the silencing of iNOS in Tca8113 cells ($P < 0.05$) (Figures 6(a) and 6(b)).

Furthermore, the effect of iNOS silencing on Tca8113 cell proliferation was evaluated using Cell Counting Kit-8. Our results showed that the proliferation of Tca8113 cells was significantly inhibited when iNOS gene was silenced ($P < 0.05$) (Figure 7).

4. Discussion

iNOS is a key enzyme in the synthesis of endogenous NO. Increased iNOS expression has been shown in a number of carcinomas including OSCC, human gastric cancer, colitis, and colon cancer [10, 21]. In this study, we further demonstrated that the expression of iNOS is correlated with tumor grade and proliferation rate in OSCC.

p53 plays an important role in apoptosis, genomic stability, and inhibition of angiogenesis and thus functions as a key tumor suppressor. However, mutant p53 proteins gain oncogenic properties favoring the insurgence, the maintenance, and the spreading of malignant tumors [22]. More than 60% of our OSCC samples were p53 positive which is consistent with the results described in the literature [23]. The detection of p53 expression in a large percentage of OSCC cases by immunohistochemistry indicated the altered status of this protein [24]. Previous reports are inconclusive in terms of the relation between p53 immunoexpression and the differentiation grade of OSCC [24–26]. Here, our results clearly showed that p53 expression is significantly correlated with the tumor stages and differentiation grade of OSCC, but not with lymph node metastasis.

In this study, we demonstrated for the first time that 5-year survival time of patients with positive iNOS expression was dramatically shorter than that of those with negative iNOS expression in OSCC. In contrast, the expression of p53 has no effect on 5-year survival time of patients with OSCC. Similarly, there was no difference in rates for overall and disease-free survival between patients with p53-positive and -negative head and neck squamous cell carcinoma [27]. However, p53 was reported to be predictive of a poor prognosis in squamous cell carcinoma of the uterine cervix [28]. It is probably due to the mutation of p53 protein in the late stages of squamous cell carcinoma.

The interaction of NO, iNOS, and p53 in tumor growth and angiogenesis is complicated and still unclear. Davis et al. reported that the activation of p53 is dependent upon iNOS expression in lung cancer [29]. iNOS is associated with the mutation of p53 in human esophageal squamous cell carcinoma [30]. To study the role of iNOS, the majority of previous studies overexpressed the iNOS isoform which could result in nonphysiological extremely high levels of NO. In this study, we also investigated the role of iNOS on tumor growth and p53 expression by decreasing endogenous iNOS expression using siRNA technique. The siRNA

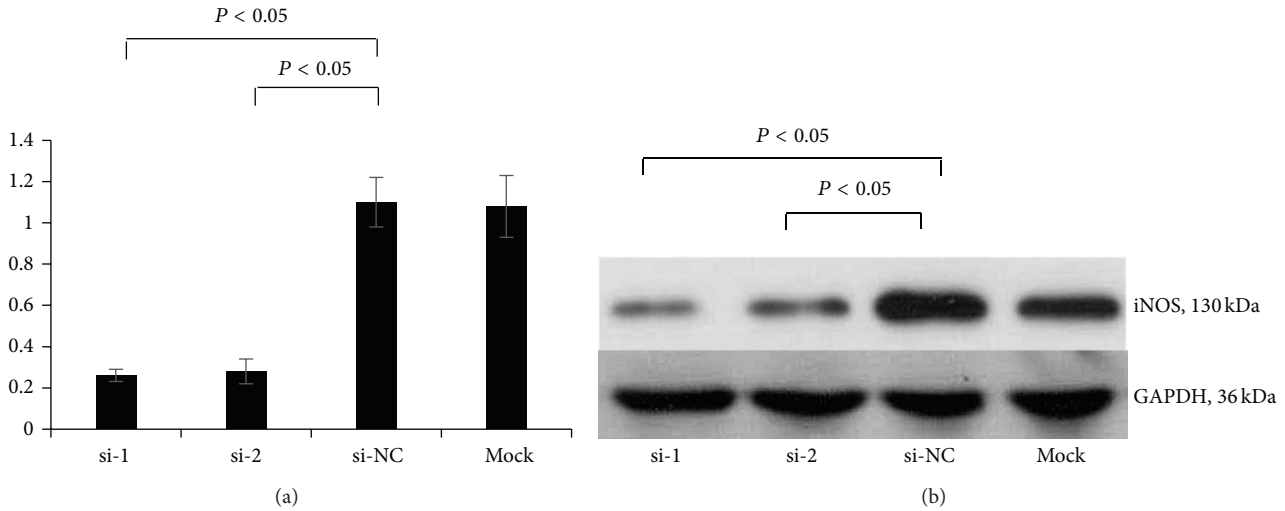

Figure 5: The expression of iNOS in Tca8113 cells transfected with iNOS-siRNA. (a) iNOS expression measured by RT-PCR; (b) iNOS expression measured by western blot. si-1: iNOS-siRNA-1; si-2: iNOS-siRNA-2; si-NC: negative control; si-MOCK: mock transfection of siRNA vector.

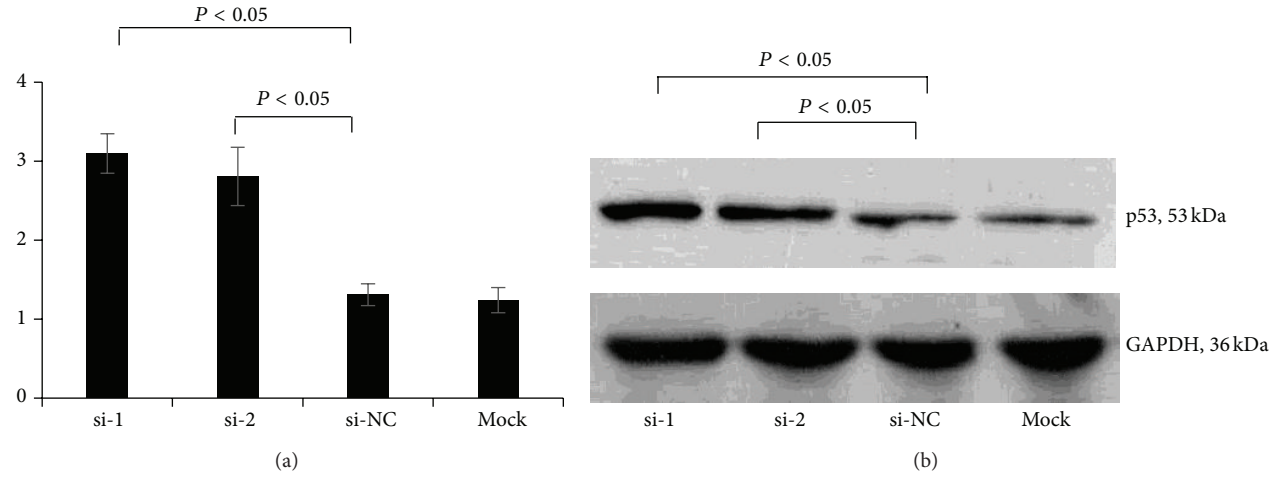

Figure 6: The expression of p53 in Tca8113 cells transfected with iNOS-siRNA. (a) p53 expression measured by RT-PCR; (b) p53 expression measured by western blot. si-1: iNOS-siRNA-1; si-2: iNOS-siRNA-2; si-NC: negative control; si-MOCK: mock transfection of siRNA vector.

transfected Tca8113 cells displayed significantly reduced growth and increase in p53 expression. Using a similar approach, Kostourou et al. reported that decreased iNOS expression resulted in the reduction of C6 cell growth [31]. Previous studies showed that silencing of mutated p53 led to the decrease of the growth of human lung adenocarcinoma cells [32]. There is still no report related to the expression of iNOS in response to the silencing of mutated p53, which will be our future objective.

All the above evidences indicated that iNOS and p53 have complex interaction in the process of tumor development. The interaction is not only related to the changes of gene and protein expression, but also to the changes of the nature and function of p53, such as activation and mutations. In the progression of OSCC tumor tissues, p53 expression is increased with the increased expression of iNOS because part of the p53 mutated and become mt-p53, which makes it a tumor-promoting factor. When the expression of iNOS was reduced in Tca8113 cells by RNA interference technology, the local NO concentration was reduced which promoted the increased expression of wt-p53 and thus led to the inhibition of tumor cell growth.

5. Conclusion

In conclusion, we have shown that (1) iNOS and p53 positivity were observed in 58.33% and 62.50% of OSCC, respectively. (2) The expression of iNOS and p53 was associated with OSCC and pathologic grade but did not correlate with lymph node metastasis. (3) The OSCC survival rate was negatively associated with iNOS expression, but not p53. (4) The interaction between p53 and iNOS is complicated.

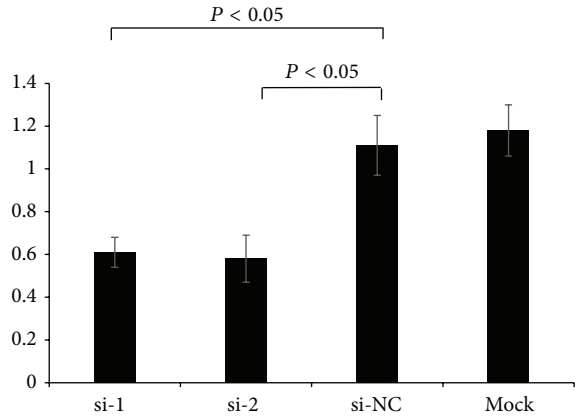

Figure 7: The effect of iNOS silencing on the proliferation of Tca8113 cells measured by CCK-8 method. si-1: iNOS-siRNA-1; si-2: iNOS-siRNA-2; si-NC: negative control; si-MOCK: mock transfection of siRNA vector.

iNOS and p53 expression was positively correlated in the progression of OSCC tumor tissues. In the tumor cells, p53 expression was upregulated in response to iNOS silencing. Together, these data further support the concept of inhibiting iNOS as a therapeutic strategy for the treatment of OSCC.

Conflict of Interests

The authors declare no conflict of interests.

Acknowledgments

This study was supported by Guangzhou Bureau of Education (no. 10A250) and Guangzhou Bureau of Health (201102A213250).

References

[1] H. H. H. W. Schmidt and U. Walter, "NO at work," *Cell*, vol. 78, no. 6, pp. 919–925, 1994.

[2] W. Xu, L. Z. Liu, M. Loizidou, M. Ahmed, and I. G. Charles, "The role of nitric oxide in cancer," *Cell Research*, vol. 12, no. 5-6, pp. 311–320, 2002.

[3] S. K. Choudhari, M. Chaudhary, S. Bagde, A. R. Gadbail, and V. Joshi, "Nitric oxide and cancer: a review," *World Journal of Surgical Oncology*, vol. 11, article 118, 2013.

[4] M. Lechner, P. Lirk, and J. Rieder, "Inducible nitric oxide synthase (iNOS) in tumor biology: the two sides of the same coin," *Seminars in Cancer Biology*, vol. 15, no. 4, pp. 277–289, 2005.

[5] P. A. Brennan, S. Dennis, D. Poller, M. Quintero, R. Puxeddu, and G. J. Thomas, "Inducible nitric oxide synthase: correlation with extracapsular spread and enhancement of tumor cell invasion in head and neck squamous cell carcinoma," *Head & Neck*, vol. 30, no. 2, pp. 208–214, 2008.

[6] M. Vakkala, K. Kahlos, E. Lakari, P. Pääkkö, V. Kinnula, and Y. Soini, "Inducible nitric oxide synthase expression, apoptosis, and angiogenesis in in situ and invasive breast carcinomas," *Clinical Cancer Research*, vol. 6, no. 6, pp. 2408–2416, 2000.

[7] P. A. Brennan, S. Sharma, J. R. Bowden, and T. Umar, "Expression of inducible nitric oxide sythase in bone metastases," *European Journal of Surgical Oncology*, vol. 29, no. 7, pp. 619–623, 2003.

[8] H. Broholm, I. Rubin, A. Kruse et al., "Nitric oxide synthase expression and enzymatic activity in human brain tumors," *Clinical Neuropathology*, vol. 22, no. 6, pp. 273–281, 2003.

[9] L. Speranza, M. A. De Lutiis, Y. B. Shaik et al., "Localization and activity of iNOS in normal human lung tissue and lung cancer tissue," *International Journal of Biological Markers*, vol. 22, no. 3, pp. 226–231, 2007.

[10] S. T. Connelly, M. Macabeo-Ong, N. Dekker, R. C. K. Jordan, and B. L. Schmidt, "Increased nitric oxide levels and iNOS overexpression in oral squamous cell carcinoma," *Oral Oncology*, vol. 41, no. 3, pp. 261–267, 2005.

[11] K. Sappayatosok, Y. Maneerat, S. Swasdison et al., "Expression of pro-inflammatory protein, iNOS, VEGF and COX-2 in oral squamous cell carcinoma (OSCC), relationship with angiogenesis and their clinico-pathological correlation," *Medicina Oral, Patologia Oral y Cirugia Bucal*, vol. 14, no. 7, pp. E319–E324, 2009.

[12] W.-L. Chen, S.-G. Zeng, H.-G. Li, H.-Z. Huang, and C.-B. Pan, "Expression of inducible nitric oxide synthase mRNA in squamous cell carcinoma of tongue," *Ai Zheng*, vol. 21, no. 3, pp. 314–318, 2002.

[13] L. E. Giono and J. J. Manfredi, "The p53 tumor suppressor participates in multiple cell cycle checkpoints," *Journal of Cellular Physiology*, vol. 209, no. 1, pp. 13–20, 2006.

[14] K. T. Bieging, S. S. Mello, and L. D. Attardi, "Unravelling mechanisms of p53-mediated tumour suppression," *Nature Reviews Cancer*, vol. 14, no. 5, pp. 359–370, 2014.

[15] W. E. Mercer, "Cell cycle regulation and the p53 tumor suppressor protein," *Critical Reviews in Eukaryotic Gene Expression*, vol. 2, no. 3, pp. 251–263, 1992.

[16] L. Weisz, A. Damalas, M. Liontos et al., "Mutant p53 enhances nuclear factor κB activation by tumor necrosis factor α in cancer cells," *Cancer Research*, vol. 67, no. 6, pp. 2396–2401, 2007.

[17] A. Zalcenstein, L. Weisz, P. Stambolsky, J. Bar, V. Rotter, and M. Oren, "Repression of the MSP/MST-1 gene contributes to the antiapoptotic gain of function of mutant p53," *Oncogene*, vol. 25, no. 3, pp. 359–369, 2006.

[18] D. P. Liu, H. Song, and Y. Xu, "A common gain of function of p53 cancer mutants in inducing genetic instability," *Oncogene*, vol. 29, no. 7, pp. 949–956, 2010.

[19] S. Strano, S. Dell'Orso, S. Di Agostino, G. Fontemaggi, A. Sacchi, and G. Blandino, "Mutant p53: an oncogenic transcription factor," *Oncogene*, vol. 26, no. 15, pp. 2212–2219, 2007.

[20] B. Leroy, L. Girard, A. Hollestelle, J. D. Minna, A. F. Gazdar, and T. Soussi, "Analysis of TP53 mutation status in human cancer cell lines: a reassessment," *Human Mutation*, vol. 35, no. 6, pp. 756–765, 2014.

[21] E. Gochman, J. Mahajna, P. Shenzer et al., "The expression of iNOS and nitrotyrosine in colitis and colon cancer in humans," *Acta Histochemica*, vol. 114, no. 8, pp. 827–835, 2012.

[22] S. Strano, S. Dell'Orso, A. M. Mongiovi et al., "Mutant p53 proteins: between loss and gain of function," *Head and Neck*, vol. 29, no. 5, pp. 488–496, 2007.

[23] A. C. Abrahao, B. V. Bonelli, F. D. Nunes, E. P. Dias, and M. G. Cabral, "Immunohistochemical expression of p53, p16 and hTERT in oral squamous cell carcinoma and potentially malignant disorders," *Brazilian Oral Research*, vol. 25, no. 1, pp. 34–41, 2011.

[24] M. Gasco and T. Crook, "The p53 network in head and neck cancer," *Oral Oncology*, vol. 39, no. 3, pp. 222–231, 2003.

[25] L. R. de Oliveira, A. Ribeiro-Silva, and S. Zucoloto, "Prognostic impact of p53 and p63 immunoexpression in oral squamous cell carcinoma," *Journal of Oral Pathology and Medicine*, vol. 36, no. 4, pp. 191–197, 2007.

[26] A. C. Abrahao, B. V. Bonelli, F. D. Nunes, E. P. Dias, and M. G. Cabral, "Immunohistochemical expression of p53, p16 and hTERT in oral squamous cell carcinoma and potentially malignant disorders," *Brazilian Oral Research*, vol. 25, no. 1, pp. 34–41, 2011.

[27] N. Oridate, A. Homma, E. Higuchi et al., "p53 expression in concurrent chemoradiotherapy with docetaxel for head and neck squamous cell carcinoma," *Auris Nasus Larynx*, vol. 36, no. 1, pp. 57–63, 2009.

[28] A. Moon, K. Y. Won, J. Y. Lee, I. Kang, and S.-K. Lee, "Expression of BDNF, TrkB, and p53 in early-stage squamous cell carcinoma of the uterine cervix," *Pathology*, vol. 43, no. 5, pp. 453–458, 2011.

[29] D. W. Davis, D. A. Weidner, A. Holian, and D. J. McConkey, "Nitric oxide-dependent activation of p53 suppresses bleomycin-induced apoptosis in the lung," *Journal of Experimental Medicine*, vol. 192, no. 6, pp. 857–869, 2000.

[30] M. Matsumoto, M. Furihata, A. Kurabayashi, K. Araki, S. Sasaguri, and Y. Ohtsuki, "Association between inducible nitric oxide synthase expression and p53 status in human esophageal squamous cell carcinoma," *Oncology*, vol. 64, no. 1, pp. 90–96, 2003.

[31] V. Kostourou, J. E. Cartwright, A. P. Johnstone et al., "The role of tumour-derived iNOS in tumour progression and angiogenesis," *British Journal of Cancer*, vol. 104, no. 1, pp. 83–90, 2011.

[32] L. L. Ma, W. J. Sun, Z. Wang, G. Y. Zh, P. Li, and S. B. Fu, "Effects of silencing of mutant p53 gene in human lung adenocarcinoma cell line Anip973," *Journal of Experimental and Clinical Cancer Research*, vol. 25, no. 4, pp. 585–592, 2006.

Hindawi Publishing Corporation
BioMed Research International
Volume 2015, Article ID 963569, 8 pages
http://dx.doi.org/10.1155/2015/963569

Clinical Study

High 15-F_{2t}-Isoprostane Levels in Patients with a Previous History of Nonmelanoma Skin Cancer: The Effects of Supplementary Antioxidant Therapy

Betânia de Jesus e Silva de Almendra Freitas,[1,2] Gustavo Rafaini Lloret,[2] Marília Berlofa Visacri,[2] Bruna Taliani Tuan,[2] Lais Sampaio Amaral,[3] Daniele Baldini,[3] Vanessa Marcílio de Sousa,[3] Laís Lima de Castro,[1] Jordana Rayane Sousa Aguiar,[1] Eder de Carvalho Pincinato,[4] Priscila Gava Mazzola,[2,3] and Patricia Moriel[2,3]

[1]*Department of Nutrition, Federal University of Piauí (UFPI), Campus Universitário Ministro Petrônio Portella, 64049-550 Teresina, PI, Brazil*
[2]*School of Medical Sciences (FCM), University of Campinas (UNICAMP), 13083-887 Campinas, SP, Brazil*
[3]*Faculty of Pharmaceutical Sciences (FCF), University of Campinas (UNICAMP), 13083-859 Campinas, SP, Brazil*
[4]*Department of Biological and Health Science Center, Mackenzie Presbyterian University, 01302-907 São Paulo, SP, Brazil*

Correspondence should be addressed to Patricia Moriel; morielpa@fcm.unicamp.br

Received 4 February 2015; Revised 10 May 2015; Accepted 14 May 2015

Academic Editor: Pierre Hainaut

Background. Phase I of this study was aimed at comparing the profiles of oxidative stress biomarkers in patients with history of nonmelanoma skin cancer (NMSC), previously treated with surgery, to the healthy subjects. Phase II aimed to evaluate the effects of supplementary antioxidant therapy on the levels of biomarkers in the case group. *Materials and Methods*. In Phase I, oxidative stress biomarkers were measured in blood samples obtained from 24 healthy subjects and 60 patients with history of NMSC previously treated with surgery. In Phase II, the 60 patients with history of NMSC were randomized into two subgroups, one receiving placebo ($n = 34$) and the other ($n = 26$) receiving vitamin C, vitamin E, and zinc supplementation for 8 weeks, followed by reevaluation of biomarkers. *Results*. In Phase I, patients with history of NMSC showed increased plasma concentrations of all biomarkers, but only 15-F_{2t}-isoprostane was significantly higher than in the healthy subjects. Risk of NMSC increased by 4% for each additional 1 pg/mL increase in 15-F_{2t}-isoprostane. In Phase II, supplementation did not significantly reduce levels of oxidative stress biomarkers. *Conclusion*. Patients with history of NMSC had significantly high 15-F_{2t}-isoprostane plasma levels; supplementation did not result in significant reduction of oxidative stress biomarkers. This trial was registered with ClinicalTrials.gov (ID NCT02248584).

1. Introduction

Oxidative stress occurs when there is disequilibrium between the generation of reactive oxygen and nitrogen species (ROS-RNS) and the cellular antioxidant system and may result in significant damage to cellular structures as well as nucleotides, proteins, and lipids. Lipid peroxidation generates a variety of relatively stable decomposition products, such as isoprostanes [1], which can be measured in plasma and urine as indirect biomarkers of cellular prooxidant status.

Substantial evidence suggests that oxidative stress is a prominent feature of many acute and chronic diseases including cancer, cardiovascular disease, and neurodegenerative pathologies, as well as being part of the normal aging process [2, 3]. Oxidant-mediated alterations may contribute to numerous skin disorders ranging from photosensitivity to cancer. This has led to the search for nontoxic antioxidants that could potentially minimize and/or reverse these changes [4].

Skin cancer is one of the most important and common cancers, with considerably more than a million new cases diagnosed each year worldwide [5]. Skin cancer is commonly grouped into two different categories, melanoma skin cancer (MSC) and nonmelanoma skin cancer (NMSC), based on the cell of origin and clinical behavior. The incidence of NMSC is much higher than that of melanoma. Fortunately, the vast majority of NMSCs are much easier to treat than MSCs and have a considerably better long-term prognosis. There are strong epidemiologic and molecular data linking all forms of skin cancer to sunlight exposure, and it is estimated that ultraviolet (UV) radiation is the primary cause of nearly 90% of NMSCs [6]. A component of sunlight is UVA radiation, which penetrates deeper into the skin than UVB due to its longer wavelengths. While UVA can indirectly damage DNA through the formation of ROS, such as the superoxide anion, hydrogen peroxide, and the hydroxyl radical [7], UVB can directly damage DNA leading to the apoptosis of sunburn cells in skin [5]. ROS may induce extensive DNA damage, lead to cross-links between DNA and proteins, and cause DNA and chromosomal aberrations that may be mutagenic [8]. ROS may also be involved in tumorigenesis through the activation of procarcinogens to generate free radicals that can attack nucleophiles [4].

The purpose of the present study was to compare the profiles of oxidative stress biomarkers, especially 15-F_{2t}-isoprostane, of patients with a history of NMSC previously treated by surgery (case group) with those of healthy subjects (comparison group) (Phase I) and to determine whether supplementation with antioxidants could influence the levels of biomarkers in the case group (Phase II).

2. Materials and Methods

This was a two-phase study composed of Phase I, with a cross-sectional study design, and Phase II, a double-blind, randomized, placebo-controlled trial, carried out between January 2011 and December 2011 in Teresina, Piauí, Brazil. The study was approved by the local ethics committee, and all participants provided a signed informed consent form authorizing use of their data.

2.1. Characterization of Groups, Recruitment, and Eligibility. In Phase I, the case group ($n = 64$) consisted of patients with a history of NMSC (squamous cell carcinoma or basal cell carcinoma) treated with surgery, recruited from a hospital in Teresina, Piauí, while the comparison group ($n = 24$) was composed of workers from a university in Teresina, Piauí, with no history of NMSC. In Phase II, the patients in the case group were randomized into two subgroups, one receiving placebo ($n = 34$) and the other receiving supplementary antioxidant therapy ($n = 26$).

The inclusion criteria for all participants were as follows: age ≥20 years; absence of comorbidities such as type 1 diabetes, severe heart disease, hepatic dysfunction, renal failure requiring dialysis, HIV infection, or MSC; no history of chemotherapy or radiotherapy in the previous 6 months; absence of severe psychiatric disease that limited comprehension; and no taking of any vitamin and/or mineral supplementation. Subjects in the case group who did not complete the entire course of supplemental therapy were excluded from the study during Phase II.

Table 1: Dietary reference intakes (UL–DRIs) and recommendations of the Institute of Medicine/National Academy Press [9, 10].

	Gender	DRI
Vitamin A	Male	625 μg/d
	Female	500 μg/d
Vitamin C	Male	75 mg/d
	Female	60 mg/d
Vitamin E	Male	12 mg/d
	Female	12 mg/d
Cuprum	Male	700 μg/d
	Female	700 μg/d
Zinc	Male	9.4 mg/d
	Female	6.8 mg/d
Selenium	Male	45 μg/d
	Female	45 μg/d

2.2. Sociodemographic Characteristics. Sociodemographic characteristics of both the comparison and case groups were collected using a standardized form that included age, gender, race, smoking and alcohol habits (yes or no), actual use of sunscreen, sunlight exposure, and family history of cancer. In the case group, information regarding histopathological parameters and tumor localization was also collected.

2.3. Anthropometric and Dietary Investigations. Anthropometric characteristics were assessed for both groups, and a food frequency questionnaire was used to estimate the daily intake of vitamins and minerals for each patient. Dietary reference intakes (DRIs) established by the Institute of Medicine of the National Academies were used to evaluate the necessity of supplemental therapy (Table 1).

2.4. Supplemental Antioxidant Therapy. The placebo group and supplemented group received, respectively, a placebo capsule containing only lactose and an identical capsule containing vitamin C (500 mg; CVS Quality, USA), vitamin E (400 IU; CVS Quality), and zinc (50 mg; Nature's Bounty, USA) per day for 60 days. The concentrations of antioxidants administered were determined according to the DRI Tolerable Upper Intake Level (UL) and recommendations of the Institute of Medicine/National Academy Press [9, 10] (Table 1).

2.5. Oxidative Stress Biomarkers. Oxidative stress biomarkers including 15-F_{2t}-isoprostane, thiobarbituric acid reactive substances (TBARS), nitrite, and total antioxidant capacity (TAC) were measured in plasma. All analyses were performed for both the comparison and case groups. The comparison group was evaluated only in Phase I. The case group was

Table 2: Comparison regarding sociodemographic characteristics from comparison and case groups.

	Comparison ($n = 24$)	Case ($n = 60$)	p value
Sociodemographic characteristics			
Age (years) (mean ± SD)	56.7 ± 11.6	62.7 ± 14.2	**0.0492**[a]
Sex (female), n (%)	19 (79.2)	39 (65.0)	0.2045[b]
Smoking, n (%)	3 (12.5)	8 (13.3)	0.6645[c]
Alcoholism, n (%)	3 (12.5)	9 (15.0)	0.7307[c]
Use of sunscreen, n (%)	6 (25.0)	41 (68.3)	**0.0003**[b]
Mean daily sunlight exposure (min) (mean ± SD)	35.0 ± 28.9	180.5 ± 123.7	<**0.0001**[a]
Family history of cancer, n (%)	4 (16.7)	42 (70.0)	<**0.0001**[b]
Race, n (%)			0.1377[b]
Caucasian	8 (33.3)	11 (18.3)	
Non-Caucasian	16 (66.7)	49 (81.7)	
Anthropometric parameters (mean ± SD)			
BMI (kg/m^2)	27.3 ± 3.5	26.5 ± 3.7	0.2710[a]
TSF (mm)	20.2 ± 6.8	18.3 ± 7.8	0.1750[a]
MUAC (cm)	30.9 ± 3.1	30.1 ± 4.5	0.1910[a]
MAMC (cm)	24.6 ± 3.0	24.5 ± 4.0	0.7100[a]
Daily intake levels (mean ± SD)			
Vitamin A (μg)	380.9 ± 197.1	558.0 ± 570.0	**0.0015**[a]
Vitamin C (mg)	162.4 ± 419.3	57.9 ± 50.6	0.2223[a]
Vitamin E (mg)	6.1 ± 14.2	9.6 ± 7.0	**0.0018**[a]
Cuprum (μg)	1040.0 ± 1009.0	800.0 ± 400.0	**0.0331**[a]
Zinc (μg)	10.1 ± 12.6	6.5 ± 3.6	**0.0317**[a]
Selenium (μg)	52.2 ± 44.5	76.2 ± 38.8	**0.0285**[a]

N = total of subjects/patients, SD = standard deviation, BMI = body mass index, TSF = triceps skinfold, MUAC = mid-upper-arm circumference, and MAMC = mid-arm muscle circumference. Statistical analysis: [a]Mann-Whitney test; [b]Chi-square test; [c]Fisher's exact test.

evaluated at two different times: (a) one day before the start of supplementation or placebo administration and (b) one day after the finish of intervention period. A total of 10 mL of venous blood was obtained from all subjects. Blood was withdrawn into blood collection tubes with EDTA or citrate as an anticoagulant and centrifuged (2500 rpm for 10 min at 4°C), and the plasma was stored at −80°C until analysis. Each test for oxidative stress biomarkers required 1 mL plasma. The plasma concentration of 15-F_{2t}-isoprostane was determined by enzyme-linked immunosorbent assay (Isoprostane Express EIA Kit; Cayman, USA). Plasma TBARS was measured using a colorimetric method as previously described [11], and the values were expressed in nmol per mL of malondialdehyde equivalents. TAC was assessed using an Antioxidant Assay Kit (Cayman, USA). Nitric oxide synthesis was assessed through nitrite measurement using the Griess assay [12] expressed in μmol of nitrite.

2.6. Data Analysis. Descriptive analyses were performed on absolute frequencies and percentages for categorical variables. Numerical variables were described by the mean and standard deviation. Statistical analyses were performed using the SAS System for Windows 9.3 program and data were analyzed using Chi-square, Fisher, Mann-Whitney, or ANOVA for repeated measures tests. Multivariate logistic regression analysis was performed to identify risk factors for NMSC. The following covariates were used: age, race, smoking, alcoholism, family history of cancer, 15-F_{2t}-isoprostane, TBARS, nitrite, and TAC, and two-sided p values < 0.05 were considered statistically significant. When the sociodemographic characteristics differed between the groups, the data were normalized and used in all regression analyses.

3. Results

3.1. Phase I. Sociodemographic characteristics, anthropometric parameters, and levels of daily vitamin intake for both groups (comparison and case groups) are detailed in Table 2. Both groups contained more women than men. Age, prolonged daily sunlight exposure, sunscreen use, and previous family history of skin cancer were all significantly higher in the case group.

Of the patients in the case group ($n = 60$), 85.0% had basal cell carcinoma, while the remaining 15.0% had squamous cell carcinoma. The face (80.0%) was the most common area affected, followed by the trunk (8.3%), neck (6.7%), and other areas (5.0%).

The case group had higher plasma concentrations of all oxidative biomarkers assessed (Figure 2(a)). However, only the increase in 15-F_{2t}-isoprostane levels was statistically significant (81.9 ± 36.4 pg/mL versus 46.2 ± 21.8 pg/mL, $p < 0.0001$). Therefore, patients with a previous history of NMSC

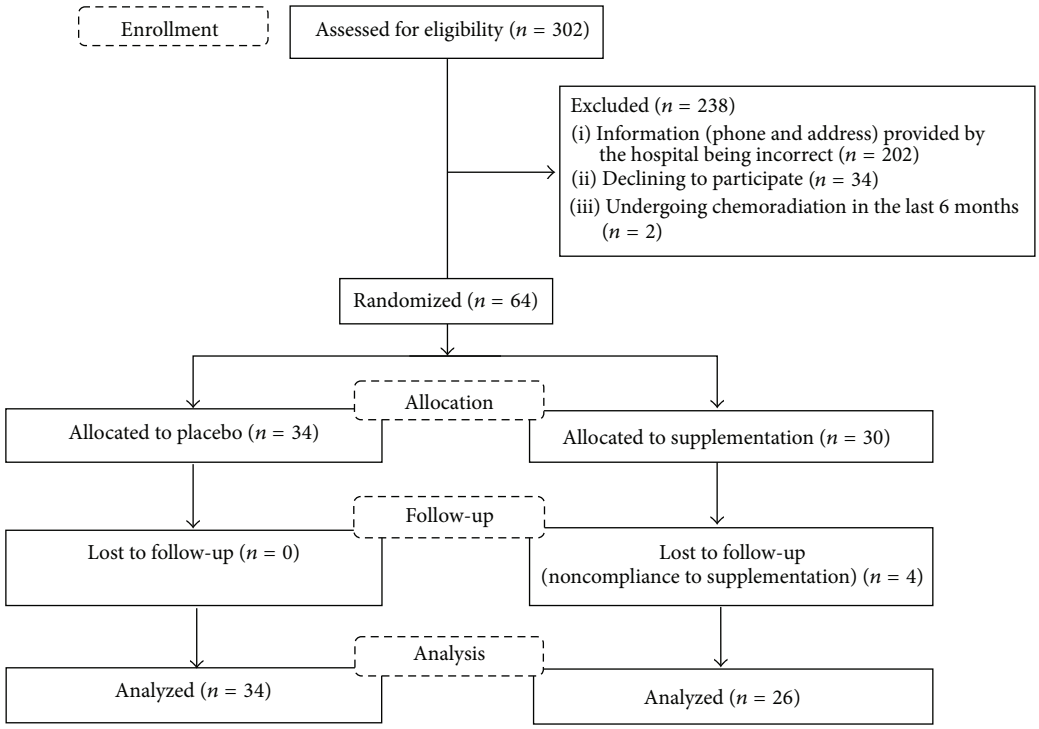

Figure 1: Flow diagram of the passage of participants (Phase II).

were considered to have a relatively prooxidant cellular state compared with healthy subjects.

Multivariate logistic regression analysis identified age ($p = 0.0050$, odds ratio (OR) = 1.121, and 95% confidence interval (CI) = 1.035–1.213) and the oxidative stress biomarker 15-F_{2t}-isoprostane ($p = 0.0099$, OR = 1.044, and 95% CI = 1.010–1.078) as risk factors associated with NMSC. The risk of NMSC increased by 12% each year and by 4% for each additional 1 pg/mL increase in 15-F_{2t}-isoprostane levels in the plasma.

Table 2 shows that levels of daily vitamin C, vitamin E, and zinc intake in the case group were lower than recommended for both genders; therefore, vitamin C, vitamin E, and zinc supplementation was clinically indicated (Phase II).

3.2. Phase II. The recruitment of participants to Phase II is described in Figure 1. Sociodemographic characteristics, anthropometric parameters, and levels of daily vitamin intake for both groups (placebo and supplemented) are detailed in Table 3. Placebo and supplementation subgroups had similar sociodemographic characteristics, except for alcoholism, which was significantly more prominent in the supplemented subgroup.

A reduction of TAC (2.3 mmol/L versus 2.1 mmol/L), 15-F_{2t}-isoprostane (87.3 pg/mL versus 76.8 pg/mL), and TBARS (90.0 nmol/L versus 60.0 nmol/L) levels after supplementation with antioxidants was observed, although these differences did not reach statistical significance compared with placebo. Compared with baseline values, the group receiving supplementation showed a reduction of both mean and median plasma levels of 15-F_{2t}-isoprostane, in addition to a more homogeneous distribution of values, which was not observed in the placebo group. The supplementation group also showed a small increase of nitrite levels (10.9 mmol/L versus 15.0 mmol/L), but this was not significantly different from that of the placebo group (Figures 2(b) and 2(c)).

4. Discussion

Owing to the increasing incidence, morbidity, and mortality of cancer worldwide, new diagnostic and screening methods are needed for early detection. In recent years, knowledge of cancer biomarkers has increased greatly and this presents numerous opportunities to improve cancer management [13]. The present study demonstrated that plasma levels of 15-F_{2t}-isoprostane were significantly higher in patients with a previous history of NMSC compared to healthy subjects. Moreover, each additional 1 pg/mL of 15-F_{2t}-isoprostane in plasma was associated with a 4% greater chance of developing NMSC. Age was also found to be a risk factor for NMSC. In addition, patients with history of NMSC had a cellular prooxidant state compared to healthy subjects.

Oxidative stress has been implicated in various pathological conditions, including cancer. When evaluating a marker for its importance *in vivo*, difficulties may arise because of analytical problems relating to its specificity and sensitivity [14]. Isoprostanes are certainly the most specific markers of lipid peroxidation but are also the most difficult to measure [14]. Several comprehensive reviews providing information on the biochemistry of isoprostanes and their utilization as markers of oxidative stress have been published in the last decade [2, 14, 15].

Table 3: Comparison regarding sociodemographic characteristics from placebo and supplemented groups before supplementation.

	Placebo (n = 34)	Supplemented (n = 26)	p value
Sociodemographic characteristics			
Age (years) (mean ± SD)	65.6 ± 13.2	59.0 ± 14.9	0.0860[a]
Sex (female), n (%)	24 (70.6)	15 (57.7)	0.2994[b]
Smoking, n (%)	4 (11.8)	4 (15.4)	0.7172[c]
Alcoholism, n (%)	2 (5.9)	7 (26.9)	**0.0323**[c]
Use of sunscreen, n (%)	22 (64.7)	19 (73.1)	0.4987[b]
Mean daily sunlight exposure (mean ± SD)	199.4 ± 130.2	155.8 ± 112.5	0.2450[a]
Family history of cancer, n (%)	24 (70.6)	18 (69.2)	0.9095[b]
Race, n (%)			0.5072[c]
Caucasian	5 (14.7)	6 (23.1)	
Non-Caucasian	29 (85.3)	20 (76.9)	
Anthropometric parameters (mean ± SD)			
BMI (kg/m^2)	27.0 ± 4.1	25.8 ± 3.2	0.3440[a]
TSF (mm)	18.1 ± 7.4	17.5 ± 8.3	0.9100[a]
MUAC (cm)	30.0 ± 4.7	30.2 ± 4.2	0.6710[a]
MAMC (cm)	24.8 ± 4.0	24.1 ± 4.1	0.7670[a]
Daily intake levels (mean ± SD)			
Vitamin A (μg)	705.3 ± 778.6	428.2 ± 232.4	0.8817[a]
Vitamin C (mg)	55.7 ± 47.6	54.2 ± 46.5	0.7326[a]
Vitamin E (mg)	9.0 ± 4.0	9.9 ± 9.3	0.6157[a]
Cuprum (μg)	950.0 ± 510.0	870.0 ± 280.0	0.0784[a]
Zinc (μg)	7.1 ± 4.4	5.8 ± 2.4	0.1321[a]
Selenium (μg)	79.8 ± 47.4	76.9 ± 21.5	0.1979[a]

N = total of subjects/patients, SD = standard deviation, BMI = body mass index, TSF = triceps skinfold, MUAC = mid-upper-arm circumference, and MAMC = mid-arm muscle circumference. Statistical analysis: [a]Mann-Whitney test; [b]Chi-square test; [c]Fisher's exact test.

Isoprostanes are prostaglandin isomers produced by peroxidation of polyunsaturated fatty acids from the cellular membrane. The most frequent isomer released into the circulation is 15-F_{2t}-isoprostane, which has been identified as a promising key biomarker to investigate the role of oxidative injury [16] in several diseases, including cancer. Barocas et al. [17] reported that increased levels of isoprostanes are present in the urine of patients with prostate cancer. Moreover, Rossner Jr. et al. [18] presented evidence that increased levels of isoprostanes may be correlated with an increased risk of breast cancer. Belli et al. [19] showed that 15-F_{2t}-isoprostane levels were increased in basal cell carcinoma and in healthy skin previously exposed to UVA irradiation. Increased levels of isoprostanes have also been reported in several acute and chronic diseases including cardiovascular and neurodegenerative pathologies and cancer, as well as during the normal aging process [16, 20].

As oxidative stress is widely believed to cause or aggravate several human pathologies as described above, it is possible that antioxidants could counteract the harmful effects caused by a prooxidant profile and prevent or treat oxidative stress-related diseases. Herein, it was observed that daily intake levels of vitamins C and E in the case group were lower than those recommended (DRI guidelines). After supplementation, there was no significant reduction in levels of oxidative stress biomarkers. However, there was a small reduction in plasma levels of all oxidative biomarkers evaluated, especially 15-F_{2t}-isoprostane. Both mean and median plasma levels of 15-F_{2t}-isoprostane were reduced after supplementation, and there was a more homogeneous distribution of values in this group. Additional studies on the modulation of isoprostanes by antioxidant nutrients have recently been published. For example, Reilly et al. [21] reported that vitamin C administered to heavy smokers for 5 days at 2 g/day significantly reduced isoprostane excretion in their urine. Moreover, Davi et al. [22, 23] described a significant reduction in urinary isoprostane excretion in patients with diabetes mellitus and hypercholesterolemia after supplemental therapy with vitamin E.

Our study did not show a significant reduction in the levels of 15-F_{2t}-isoprostane after supplementation with vitamin C, vitamin E, and zinc for 60 days. However a study conducted by Dietrich et al. [24], in which patients were supplemented for 60 days with vitamin C at 500 mg/day and vitamin E at 300 mg/day, showed a statistically significant reduction in the plasma levels of 15-F_{2t}-isoprostane. These doses were similar to those used by our study. In a study using doses of vitamin C lower than 500 mg/day and doses of vitamin E lower than 300 mg/day, a longer period of supplementation did not lead to showing a significant reduction in plasma levels of biomarkers of oxidative stress [25]. In a study by Murer et al. [26], there was a significant reduction of over 30% (p = 0.014) of 15-F_{2t}-isoprostane levels in the urine of obese children after supplementation with 500 mg/day of

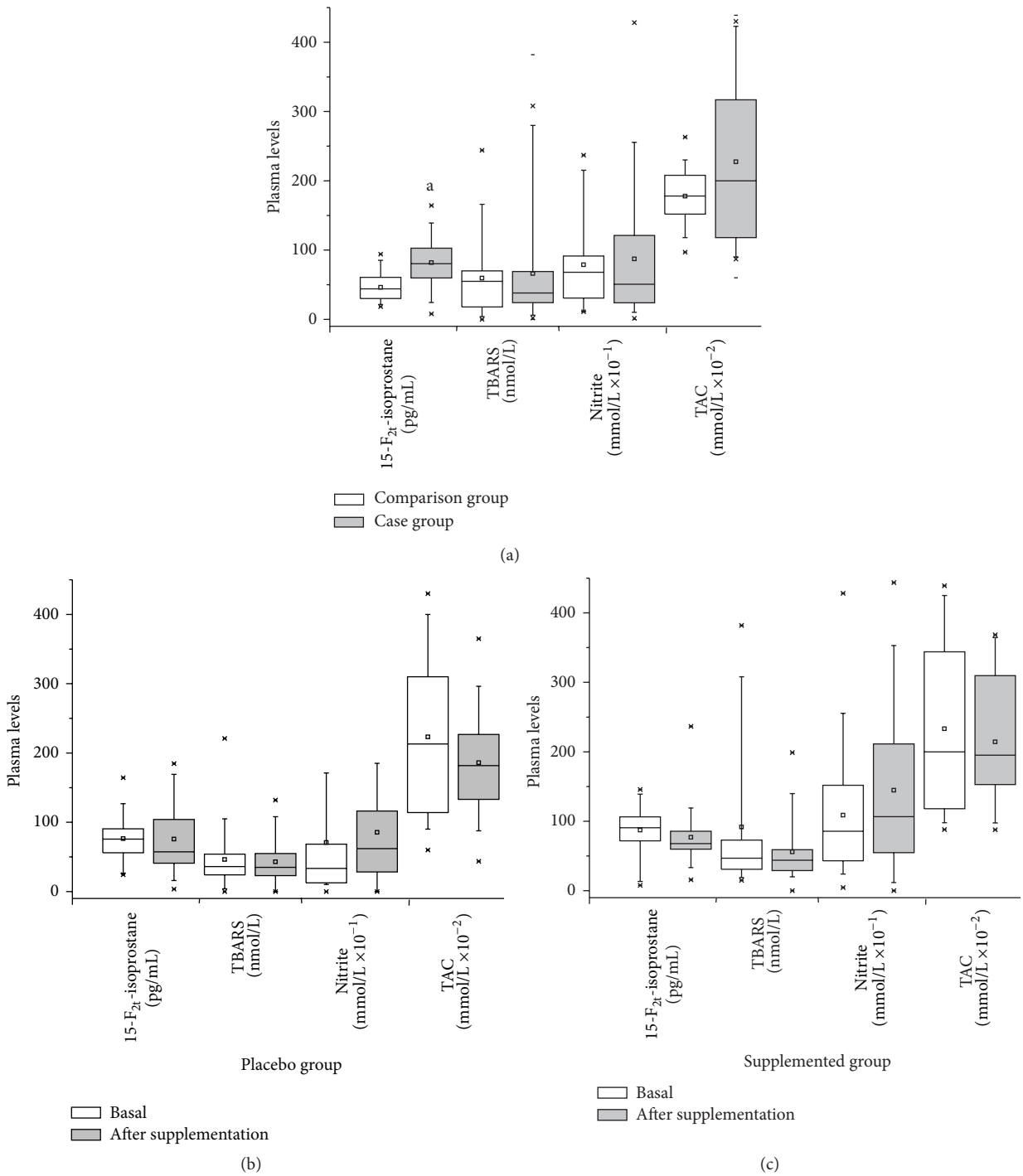

Figure 2: Mean values of oxidative stress biomarkers from each group present in the study: (a) Phase I/comparison and case groups, (b) Phase II/case group (placebo): basal and after supplementation, and (c) Phase II/case group (supplemented): basal and after supplementation. ANOVA for repeated measures statistical test; [a]statistically significant difference in relation to comparison group.

vitamin C, 400 IU/day of vitamin E, and 50 mg/day of selenium for 119 days.

In a recent study by Roberts II et al. [27], the influence of the dose of vitamin E on the reduction of 15-F_{2t}-isoprostane was examined in patients with coronary artery disease. The study was initially carried out with patients supplemented with 3200 IU/day vitamin E for 20 weeks and then participants were supplemented with a dose of 0, 100, 200, 400, 800, 1600, or 3200 IU/day vitamin E for 16 weeks. Maximum suppression of plasma levels of 15-F_{2t}-isoprostane did not occur until the 16th week of supplementation and the percentage reduction in plasma concentrations of 15-F_{2t}-isoprostane only reached significance at doses of 1600 IU/day and 3200 IU/day. These data reveal the dose-dependent

effects of antioxidant supplementation for the reduction of biomarkers of oxidative stress and indicate that the dose and time of supplementation should be chosen carefully to achieve the desired result.

This study has some limitations: a relatively small sample size; a short period of antioxidant supplementation; a lack of information about cancer types (primarily skin cancer) in families; a lack of past information about smoking, alcohol habits, use of sunscreen, and sunlight exposure; and a lack of a robust classification for smoking, alcohol habits, and use of sunscreen. In addition, the results of the immunoassays could be confounded by the structural similarities between isoprostanes and some prostaglandins; therefore, 15-F_{2t}-isoprostane should preferably be quantified by mass spectrometry.

5. Conclusion

The present study demonstrated that patients with a history of NMSC had a statistically significant increase in plasma levels of 15-F_{2t}-isoprostane. This suggests that oxidative stress may play an important role in the pathogenesis of skin cancers. Moreover, to the authors' knowledge, this is the first demonstration that increased plasma levels of 15-F_{2t}-isoprostane are a risk factor for NMSC. The supplementary antioxidant therapy did not cause significant reduction in levels of oxidative stress biomarkers, so there is need for further evaluation of these supplements as long-term adjunctive therapy.

Conflict of Interests

The authors declare no conflict of interests.

Acknowledgments

The authors would like to thank the hospital medical staff for their support and collaboration during the research as well as São Paulo Research Foundation (FAPESP) and the National Council for Scientific and Technological Development (CNPq) (Grant no. 482958/2011-1) for financial support.

References

[1] G. L. Milne, H. Yin, and J. D. Morrow, "Human biochemistry of the isoprostane pathway," *The Journal of Biological Chemistry*, vol. 283, no. 23, pp. 15533–15537, 2008.

[2] P. Montuschi, P. J. Barnes, and L. J. Roberts II, "Isoprostanes: markers and mediators of oxidative stress," *The FASEB Journal*, vol. 18, no. 15, pp. 1791–1800, 2004.

[3] B. Halliwell and M. Grootveld, "The measurement of free radical reactions in humans. Some thoughts for future experimentation," *FEBS Letters*, vol. 213, no. 1, pp. 9–14, 1987.

[4] D. R. Bickers and M. Athar, "Oxidative stress in the pathogenesis of skin disease," *Journal of Investigative Dermatology*, vol. 126, no. 12, pp. 2565–2575, 2006.

[5] H. W. Rogers, M. A. Weinstock, A. R. Harris et al., "Incidence estimate of nonmelanoma skin cancer in the United States, 2006," *Archives of Dermatology*, vol. 146, no. 3, pp. 283–287, 2010.

[6] J. D'Orazio, S. Jarrett, A. Amaro-Ortiz, and T. Scott, "UV radiation and the skin," *International Journal of Molecular Sciences*, vol. 14, no. 6, pp. 12222–12248, 2013.

[7] F. L. Meyskens Jr., P. Farmer, and J. P. Fruehauf, "Redox regulation in human melanocytes and melanoma," *Pigment Cell Research*, vol. 14, no. 3, pp. 148–154, 2001.

[8] M. Athar, "Oxidative stress and experimental carcinogenesis," *Indian Journal of Experimental Biology*, vol. 40, no. 6, pp. 656–667, 2002.

[9] Institute of Medicine, *DRIs—Dietary Reference Intakes for Vitamin C, Vitamin E, Selenium and Carotenoids*, Institute of Medicine, National Academy Press, 2000.

[10] Institute of Medicine, *DRIs—Dietary Reference Intakes for Vitamin A, Vitamin K, Arsenic, Boron, Chromium, Cooper, Iodine, Iron, Manganese, Molybdenum, Nickel, Silicon, Vanadium, and Zinc*, National Academy Press, Washington, DC, USA, 2002.

[11] D. M. Attia, R. Goldschmeding, M. A. Attia, P. Boer, H. A. Koomans, and J. A. Joles, "Male gender increases sensitivity to renal injury in response to cholesterol loading," *The American Journal of Physiology—Renal Physiology*, vol. 284, no. 4, pp. F718–F726, 2003.

[12] E. Tatsch, G. V. Bochi, R. Da Silva Pereira, H. Kober, J. R. De Oliveira, and R. N. Moresco, "Effects of anticoagulants and storage temperature on blood nitrite levels," *Brazilian Journal of Pathology and Laboratorial Medicine*, vol. 47, no. 2, pp. 147–150, 2011.

[13] A. N. Bhatt, R. Mathur, A. Farooque, A. Verma, and B. S. Dwarakanath, "Cancer biomarkers—current perspectives," *Indian Journal of Medical Research*, vol. 132, no. 8, pp. 129–149, 2010.

[14] M. Janicka, A. Kot-Wasik, J. Kot, and J. Namieśnik, "Isoprostanes-biomarkers of lipid peroxidation: their utility in evaluating oxidative stress and analysis," *International Journal of Molecular Sciences*, vol. 11, no. 11, pp. 4631–4659, 2010.

[15] B. Piłacik, T. W. Nofer, and W. Wąsowicz, "F2-isoprostanes biomarkers of lipid peroxidation: their utility in evaluation of oxidative stress induced by toxic agents," *International Journal of Occupational Medicine and Environmental Health*, vol. 15, no. 1, pp. 19–27, 2002.

[16] P. Montuschi, P. Barnes, and L. J. Roberts II, "Insights into oxidative stress: the isoprostanes," *Current Medicinal Chemistry*, vol. 14, no. 6, pp. 703–717, 2007.

[17] D. A. Barocas, S. Motley, M. S. Cookson et al., "Oxidative stress measured by urine F2-isoprostane level is associated with prostate cancer," *Journal of Urology*, vol. 185, no. 6, pp. 2102–2107, 2011.

[18] P. Rossner Jr., M. D. Gammon, M. B. Terry et al., "Relationship between urinary 15-F_{2t}-isoprostane and 8-oxodeoxyguanosine levels and breast cancer risk," *Cancer Epidemiology Biomarkers and Prevention*, vol. 15, no. 4, pp. 639–644, 2006.

[19] R. Belli, P. Amerio, L. Brunetti et al., "Elevated 8-isoprostane levels in basal cell carcinoma and in UVA irradiated skin," *International Journal of Immunopathology and Pharmacology*, vol. 18, no. 3, pp. 497–502, 2005.

[20] D. Praticò, V. M.-Y. Lee, J. Q. Trojanowski, J. Rokach, and G. A. Fitzgerald, "Increased F2-isoprostanes in Alzheimer's disease: evidence for enhanced lipid peroxidation *in vivo*," *The FASEB Journal*, vol. 12, no. 15, pp. 1777–1783, 1998.

[21] M. Reilly, N. Delanty, J. A. Lawson, and G. A. FitzGerald, "Modulation of oxidant stress in vivo in chronic cigarette smokers," *Circulation*, vol. 94, no. 1, pp. 19–25, 1996.

[22] G. Davi, G. Ciabattoni, A. Consoli et al., "In vivo formation of 8-iso-prostaglandin F_2 and platelet activitation in diabetes mellitus. Effects of improved metabolic control and vitamin E supplementation," *Circulation*, vol. 99, pp. 224–229, 1999.

[23] G. Davi, P. Alessandrini, A. Mezzetti et al., "*In vivo* formation of 8-epi-prostaglandin $F_{2\alpha}$ is increased in hypercholesterolemia," *Arteriosclerosis, Thrombosis, and Vascular Biology*, vol. 17, no. 11, pp. 3230–3235, 1997.

[24] M. Dietrich, G. Block, M. Hudes et al., "Antioxidant supplementation decreases lipid peroxidation biomarker F2-isoprostanes in plasma of smokers," *Cancer Epidemiology, Biomarkers and Prevention*, vol. 11, no. 1, pp. 7–13, 2002.

[25] R. A. Jacob, G. M. Aiello, C. B. Stephensen et al., "Moderate antioxidant supplementation has no effect on biomarkers of oxidant damage in healthy men with low fruit and vegetable intakes," *Journal of Nutrition*, vol. 133, no. 3, pp. 740–743, 2003.

[26] S. B. Murer, I. Aeberli, C. P. Braegger et al., "Antioxidant supplements reduced oxidative stress and stabilized liver function tests but did not reduce inflammation in a randomized controlled trial in obese children and adolescents," *Journal of Nutrition*, vol. 144, no. 2, pp. 193–201, 2014.

[27] L. J. Roberts II, J. A. Oates, M. F. Linton et al., "The relationship between dose of vitamin E and suppression of oxidative stress in humans," *Free Radical Biology and Medicine*, vol. 43, no. 10, pp. 1388–1393, 2007.

Hindawi Publishing Corporation
BioMed Research International
Volume 2015, Article ID 801353, 7 pages
http://dx.doi.org/10.1155/2015/801353

Review Article

Identification of Human Herpesvirus 8 Sequences in Conjunctiva Intraepithelial Neoplasia and Squamous Cell Carcinoma of Ugandan Patients

Noemy Starita,[1] Clorinda Annunziata,[1] Keith M. Waddell,[2] Luigi Buonaguro,[1] Franco M. Buonaguro,[1] and Maria Lina Tornesello[1]

[1]*Molecular Biology and Viral Oncology, Istituto Nazionale Tumori "Fondazione G Pascale", IRCCS, 80131 Naples, Italy*
[2]*Departments of Ophthalmology and Paediatrics, Mbarara University of Science and Technology, P.O. Box 1410, Mbarara, Uganda*

Correspondence should be addressed to Maria Lina Tornesello; ml.tornesello@istitutotumori.na.it

Received 22 April 2015; Revised 18 June 2015; Accepted 28 June 2015

Academic Editor: Yanjin Zhang

The incidence of squamous cell carcinoma of the conjunctiva is particularly high in sub-Saharan Africa with temporal trends similar to those of Kaposi sarcoma (KS). Human herpesvirus type 8 (HHV8), has not yet been investigated in conjunctiva tumors. In this study biopsies and PBMCs of conjunctiva neoplasia patients along with nonneoplastic conjunctiva tissues have been analyzed for HHV8 sequences by PCR targeting ORF26. All amplimers were subjected to nucleotide sequencing followed by phylogenetic analysis. HHV8 DNA has been identified in 12 out of 48 (25%) HIV-positive, and in 2 out of 24 (8.3%) HIV-negative conjunctiva neoplastic tissues and in 4 out of 33 (12.1%) PBMC samples from conjunctiva neoplasia diseased patients as well as in 4 out of 60 (6.7%) nontumor conjunctiva tissues. The viral load ranged from 1 to 400 copies/10^5 cells. Phylogenetic analysis showed that the majority of HHV8 ORF26 amplimers clustered with subtypes R ($n = 11$) and B2 ($n = 6$). This variant distribution is in agreement with that of HHV8 variants previously identified in Ugandan KS cases. The presence of HHV8 in conjunctiva tumors from HIV-positive patients warrants further studies to test whether HHV8 products released by infected cells may have paracrine effects on the growth of conjunctiva lesions.

1. Introduction

The incidence of squamous cell carcinoma of the conjunctiva (CSCC) has shown a dramatic increase in the sub-Saharan African populations during the HIV/AIDS era [1–5]. In Uganda the incidence has increased more than tenfold between 1960–1971 and 1995–1997 and has remained high during the period 1991–2010 [6]. Similarly, a 10-fold increase in the incidence of conjunctival carcinoma has been reported in Harare, Zimbabwe, during the period 1991–2004 [3]. This finding supported the hypothesis that HIV-related immune suppression could facilitate the oncogenic process of other oncogenic agents infecting the conjunctival mucosa. Several viruses have been searched in HIV-positive and HIV-negative conjunctival neoplasia, including cutaneous and mucosal human papillomaviruses [7–9], but the etiologic mechanism of such tumor remains still unclear.

Human herpesvirus type 8 (HHV8) is the causal agent of all clinical forms of Kaposi sarcoma, of two B-cell tumors, namely, primary effusion lymphoma and multicentric Castleman disease, and the recently described HHV8 inflammatory cytokine syndrome [10–14]. Kaposi sarcoma is a vascular lesion which frequently develops in mucocutaneous sites including the ocular surface [15–17]. Indeed, Kaposi sarcoma of the conjunctiva and ocular adnexa were observed in approximately 5% of HIV/AIDS patients before HAART [18].

The HHV8 encodes several homologues of human proteins, such as viral G protein-coupled receptor (vGPCR), viral interferon regulatory factors 1–4 (vIRF 1–4), viral interleukin 6 (vIL-6), viral Fas-associated death domain-like IL-1-converting enzyme inhibitory protein (vFLIP), and vBCL2 that are able to promote cell survival, immune evasion, angiogenesis, and inflammation [19]. Moreover, HHV8 vGPCR induces secretion of vascular endothelial

growth factor (VEGF), IL-6, and platelet derived growth factor (PDGF) which, together with the vIL-6 and vFLIP, deregulate via autocrine and paracrine mechanisms the proliferation and apoptosis of uninfected cells surrounding those harboring replicating virus [20, 21]. Moreover, in the HHV8 inflammatory cytokine syndrome the symptoms are associated with excess lytic activation of the virus, elevated levels of HHV8 vIL-6, IL-6, and viral loads [22].

The HHV8 has been shown to infect a variety of cells including endothelial, epithelial, and B cells as well as monocytes and CD34+ hematopoietic progenitor stem cells [23, 24]. The viral DNA has been found in normal skin, plasma, and PBMCs of a significant fraction of Kaposi sarcoma patients [25]. In Uganda, where Kaposi sarcoma is endemic, HHV8 in plasma was detected in 8.7% of the general population [26]. Among HIV-positive patients with no diagnosis of Kaposi sarcoma, HHV8 DNA has been identified in PBMCs in 13% of patients in association with lower CD4+ cell counts and higher plasma HIV RNA [27].

DNA sequences of HHV8 have been also detected in non-Kaposi skin lesions of transplant recipients, in pemphigus vulgaris and mycosis fungoides lesions, in angiosarcomas, and in angiolymphoid hyperplasia [28]. No study systematically searched for HHV8 DNA in conjunctival neoplastic lesions.

This study aimed to analyze the prevalence of HHV8 DNA in conjunctival neoplasia biopsies at different stages of malignancy, including conjunctival intraepithelial lesions grades 1 to 3 (CIN1, -2, or -3), in invasive conjunctival squamous cell carcinoma (CSCC) and in PBMCs from conjunctiva neoplasia HIV-positive and HIV-negative patients as well as in conjunctival tissues from healthy control subjects.

2. Materials and Methods

2.1. Patients and Specimens. Conjunctival biopsies from 72 patients with conjunctival neoplasia from 60 conjunctiva subjects with nonneoplastic were obtained at seven countrywide eye clinics in Southern Uganda from all subjects who gave informed consent to participate in the study. Peripheral blood mononuclear cells (PBMCs) obtained from 33 conjunctiva neoplasia patients, whose surgical biopsies were not available, were also included in the study. The study protocol was approved by the local ethical review board. All cases and controls were previously characterized in terms of histology, DNA quality, HIV serology, and cutaneous and mucosal HPV DNA positivity [7, 29]. DNA extraction was performed with similar procedures for both types of samples (frozen biopsies and PBMCs). Briefly samples were digested with proteinase K (150 μg/mL at 60°C for 30 min) in lysis buffer (10 mM Tris-HCl pH 7.6, 5 mM EDTA, 150 mM NaCl, and 1% SDS), followed by DNA purification with phenol and phenol-chloroform-isoamyl alcohol (25 : 24 : 1) extraction and ethanol precipitation in 0.3 M sodium acetate (pH 4.6).

2.2. PCR Amplification of HHV8 ORF26. The HHV8 ORF26 was amplified by nested PCR using oligoprimers and reaction conditions previously described [31, 32]. In particular, rightward ORF26 has been amplified with outer oligonucleotides LGH2574L (5′-CAGAAACAGGGCTAGGTAC-3′) and LGH2575R (5′-GTGCTTGACGATCTGTCC-3′) and with inner oligonucleotides SJF (5′-CTATCTTCAGAG-TCTCAG-3′) and SJR (5′-TAGGTACACACAATTTTG-3′); leftward ORF26 has been amplified with outer oligonucleotides LGH1701R (5′-GGATCCCTCTGACAACC-3′) and SJ2R (5′-GCCAAGATTAAATATAGAACTGAG-3′) and inner oligonucleotides LGH1701R and SJ1R (5′-AATATA-GAACTGAGACTCTGAAG-3′) (Table 1). PCR amplification reactions were performed in 50 μL reaction mixture containing 100 to 300 ng of target DNA, 5 pmol of each primer, 2.5 mM $MgCl_2$, 50 μM of each dNTP, and 5 μL Hot Master buffer and 2.5 U of Hot Master Taq DNA Polymerase (5 Prime GmbH, Hamburg, Germany). DNA was amplified in a Perkin-Elmer GeneAmp PCR System 9700 thermal cycler with the following steps: an initial 2 min denaturation at 94°C, followed by 45 amplification cycles of 55°C for 45 sec, 68°C for 1 min, 94°C for 15 sec, and a 5 min final elongation at 68°C. A reaction mixture containing genomic DNA, extracted from NIH 3T3 murine cell line, was used as negative control and was included in every set of 5 clinical specimens. All HHV8 amplimers were subjected to bidirectional direct sequencing analysis.

2.3. HHV8 Real Time PCR. A SYBR Green real time PCR method was used to determine HHV8 viral load in all DNA samples. Specially, oligoprimers ORF26LR1F1 (5′-GCAGTATCTATCCAAGTG-3′) and ORF26LR2R2 (5′-ACAGATCGTCAAGCA-3′) producing a 434 bp product were designed with Beacon Designer software (Premier Biosoft) and used for real time PCR (Table 1). HHV8 viral load quantization was performed in the Bio-Rad CFX96 real time PCR Detection System using 300 ng of template DNA, 12.5 μL of iQ SYBR Green supermix (Bio Rad), and 5 pmol each of forward and reverse primers in a final volume of 25 μL. Thermal cycling consisted of a denaturation step at 95°C for 3 min, followed by 50 cycles of 55°C annealing for 30 s, 72°C extension for 30 s, and 95°C denaturation for 30 s. A standard curve was constructed using serial dilutions (1.0 to 10^7 copies of BCBL1 cell line, containing 70 copies per cell of HHV8 DNA). Three replicates were performed for each sample and real time PCR data were analyzed using BioRad CFX manager software. The averaged copy numbers in samples were calculated according to the standard curve and were represented as copies of viral DNA per 10^5 cells. The amount of human genomic DNA in each sample was also determined by real time PCR targeting human β-globin gene (GH20, 5′-GAAGAGCCAAGGACAGGTAC-3′, and PC04, 5′-CAACTTCATCCACGTTCACC-3′) and the quantification of human β-globin gene was used to normalize the target DNA.

2.4. Nucleotide Sequencing and Phylogenetic Analysis. Aliquots of HHV8 PCR amplified products were subjected to bidirectional direct sequencing analysis by Eurofins Genomics (Milan, Italy) using the fluorescent dye terminator technology and ABI 3730 DNA sequencers (Applied BioSystems, Foster City, CA). This Sanger based technique

Table 1: PCR primer sequences used to amplify HHV8 ORF26 regions by standard PCR and real time PCR.

Method	Locus	Primer name	Sequences (5′-3′)	Nucleotide position	Size	Reference
PCR outer	ORF26-3′	LGH2575-R	GTGCTTGACGATCTGTCC	47,638–47,655	620 bp	[30]
		LGH2574-L	CAGAAACAGGGCTAGGTAC	48,239–48,257		
PCR inner	ORF26-3′	SJ-F	CTATCTTCAGAGTCTCAG	47,844–47,861	402 bp	[31]
		SJ-R	TAGGTACACACAATTTTG	48,228–48,245		
PCR outer	ORF26-5′	LGH1701R	GGATCCCTCTGACAACC	47,292–47,309		
		SJ-R2	GCCAAGATTAAATATAGAACTGAG	47,857–47,880	589 bp	[31]
PCR inner	ORF26-5′	LGH1701R	GGATCCCTCTGACAACC	47,292–47,309		
		SJ-R1	AATATAGAACTGAGACTCTGAAG	47,848–47,870	579 bp	[31]
Real time PCR	ORF26-3′	ORF26LR1F1	GCAGTATCTATCCAAGTG	47,220–47,237		
		ORF26LR2R2	ACAGATCGTCAAGCA	47,639–47,653	434 bp	This study

Nucleotide positions are given on the GenBank sequence number NC_009333.

is capable of detecting mixtures of viral variants when each variant represents >15% of the viral population. Nucleotide sequences were edited with Chromas Lite 2.01 (http://www.technelysium.com.au/chromas.html) and converted to FASTA format. Multiple sequence alignments of HHV8 sequences from the present study and reference strains reported in the GenBank were performed with clustal W tool of MegAlign program of the Lasergene software (DNASTAR Inc., V7.0.0). Reference sequences for each HHV8 ORF26 subtype were DQ984689.1 (BCBLR, A/C), DQ984768.1 (HKS15, R), DQ984785.1 (431K, B1), DQ984789.1 (021K, B2), and DQ984759.1 (HKS21, J).

2.5. Statistical Analysis. Statistical analysis was performed with Epi Info 6 Statistical Analysis System software (Version 6.04b, 1997, Centers for Disease Control and Prevention, USA). Unpaired t-test was used for comparisons of continuous variables (i.e., age); Mantel-Haenszel corrected χ^2 test and, where appropriate, two-sided Fisher's exact test were used for comparison of categorical data. Differences were considered to be statistically significant when P values were less than 0.05.

Table 2: Distribution of known variables between conjunctival neoplasia cases and controls.

	Conjunctiva neoplastic tissues $N = 72$ (%)	Conjunctiva control tissue* $N = 60$ (%)	P value
Sex			0.724
M	31 (43.1)	24 (40.0)	
F	41 (56.9)	36 (60.0)	
Age			0.584
≤30 years	31 (43.1)	23 (38.3)	
>30 years	41 (56.9)	37 (61.7)	
HHV8 PCR			0.034
Positive	14 (19.4)	4 (6.7)	
Negative	58 (80.5)	56 (93.3)	
HIV serology†			0.004
Positive	48 (66.7)	15 (38.5)	
Negative	24 (33.3)	24 (61.5)	

*Two pingueculae, 1 pterygium, and 1 papilloma of the conjunctiva were included in the control group.
†21 control subjects with undetermined HIV serology were not included.

3. Results

Overall, HHV8 DNA has been detected in 14 out of 72 (19.4%) conjunctiva neoplastic tissues and in 4 out of 60 (6.7%) control tissues (Table 2). The prevalence of HHV8 DNA was found to be significantly different between cases and controls ($P = 0.034$). Following stratification of patients by HIV status the HHV8 DNA was found in 12 out of 48 (25%) HIV-positive and in 2 out of 24 (8.3%) HIV-negative conjunctiva neoplastic tissues (Table 3). The difference in HHV8 prevalence between these two groups was of borderline significance (Fisher's exact test two-tailed $P = 0.120$), due to the limited sample size of controls with known HIV serostatus. HHV8 DNA has been identified in 4 out of 33 (12.1%) PBMC samples of conjunctiva neoplasia diseased patients, for which conjunctiva biopsies were not available. The histology of the 72 conjunctival neoplasia patients identified 24 (33.3%) lesions as invasive conjunctiva squamous carcinoma, 17 (23.6%) as conjunctiva intraepithelial neoplasia grade 3 (CIN3), 16 (22.2%) as CIN2, and 15 (20.8%) as CIN1. The frequency of HHV8 infection among cases, grouped by histological types, was 20.8% (5/24) in the CSCC, 23.5% (4/17) in the CIN3, 25% (4/16) in CIN2, and 6.7% (1/15) in CIN1. Therefore, HHV8 detection frequency seems not associated with more advanced disease stages.

To quantify HHV8 viral load in conjunctiva DNA samples, serial dilution of DNA extracted from BCBL-1 cell line (range, 1×10^0 to 1×10^6 cells) in the background of human DNA was amplified with HHV8 and human β-globin oligonucleotides by real time PCR. The estimated HHV8 copy number was 70 per BCBL-1 cell, which is in agreement with the value reported in the literature [33]. Of the 72 conjunctiva neoplasia DNA samples tested by real time PCR, 18 (25%) were positive for HHV8 DNA with viral loads ranging from 1 to 400 copies/10^5 cells in different samples.

Amplimers obtained by nested PCR from 17 DNA samples were sequenced across the rightward and leftward

Table 3: Distribution of HHV8 in HIV-positive and HIV-negative conjunctival neoplasia samples and controls.

HIV status	Conjunctiva neoplastic tissues N (%)	Conjunctiva control tissue* $N^{\dagger}$ (%)	P value
HIV positive			0.347‡
HHV8-Pos	12 (25.0)	2 (13.3)	
HHV8-Neg	36 (75.0)	13 (86.7)	
HIV negative			1.000‡
HHV8-Pos	2 (8.3)	1 (4.2)	
HHV8-Neg	22 (91.7)	23 (95.8)	

*Two pingueculae, 1 pterygium, and 1 papilloma of the conjunctiva were included in the control group.

†21 control subjects with undetermined HIV serology were not included.

‡Fisher's exact test, two-tailed.

ORF26 locus. All nucleotide differences between samples are described in Table 4. HHV8 ORF26 sequences mainly belong to B2 (10 out of 17, 58.8%), R (5 out of 17, 29.4%), B1 (1 out of 17, 5.9%), and J (1 out of 17, 5.9%) subtypes, following the nomenclature proposed by Zong et al. (2007) [30]. No multiple infections with different HHV8 variants were identified by nucleotide sequencing analysis.

4. Discussion

HHV8 has been clearly associated with proliferative disorders such as Kaposi sarcoma, primary effusion lymphoma, and multicentric Castleman's disease [10]. Several viral genes, such as v-GPCR, vIRF 1–4, vFLIP, and vIL-6, mainly expressed during the lytic phase of viral replication have been recognized as transforming factors acting through autocrine and paracrine mechanisms [21, 34]. In fact, it has been shown that in Kaposi sarcoma tumors only few HHV8 infected cells undergo lytic reactivation and express a large number of viral proteins, which in turn contribute to angiogenesis in Kaposi tumors promoting the secretion of cellular or viral factors in a paracrine manner [21]. These paracrine proangiogenic properties raise the question whether HHV8 might be implicated in the pathogenesis of vascular proliferative lesions other than Kaposi sarcoma.

In this study HHV8 sequences have been identified in 25% and 8% of HIV-positive and HIV-negative conjunctival neoplasia samples, respectively, suggesting a major effect of HIV-related immune suppression in HHV8 replication. The phylogenetic analysis of the conserved ORF26 amplimers indicated that subtypes R and B2 were the most common variants in conjunctiva samples, in agreement with previous results on HHV8 variant distribution in Ugandan Kaposi sarcoma cases [32]. Furthermore, the similar frequency rate of HHV8 positivity in invasive tumors compared to CIN2 and CIN3 lesions suggests that the virus might be involved in early phases of tumor development but is unlikely involved in tumor progression.

HHV8 loads have been evaluated in conjunctiva neoplasia samples and found to be in the range of 1 to 400 copies/10^5 cells. These values are comparable to those observed in PBMCs of HIV-related Kaposi sarcoma patients and are probably correlated to the immune status of subjects [35]. The results obtained so far are not sufficient to differentiate whether HHV8 has a direct role in the development of conjunctival carcinoma or is a bystander vehiculated by infected PBMCs in the high vascularized conjunctival lesions. However, in both cases it is possible to postulate a paracrine effect of the viral products enhancing angiogenesis and tumorigenesis in conjunctival mucosa.

The presence of HHV8 DNA has been investigated in several other disorders with controversial results. Nishimoto et al. identified HHV8 DNA sequences in a variable fraction of skin lesions such as Bowen's disease, actinic keratoses, leukoplakia, Paget's disease, melanoma, neurofibroma, and chronic dermatitis [36]. However, several other studies failed to confirm such association [37, 38].

McDonagh et al. described the presence of HHV8 DNA sequences in vascular proliferations including angiosarcomas (29%) and haemangiomas (5%) [39]. However, Lebbe et al. reported no association between HHV8 and non-Kaposi sarcoma vascular lesions in their patients [40].

More recently, few studies reported the detection of low levels of HHV8 DNA in lymphoproliferative diseases such as large-plaque parapsoriasis and mycosis fungoides [41, 42], but not confirmed in other studies [43–45]. Kreuter et al. hypothesized that this association may depend on high HHV8 seroprevalence in some geographic regions or HHV8 reactivation in immune compromised patients [42].

Moreover, Nalwoga et al. have recently shown that in Uganda, where malaria is highly endemic, the positivity for malaria antibodies is strongly associated with HHV8 seropositivity suggesting that malaria exposure may facilitate HHV8 reactivation, viral transmission, and related diseases [46].

Seroprevalence of HHV8 in Uganda is very high, ranging from 36% to 60% in the general population [47–49]. More recently high prevalence of HHV8 DNA has been detected in the plasma of HHV8 seropositive Ugandan subjects enrolled in a HIV/AIDS survey [26]. In their study, Shebl et al. found plasma viral DNA in 14% of HHV8 seropositive and 2% of HHV8 seronegative subjects suggesting that replicating virus is very common in the blood of Ugandan subjects, where HHV8 infection and Kaposi sarcoma are endemic.

This study has several limitations including the small sample size of controls with known HIV serostatus and the lack of material to evaluate HHV8 mRNA levels in conjunctiva samples. However this is the first study designed to systematically detect HHV8 DNA sequences in conjunctiva neoplasia at different grade of malignancy and the obtained results warrant further epidemiological and molecular studies.

5. Conclusions

In conclusion, HHV8 DNA sequences are detected in a significant fraction of HIV-positive conjunctival neoplasia cases from Uganda. The results obtained so far are not sufficient to determine whether HHV8 is a bystander vehiculated

Table 4: Nucleotide changes identifying distinct subgroups of HHV8 genomes within the ORF26 gene locus. Dashes indicate identities to the prototype. Absence of genetic variations relative to the references is marked with dashes, whereas presence of variant nucleotides is indicated by the nucleotide corresponding letter. An empty space indicates sequence not available. ∧ indicates nucleotide insertion; δ indicates nucleotide deletion. The numbering system conforms to that used by Tornesello et al. [32].

Sample name	73 33	98 31	10 32	35 25	08 26	12 22	13 22	13 29	14 21	15 18	17 17	20 16	49 10	45 05	56 20	66 28	69 39	94 04	17 17	12 23	25 34	59 45	02 52	16 62	25 75	ORF26 class
BCBLR	G	T	C	G	C	G	A	A	A	C	C	G	G	C	∧	G	G	G	C	C	C	G	G	T	G	A/C
HKS15		C	—	—	T	—	—	C	—	—	—	—	T	—	0	δ	δ	T	T	—	—	—	—	—	—	R
CIN3.110	—	C	—	—	T	—	—	C	—	—	—	—	T	—												R
CIN3.179	—	C	—	—	T	—	—	C	—	—	—	—	T	—												R
CIN2.136	—	C	—	—	T	—	—	C	—	—	—	—	T	—												R
CIN2.169	—	C	—	—	T	—	—	C	—	—	—	—	T	—	0	δ	δ	T	T	—	—	—	—	—	—	R
CIN1.173	—	C	—	—	T	—	—	C	—	—	—	—	T	—	0	δ	δ	T	T	—	—	—	—	—	—	R
431K		C	—	—	—	—	G	C	—	—	—	—	—	—	0	T	A	—	—	T	—	C	—	C	A	B1
SCC.193	—	C	—	—	—	—	G	C	—	—	—	—	—	—	0	T	A	—	—	T	—	C	—	C	A	B1
021K		C	A	—	—	—	G	C	—	—	—	—	—	—	0	T	A	—	—	T	—	C	—	C	A	B2
SCC.108	—	C	A	—	—	—	G	C	—	—	—	—	—	—	0	T	A	—	—	T	—	C	—	C	A	B2
SCC.144	—	C	A	—	—	—	G	C	—	—	—	—	—	—												B2
SCC.218	—	C	A	—	—	—	G	C	—	—	—	—	—	—												B2
CIN3.99	—	C	A	—	—	—	G	C	—	—	—	—	—	—												B2
CIN3.167	—	C	A	—	—	—	G	C	—	—	—	—	—	—												B2
CIN2.138	—	C	A	—	—	—	G	C	—	—	—	—	—	—												B2
CIN2.143	—	C	A	—	—	—	G	C	—	—	—	—	—	—	0	T	A	—	—	T	—	C	—	C	A	B2
CTR.142	—	C	A	—	—	—	G	C	—	—	—	—	—	—												B2
CTR.143	—	C	A	—	—	—	G	C	—	—	—	—	—	—												B2
CTR.149	—	C	A	—	—	—	G	C	—	—	—	—	—	—												B2
HKS21		C	A	T	—	—	G	C	—	—		—	—	—	0	—	—	—	—	—	—	—	—	—	—	J
SCC.142	—	C	A	T	—	—	G	C	—	—	—	—	—	—												J

by infected PBMCs in the high vascularized conjunctival lesions or is able to infect cells populating the conjunctiva. Further studies are needed to determine if the expression and secretion of viral and human inflammatory factors, such as vIL6 and the human homologue, contribute to angiogenesis and tumorigenesis of conjunctival neoplasia in a paracrine fashion.

Abbreviations

HHV8: Human herpesvirus type 8
CIN: Conjunctival intraepithelial neoplasia
CSCC: Conjunctival squamous cell carcinoma
KS: Kaposi sarcoma
HIV: Human immunodeficiency virus.

Conflict of Interests

The authors declare that there is no conflict of interests regarding the publication of this paper.

Acknowledgments

The authors thank Dr. Sebastian Lucas for the histopathological characterization of all conjunctival biopsies analyzed in the study. This work was supported by grants from Ministero della Salute, Ricerca Corrente 2014 no. 2610139, and the ICSC-World Laboratory (Project MCD-2/7).

References

[1] K. M. Waddell, S. Lewallen, S. B. Lucas, C. Atenyi-Agaba, C. S. Herrington, and G. Liomba, "Carcinoma of the conjunctiva and HIV infection in Uganda and Malawi," *British Journal of Ophthalmology*, vol. 80, no. 6, pp. 503–508, 1996.

[2] M. Guech-Ongey, E. A. Engels, J. J. Goedert, R. J. Biggar, and S. M. Mbulaiteye, "Elevated risk for squamous cell carcinoma of the conjunctiva among adults with AIDS in the United States," *International Journal of Cancer*, vol. 122, no. 11, pp. 2590–2593, 2008.

[3] E. Chokunonga, M. Z. Borok, Z. M. Chirenje, A. M. Nyakabau, and D. M. Parkin, "Trends in the incidence of cancer in the

black population of Harare, Zimbabwe 1991–2010," *International Journal of Cancer*, vol. 133, no. 3, pp. 721–729, 2013.

[4] S. M. Mbulaiteye, K. Bhatia, C. Adebamowo, and A. J. Sasco, "HIV and cancer in Africa: mutual collaboration between HIV and cancer programs may provide timely research and public health data," *Infectious Agents and Cancer*, vol. 6, no. 1, article 16, 2011.

[5] S. N. Akarolo-Anthony, L. D. Maso, F. Igbinoba, S. M. Mbulaiteye, and C. A. Adebamowo, "Cancer burden among HIV-positive persons in Nigeria: preliminary findings from the Nigerian AIDS-cancer match study," *Infectious Agents and Cancer*, vol. 9, no. 1, article 1, 2014.

[6] H. R. Wabinga, S. Nambooze, P. M. Amulen, C. Okello, L. Mbus, and D. M. Parkin, "Trends in the incidence of cancer in Kampala, Uganda 1991–2010," *International Journal of Cancer*, vol. 135, no. 2, pp. 432–439, 2014.

[7] M. L. Tornesello, M. L. Duraturo, K. M. Waddell et al., "Evaluating the role of human papillomaviruses in conjunctival neoplasia," *British Journal of Cancer*, vol. 94, no. 3, pp. 446–449, 2006.

[8] C. Ateenyi-Agaba, E. Weiderpass, M. Tommasino et al., "Papillomavirus infection in the conjunctiva of individuals with and without AIDS: an autopsy series from Uganda," *Cancer Letters*, vol. 239, no. 1, pp. 98–102, 2006.

[9] C. Ateenyi-Agaba, S. Franceschi, F. Wabwire-Mangen et al., "Human papillomavirus infection and squamous cell carcinoma of the conjunctiva," *British Journal of Cancer*, vol. 102, no. 2, pp. 262–267, 2010.

[10] F. M. Buonaguro, M. L. Tornessello, L. Buonaguro et al., "Kaposi's sarcoma: aetiopathogenesis, histology and clinical features," *Journal of the European Academy of Dermatology and Venereology*, vol. 17, no. 2, pp. 138–154, 2003.

[11] Y. Chang, E. Cesarman, M. S. Pessin et al., "Identification of herpesvirus-like DNA sequences in AIDS-associated Kaposi's sarcoma," *Science*, vol. 266, no. 5192, pp. 1865–1869, 1994.

[12] E. Cesarman, Y. Chang, P. S. Moore, J. W. Said, and D. M. Knowles, "Kaposi's sarcoma-associated herpesvirus-like DNA sequences in AIDS-related body-cavity-based lymphomas," *The New England Journal of Medicine*, vol. 332, no. 18, pp. 1186–1191, 1995.

[13] J. Soulier, L. Grollet, E. Oksenhendler et al., "Kaposi's sarcoma-associated herpesvirus-like DNA sequences in multicentric Castleman's disease," *Blood*, vol. 86, no. 4, pp. 1276–1280, 1995.

[14] M. Bhutani, M. N. Polizzotto, T. S. Uldrick, and R. Yarchoan, "Kaposi sarcoma–associated herpesvirus-associated malignancies: epidemiology, pathogenesis, and advances in treatment," *Seminars in Oncology*, vol. 42, no. 2, pp. 223–246, 2015.

[15] R. A. Schwartz, G. Micali, M. R. Nasca, and L. Scuderi, "Kaposi sarcoma: a continuing conundrum," *Journal of the American Academy of Dermatology*, vol. 59, no. 2, pp. 179–206, 2008.

[16] L. Pantanowitz and B. J. Dezube, "Kaposi sarcoma in unusual locations," *BMC Cancer*, vol. 8, article 190, 2008.

[17] E. Ruocco, V. Ruocco, M. L. Tornesello, A. Gambardella, R. Wolf, and F. M. Buonaguro, "Kaposi's sarcoma: etiology and pathogenesis, inducing factors, causal associations, and treatments: facts and controversies," *Clinics in Dermatology*, vol. 31, no. 4, pp. 413–422, 2013.

[18] J. D. Shuler, G. N. Holland, S. A. Miles, B. J. Miller, and I. Grossman, "Kaposi sarcoma of the conjunctiva and eyelids associated with the acquired immunodeficiency syndrome," *Archives of Ophthalmology*, vol. 107, no. 6, pp. 858–862, 1989.

[19] E. A. Mesri, E. Cesarman, and C. Boshoff, "Kaposi's sarcoma and its associated herpesvirus," *Nature Reviews Cancer*, vol. 10, no. 10, pp. 707–719, 2010.

[20] E. A. Mesri, M. A. Feitelson, and K. Munger, "Human viral oncogenesis: a cancer hallmarks analysis," *Cell Host and Microbe*, vol. 15, no. 3, pp. 266–282, 2014.

[21] S. Gramolelli and T. F. Schulz, "The role of Kaposi sarcoma-associated herpesvirus in the pathogenesis of Kaposi sarcoma," *The Journal of Pathology*, vol. 235, no. 2, pp. 368–380, 2014.

[22] T. S. Uldrick, V. Wang, D. O'Mahony et al., "An interleukin-6-related systemic inflammatory syndrome in patients co-infected with kaposi sarcoma-associated herpesvirus and HIV but without Multicentric Castleman disease," *Clinical Infectious Diseases*, vol. 51, no. 3, pp. 350–358, 2010.

[23] W. Wu, J. Vieira, N. Fiore et al., "KSHV/HHV-8 infection of human hematopoietic progenitor (CD34+) cells: persistence of infection during hematopoiesis in vitro and in vivo," *Blood*, vol. 108, no. 1, pp. 141–151, 2006.

[24] B. Chandran, "Early events in Kaposi's sarcoma-associated herpesvirus infection of target cells," *Journal of Virology*, vol. 84, no. 5, pp. 2188–2199, 2010.

[25] M. Corbellino, L. Poirel, G. Bestetti et al., "Restricted tissue distribution of extralesional Kaposi's sarcoma-associated herpesvirus-like DNA sequences in AIDS patients with Kaposi's sarcoma," *AIDS Research and Human Retroviruses*, vol. 12, no. 8, pp. 651–657, 1996.

[26] F. M. Shebl, B. Emmanuel, L. Bunts et al., "Population-based assessment of kaposi sarcoma-associated herpesvirus DNA in plasma among Ugandans," *Journal of Medical Virology*, vol. 85, no. 9, pp. 1602–1610, 2013.

[27] J. Min and D. A. Katzenstein, "Detection of Kaposi's sarcoma-associated herpesvirus in peripheral blood cells in human immunodeficiency virus infection: association with Kaposi's sarcoma, CD4 cell count, and HIV RNA levels," *AIDS Research and Human Retroviruses*, vol. 15, no. 1, pp. 51–55, 1999.

[28] D. V. Ablashi, L. G. Chatlynne, J. E. Whitman Jr., and E. Cesarman, "Spectrum of Kaposi's sarcoma-associated herpesvirus, or human herpesvirus 8, diseases," *Clinical Microbiology Reviews*, vol. 15, no. 3, pp. 439–464, 2002.

[29] M. L. Tornesello, K. M. Waddell, M. L. Duraturo et al., "TP53 codon 72 polymorphism and risk of conjunctival squamous cell carcinoma in Uganda," *Cancer Detection and Prevention*, vol. 29, no. 6, pp. 501–508, 2005.

[30] J.-C. Zong, H. Kajumbula, W. Boto, and G. S. Hayward, "Evaluation of global clustering patterns and strain variation over an extended ORF26 gene locus from Kaposi's sarcoma herpesvirus," *Journal of Clinical Virology*, vol. 40, no. 1, pp. 19–25, 2007.

[31] S. Jalilvand, M. L. Tornesello, F. M. Buonaguro et al., "Molecular epidemiology of human herpesvirus 8 variants in Kaposi's sarcoma from Iranian patients," *Virus Research*, vol. 163, no. 2, pp. 644–649, 2012.

[32] M. L. Tornesello, B. Biryahwaho, R. Downing et al., "Human herpesvirus type 8 variants circulating in Europe, Africa and North America in classic, endemic and epidemic Kaposi's sarcoma lesions during pre-AIDS and AIDS era," *Virology*, vol. 398, no. 2, pp. 280–289, 2010.

[33] F. Lallemand, N. Desire, W. Rozenbaum, J.-C. Nicolas, and V. Marechal, "Quantitative analysis of human herpesvirus 8 viral load using a real-time PCR assay," *Journal of Clinical Microbiology*, vol. 38, no. 4, pp. 1404–1408, 2000.

[34] Y. B. Choi and J. Nicholas, "Autocrine and paracrine promotion of cell survival and virus replication by human herpesvirus 8 chemokines," *Journal of Virology*, vol. 82, no. 13, pp. 6501–6513, 2008.

[35] A.-G. Marcelin, I. Gorin, P. Morand et al., "Quantification of Kaposi's sarcoma-associated herpesvirus in blood, oral mucosa, and saliva in patients with Kaposi's sarcoma," *AIDS Research and Human Retroviruses*, vol. 20, no. 7, pp. 704–708, 2004.

[36] S. Nishimoto, R. Inagi, K. Yamanishi, K. Hosokawa, M. Kakibuchi, and K. Yoshikawa, "Prevalence of human herpesvirus-8 in skin lesions," *British Journal of Dermatology*, vol. 137, no. 2, pp. 179–184, 1997.

[37] C. Boshoff, S. Talbot, M. Kennedy, J. O'Leary, T. Schulz, and Y. Chang, "HHV8 and skin cancers in immunosuppressed patients," *The Lancet*, vol. 347, no. 8997, pp. 338–339, 1996.

[38] S. Kohler, O. W. Kamel, P. P. Chang, and B. R. Smoller, "Absence of human herpesvirus 8 and Epstein-Barr virus genome sequences in cutaneous epithelial neoplasms arising in immunosuppressed organ-transplant patients," *Journal of Cutaneous Pathology*, vol. 24, no. 9, pp. 559–563, 1997.

[39] D. P. McDonagh, J. Liu, M. J. Gaffey, L. J. Layfield, N. Azumi, and S. T. Traweek, "Detection of Kaposi's sarcoma-associated herpesvirus-like DNA sequence in angiosarcoma," *The American Journal of Pathology*, vol. 149, no. 4, pp. 1363–1368, 1996.

[40] C. Lebbe, C. Pellet, B. Flageul et al., "Sequences of human herpesvirus 8 are not defected in various non-Kaposi sarcoma vascular lesions," *Archives of Dermatology*, vol. 133, no. 7, pp. 919–920, 1997.

[41] E. Trento, C. Castilletti, C. Ferraro et al., "Human herpesvirus 8 infection in patients with cutaneous lymphoproliferative diseases," *Archives of Dermatology*, vol. 141, no. 10, pp. 1235–1242, 2005.

[42] A. Kreuter, S. Bischoff, M. Skrygan et al., "High association of human herpesvirus 8 in large-plaque parapsoriasis and mycosis fungoides," *Archives of Dermatology*, vol. 144, no. 8, pp. 1011–1016, 2008.

[43] R. Pawson, D. Catovsky, and T. F. Schulz, "Lack of evidence of HHV-8 in mature T-cell lymphoproliferative disorders," *The Lancet*, vol. 348, no. 9039, pp. 1450–1451, 1996.

[44] E. Nagore, E. Ledesma, C. Collado, V. Oliver, A. Pérez-Pérez, and A. Aliaga, "Detection of Epstein-Barr virus and human herpesvirus 7 and 8 genomes in primary cutaneous T- and B-cell lymphomas," *British Journal of Dermatology*, vol. 143, no. 2, pp. 320–323, 2000.

[45] W. Kempf, M. E. Kadin, H. Kutzner et al., "Lymphomatoid papulosis and human herpesviruses—a PCR-based evaluation for the presence of human herpesvirus 6, 7 and 8 and related herpesviruses," *Journal of Cutaneous Pathology*, vol. 28, no. 1, pp. 29–33, 2001.

[46] A. Nalwoga, S. Cose, K. Wakeham et al., "Association between malaria exposure and Kaposi's sarcoma-associated herpes virus seropositivity in Uganda," *Tropical Medicine & International Health*, vol. 20, no. 5, pp. 665–672, 2015.

[47] B. Biryahwaho, S. C. Dollard, R. M. Pfeiffer et al., "Sex and geographic patterns of human herpesvirus 8 infection in a nationally representative population-based sample in Uganda," *The Journal of Infectious Diseases*, vol. 202, no. 9, pp. 1347–1353, 2010.

[48] C. Mbondji-Wonje, V. Ragupathy, S. Lee, O. Wood, B. Awazi, and I. K. Hewlett, "Seroprevalence of human herpesvirus-8 in HIV-1 infected and uninfected individuals in Cameroon," *Viruses*, vol. 5, no. 9, pp. 2253–2259, 2013.

[49] S. M. Mbulaiteye, R. J. Biggar, R. M. Pfeiffer et al., "Water, socioeconomic factors, and human herpesvirus 8 infection in Ugandan children and their mothers," *Journal of Acquired Immune Deficiency Syndromes*, vol. 38, no. 4, pp. 474–479, 2005.

Hindawi Publishing Corporation
BioMed Research International
Volume 2015, Article ID 120749, 6 pages
http://dx.doi.org/10.1155/2015/120749

Research Article

CT Perfusion Characteristics Identify Metastatic Sites in Liver

Yuan Wang,[1] Brian P. Hobbs,[1] and Chaan S. Ng[2]

[1]*Department of Biostatistics, The University of Texas MD Anderson Cancer Center, Houston, TX 77030, USA*
[2]*Department of Diagnostic Radiology, The University of Texas MD Anderson Cancer Center, Houston, TX 77030, USA*

Correspondence should be addressed to Brian P. Hobbs; bphobbs@mdanderson.org

Received 4 April 2015; Revised 29 May 2015; Accepted 7 June 2015

Academic Editor: Franco M. Buonaguro

Tissue perfusion plays a critical role in oncology because growth and migration of cancerous cells require proliferation of new blood vessels through the process of tumor angiogenesis. Computed tomography (CT) perfusion is an emerging functional imaging modality that measures tissue perfusion through dynamic CT scanning following intravenous administration of contrast medium. This noninvasive technique provides a quantitative basis for assessing tumor angiogenesis. CT perfusion has been utilized on a variety of organs including lung, prostate, liver, and brain, with promising results in cancer diagnosis, disease prognostication, prediction, and treatment monitoring. In this paper, we focus on assessing the extent to which CT perfusion characteristics can be used to discriminate liver metastases from neuroendocrine tumors from normal liver tissues. The neuroendocrine liver metastases were analyzed by distributed parameter modeling to yield tissue blood flow (BF), blood volume (BV), mean transit time (MTT), permeability (PS), and hepatic arterial fraction (HAF), for tumor and normal liver. The result reveals the potential of CT perfusion as a tool for constructing biomarkers from features of the hepatic vasculature for guiding cancer detection, prognostication, and treatment selection.

1. Introduction

Tumor angiogenesis is the process of proliferation of new blood vessel during the growth and spread of tumors. Quantification of this process provides assessment of tumor growth at early stages and can provide prognostic, predictive, and surrogate power. In general, the tumor vessels increase in density over time, and they also function abnormally. For example, tumor vessels tend to be less leaky and more easily compressed [1]. This limits the traditional morphological imaging techniques, which emphasize the quantification simply of structural information. Computed tomography (CT) perfusion is an emerging functional imaging modality that measures characteristics pertaining to the vascular perfusion of tissues. Perfusion imaging, which provides a quantitative basis for assessing vasculature heterogeneity induced by tumor angiogenesis, has much potential in cancer detection, disease prognostication, and treatment monitoring. Many other imaging technologies such as magnetic resonance (MR) imaging, ultrasound (US), and positron emission tomography (PET) are being developed to measure perfusion characteristics [2]. Compared to these techniques, CT perfusion is most widely used because it can easily be integrated into routine CT imaging without additional technical training. Moreover, the wide availability of standardized CT imaging makes CT perfusion more accessible compared with other tools.

CT perfusion has been utilized in a number of organs including prostate, colorectal, liver, head and neck, and lung [3]. By providing functional information about the microenvironment surrounding tumor tissue, CT perfusion can assist cancer diagnosis, treatment prognostication, prediction, and monitoring. It has shown promising results for diagnosing primary or metastatic tumors [4]. It also enables assessment of tumor vascularity and perfusion changes that result from chemotherapy and radiation therapy. Moreover, it has been suggested that tumors with high vascularity tend to be more aggressive and respond poorly to chemotherapy and radiation therapy [5].

In this paper, we review the CT perfusion technology and discuss its application to a case study to assess the extent to which CT perfusion characteristics can be used to

discriminate liver metastases from neuroendocrine tumors from normal liver tissues. Liver is the second most common metastatic site after lymph nodes. Early detection is the key for successful treatment of liver tumors. Currently, diagnosis and treatment monitoring of liver cancer is mostly performed using morphological imaging such as MR, CT, and US. With the introduction of molecularly targeted therapies, these approaches may not fully access tumor information. Assessment of perfusion provides functional information of the tissue microenvironment. A variety of perfusion parameters have been produced to characterize tissue perfusion. The most frequently encountered parameters are blood flow (BF), the rate of blood passing through the vasculature in a tissue region, measured in mL/min/100 g; blood volume (BV), the volume of blood that is actually flowing within the vasculature in a tissue region, measured in mL/100 g; mean transit time (MTT), the average time for blood traversing from the arterial input to the venous outlet, measured in seconds. Both BF and BV correlate with the density of microvessels. Increased number of vessels would increase BF and BV correspondingly. MTT reflects perfusion pressure in a way that higher perfusion pressure pushes blood traveling at a higher velocity and results in a shorter mean transit time. Permeability surface area product (PS) is another widely studied perfusion parameter; it is the product of permeability and the total surface area of capillary endothelium in a unit mass of tissue, measured in units of mL/min/100 g. PS is a surrogate measure of vascular leakiness and it reflects the flux of solutes from blood plasma to the interstitial space. In the study of liver, hepatic arterial fraction (HAF) is another important parameter. The liver has a dual system of blood supply from the hepatic artery and the portal vein. HAF, which is the proportion of liver blood supplied by the hepatic artery, provides a measure of liver perfusion derived from arterial rather than portal blood.

Existing studies have shown that perfusion characteristics correlate well with the presence of tumor vessels [6]. The relationship between perfusion parameters and tumor angiogenesis is complex [3, 6, 7]. The growth and spread of tumor rely heavily on proliferation of new blood vessels. The increased density of microvessels will result in increased tumor perfusion and consequently changes in the distributions of perfusion parameters [8]. Guyennon et al. [9] have demonstrated that, compared with healthy tissues, metastatic neuroendocrine tumors had significantly higher blood flow, blood volume, and permeability surface area product and significantly shorter MTT. Reiner et al. [10] have shown significantly increased hepatic arterial perfusion and decreased portal venous perfusion in colorectal cancer. Moreover, the difference in permeability of malignant and normal tissues varies with the target organ. Permeability levels for brain tumor are considerably higher, while in other organs the difference is generally lower in comparison to brain [8]. In general, tumor vessels tend to have incomplete basement membranes which lead to increased permeability and leakage space. Our study yielded statistically significant evidence to suggest that four perfusion characteristics, BF, MTT, PS, and HAF, effectively discriminate between ROIs that contain neuroendocrine metastases from sites containing healthy liver tissues.

2. Materials and Methods

The study focused on patients with neuroendocrine liver metastases who underwent CT perfusion of a target lesion in the liver, in which malignancy was determined clinically or radiologically. The study collected data between April 2007 and September 2009 on 16 patients. CT perfusion images (Figure 1) were obtained from a dual phase protocol spanning a duration of 590 seconds (s). The images were obtained with a 64-row multidetector CT scanner (VCT, GE Healthcare, Waukesha, WI). The scans were obtained in two phases: Phase 1, cine acquisition during a breath-hold, followed by Phase 2, consisting of intermittent short breath-hold helical scans. The dataset analyzed here consisted of fifty-nine 8-slice cine images temporally sampled at 0.5 s from the Phase 1 acquisition, together with eight anatomically matched images from the Phase 2 acquisition. Five perfusion characteristics were acquired: blood flow (BF), blood volume (BV), mean transit time (MTT), permeability surface area product (PS), and hepatic arterial fraction (HAF). Figure 1 illustrates the five CTp characteristics obtained for a single patient at the end of the acquisition duration. Our analysis used the average BF, BV, MTT, PS, and HAF values obtained at acquisition time 590 s, a duration that was shown to yield stable acquisition in the liver. The values of the CTp characteristics were averaged over all 8 slices of the acquired CT perfusion images. More information of the study is available in [11].

2.1. Acquisition of CT Perfusion. Typically, CT perfusion acquisition requires intravenous injection of iodinated contrast medium and repeated CT data from the target tissue. The contrast medium passes through human body within the intravascular space and the extravascular extracellular space. The tissue enhancement is proportional to the local concentration of the contrast medium at any given time. By tracking the local concentration of the contrast medium in the tissue over time, the time-intensity curve can be observed for any region of interest (ROI). The distribution of contrast medium largely reveals blood flow and perfusion. Different approaches have been developed to estimate perfusion parameters. One approach is the distributed parameter model, which uses the deconvolution of the tissue and vascular time-intensity curves [12]. For the distributed parameter model, the tissue and vascular time-intensity curves over the whole acquisition are used for calculating perfusion parameters.

The quality of the resulting perfusion data depends on the manner in which the data is acquired. When specifying an acquisition protocol, investigators must determine several factors that could affect the quality of the resultant perfusion measurements. In particular, these include duration of scan acquisition, temporal sampling frequency, and the preenhancement set point. Additionally, some imaging preprocessing, such as motion correction, may be necessary.

2.1.1. Duration of Scan. In current clinical applications of CT perfusion in liver, the durations of acquisitions vary between half a minute and 10 minutes. Reduced acquisition

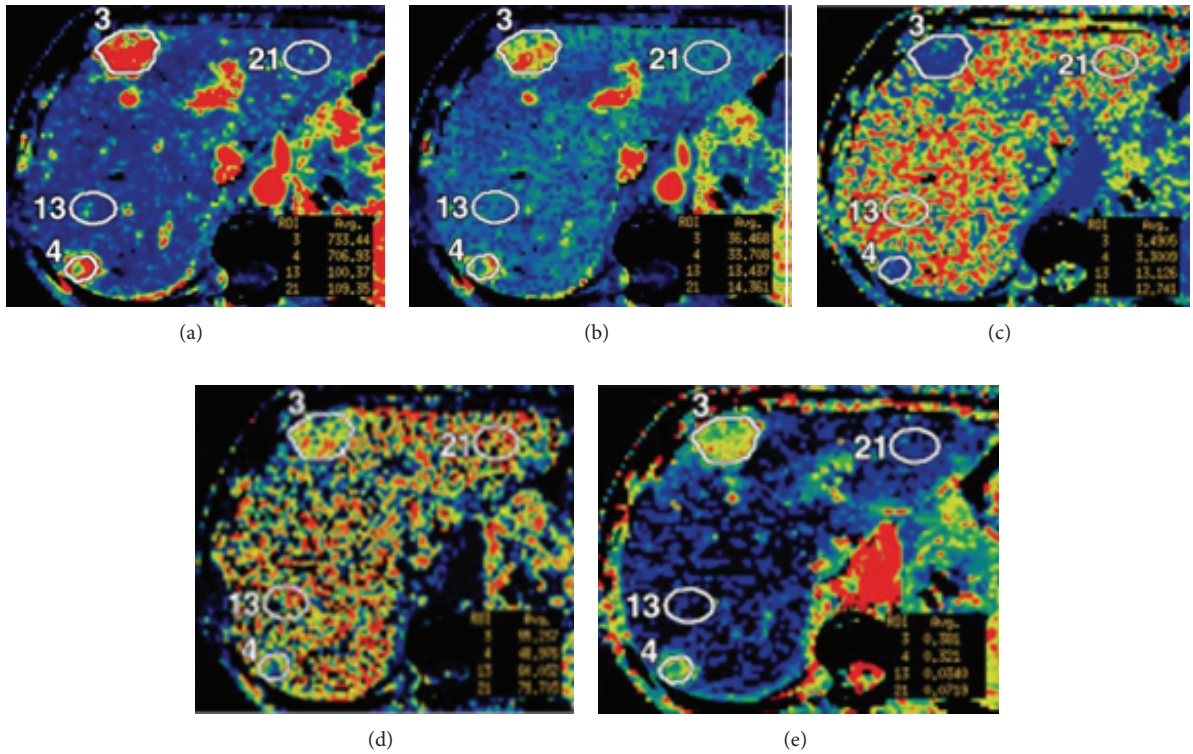

Figure 1: Maps for BF, BV, MTT, PS, and HAF at acquisition durations of 590 seconds ((a)–(e), resp.). BF is expressed in mL/min per 100 g; BV, in mL/100 g; MTT, in seconds; and PS, in mL/min per 100 g.

duration offers less radiation exposure but may compromise the quality of the CT perfusion parameter values. Ng et al. [13] have shown in a study of lung cancer that CT perfusion parameter values derived from deconvolution modeling can be markedly affected by the acquisition duration. Ng et al. [11] described that determination of appropriate and sufficiently long acquisition durations depends on the degree of confidence required for those parameters. Moreover, the results can vary depending on the specific parameter of interest. 160 s was required to obtain at least low confidence of stability for any of the CT perfusion parameters in liver. PS requires longer acquisition time when compared with BF, BV, MTT, and HAF.

2.1.2. Sampling Interval. Another factor that affects the overall radiation exposure is the frequency of CT scan, or the sampling interval (SI). The CT images are acquired at relatively high temporal sampling frequencies, typically with a temporal sampling interval of 1 second or less. The overall radiation exposure could be reduced if the temporal SI could be increased. Ng et al. [14] investigated the effect of SIs on CT perfusion parameter values in liver tumors and normal tissue and, in particular, one that implements the dual vascular (arterial and portal venous) inputs that are relevant to this particular organ. They have shown that increasing SIs beyond 1 second yielded significantly different CT perfusion parameter values when compared with the reference values at SI of 0.5 seconds.

2.1.3. Preenhancement Set Point. Perfusion parameters calculated using the distributed parameter model also depend on the input tissue and vascular time-intensity curves. The preenhancement set point (T_1), that is, the time when the arterial concentration first begins to rise, is one crucial factor in defining these time-intensity curves. This is a user-defined variable and is inevitably subject to observer variation. There have been a few studies that have investigated the potential effects of the positioning of T_1 on CT perfusion parameter values using distributed parameter modeling. Sanelli et al. [15] have shown that, in the study of brain, variations in the delineation of T_1 could lead to significant change in the resultant CT perfusion parameter values. Ng et al. [16] compared varying preenhancement displacements in a study of liver metastases and showed that the absolute values of CT perfusion parameters were affected by the positioning of T_1. Moreover, positive displacements in T_1 greater than or equal to 1.0 second were more deleterious than corresponding negative displacements, when comparing the impact on CTp values in relation to the reference.

2.2. Statistical Analysis. Receiver operating characteristics (ROCs) were computed to evaluate the extent to which perfusion characteristics acquired using CT can be used to discriminate between ROIs that contain liver metastases from those with healthy liver tissues. Univariate logistic regression analysis was implemented to estimate the extent to which the odds that given ROI contains a metastatic lesion change

Table 1: Summary of raw data by CT perfusion parameter. BF, in mL/min/100 g; BV, in mL/100 g; MTT, in seconds; PS, in mL/min/100 g; HAF, ratio without units.

Parameter	Tumor		Normal liver	
	Median	Interquartile range	Median	Interquartile range
BF	203.6	138.8–361.9	133.50	94.01–174.50
BV	16.61	9.93–23.02	14.58	11.81–18.61
MTT	6.151	5.057–7.116	8.908	7.826–9.470
PS	55.39	42.67–62.71	82.90	74.31–89.35
HAF	0.4336	0.3625–0.5360	0.21070	0.07761–0.28670

Table 2: Results of statistical analyses for association between ROI status (metastatic site versus healthy liver tissue) and perfusion parameters. p values obtained from logistic regression are provided for each characteristic as well as the corresponding AUC.

	p value	AUC
BF	0.00444	0.7407
BV	0.586	0.5793
PS	0.000475	0.9407
MTT	0.000318	0.9215
HAF	0.001201	0.9096

as function of each of the five characteristics separately. For each characteristic, two-sided Wald tests were applied to test for a trend. We report the resulting p values as well as the corresponding areas under the ROC curves (AUCs). Bonferroni correction was applied to adjust for multiple comparisons among the five comparisons. A p value of 0.01 was used to confer statistical significance. Additionally, multiple logistic regression was used to evaluate the extent to which discrimination could be improved in multivariate analysis. All plots and analyses were performed using the statistical software R 3.0.1 (R Foundation, Vienna, Austria).

3. Results

Table 1 provides summary statistics for each characteristic for metastatic tumor and normal liver ROIs. Table 2 provides the p values that result from univariate logistic regression analysis as well as the AUCs. Figure 2 shows the ROCs for classifying liver metastases from normal tissue using perfusion parameters BF, PS, MTT, and HAF, respectively. With the exception of BV, the CT perfusion characteristics were significantly associated with ROI status (tumor versus normal liver). Moreover, MTT, PS, and HAF were highly associated with the presence of a metastatic ROI, with tissues surrounding liver tumors exhibiting significantly elevated HAF and decreased MTT and PS. PS demonstrated the highest utility for discriminating ROIs with tumor from normal liver ROIs with an AUC of 0.94 on univariate analysis. The AUCs aforementioned were obtained from univariate analysis of each characteristic. Our ability to discriminate tumor from normal ROIs was improved using multivariate logistic regression analysis based on all five perfusion parameters, AUC = 0.97.

The aforementioned results and statistical models pertain to analysis of the extent of association between perfusion parameters and pathologic status. Naturally, the results for predicting metastatic sites are attenuated using these approaches. However, owing to the fact that perfusion characteristics tend to be highly correlated among ROIs within a given patient due to shared features of the hepatic vasculature, predictive detection of metastatic sites can be improved using models that account for interparameter and inter-ROI dependence. For example, increased microvessel density often leads to higher blood flow, higher blood volume, and lower MTT. Moreover, the extent of interdependence varies substantially in magnitude and direction between vasculatures surrounding malignant and healthy tissues, providing additional signal for detecting sites where angiogenesis is taking place within the tumor microenvironment. Wang et al. [17] proposed a spatial multivariate Bayesian approach to quadratic discriminant analysis that can be used to predict the status of multiple ROIs simultaneously. The multivariate model was shown to dramatically improve performance for predicting the status of liver ROIs using the perfusion characteristics acquired in our study. In fact, the simultaneous Bayesian method properly predicted the status of every ROI that contains a metastasis.

4. Discussion

Over the past two decades, the development of fast CT scanners and the improvement of analysis techniques have made CT perfusion a promising tool for quantitative analysis of tissue perfusion through features that characterize biological processes associated with tumor angiogenesis. Our study suggests that perfusion parameters obtained in liver effectively discriminate between ROIs that contain neuroendocrine metastases from sites containing healthy liver tissues. Moreover, the resulting characteristics are potentially useful for prognostication and staging, since it has been demonstrated that tumors exhibiting high vascularity tend to be more aggressive and respond poorly to chemotherapy and radiation therapy. CT perfusion also offers the potential for quantitative assessment of treatment response since it enables evaluation of tumor vascularity and perfusion changes that occur following chemotherapy and radiation therapy. This promising technology may realize its full potential as a tool for constructing biomarkers from features of the hepatic vasculature for guiding cancer detection, prognostication,

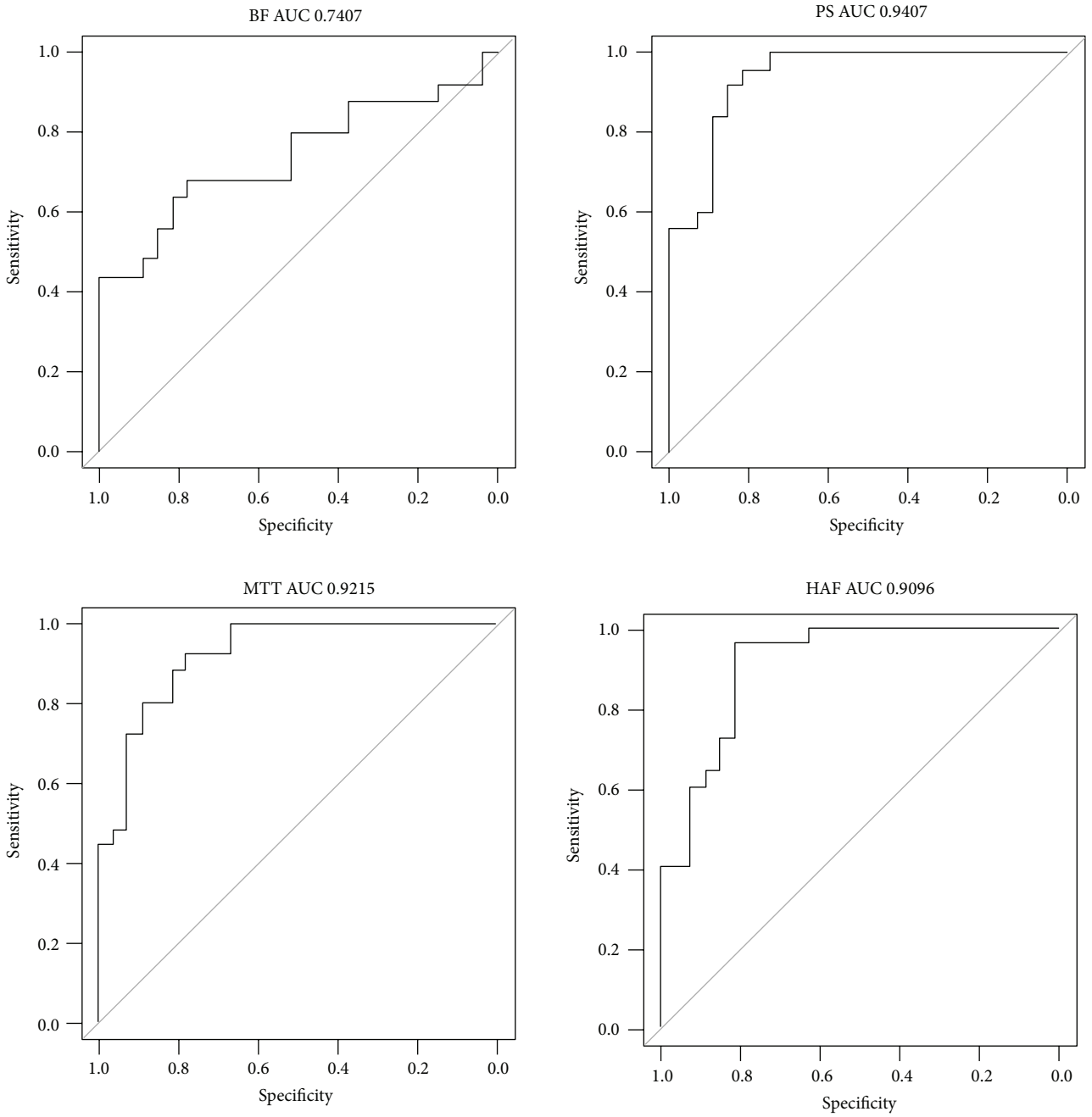

Figure 2: ROCs for classifying liver metastases from normal tissue using perfusion parameters BF, PS, MTT, and HAF with corresponding AUCs: 0.74, 0.94, 0.92, and 0.91, respectively.

and treatment selection through the implementation of multivariate models that leverage the sources of interdependence between parameters and ROIs. Additionally, multivariate modeling enhances the understanding of vascular heterogeneity.

Conflict of Interests

The authors declare that there is no conflict of interests regarding the publication of this paper.

References

[1] K. Miles, C. Charnsangavej, F. Lee, E. Fishman, K. Horton, and T.-Y. Lee, "Application of CT in the investigation of angiogenesis in oncology," *Academic Radiology*, vol. 7, no. 10, pp. 840–850, 2000.

[2] A. K. Dixon and F. J. Gilbert, "Standardising measurement of tumour vascularity by imaging: recommendations for ultrasound, computed tomography, magnetic resonance imaging and positron emission tomography," *European Radiology*, vol. 22, no. 7, pp. 1427–1429, 2012.

[3] K. A. Miles, T.-Y. Lee, V. Goh et al., "Current status and guidelines for the assessment of tumour vascular support with dynamic contrast-enhanced computed tomography," *European Radiology*, vol. 22, no. 7, pp. 1430–1441, 2012.

[4] S. Bisdas, M. Baghi, J. Wagenblast et al., "Differentiation of benign and malignant parotid tumors using deconvolution-based perfusion CT imaging: feasibility of the method and initial results," *European Journal of Radiology*, vol. 64, no. 2, pp. 258–265, 2007.

[5] D. V. Sahani, S. P. Kalva, L. M. Hamberg et al., "Assessing tumor perfusion and treatment response in rectal cancer with multisection CT: initial observations," *Radiology*, vol. 234, no. 3, pp. 785–792, 2005.

[6] S. H. Kim, A. Kamaya, and J. K. Willmann, "CT perfusion of the liver: principles and applications in oncology," *Radiology*, vol. 272, no. 2, pp. 322–344, 2014.

[7] V. Goh, S. Halligan, F. Daley, D. M. Wellsted, T. Guenther, and C. I. Bartram, "Colorectal tumor vascularity: quantitative assessment with multidetector CT—do tumor perfusion measurements reflect angiogenesis?" *Radiology*, vol. 249, no. 2, pp. 510–517, 2008.

[8] K. A. Miles, "Functional computed tomography in oncology," *European Journal of Cancer*, vol. 38, no. 16, pp. 2079–2084, 2002.

[9] A. Guyennon, M. Mihaila, J. Palma, C. Lombard-Bohas, J. A. Chayvialle, and F. Pilleul, "Perfusion characterization of liver metastases from endocrine tumors: computed tomography perfusion," *World Journal of Radiology*, vol. 2, no. 11, pp. 449–454, 2010.

[10] C. S. Reiner, R. Goetti, I. A. Burger et al., "Liver perfusion imaging in patients with primary and metastatic liver malignancy: prospective comparison between ^{99m}Tc-MAAspect and dynamic CT perfusion," *Academic Radiology*, vol. 19, no. 5, pp. 613–621, 2012.

[11] C. S. Ng, B. P. Hobbs, A. G. Chandler et al., "Metastases to the liver from neuroendocrine tumors: effect of duration of scan acquisition on CT perfusion values," *Radiology*, vol. 269, no. 3, pp. 758–767, 2013.

[12] T. Y. Lee, "Functional CT: physiological models," *Trends in Biotechnology*, vol. 20, no. 8, pp. S3–S10, 2002.

[13] C. S. Ng, A. G. Chandler, W. Wei et al., "Effect of duration of scan acquisition on CT perfusion parameter values in primary and metastatic tumors in the lung," *European Journal of Radiology*, vol. 82, no. 10, pp. 1811–1818, 2013.

[14] C. S. Ng, B. P. Hobbs, W. Wei et al., "Effect on perfusion values of sampling interval of computed tomographic perfusion acquisitions in neuroendocrine liver metastases and normal liver," *Journal of Computer Assisted Tomography*, vol. 39, no. 3, pp. 373–382, 2015.

[15] P. C. Sanelli, M. H. Lev, J. D. Eastwood, R. G. Gonzalez, and T. Y. Lee, "The effect of varying user-selected input parameters on quantitative values in CT perfusion maps," *Academic Radiology*, vol. 11, no. 10, pp. 1085–1092, 2004.

[16] C. S. Ng, A. G. Chandler, J. C. Yao et al., "Effect of pre-enhancement set point on computed tomographic perfusion values in normal liver and metastases to the liver from neuroendocrine tumors," *Journal of Computer Assisted Tomography*, vol. 38, no. 4, pp. 526–534, 2014.

[17] Y. Wang, B. P. Hobbs, J. Hu, C. S. Ng, and K. A. Do, "Predictive classification of correlated targets with application to detection of metastatic cancer using functional CT imaging," *Biometrics*, 2015.

Hindawi Publishing Corporation
BioMed Research International
Volume 2015, Article ID 490531, 16 pages
http://dx.doi.org/10.1155/2015/490531

Review Article

Glycosylation-Based Serum Biomarkers for Cancer Diagnostics and Prognostics

Alan Kirwan,[1] Marta Utratna,[1] Michael E. O'Dwyer,[2] Lokesh Joshi,[1] and Michelle Kilcoyne[1,3]

[1]*Glycoscience Group, National Centre for Biomedical Engineering Science, National University of Ireland Galway, Galway, Ireland*
[2]*Department of Hematology, National University of Ireland Galway, Galway, Ireland*
[3]*Carbohydrate Signalling Group, Microbiology, School of Natural Sciences, National University of Ireland Galway, Galway, Ireland*

Correspondence should be addressed to Michelle Kilcoyne; michelle.kilcoyne@nuigalway.ie

Received 2 April 2015; Revised 28 May 2015; Accepted 31 May 2015

Academic Editor: Maria Lina Tornesello

Cancer is the second most common cause of death in developed countries with approximately 14 million newly diagnosed individuals and over 6 million cancer-related deaths in 2012. Many cancers are discovered at a more advanced stage but better survival rates are correlated with earlier detection. Current clinically approved cancer biomarkers are most effective when applied to patients with widespread cancer. Single biomarkers with satisfactory sensitivity and specificity have not been identified for the most common cancers and some biomarkers are ineffective for the detection of early stage cancers. Thus, novel biomarkers with better diagnostic and prognostic performance are required. Aberrant protein glycosylation is well known hallmark of cancer and represents a promising source of potential biomarkers. Glycoproteins enter circulation from tissues or blood cells through active secretion or leakage and patient serum is an attractive option as a source for biomarkers from a clinical and diagnostic perspective. A plethora of technical approaches have been developed to address the challenges of glycosylation structure detection and determination. This review summarises currently utilised glycoprotein biomarkers and novel glycosylation-based biomarkers from the serum glycoproteome under investigation as cancer diagnostics and for monitoring and prognostics and includes details of recent high throughput and other emerging glycoanalytical techniques.

1. Introduction

Cancer is the second most common cause of death in developed countries. According to a survey of worldwide cancer rates, there were approximately 14 million newly diagnosed cases and estimated 6,234,000 cancer-related deaths in 2012 [1]. The most commonly diagnosed and leading causes of cancer-related deaths worldwide are malignancies of the lung, bronchus, and trachea in males and breast cancers in females (Figure 1).

Due to a lack of early symptoms and a hesitation to seek medical investigation, many cancer cases are discovered late, when the disease is at a relatively advanced stage. Survival rate is strongly correlated with the stage at which the disease is diagnosed. The early detection of the disease and the development of minimally invasive screening methods that have wide patient acceptability is the most promising approach for improving the long-term survival of cancer patients.

Recent advances in molecular biology tools and computational methods have enabled the identification of novel cancer biomarkers. Biomarkers are currently used as a complementary strategy to imaging or histopathology techniques and aim to provide minimally invasive and source-effective information which can be prognostic and predictive [2].

The current clinically approved cancer biomarkers have greatest value when applied to patients with widespread cancer. However, despite years of effort and a plethora of publications suggesting novel screening tools, single biomarkers with satisfactory sensitivity (ability to detect individuals with the disease) and specificity (ability to distinguish individuals with the disease from those that are either normal or have some other condition) have not been identified for the most common cancers [3]. This is possibly due to the molecular

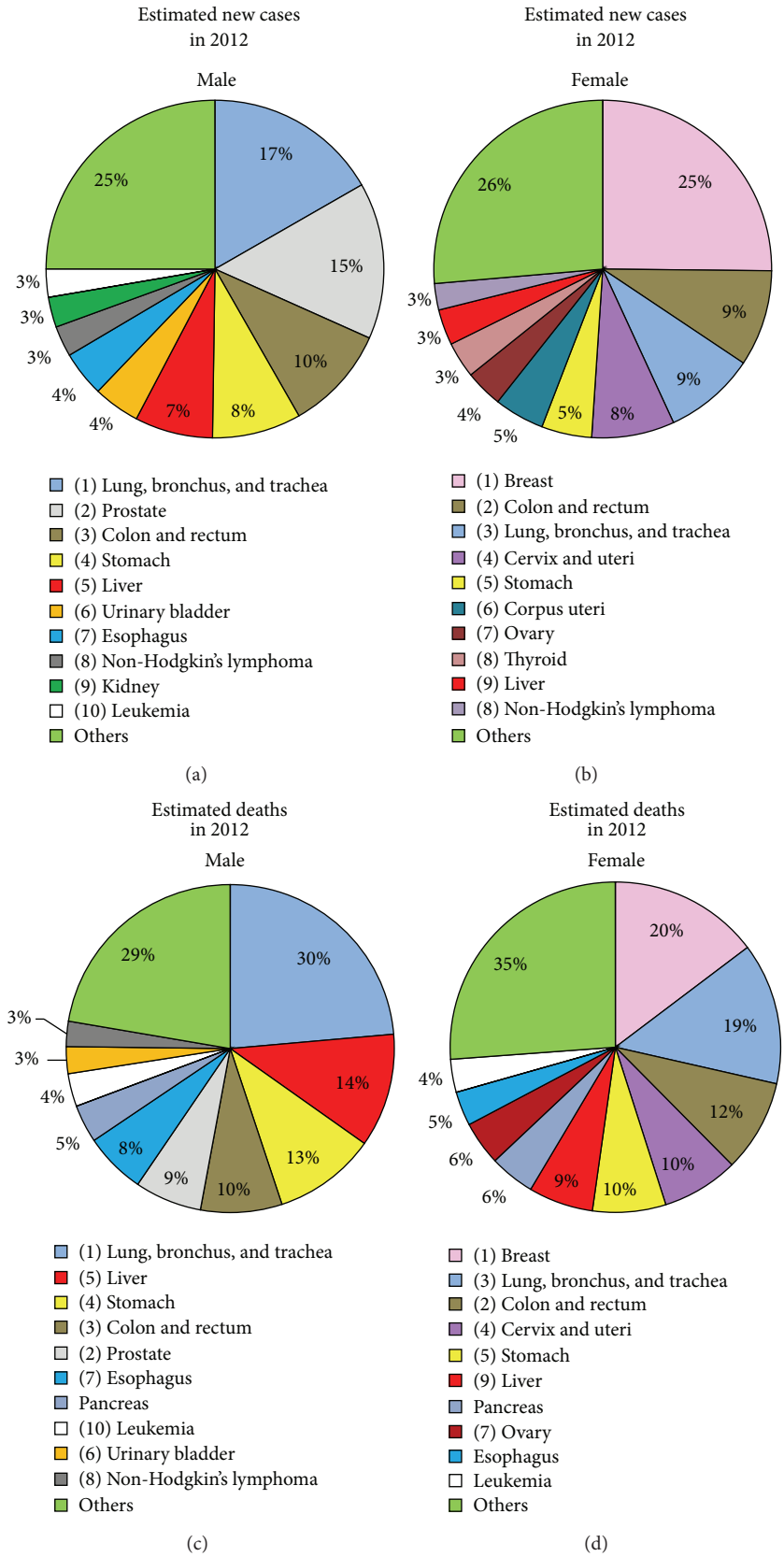

Figure 1: Global cancer statistics. Based on data for 2012 from Torre et al., 2015 [1]. (a) and (b) depict the top 10 most frequently diagnosed types of cancer as a percentage of all detected ones. (c) and (d) represent the top 10 causes of death with each type as a percentage of all cancer-related deaths.

Table 1: List of FDA-approved cancer biomarkers currently used in clinical practice.

Marker	Full name	Cancer types	Detection type	Clinical applications	Year of FDA approval
AFP	α-Fetoprotein	Liver	Protein concentrations and core fucosylation (for AFP-L3)	Diagnosis, staging, detecting recurrence, and monitoring therapy	1992/2008
PSA, Pro2PSA	Prostate-specific antigen	Prostate	Protein concentrations	Screening, discriminating cancer from benign disease	1986/1994/2012
CA125 (MUC16)	Cancer antigen 125	Ovarian	Protein concentrations	Monitoring therapy, detecting recurrence	1997/2011
HE4 (WFDC2)	Human epididymis protein 4	Ovarian	Protein concentrations	Monitoring therapy, detecting recurrence	2008
OVA1 test (multiple proteins)	β-2 Microglobulin + CA 125II (up), apolipoprotein A1 + prealbumin + transferrin (down)	Ovarian	Protein concentrations	Prediction	2009
ROMA test	HE4 + CA125	Ovarian	Protein concentrations	Prediction	2011
CA15-3 (MUC1)	Cancer antigen 15-3	Breast	Sialylated *O*-linked oligosaccharide on MUC1	Monitoring therapy	1997
CA27-29	Cancer antigen 27-29	Breast	MUC1 protein levels	Monitoring therapy	2002
CA19-9	Carbohydrate antigen 19-9 or cancer antigen 19-9	Pancreatic, ovarian	SLe[a] on mucin glycoproteins and gangliosides	Monitoring therapy	2002
CEA	Carcinoembryonic antigen	Colon, gastric, pancreatic, lung, and breast	Protein concentrations	Monitoring therapy, detecting recurrence	1985
HER2/neu	Human epidermal growth factor receptor 2	Breast	Protein concentrations	Therapy choice	1998
Tg	Thyroglobulin	Thyroid	Protein concentrations	Monitoring therapy	1997
hCG	Human chorionic gonadotropin	Testicular, ovarian	Protein concentrations	Diagnosis, staging, detecting recurrence, and monitoring therapy	Not approved

heterogeneity of tumours from patient to patient and the fact that an individual organ can contain a tumour of several stages in the same tissue [4]. Moreover, the majority of cancer biomarkers are elevated in benign diseases, and some biomarkers are undetectable in early stage cancers. However, in most cases extremely abnormal biomarker concentrations correlate to a poor prognosis and inform clinicians that a more aggressive treatment method is required [3]. Thus, despite their limitations, a variety of biomarkers are routinely used in clinical laboratories (Table 1) [5]. Increasing clinical technical capabilities and better characterization of existing biomarkers might contribute to the introduction of multimarker combinations with better diagnostic, monitoring, and prognostic performance and to the discovery of new candidate biomarkers.

Aberrant glycosylation of proteins is a well-known hallmark of cancer and represents a valuable source of information [6, 7]. However, in contrast to proteins and nucleic acids, biosynthesis of oligosaccharides in mammals is not template driven [8]. The structural complexity of carbohydrates underpins their wide range of biological roles and involvement in many cell-cell and cell-matrix interactions related to cancer through modulation of adhesion and cell trafficking [9]. Interestingly, the majority of the human serum proteome is made up of glycoproteins [10]. Proteins enter the circulatory system from tissues or blood cells through active secretion or leakage, including necrotic and apoptotic processes. Thus, carbohydrate structures of great complexity fluctuate in response to multiple stimuli reflecting the physiological and pathological state of the organism. Serum, with its ease of accessibility from the peripheral blood and reduced risk to the patient due to the minimally invasive nature of harvesting, is an attractive option from a clinical and diagnostic perspective [2].

Many technical approaches have been undertaken to describe glycosylation changes associated with cellular conditions and to address the challenges of carbohydrate structure detection and determination [11–16]. In many cases, specific cancer-associated carbohydrate alterations (reviewed elsewhere [6, 17]) can be detected using the separation of oligosaccharides released from glycoproteins by hydrophilic-interaction chromatography (HILIC) high performance liquid chromatography (HPLC), capillary electrophoresis (CE), and mass spectrometry (MS). Monoclonal antibodies and

Table 2: Clinical trials using blood/plasma or serum carbohydrate analysis to diagnose and monitor cancer. Information on recent clinical trials (https://clinicaltrials.gov/) that involve analysis of glycosylation-based biomarkers in blood components to monitor and diagnose various cancers. *Status of trials was correct at time of submission (April 2015).

Trial title	Description of trial	Status*	Clinicaltrials.gov identifier
Glycoprotein and Glycan in Patients with Stage I, Stage II, and Stage III or Stage IV Cervical Cancer Undergoing Surgery to Remove Pelvic and Abdominal Lymph Nodes	Studying samples of tumor tissue and blood from patients to identify cancer biomarkers; the current primary objectives of this study are to detect the presence of T-synthase or COSMIC. Measuring the level of staining for Tn and STn antigens as well as measuring the differences in expression of 50 different genes on a customized glycogen array and differences in 10 carbohydrate structures using a customized glycan array.	Study is ongoing but not recruiting	NCT00460356
The Association between Alpha 1 Acid Glycoprotein Level and Outcome Metastatic Cancer Treated with Docetaxel	The association between the baseline plasma level of alpha 1 acid glycoprotein and progression-free survival of docetaxel based therapies in patients with metastatic nonsmall cell lung carcinoma, breast cancer, gastric cancer, prostate cancer, and bladder cancer.	Study is not yet open for participant recruitment	NCT00897962
Blood Glycan Biomarkers in Women with Stage IV Breast Cancer	Profiling serum glycan biomarkers in patients with metastatic breast cancer, healthy controls, and patients with noncancer medical illness.	Study is active but no longer recruiting	NCT00897962
Glycan Analysis in Diagnosing Cancer in Women with Ovarian Epithelial Cancer and in Healthy Female Analysis	Comparison of a new assay to the standard CA125 assay.	Study is currently recruiting participants	NCT00628654

lectins, carbohydrate-binding proteins which are highly specific for various carbohydrate moieties [18], are also commonly employed for the detection of abnormal structures and the proportion of alterations can be quantified [14, 19–21].

The aim of this review is to summarise the current status and the potential for contribution of the serum glycoproteome to cancer diagnostics, monitoring, and prognostics. Glycosylation-based cancer biomarkers which have crossed the boundary from the laboratory into routine clinical use (Table 1) and those which are under development (Table 2), together with the most recent advantages of high throughput (HTP) and other emerging analytical techniques, are described.

2. Clinically Approved Biomarkers

2.1. α-Fetoprotein (AFP). The presence of α-fetoprotein (AFP), a glycoprotein of approximately 70 kDa, was initially reported in the serum of the human fetus in 1956 [22]. AFP is mainly produced by the yolk sac and the fetal liver, reaching its maximum concentration of 3–5 × 10^6 μg/L at the end of the first trimester [23]. The concentration of AFP in fetal serum decreases to approximately 1–20 × 10^5 μg/L at term and rapidly declines after birth to adult reference values (0.5–15 μg/L) reached at 2 years of age. Elevated concentrations of AFP also appear in maternal serum during pregnancy and peak at about weeks 30–32 of gestation (200–300 μg/L). Under certain pathological conditions, the expression of AFP is elevated and high serum concentrations are usually an indication of underlying diseases, including hepatocellular carcinoma (HCC), pancreatic and gastrointestinal carcinomas, germ cell tumours of the testis, and brain tumours [24]. Despite its low specificity for individual cancer types, AFP is the best-studied serological biomarker for HCC which is the most common type of liver cancer. Liver cancer is the fifth most frequent type of cancer diagnosed in males worldwide and the second most common in terms of number of cancer-related deaths in males (Figure 1). In a systematic review which evaluated AFP concentrations at all stages of HCC [25], sensitivities of 41–65% and specificities of 80–94% were reported for a cut-off of 20 ng/mL. AFP concentrations are correlated with increased HCC tumour size but have poor sensitivity at early stages, which is insufficient for early detection of cancer [26]. However, a sensitivity of 66% was reported for early stage HCC using a lower cut-off of 10.9 ng/mL [27].

AFP has a single *N*-linked oligosaccharide with a biantennary complex-type structure which has altered terminal sialylation and core fucosylation during cancer (Figure 2). This fucosylation is detectable by the lectin *Lens culinaris* agglutinin (LCA) and increased fucosylation can be correlated with HCC progression [28]. Due to the limitation of AFP concentration for early detection of HCC, the proportion of the LCA-reactive fraction of AFP (AFP-L3) compared to total AFP has been proposed as an improved biomarker [12, 29]. With a 10% cut-off for AFP-L3/AFP, a specificity of 90% and sensitivity of 60% for this biomarker were achieved for all stages of HCC, for those patients with AFP concentrations exceeding 10 ng/mL, including the early disease stages. The United States (U.S.) Food and Drug Administration (FDA) approved a laboratory test for AFP-L3 in 2006 for determining the risk of developing liver cancer [20]. The development of a highly sensitive assay for AFP-L3 enabled measurement in individuals with AFP

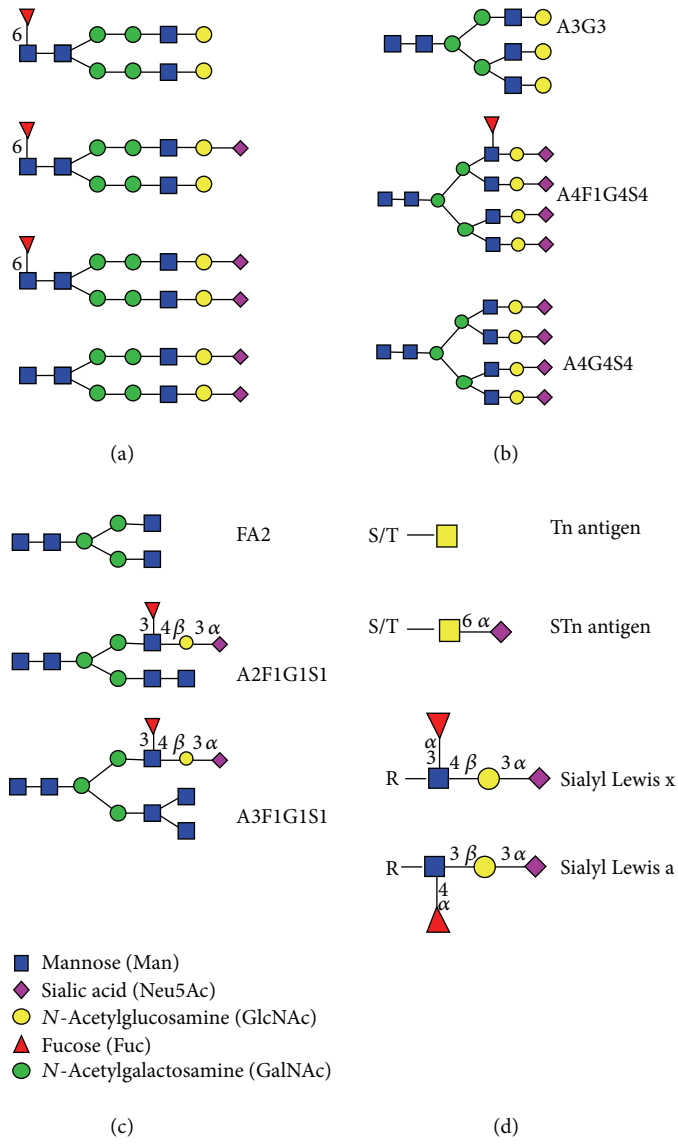

Figure 2: Altered carbohydrate structures expressed in various cancers. (a) *N*-linked oligosaccharides expressed on AFP in HCC patients, the majority of which have core fucosylation based on Johnson et al. [160]. (b) *N*-linked oligosaccharide structures which change in abundance as the cancer progresses according to Saldova et al. [41]. (c) *N*-linked oligosaccharide structures that are upregulated in lymph node metastasis positive breast cancers based on Pierce et al. [159]. (d) Tumour associated carbohydrate structures.

concentrations as low as 2 ng/mL and the accuracy of this biomarker is under further investigation [30, 31]. The activity of α-(1, 6)-fucosyltransferase was also correlated with HCC progression [32]. The addition of measuring the enzymatic activity of α-fucosidase, which specifically removes the fucose residue from the *N*-linked oligosaccharide of AFP-L3, can further increase the specificity and sensitivity for the early detection of primary HCC [33]. Coupling the use of the AFP cut-off concentration of 20 ng/mL to classify patients as AFP-positive or AFP-negative [21] with the ratio of fucosylated paraoxonase 1 to paraoxonase can be used to distinguish between HCC and liver cirrhosis (LC) with a sensitivity of 90% and a specificity of 75% in AFP-negative patients. These results were confirmed in a small cohort of patients (20 HCC, 20 LC) in which 17 patients were correctly diagnosed with HCC, providing support for the use of multiple biomarkers as a means of diagnosing early stage cancers [21].

2.2. Prostate-Specific Antigen (PSA). Prostate-specific antigen (PSA), also known as gamma-seminoprotein, kallikrein-3, and KLK3, has been widely used to screen for prostate cancer in men. Prostate cancer is the second most commonly diagnosed cancer and the fifth leading cause of cancer-related deaths in men (Figure 1). PSA is member of the kallikrein family of peptidases and is secreted by the prostate epithelium and periurethral glands. It is a 28.4 kDa glycoprotein with one *N*-linked glycosylation site and is further subcategorized into glycosylated (gp28, gp22, gp18, and gp12) or nonglycosylated (p26-full length nonglycosylated PSA, p20, p16, p10, and p6) peptides [34]. The function of PSA is to liquefy semen

in the seminal coagulum to enable sperm to swim in the ejaculate.

Disruption of the prostatic epithelium in inflammation and prostate disorders, including benign prostatic hyperplasia (BPH) and prostate cancer, causes diffusion of PSA into the tissue around the epithelium and leads to elevated concentrations of circulating PSA in these conditions. PSA is present in small quantities in the serum of men with healthy prostates (up to 2.5 ng/mL before their 40 s and around 6.5 ng/mL after 70 years of age) but concentrations above 4 ng/mL are considered indicative of prostate cancer or BPH [35]. PSA as a diagnostic by itself currently has a low specificity and has led to extensive overdiagnosis, overtreatment, and potential harm, especially from unnecessary biopsies. However, serum PSA screening in conjunction with a digital rectal exam (DRE) and Gleason scoring of prostate biopsy samples has been approved by the FDA for the early detection of prostate cancer [36, 37]. Recent approaches for improving the specificity and sensitivity of the serum PSA test include research into the individual molecular forms of PSA (proPSA, benign PSA, and intact PSA), kallikreins other than PSA, calculating the proportion of total PSA complexed with α1-chymotrypsin and α2-macroglobulin (tPSA) compared to free PSA (fPSA), comparing PSA with other markers such as prostate cancer antigen 3 (PCA3) [38] and examining PSA modifications such as glycosylation [39–41].

Several studies have reported altered fucosylation and sialylation in PSA and other proteins isolated from the serum of prostate cancer patients [42, 43]. Serum PSA contains an additional α-(2,3)-linked sialic acid to the terminal galactose residue on *N*-linked oligosaccharides in prostate cancer when compared to healthy individuals [39, 44] (Figure 2). The binding of prostate cancer-associated PSA to the α-(2,3)-linked sialic acid-recognizing lectin *Maackia amurensis* agglutinin (MAA) was more intense compared to PSA from a healthy individual [13]. Analysis of PSA by 2D electrophoresis identified five PSA glycoforms (F1, F2, F3, F4, and F5) in prostate cancer and BPH sera [40]. The F5 glycoform was nonglycosylated and the F4 glycoform had a lower degree of sialylation compared to the F1–F3 glycoforms. The *N*-linked oligosaccharides on the most abundant PSA glycoform F3 had a greater proportion of α-(2,3)-linked sialic acid and a decrease in core fucosylation in prostate cancer (Figure 2). The relative percentage of F3 (%F3) compared to all glycoforms (F1–F5) negatively correlated with the stage of prostate cancer while the relative percentages of the F4 (%F4) glycoform, which contained monosialylated *N*-linked oligosaccharides (Figure 2), were increased in prostate cancer patients [40].

Li et al. [45] showed that fucosylated PSA had better predictive power to differentiate between aggressive and nonaggressive forms of prostate cancer compared to total PSA. Yoneyama et al. [46] used a magnetic microbead-based immunoassay and a free serum PSA glycoform that terminates in α-(2,3)-linked sialic acid to develop a more sensitive diagnostic PSA assay. The novel assay has a sensitivity of 90.2% and a specificity of 64.2% when used on a cohort of patients with (n = 138) and without (n = 176) prostate cancer. This method was more sensitive and accurate than either PSA alone or percentage of fPSA in diagnosing prostate cancer in these patients.

Routine differentiation between prostate cancer and BPH is far from clear-cut and on-going research concentrates on the altered microheterogeneity of each PSA glycoform to distinguish between the two conditions [47, 48].

2.3. MUC16 (CA125). MUC16, initially named cancer antigen 125 (CA125), was first described as a biomarker in a screen of monoclonal antibodies developed against the OVCA433 ovarian cancer cell line [49]. MUC16 is a membrane-spanning mucin and the largest mucin known to date. It has a molecular mass as high as 2×10^6 Da [50, 51]. MUC16 is expressed by the various normal epithelial cells of the human body, including bronchial, endometrial, ovarian, and corneal. MUC16 protects the cells and sheds its extracellular portion into the bloodstream. Soon after its discovery, MUC16 was established as a serum biomarker for diagnosing and monitoring stability or progression in ovarian cancer [52]. However, observations of other conditions including nongynecological cancers and benign conditions such as endometriosis, as well as individuals during menstruation and pregnancy, reported elevated MUC16 serum concentrations [53]. Despite being nonspecific and unreliable for diagnosing early stage ovarian cancer, monitoring serum MUC16 together with ultrasonography is a standard procedure for detection of ovarian malignancies [54].

Several studies have reported attempts to use MUC16 glycoforms to discriminate between endometriosis and ovarian cancer and to evaluate the clinical stage, cytological grade, and histological type of ovarian cancer [55–57]. Varying concentrations of sialyl-Tn antigen (STn, Neu5Ac-α-(2,6)-GalNAc-α-*O*-Ser/Thr) were expressed in MUC16-enriched fractions from the peritoneal fluid of patients with endometriosis and ovarian cancer [55]. A lectin microarray analysis of selected carbohydrate structures, including STn and Tn (GalNAc-α-*O*-Ser/Thr) (Figure 2), on MUC16 and MUC1 (CA15-3) was able to distinguish benign ovarian neoplasms from invasive epithelial ovarian/tubule cancer with a specificity of 61.1% and 90% sensitivity [56]. This HTP method is a promising approach for differential diagnosis and requires further investigation in other cancers.

2.4. Human Epididymis Protein 4 (HE4). Human epididymis protein 4 (HE4, also known as WFDC2) was first identified in differential cDNA screening of human epididymal tissue [58, 59]. HE4 is a small (23–27 kDa), secretory protein with hydrophobic amino acids at the N-terminus consistent with a signal peptide which cleaves to yield a mature secretory polypeptide with a consensus site for *N*-linked glycosylation at amino acid position 15. HE4 contains two whey acidic protein (WAP) domains characterized by a four-disulfide core arrangement of 50 amino acids, including eight cysteines. Based on gene expression data, the HE4 gene is one of the most frequently upregulated genes in epithelial ovarian carcinomas [60, 61]. HE4 has also been shown to be expressed and secreted as a glycoprotein by ovarian carcinoma cells [62]. Moreover, HE4 expression is lower than MUC16 in benign gynecological conditions

and low-malignant potential tumours and HE4 is found in a fraction of endometrial and ovarian cancers which are deficient for MUC16 expression.

In June 2008, the HE4 enzyme immunoassay (EIA) test kit (Fujirebio Diagnostics, Sweden) and, in March 2010, the ARCHITECT HE4 automated version (Abbott Diagnostics, UK) were approved by the FDA as substantially equivalent to a MUC16 assay for ovarian cancer. The HE4 EIA is a solid-phase, noncompetitive immunoassay based on the direct sandwich technique, which measures concentrations between 15 pM and 900 pM [63]. The most recent review of the performance of the HE4 and MUC16 in multiple studies concluded that HE4 exhibits a significantly higher specificity than MUC16 (93% *versus* 78%, resp.) and outperforms MUC16 in identifying patients with early stage ovarian cancer [64]. In September 2011, the FDA approved the combination of the HE4 test with the MUC16 test in the Risk of Ovarian Malignancy Algorithm (ROMA) test, to determine the likelihood of finding malignancy at surgery in premenopausal or postmenopausal women presenting with an ovarian adnexal mass [65, 66]. A study involving 349 female patients with pelvic masses and with different menopausal status confirmed that the ROMA test outperforms the individual biomarkers in their ability to detect both early and late stage ovarian cancers, and this reached statistical significance in postmenopausal women [67].

Despite the fact that HE4 was shown to be glycosylated [62, 68], there has only been limited studies addressing the role of glycosylation for HE4 function [69] and none on the diagnostic or prognostic capability of different glycoforms. Further studies of HE4 glycoforms may lead to insights in to the occurrence, development, or migration of cancerous cells and facilitate early diagnosis or improve the therapeutic options in ovarian cancer.

2.5. MUC1 (CA15-3/CA27.29). MUC1, also known as cancer antigen 15-3 (CA15-3), MAM6, milk mucin antigen, and CA27.29 [70], is a transmembrane mucin expressed by most glandular epithelial cells as a high molecular mass glycoprotein which is heavily substituted with *O*-linked oligosaccharides. It was first identified in human milk, where it is shed from lactating mammary epithelial cells which surround the fat globules [71, 72]. MUC1 was identified on the surface of many types of cancer cells, for example, breast and ovarian, lung, pancreatic, and prostate cancers [70]. It is shed into the blood stream where it can be found in the serum of cancer patients in considerable amounts by certain therapeutic antibodies. To date, multiple monoclonal antibodies, recognizing different portions of the molecule, have been developed against the mucinous antigens of MUC1 [73–75]. Thus, in many publications, the terms CA15-3- and CA27.29-targeting epitopes of MUC1 protein are used interchangeably. Despite the lack of specificity, MUC1-directed assays in combination with other serum biomarkers are routinely used in the complex diagnosis of breast cancer [76]. The anti-CA27.29 monoclonal antibody developed against one of the MUC-1-associated epitopes binds to an eight-amino-acid sequence that partially overlaps the antigen binding site for the DF3 antibody [77]. Thus, it provides comparable results to the first results reported in MUC1 tests assessed by anti-CA15-3 radioimmunoassay [74, 77]. However, serum monitoring with the CA27.29 antibody cannot distinguish stage I from stage II patients and CA27.29 monitoring is primarily used in metastatic breast cancer to detect treatment failure in the absence of readily measurable disease [74].

The altered glycosylation of serum MUC1 in breast cancer is another possibility for the early diagnosis of breast cancer. MUC1 in breast malignancies is more heavily glycosylated in comparison to MUC1 from a healthy tissue and MUC1 peptide fragments bearing aberrant *O*-linked oligosaccharides are secreted from epithelial cell surfaces to serum [78]. The *O*-linked oligosaccharides on the MUC1 shed in to serum of an advanced breast cancer (ABC) patients were analysed by HPLC [79]. Mucin type core 1 *O*-linked oligosaccharide structures dominated (83%) over core 2 structures (17%) and the majority of structures had high levels of sialylation. Additionally, truncated structures of MUC1 are observed on tumor cells with short, often prematurely sialylated side chains of oligosaccharides, including the Thomsen-Friedenreich antigen (T antigen), its precursor (Tn antigen), and their respective sialylated derivatives STn and α-(2,6)-sialylated T antigen (Figure 2). Because MUC1 antigen is abundantly expressed and aberrantly glycosylated in carcinomas, the tumor associated glycopeptides and epitopes which are masked in normal cells are considered an attractive target in cancer immunotherapy and immunodiagnostics and have been the subject of intensive research efforts [80–82].

2.6. Human Epidermal Growth Factor Receptor 2 (HER2). The human epidermal growth factor receptor 2 (HER2) is encoded by the ERBB2 gene and is also known as cluster of differentiation 340 (CD340) or protooncogene Neu. It is a 185 kDa glycoprotein consisting of three domains; a 105 kDa extracellular domain (ECD), a transmembrane lipophilic segment, and an intracellular domain with tyrosine kinase activity. The ECD portion can be released by cleavage from the HER2 receptor and shed into serum [83]. Overexpression of HER2 is observed in 20–30% of breast cancers, resulting in an aggressive tumour phenotype, reduced survival, and possible treatment eligibility with the monoclonal antibody trastuzumab or other therapies targeted against the HER2 receptor protein [84, 85]. The prognostic value of HER2 ECD combined with MUC1 in early breast cancer was shown to be valuable in identifying high-risk breast cancer patients. These two independent indicators of a worse disease-free survival are used to identify patients in need of more aggressive therapies and intensified surveillance [86]. HER2 ECD has also been shown to be a potential diagnostic and prognostic biomarker in HER2-positive gastric cancer. Not only was there a direct correlation between serum and tumour HER2 concentration, there was also a correlation between serum HER2 concentration and patient responses to chemotherapy [87].

Although the ECD of HER2 contains several potential *N*-linked glycosylation sites, studies of its glycoforms have been limited to an examination of how HER2 glycosylation affected the specificities of a panel of anti-HER2 antibodies

[88]. HER2 oligosaccharide structures have not yet been elucidated.

2.7. Carcinoembryonic Antigen (CEA). Carcinoembryonic antigen (CEA) has molecular weight of approximately 180 kDa, belongs to the immunoglobulin superfamily, and is a glycosylphosphatidylinositol-anchored cell surface glycoprotein. CEA is normally produced by mucosal cells in gastrointestinal tissue during fetal development and the expression decreases before birth, with the highest concentrations in the second trimester 80–100 ng/mL in amniotic fluid at week 19, reducing to 50 ng/mL at full term [89]. CEA is not elevated in maternal serum during pregnancy since it does not cross the placenta and is present only at very low concentrations in healthy adult serum of both genders (less than 2.5 ng/mL). However, CEA serum concentrations are elevated for heavy smokers, who express up to 5 ng/mL, and under certain pathological conditions, including colorectal, gastric, pancreatic, nonsmall cell lung, and breast carcinomas [90]. CEA is the primary biomarker used for the staging of colorectal carcinoma and monitoring the recurrence or spread of colon cancer after surgical resection, as rising concentrations of CEA precede other clinical indicators by several months [91, 92].

N-linked oligosaccharides account for more than 50% of the molecular mass of CEA and it is hypothesized that the reduction in mass of human colonic CEA to 170 kDa is as a result of alterations in glycosylation [93, 94]. CEA expressed by CD44-double knockdown LS174T colon carcinoma cells is more densely substituted with sialylated and fucosylated epitopes than CEA on wild-type LS174T cells [95]. The avidity of the altered glycoforms of CEA for selectins was increased when compared to glycoforms from the wild-type cells, which may contribute to metastatic dissemination [95]. However, further studies are required for CEA glycosylation and the role of this glycosylation and to investigate whether these potentially altered glycoforms can enhance the diagnostic ability of CEA.

2.8. Carbohydrate Antigen (CA19-9). Carbohydrate antigen 19-9 (CA19-9), or cancer antigen 19-9, is the sialyl Le^a (sLe^a) blood group structure which is recognised by the antibody N-19-9 [96] (Figure 2). CA19-9 is used primarily in combination with other biomarkers (e.g., CEA) for the monitoring and management of pancreatic cancer [90]. CA19-9 is also currently recognised as one of the most common tumour markers for colorectal, gastric, and hepatocellular cancer [97]. The latter three types of cancer contribute to 28% and 16% of cancer-associated deaths in males and females, respectively (Figure 1). The biggest disadvantage of using the CA19-9 testing is that sLe^a structure is neither exclusively expressed for a specific tumour type nor is it expressed in cancer only, but it is expressed at a lower concentration in tissue and serum of healthy individuals of appropriate blood types. Additionally, patients who are genotypically negative for the Le^a antigen cannot produce CA19-9, even when affected by cancer [98].

Increased expression of CA19-9 is used to indicate the presence of pancreatic cancer before any evidence of disease is obtained with other methods [99] and strictly correlates with the clinical response after pancreatectomy. Thus, it is used for the monitoring of disease recurrence [100]. Similarly, CA19-9 testing in combination with other biomarkers was recommended in multiple studies for estimating the relapse of gastric carcinoma after surgery [101, 102]. Recently, CA19-9 has been used as a prognostic biomarker for HCC and postoperative cholangiocarcinoma patients. In HCC, patients serum concentrations in excess of 100 U/mL independently predicts poorer overall survival while, in cholangiocarcinoma patients, serum CA19-9 concentrations in excess of 150 U/mL were associated with a worse overall survival [97, 103].

2.9. Thyroglobulin (Tg). Thyroglobulin (Tg) is a 660 kDa dimeric glycoprotein with 20 potential *N*-linked glycosylation sites, of which 16 sites were shown to be glycosylated in the mature protein [104]. Tg is produced by the follicular cells of the thyroid and is used by the thyroid gland as a substrate for the synthesis of thyroxine and triiodothyronine and for the storage of the inactive forms of thyroid hormone and iodine. Serum Tg concentration is a biomarker for monitoring postoperative thyroid cancer recurrence [105, 106]. However, the usefulness of preoperative Tg measurements (partly related to difficulties with antibody interference and nonspecific recognition) remains unclear [107–110]. The glycosylation of Tg is well known and carbohydrate structures correlated with Tg function playing a role in the secretion of Tg, transportation of Tg to cell compartments, iodination, hormone synthesis, and immunoreactivity [104].

Structure elucidation of Tg glycosylation in cancer has not been performed to date but may be useful for thyroid cancer diagnostics. Preliminary studies showed that the interaction of lectin LCA with Tg from thyroid carcinoma was significantly lower than that in normal thyroid tissue and in patients with benign thyroid tumor [111, 112]. The percentage of LCA-reactive Tg could discriminate between benign and malignant lesions [113]. It was also found that the percentage of LCA-reactive Tg was significantly decreased in thyroid carcinoma patients who were positive for lymph node metastasis compared to thyroid carcinoma patients who were negative for lymph node metastasis [112].

3. Potential Novel Biomarkers

The translation of biomarkers from discovery to clinical practice is still ongoing for hundreds of potential biomarkers which have been identified and published. The validation process of a putative biomarker requires time, hundreds of specimens, and large cohorts of patients to be shown reproducibly. Examples of promising biomarkers routinely checked in clinical practice but not approved for specific cancer due to low specificity or sensitivity are described below.

3.1. Human Chorionic Gonadotropin (hCG). Human chorionic gonadotropin (hCG) is a heterodimeric glycoprotein hormone produced by the placenta and comprises an α-subunit and a β-subunit that can vary in glycosylation [114]. The α-subunit structure is common to luteinizing hormone,

follicle stimulating hormone, and thyroid stimulating hormone while the β-subunits of the aforementioned hormones display various degrees of homology with each other, conferring the distinct biological activity of each heterodimer. In addition, two variants of hCG, regular and hyperglycosylated, have independent activities. The regular form maintains the arteries and the vascular supply of the placenta during the full course of pregnancy while the hyperglycosylated hCG (hCG with *O*-linked oligosaccharides) is responsible for embryo implantation during pregnancy [115].

The hyperglycosylated form of hCG is also expressed by several tumours, including male germ cell tumours (GCTs) and choriocarcinomas [114], and has been suggested to play a central role in cancer invasion [116]. High concentrations of hCG are usually indicative of adverse prognosis for cancer progression [114, 117]. More complex carbohydrate structures were reported for cancer-related hCG when compared to hCG expressed during pregnancy [118, 119]. However, the relative proportion of hCG isoforms may vary among healthy and diseased states and false positive hCG results are a major problem in the management of gestational trophoblastic disease and cancer [120]. While hCG is well-known indicator of tumours, it has not been approved for this application by the FDA.

3.2. α-1-Antitrypsin (A1AT). A1AT is a 52 kDa serine protease inhibitor with three potential glycosylation sites which is produced mainly by hepatocytes and is upregulated in the serum of lung cancer patients [121–124]. A1AT is present in various different glycoforms which can be used to distinguish between various subtypes of lung cancer and benign pulmonary diseases (BPDs) [124]. The galactosylated A1AT and fucosylated A1AT glycoforms can both distinguish nonsmall cell lung carcinoma (NSCLC) ($n = 23$) from BPD ($n = 25$) with identical degrees of accuracy (AUC = 0.834). Fucosylated A1AT can also efficiently distinguish adenocarcinoma ($n = 28$) from BPD (AUC 0.919). The poly-*N*-acetyllactosamine (polyLacNac) A1AT glycoform can distinguish between small cell lung carcinoma and BPD with a high degree of accuracy (AUC = 0.905) [124]. While the preliminary data is promising, these biomarkers were only examined on 81 patients and need to be investigated in a larger cohort of patients.

3.3. Fucosylated Haptoglobin (Fuc-Hpt). Haptoglobin is a 40 kDa glycoprotein that is produced mainly in the liver and has a low proportion of fucosylation in healthy individuals [125, 126]. Highly fucosylated haptoglobin (Fuc-Hpt) was identified as a potential biomarker in pancreatic cancer upon *Aleuria aurantia* lectin (AAL) blot analysis of the serum of pancreatic cancer patients [127]. Fuc-Hpt has also been shown to be upregulated in the serum of pancreatic cancer patients, with increased branching and fucosylation of the antennae of the *N*-linked oligosaccharides on the beta chain of Hpt [128]. Fuc-Hpt of pancreatic cancer patients had more intense binding to AAL compared to the healthy controls [125]. The concentrations of Fuc-Hpt in 300 pancreatic cancer patients and 315 healthy volunteers were analysed using lectin-based ELISAs. Fuc-Hpt concentrations were significantly higher in the pancreatic cancer patients ($P < 0.01$) and the ELISA had an AUC of 0.91, a sensitivity of 85.1%, and a specificity of 82.3% [129]. Fuc-Hpt was also elevated in certain colorectal cancer patients, in relation to the proximity of the tumour to the liver and distance metastasis. When Fuc-Hpt was combined with CEA, it was shown that it had the potential to be a novel prognostic marker in colorectal cancer [125, 130]. Fuc-Hpt could also be a potential prognostic biomarker in prostate cancer, as it significantly correlated with Gleason scores and biochemical recurrence after radical prostatectomy. PSA also correlated with overall and progression-free survival and the clinical stage of prostate cancer [131].

3.4. YKL-40. YKL-40, also known as chitinase-3-like 1 (CHI3L1) or human cartilage glycoprotein-39, is a 40 kDa secreted glycoprotein with two potential *N*-linked glycosylation sites which has been proposed as a biomarker in a variety of cancers but has not received FDA approval [132]. High serum concentrations of YKL-40 have previously been associated with high risk disease and increased bone destruction [133, 134]. YKL-40 was investigated as a prognostic marker in multiple myeloma (MM) [135]. A study carried out in 230 MM patients showed that age-corrected serum YKL-40 concentration is an independent prognostic biomarker in MM and indicates a quicker progression to the first skeletal related complications (e.g., bone lesions) [135]. The data shown is promising but a larger multicentre clinical trial is required before YKL-40 can be accepted as a prognostic marker in MM.

4. Carbohydrates as Potential Serum Biomarkers

Advances in HTP glycoanalytical methods have led to investigation of the carbohydrate structures present on glycoproteins in the serum of cancer patients and healthy controls. Many research groups have evaluated whether the variation in structure and/or abundance of these carbohydrates can distinguish between cancer patients and healthy controls [136–139]. This section presents the most recent publications (from 2010 to the present) on alterations in carbohydrate structures on serum glycoproteins of cancer patients and their potential utility as clinical biomarkers.

4.1. Ovarian Cancer. The biomarker currently used to diagnose ovarian cancer, MUC16, can only detect late stage ovarian cancer and cannot distinguish between ovarian cancers and benign ovarian diseases (BOD). Enzyme-released *N*-linked oligosaccharides from the serum of patients with ovarian cancer and BOD were analyzed by MS [138, 140]. MS analysis revealed a panel of *N*-linked oligosaccharides which could accurately distinguish between ovarian cancer and BOD with greater sensitivity (81–84%) and specificity (83%) than MUC16 (sensitivity = 78%) when tested on a small cohort of patients (37 ovarian patients and 23 healthy controls [140] and 20 ovarian cancer patients, 20 BOD patients, and 33 healthy controls [138]). The use of carbohydrates as

improved biomarkers for diagnosing ovarian cancer compared to MUC16 is currently being investigated in a clinical trial (NCT00628654, Table 2).

Increased sialylation is a common glycosylation alteration in various cancer types and sialylation has been investigated as a possible cancer biomarker [141–143]. Measuring the alteration in the serum concentrations of both sialic acid and hydroxyproline distinguishes between ovarian cancer and healthy controls [144]. This assay outperformed the MUC16 and HE4 assays in the diagnosis of ovarian cancer [44]. However, this assay was not significantly better than the ROMA test, which currently remains the best method for diagnosing and monitoring ovarian cancer [66].

4.2. Gastric Cancer. Gastric cancer is the second most common cause of cancer-related death (Table 1). Studies have shown that the infections with *Helicobacter pylori* which cause gastritis can progress to gastric adenocarcinoma [145–148]. *H. pylori* infection is associated with a sixfold increased risk of gastric cancer [149]. *H. pylori* infection also causes peptic ulcer disease but, unlike gastritis, it is inversely correlated to gastric cancer. However, there are currently no methods for the early stage detection of gastric cancer and most cases present with advanced or metastatic disease [150]. MS was used to investigate whether alterations in the structure or abundance of *N*-linked oligosaccharides in the serum of gastric cancer patients ($n = 36$) could distinguish them from patients with gastritis ($n = 18$) or duodenal ulcers ($n = 18$) [139]. Gastric cancer patients had altered serum *N*-linked glycosylation when compared to patients with gastritis. Gastric cancer patients showed reductions in high-mannose type *N*-linked oligosaccharides, those with one complex-type antenna and bigalactosylated biantennary structures and increased levels of nongalactosylated biantennary *N*-linked oligosaccharides [139]. Significant differences in *N*-linked oligosaccharides only existed between gastric cancer and gastritis patients. While these results will need to be confirmed in a larger cohort of patients, it does support the use of serum glycosylation as potential diagnostic biomarkers in gastric cancer.

4.3. Pancreatic Cancer. Alpha-1-acid glycoprotein (AGP), a 40 kDa acute phase serum glycoprotein with five complex-type *N*-linked oligosaccharides attached to the polypeptide backbone, shows variations in abundance and glycosylation in various different cancers [151]. The structures of the *N*-linked oligosaccharides on AGP from patients with pancreatic cancer ($n = 6$) and patients with chronic pancreatitis ($n = 2$) were analysed using LC-MS to investigate their potential as diagnostic biomarkers [152]. There was an increase in fucosylated triantennary trisialylated and fucosylated tetra-antennary trisialylated *N*-linked oligosaccharides in the pancreatic patients when compared to the pancreatitis patients. The increased abundance of these *N*-linked oligosaccharides also differed between the various stages of pancreatic cancer and could be potentially used as prognostic biomarkers [152]. While the sample size used in this study was too small for a statistical analysis to be carried out, a larger cohort of patients can confirm whether these glycosylation alterations can be used as diagnostic and prognostic markers.

Current clinical interest in AGP is related to its abundance in the serum of cancer patients. The serum concentration of AGP affects the pharmacokinetics and dynamics of the chemotherapeutic drug docetaxel and may predict a patient's reaction to the therapy [153]. The effect of AGP on docetaxel therapy is currently being examined in a large scale clinical trial (Table 2).

Another serum glycoprotein that is abnormally glycosylated in pancreatic cancer is ceruloplasmin. Ceruloplasmin is an acute-phase protein that is produced by the liver and secreted into the plasma. Ceruloplasmin has four *N*-linked glycosylation sites with complex type, bi-, tri-, and tetra-antennary structures, fucosylated and sialylated, containing the sialyl Lewis x (sLe^x) epitope (Figure 2) [154]. Analysis of the *N*-linked oligosaccharides on ceruloplasmin using MS showed that it had a trend towards higher proportions of sLe^x in pancreatic patients ($n = 20$), when compared to healthy controls ($n = 13$) and patients with chronic pancreatitis ($n = 14$) [155]. A larger sample size is required before it can be confirmed whether the trend of higher sLe^x expression on ceruloplasmin can be used as biomarker for pancreatic cancer diagnosis and progression.

4.4. Colon Cancer. The expression of the cancer-related epitopes sLe^x and sLe^a on glycoproteins present in the serum of colon cancer patients was analysed using a novel antibody microarray [156]. A panel of five serum glycoproteins were identified that could distinguish between stage 3 and stage 4 colon cancer patients and healthy controls with an AUC of 90%. Although the glycoproteins were not named, they may represent novel biomarkers that could improve the sensitivity of current tests for colorectal cancer.

4.5. Oesophageal Cancer. LC-MS was used to determine the site specific alterations in *N*-linked oligosaccharides in oesophageal cancers [137]. This novel method was applied to serum isolated from patients with oesophageal cancer ($n = 15$) and disease-free controls ($n = 15$). The study also included patients with diseases that can develop into oesophageal cancer, for example, high grade dysplasia ($n = 12$) and Barrett's disease ($n = 7$) [137, 157, 158]. Significant alterations in site-specific glycosylation were successfully identified on the serum proteins vitronectin, ceruloplasmin, alpha-2-macroglobulin, and complement factor 1 between oesophageal cancer and control patients. These findings will have to be verified in a larger cohort of patients before any definitive conclusions can be made.

4.6. Breast Cancer. Increased sialylation, changes in fucosylation, and higher proportions of sialyl Lewis x were reported in *N*-linked oligosaccharide structures in serum from breast cancer patients [19]. The abundance of sLe^x containing *N*-linked oligosaccharides was investigated in the serum from 52 breast cancer patients and 134 patients with benign breast disease using exoglycosidase digestion and HPLC analysis to determine whether it could be used as a diagnostic/prognostic tool. While there was no significant

difference in serum glycosylation between early stage breast cancer and benign breast disease, there were differences in serum glycosylation between breast cancer patients with lymph-node positive and lymph-node negative breast cancer. Patients with lymph-node positive breast cancer showed increased proportions of biantennary (FA2) and terminally sialylated *N*-linked oligosaccharides (A3F1G1S1 and A2F1G1S1) containing the sLe^x structure in their serum when compared to lymph node-negative patients with early breast cancer [159]. These results need to be confirmed in a larger cohort of patients to verify the prognostic utility of serum glycan analysis in breast cancer.

4.7. Prostate Cancer. Analysis of serum glycosylation using HPLC and exoglycosidase digestion showed taht there were differences in fucosylation and sialylation between prostate cancer patients and patients with BPH. Serum form prostate cancer patients had increased core fucosylation, as well as increased expression of α-(2,3)-linked sialic acid when compared to serum BPH patients [41]. These alterations in serum glycosylation could also distinguish between different stages of prostate cancer. Triantennary trigalactosylated (A3G3) and tetra-antennary tetrasialylated *N*-linked oligosaccharides with outer arm fucose (A4FS4) (Figure 2) were significantly decreased on serum PSA from patients with a Gleason score of 7 (more aggressive cancer and a higher chance of relapse) compared to a Gleason score of 5. In contrast, tetra-antennary tetrasialylated *N*-linked oligosaccharides (A4S4) (Figure 2) were increased in the serum of PSA patients with a Gleason score of 7. The serum glycome analysis was better than PSA at distinguishing between BPH and prostate cancer and at distinguishing between patients with a Gleason score of 7 and patients with a Gleason score of 5 [41]. While the results of this study are promising, they must be confirmed in a larger cohort of patients.

5. Conclusions

Research into cancer-specific alterations in glycosylation of serum glycoproteins has provided a promising source of novel biomarkers. Various groups have reported that altered glycoforms of serum glycoproteins can be used to diagnose and monitor various cancers with greater sensitivity and specificity than the currently used biomarkers [21, 44, 156]. Preliminary data has shown that serum glycome analysis is potentially a very sensitive method of discriminating between cancer and control patients or patients with related benign conditions and can detect cancers at a much earlier stage than the currently used biomarkers [139, 140]. Given the possible diagnostic power of glycoproteins and serum glycome analysis, glycosylation-based biomarkers are currently one of the most promising areas of biomarker discovery.

Conflict of Interests

The authors declare that there is no conflict of interests regarding the publication of this paper.

Acknowledgments

The authors thank Science Foundation Ireland (SFI) and Enterprise Ireland for a Technology Innovation Development Award (13/TIDA/B2687) (Michelle Kilcoyne and Marta Utratna), SFI for support of the Alimentary Glycoscience Research Cluster (08/SRC/B1393) (Lokesh Joshi), and Cancer Care West (Maura Burke fellowship) and the Hardiman Fellowship, NUI Galway, for funding a PhD scholarship (Alan Kirwan).

References

[1] L. A. Torre, F. Bray, R. L. Siegel, J. Ferlay, J. Lortet-Tieulent, and A. Jemal, "Global cancer statistics, 2012," *CA: A Cancer Journal for Clinicians*, vol. 65, no. 2, pp. 87–108, 2015.

[2] K. Strimbu and J. A. Tavel, "What are biomarkers?" *Current Opinion in HIV and AIDS*, vol. 5, no. 6, pp. 463–466, 2010.

[3] J. A. Ludwig and J. N. Weinstein, "Biomarkers in cancer staging, prognosis and treatment selection," *Nature Reviews Cancer*, vol. 5, no. 11, pp. 845–856, 2005.

[4] S. M. Hanash, S. J. Pitteri, and V. M. Faca, "Mining the plasma proteome for cancer biomarkers," *Nature*, vol. 452, no. 7187, pp. 571–579, 2008.

[5] S. Yotsukura and H. Mamitsuka, "Evaluation of serum-based cancer biomarkers: a brief review from a clinical and computational viewpoint," *Critical Reviews in Oncology/Hematology*, vol. 93, no. 2, pp. 103–115, 2014.

[6] M. N. Christiansen, J. Chik, L. Lee, M. Anugraham, J. L. Abrahams, and N. H. Packer, "Cell surface protein glycosylation in cancer," *Proteomics*, vol. 14, no. 4-5, pp. 525–546, 2014.

[7] S. R. Stowell, T. Z. Ju, and R. D. Cummings, "Protein glycosylation in cancer," *Annual Review of Pathology: Mechanisms of Disease*, vol. 10, no. 1, pp. 473–510, 2015.

[8] R. G. Spiro, "Protein glycosylation: nature, distribution, enzymatic formation, and disease implications of glycopeptide bonds," *Glycobiology*, vol. 12, no. 4, pp. 43R–56R, 2002.

[9] S. V. Glavey, D. Huynh, M. R. Reagan et al., "The cancer glycome: carbohydrates as mediators of metastasis," *Blood Reviews*, 2015.

[10] N. L. Anderson and N. G. Anderson, "The human plasma proteome: history, character, and diagnostic prospects," *Molecular & Cellular Proteomics*, vol. 1, no. 11, pp. 845–867, 2002.

[11] S. Saussez, H. Marchant, N. Nagy et al., "Quantitative glycohistochemistry defines new prognostic markers for cancers of the oral cavity," *Cancer*, vol. 82, no. 2, pp. 252–260, 1998.

[12] K. Shiraki, K. Takase, Y. Tameda, M. Hamada, Y. Kosaka, and T. Nakano, "A clinical study of lectin-reactive alpha-fetoprotein as an early indicator of hepatocellular carcinoma in the follow-up of cirrhotic patients," *Hepatology*, vol. 22, no. 3, pp. 802–807, 1995.

[13] C. Ohyama, M. Hosono, K. Nitta et al., "Carbohydrate structure and differential binding of prostate specific antigen to *Maackia amurensis* lectin between prostate cancer and benign prostate hypertrophy," *Glycobiology*, vol. 14, no. 8, pp. 671–679, 2004.

[14] Y. Mechref, Y. Hu, A. Garcia, and A. Hussein, "Identifying cancer biomarkers by mass spectrometry-based glycomics," *Electrophoresis*, vol. 33, no. 12, pp. 1755–1767, 2012.

[15] S. A. Svarovsky and L. Joshi, "Cancer glycan biomarkers and their detection—past, present and future," *Analytical Methods*, vol. 6, no. 12, pp. 3918–3936, 2014.

[16] S. V. Glavey, S. Manier, A. Natoni et al., "The sialyltransferase ST3GAL6 influences homing and survival in multiple myeloma," *Blood*, vol. 124, no. 11, pp. 1765–1776, 2014.

[17] F. Dall'Olio, N. Malagolini, M. Trinchera, and M. Chiricolo, "Mechanisms of cancer-associated glycosylation changes," *Frontiers in Bioscience*, vol. 17, no. 2, pp. 670–699, 2012.

[18] H. Ghazarian, B. Idoni, and S. B. Oppenheimer, "A glycobiology review: carbohydrates, lectins and implications in cancer therapeutics," *Acta Histochemica*, vol. 113, no. 3, pp. 236–247, 2011.

[19] Z. Kyselova, Y. Mechref, P. Kang et al., "Breast cancer diagnosis and prognosis through quantitative measurements of serum glycan profiles," *Clinical Chemistry*, vol. 54, no. 7, pp. 1166–1175, 2008.

[20] R. K. Sterling, L. Jeffers, F. Gordon et al., "Clinical utility of AFP-L3% measurement in North American patients with HCV-related cirrhosis," *The American Journal of Gastroenterology*, vol. 102, no. 10, pp. 2196–2205, 2007.

[21] S. Zhang, K. Jiang, Q. Zhang, K. Guo, and Y. Liu, "Serum fucosylated paraoxonase 1 as a potential glycobiomarker for clinical diagnosis of early hepatocellular carcinoma using ELISA Index," *Glycoconjugate Journal*, vol. 32, no. 3-4, pp. 119–125, 2015.

[22] C. G. Bergstrand and B. Czar, "Demonstration of a new protein fraction in serum from the human fetus," *Scandinavian Journal of Clinical and Laboratory Investigation*, vol. 8, no. 2, p. 174, 1956.

[23] G. J. Mizejewski, "Alpha-fetoprotein (AFP)-derived peptides as epitopes for hepatoma immunotherapy: a commentary," *Cancer Immunology, Immunotherapy*, vol. 58, no. 2, pp. 159–170, 2009.

[24] S. Saito, H. Ojima, H. Ichikawa, S. Hirohashi, and T. Kondo, "Molecular background of α-fetoprotein in liver cancer cells as revealed by global RNA expression analysis," *Cancer Science*, vol. 99, no. 12, pp. 2402–2409, 2008.

[25] S. Gupta, S. Bent, and J. Kohlwes, "Test characteristics of α-fetoprotein for detecting hepatocellular carcinoma in patients with hepatitis C: a systematic review and critical analysis," *Annals of Internal Medicine*, vol. 139, no. 1, pp. 46–50, 2003.

[26] R. Saffroy, P. Pham, M. Reffas, M. Takka, A. Lemoine, and B. Debuire, "New perspectives and strategy research biomarkers for hepatocellular carcinoma," *Clinical Chemistry and Laboratory Medicine*, vol. 45, no. 9, pp. 1169–1179, 2007.

[27] J. A. Marrero, "Modern diagnosis of hepatocellular carcinoma: utilization of liver biopsy and genomic markers," *Journal of Hepatology*, vol. 50, no. 4, pp. 659–661, 2009.

[28] M. Kobayashi, T. Kuroiwa, T. Suda et al., "Fucosylated fraction of alpha-fetoprotein, L3, as a useful prognostic factor in patients with hepatocellular carcinoma with special reference to low concentrations of serum alpha-fetoprotein," *Hepatology Research*, vol. 37, no. 11, pp. 914–922, 2007.

[29] T. Nakagawa, E. Miyoshi, T. Yakushijin et al., "Glycomic analysis of alpha-fetoprotein L3 in hepatoma cell lines and hepatocellular carcinoma patients," *Journal of Proteome Research*, vol. 7, no. 6, pp. 2222–2233, 2008.

[30] H. Toyoda, T. Kumada, T. Tada et al., "Clinical utility of highly sensitive Lens culinaris agglutinin-reactive alpha-fetoprotein in hepatocellular carcinoma patients with alpha-fetoprotein <20 ng/mL," *Cancer Science*, vol. 102, no. 5, pp. 1025–1031, 2011.

[31] K. Oda, A. Ido, T. Tamai et al., "Highly sensitive lens culinaris agglutinin-reactive α-fetoprotein is useful for early detection of hepatocellular carcinoma in patients with chronic liver disease," *Oncology Reports*, vol. 26, no. 5, pp. 1227–1233, 2011.

[32] T. Tada, T. Kumada, H. Toyoda et al., "Relationship between *Lens culinaris* agglutinin-reactive α-fetoprotein and pathologic features of hepatocellular carcinoma," *Liver International*, vol. 25, no. 4, pp. 848–853, 2005.

[33] M. G. Giardina, M. Matarazzo, R. Morante et al., "Serum α-L-fucosidase activity and early detection of hepatocellular carcinoma: a prospective study of patients with cirrhosis," *Cancer*, vol. 83, no. 12, pp. 2468–2474, 1998.

[34] T. Isono, T. Tanaka, S. Kageyama, and T. Yoshiki, "Structural diversity of cancer-related and non-cancer-related prostate-specific antigen," *Clinical Chemistry*, vol. 48, no. 12, pp. 2187–2194, 2002.

[35] M. V. Dwek, A. Jenks, and A. J. C. Leathem, "A sensitive assay to measure biomarker glycosylation demonstrates increased fucosylation of prostate specific antigen (PSA) in patients with prostate cancer compared with benign prostatic hyperplasia," *Clinica Chimica Acta*, vol. 411, no. 23-24, pp. 1935–1939, 2010.

[36] W. J. Catalona, D. S. Smith, T. L. Ratliff et al., "Measurement of prostate-specific antigen in serum as a screening test for prostate cancer," *The New England Journal of Medicine*, vol. 324, no. 17, pp. 1156–1161, 1991.

[37] H. B. Carter, P. C. Albertsen, M. J. Barry et al., "Early detection of prostate cancer: AUA guideline," *Journal of Urology*, vol. 190, no. 2, pp. 419–426, 2013.

[38] M. J. G. Bussemakers, A. van Bokhoven, G. W. Verhaegh et al., "DD3: a new prostate-specific gene, highly overexpressed in prostate cancer," *Cancer Research*, vol. 59, no. 23, pp. 5975–5979, 1999.

[39] M. Tajiri, C. Ohyama, and Y. Wada, "Oligosaccharide profiles of the prostate specific antigen in free and complexed forms from the prostate cancer patient serum and in seminal plasma: a glycopeptide approach," *Glycobiology*, vol. 18, no. 1, pp. 2–8, 2008.

[40] A. Sarrats, J. Comet, G. Tabarés et al., "Differential percentage of serum prostate-specific antigen subforms suggests a new way to improve prostate cancer diagnosis," *Prostate*, vol. 70, no. 1, pp. 1–9, 2010.

[41] R. Saldova, Y. Fan, J. M. Fitzpatrick, R. W. G. Watson, and P. M. Rudd, "Core fucosylation and α2-3 sialylation in serum N-glycome is significantly increased in prostate cancer comparing to benign prostate hyperplasia," *Glycobiology*, vol. 21, no. 2, pp. 195–205, 2011.

[42] Z. Kyselova, Y. Mechref, M. M. Al Bataineh et al., "Alterations in the serum glycome due to metastatic prostate cancer," *Journal of Proteome Research*, vol. 6, no. 5, pp. 1822–1832, 2007.

[43] R. Peracaula, S. Barrabés, A. Sarrats, P. M. Rudd, and R. De Llorens, "Altered glycosylation in tumours focused to cancer diagnosis," *Disease Markers*, vol. 25, no. 4-5, pp. 207–218, 2008.

[44] R. Peracaula, G. Tabarés, L. Royle et al., "Altered glycosylation pattern allows the distinction between prostate-specific antigen (PSA) from normal and tumor origins," *Glycobiology*, vol. 13, no. 6, pp. 457–470, 2003.

[45] Q. K. Li, L. Chen, M. Ao et al., "Serum Fucosylated Prostate-specific Antigen (PSA) improves the differentiation of aggressive from non-aggressive prostate cancers," *Theranostics*, vol. 5, no. 3, pp. 267–276, 2015.

[46] T. Yoneyama, C. Ohyama, S. Hatakeyama et al., "Measurement of aberrant glycosylation of prostate specific antigen can improve specificity in early detection of prostate cancer," *Biochemical and Biophysical Research Communications*, vol. 448, no. 4, pp. 390–396, 2014.

[47] A. Vegvari, M. Rezeli, C. Sihlbom et al., "Molecular micro-heterogeneity of prostate specific antigen in seminal fluid by

mass spectrometry," *Clinical Biochemistry*, vol. 45, no. 4-5, pp. 331–338, 2012.

[48] S. Goč and M. Janković, "Evaluation of molecular species of prostate-specific antigen complexed with immunoglobulin m in prostate cancer and benign prostatic hyperplasia," *Disease Markers*, vol. 35, no. 6, pp. 847–855, 2013.

[49] R. C. Bast Jr., M. Feeney, H. Lazarus, L. M. Nadler, R. B. Colvin, and R. C. Knapp, "Reactivity of a monoclonal antibody with human ovarian carcinoma," *The Journal of Clinical Investigation*, vol. 68, no. 5, pp. 1331–1337, 1981.

[50] F.-G. Hanisch, G. Uhlenbruck, J. Peter-Katalinic, and H. Egge, "Structural studies on oncofetal carbohydrate antigens (Ca 19-9, Ca 50, and Ca 125) carried by O-linked sialyl-oligosaccharides on human amniotic mucins," *Carbohydrate Research*, vol. 178, no. 1, pp. 29–47, 1988.

[51] H. M. Davis, V. R. Zurawski Jr., R. C. Bast Jr., and T. L. Klug, "Characterization of the CA 125 antigen associated with human epithelial ovarian carcinomas," *Cancer Research*, vol. 46, part 1, no. 12, pp. 6143–6148, 1986.

[52] R. C. Bast, T. L. Klug, E. St John et al., "A radioimmunoassay using a monoclonal antibody to monitor the course of epithelial ovarian cancer," *The New England Journal of Medicine*, vol. 309, no. 15, pp. 883–887, 1983.

[53] M. Muyldermans, F. J. Cornillie, and P. R. Koninckx, "CA125 and endometriosis," *Human Reproduction Update*, vol. 1, no. 2, pp. 173–187, 1995.

[54] C. S. Marcus, G. L. Maxwell, K. M. Darcy, C. A. Hamilton, and W. P. McGuire, "Current approaches and challenges in managing and monitoring treatment response in ovarian cancer," *Journal of Cancer*, vol. 5, no. 1, pp. 25–30, 2014.

[55] K. Akita, S. Yoshida, Y. Ikehara et al., "Different levels of sialyl-Tn antigen expressed on MUC16 in patients with endometriosis and ovarian cancer," *International Journal of Gynecological Cancer*, vol. 22, no. 4, pp. 531–538, 2012.

[56] K. Chen, A. Gentry-Maharaj, M. Burnell et al., "Microarray Glycoprofiling of CA125 improves differential diagnosis of ovarian cancer," *Journal of Proteome Research*, vol. 12, no. 3, pp. 1408–1418, 2013.

[57] S. Ricardo, L. Marcos-Silva, D. Pereira et al., "Detection of glyco-mucin profiles improves specificity of MUC16 and MUC1 biomarkers in ovarian serous tumours," *Molecular Oncology*, vol. 9, no. 2, pp. 503–512, 2014.

[58] C. Kirchhoff, "Molecular characterization of epididymal proteins," *Reviews of Reproduction*, vol. 3, no. 2, pp. 86–95, 1998.

[59] C. Kirchhoff, I. Habben, R. Iveli, and N. Krull, "A major human epididymis-specific cDNA encodes a protein with sequence homology to extracellular proteinase inhibitors," *Biology of Reproduction*, vol. 45, no. 2, pp. 350–357, 1991.

[60] M. Schummer, W. V. Ng, R. E. Bumgarner et al., "Comparative hybridization of an array of 21,500 ovarian cDNAs for the discovery of genes overexpressed in ovarian carcinomas," *Gene*, vol. 238, no. 2, pp. 375–385, 1999.

[61] C. D. Hough, C. A. Sherman-Baust, E. S. Pizer et al., "Large-scale serial analysis of gene expression reveals genes differentially expressed in ovarian cancer," *Cancer Research*, vol. 60, no. 22, pp. 6281–6287, 2000.

[62] R. Drapkin, H. H. von Horsten, Y. Lin et al., "Human epididymis protein 4 (HE4) is a secreted glycoprotein that is overexpressed by serous and endometrioid ovarian carcinomas," *Cancer Research*, vol. 65, no. 6, pp. 2162–2169, 2005.

[63] K. D. Steffensen, M. Waldstrøm, I. Brandslund, and A. Jakobsen, "Prognostic impact of prechemotherapy serum levels of HER2, CA125, and HE4 in ovarian cancer patients," *International Journal of Gynecological Cancer*, vol. 21, no. 6, pp. 1040–1047, 2011.

[64] S. Ferrarow, F. Braga, M. Lanzoni, P. Boracchi, E. M. Biganzoli, and M. Panteghini, "Serum human epididymis protein 4 vs carbohydrate antigen 125 for ovarian cancer diagnosis: a systematic review," *Journal of Clinical Pathology*, vol. 66, no. 4, pp. 273–281, 2013.

[65] M. Montagnana, E. Danese, O. Ruzzenente et al., "The ROMA (Risk of Ovarian Malignancy Algorithm) for estimating the risk of epithelial ovarian cancer in women presenting with pelvic mass: is it really useful?" *Clinical Chemistry and Laboratory Medicine*, vol. 49, no. 3, pp. 521–525, 2011.

[66] M. A. Karlsen, N. Sandhu, C. Høgdall et al., "Evaluation of HE4, CA125, risk of ovarian malignancy algorithm (ROMA) and risk of malignancy index (RMI) as diagnostic tools of epithelial ovarian cancer in patients with a pelvic mass," *Gynecologic Oncology*, vol. 127, no. 2, pp. 379–383, 2012.

[67] M. T. Sandri, F. Bottari, D. Franchi et al., "Comparison of HE4, CA125 and ROMA algorithm in women with a pelvic mass: correlation with pathological outcome," *Gynecologic Oncology*, vol. 128, no. 2, pp. 233–238, 2013.

[68] N. Chhikara, M. Saraswat, A. K. Tomar, S. Dey, S. Singh, and S. Yadav, "Human epididymis protein-4 (HE-4): a novel cross-class protease inhibitor," *PLoS ONE*, vol. 7, no. 11, Article ID e47672, 2012.

[69] L. Hua, Y. Liu, S. Zhen, D. Wan, J. Cao, and X. Gao, "Expression and biochemical characterization of recombinant human epididymis protein 4," *Protein Expression and Purification*, vol. 102, pp. 52–62, 2014.

[70] S. Nath and P. Mukherjee, "MUC1: a multifaceted oncoprotein with a key role in cancer progression," *Trends in Molecular Medicine*, vol. 20, no. 6, pp. 332–342, 2014.

[71] M. Shimizu and K. Yamauchi, "Isolation and characterization of mucin-like glycoprotein in human milk fat globule membrane," *Journal of Biochemistry*, vol. 91, no. 2, pp. 515–524, 1982.

[72] J. Hilkens, F. Buijs, J. Hilgers et al., "Monoclonal antibodies against human milk-fat globule membranes detecting differentiation antigens of the mammary gland and its tumors," *International Journal of Cancer*, vol. 34, no. 2, pp. 197–206, 1984.

[73] S. B. Ho, G. A. Niehans, C. Lyftogt et al., "Heterogeneity of mucin gene expression in normal and neoplastic tissues," *Cancer Research*, vol. 53, no. 3, pp. 641–651, 1993.

[74] M. Gion, R. Mione, A. E. Leon et al., "CA27.29: a valuable marker for breast cancer management. A confirmatory multicentric study on 603 cases," *European Journal of Cancer*, vol. 37, no. 3, pp. 355–363, 2001.

[75] S. Schoonooghe, I. Burvenich, L. Vervoort, F. De Vos, N. Mertens, and J. Grooten, "PH1-derived bivalent bibodies and trivalent tribodies bind differentially to shed and tumour cell-associated MUC1," *Protein Engineering, Design & Selection*, vol. 23, no. 9, pp. 721–728, 2010.

[76] S. E. Baldus, K. Engelmann, and F.-G. Hanisch, "MUC1 and the MUCs: a family of human mucins with impact in cancer biology," *Critical Reviews in Clinical Laboratory Sciences*, vol. 41, no. 2, pp. 189–231, 2004.

[77] D. F. Hayes, H. Sekine, T. Ohno, M. Abe, K. Keefe, and D. W. Kufe, "Use of a murine monoclonal antibody for detection of circulating plasma DF3 antigen levels in breast cancer patients,"

The Journal of Clinical Investigation, vol. 75, no. 5, pp. 1671–1678, 1985.

[78] J.-H. Park, T. Nishidate, K. Kijima et al., "Critical roles of mucin 1 glycosylation by transactivated polypeptide *N*-acetylgalactosaminyltransferase 6 in mammary carcinogenesis," *Cancer Research*, vol. 70, no. 7, pp. 2759–2769, 2010.

[79] S. J. Storr, L. Royle, C. J. Chapman et al., "The O-linked glycosylation of secretory/shed MUC1 from an advanced breast cancer patient's serum," *Glycobiology*, vol. 18, no. 6, pp. 456–462, 2008.

[80] U. Westerlind, A. Hobel, N. Gaidzik, E. Schmitt, and H. Kunz, "Synthetic vaccines consisting of tumor-associated MUC1 glycopeptide antigens and a T-cell epitope for the induction of a highly specific humoral immune response," *Angewandte Chemie*, vol. 47, no. 39, pp. 7551–7556, 2008.

[81] N. Gaidzik, U. Westerlind, and H. Kunz, "The development of synthetic antitumour vaccines from mucin glycopeptide antigens," *Chemical Society Reviews*, vol. 42, no. 10, pp. 4421–4442, 2013.

[82] A. Kaiser, N. Gaidzik, U. Westerlind et al., "A synthetic vaccine consisting of a tumor-associated sialyl-T_N-MUC1 tandem-repeat glycopeptide and tetanus toxoid: induction of a strong and highly selective immune response," *Angewandte Chemie International Edition*, vol. 48, no. 41, pp. 7551–7555, 2009.

[83] V. Ludovini, S. Gori, M. Colozza et al., "Evaluation of serum HER2 extracellular domain in early breast cancer patients: correlation with clinicopathological parameters and survival," *Annals of Oncology*, vol. 19, no. 5, pp. 883–890, 2008.

[84] B. A. Gusterson, "Identification and interpretation of epidermal growth factor and c-erbB-2 overexpression," *European Journal of Cancer*, vol. 28, no. 1, pp. 263–267, 1992.

[85] A. C. Wolff, M. E. Hammond, J. N. Schwartz et al., "American Society of Clinical Oncology/College of American Pathologists guideline recommendations for human epidermal growth factor receptor 2 testing in breast cancer," *Archives of Pathology & Laboratory Medicine*, vol. 131, no. 1, pp. 18–43, 2007.

[86] D. Di Gioia, M. Dresse, D. Mayr, D. Nagel, V. Heinemann, and P. Stieber, "Serum HER2 in combination with CA 15-3 as a parameter for prognosis in patients with early breast cancer," *Clinica Chimica Acta*, vol. 440, pp. 16–22, 2015.

[87] K. Oyama, S. Fushida, T. Tsukada et al., "Evaluation of serum HER2-ECD levels in patients with gastric cancer," *Journal of Gastroenterology*, vol. 50, no. 1, pp. 41–45, 2015.

[88] J. T. Garrett, S. Rawale, S. D. Allen et al., "Novel engineered trastuzumab conformational epitopes demonstrate in vitro and in vivo antitumor properties against HER-2/neu," *Journal of Immunology*, vol. 178, no. 11, pp. 7120–7131, 2007.

[89] H. Gadler, K. Bremme, B. Wahren, and S. Hammarstrom, "CEA and NCA in amniotic fluid of normal and abnormal pregnancies," *Cancer*, vol. 42, no. 3, pp. 1579–1584, 1978.

[90] X. G. Ni, X. F. Bai, Y. L. Mao et al., "The clinical value of serum CEA, CA19-9, and CA242 in the diagnosis and prognosis of pancreatic cancer," *European Journal of Surgical Oncology*, vol. 31, no. 2, pp. 164–169, 2005.

[91] R. Goslin, G. Steele Jr., J. MacIntyre et al., "The use of preoperative plasma CEA levels for the stratification of patients after curative resection of colorectal cancers," *Annals of Surgery*, vol. 192, no. 6, pp. 747–751, 1980.

[92] M. J. Duffy, "Carcinoembryonic antigen as a marker for colorectal cancer: is it clinically useful?" *Clinical Chemistry*, vol. 47, no. 4, pp. 624–630, 2001.

[93] R. J. Paxton, G. Mooser, H. Pande, T. D. Lee, and J. E. Shively, "Sequence analysis of carcinoembryonic antigen: identification of glycosylation sites and homology with the immunoglobulin supergene family," *Proceedings of the National Academy of Sciences of the United States of America*, vol. 84, no. 4, pp. 920–924, 1987.

[94] M. Garcia, C. Seigner, C. Bastid, R. Choux, M. J. Payan, and H. Reggio, "Carcinoembryonic antigen has a different molecular weight in normal colon and in cancer cells due to *N*-glycosylation differences," *Cancer Research*, vol. 51, no. 20, pp. 5679–5686, 1991.

[95] S. N. Thomas, F. Zhu, R. L. Schnaar, C. S. Alves, and K. Konstantopoulos, "Carcinoembryonic antigen and CD44 variant isoforms cooperate to mediate colon carcinoma cell adhesion to E- and L-selectin in shear flow," *Journal of Biological Chemistry*, vol. 283, no. 23, pp. 15647–15655, 2008.

[96] H. Koprowski, M. Herlyn, Z. Steplewski, and H. F. Sears, "Specific antigen in serum of patients with colon carcinoma," *Science*, vol. 212, no. 4490, pp. 53–55, 1981.

[97] C. C. Hsu, A. Goyal, A. Iuga et al., "Elevated CA19-9 is associated with increased mortality in a prospective cohort of hepatocellular carcinoma patients," *Clinical and Translational Gastroenterology*, vol. 6, no. 2, p. e74, 2015.

[98] E. M. Vestergaard, H. O. Hein, H. Meyer et al., "Reference values and biological variation for tumor marker CA 19-9 in serum for different Lewis and secretor genotypes and evaluation of secretor and Lewis genotyping in a Caucasian population," *Clinical Chemistry*, vol. 45, no. 1, pp. 54–61, 1999.

[99] D. P. O'Brien, N. S. Sanayake, C. Jenkinson et al., "Serum CA19-9 is significantly upregulated up to 2 years before diagnosis with pancreatic cancer: implications for early disease detection," *Clinical Cancer Research*, vol. 21, no. 3, pp. 622–631, 2014.

[100] F. Safi, W. Schlosser, G. Kolb, and H. G. Beger, "Diagnostic value of CA 19-9 in patients with pancreatic cancer and nonspecific gastrointestinal symptoms," *Journal of Gastrointestinal Surgery*, vol. 1, no. 2, pp. 106–112, 1997.

[101] D. Marrelli, E. Pinto, A. de Stefano, M. Farnetani, L. Garosi, and F. Roviello, "Clinical utility of CEA, CA 19-9, and CA 72-4 in the follow-up of patients with resectable gastric cancer," *The American Journal of Surgery*, vol. 181, no. 1, pp. 16–19, 2001.

[102] Y. Takahashi, T. Takeuchi, J. Sakamoto et al., "The usefulness of CEA and/or CA19-9 in monitoring for recurrence in gastric cancer patients: a prospective clinical study," *Gastric Cancer*, vol. 6, no. 3, pp. 142–145, 2003.

[103] W.-K. Cai, J. J. Lin, G. H. He, H. Wang, J. H. Lu, and G. S. Yang, "Preoperative serum CA19-9 levels is an independent prognostic factor in patients with resected hilar cholangiocarcinoma," *International Journal of Clinical and Experimental Pathology*, vol. 7, no. 11, pp. 7890–7898, 2014.

[104] S.-X. Yang, H. G. Pollock, and A. B. Rawitch, "Glycosylation in human thyroglobulin: location of the N-linked oligosaccharide units and comparison with bovine thyroglobulin," *Archives of Biochemistry and Biophysics*, vol. 327, no. 1, pp. 61–70, 1996.

[105] J.-D. Lin, "Thyroglobulin and human thyroid cancer," *Clinica Chimica Acta*, vol. 388, no. 1-2, pp. 15–21, 2008.

[106] R. Petric, A. Perhavec, B. Gazic, and N. Besic, "Preoperative serum thyroglobulin concentration is an independent predictive factor of malignancy in follicular neoplasms of the thyroid gland," *Journal of Surgical Oncology*, vol. 105, no. 4, pp. 351–356, 2012.

[107] C. A. Spencer, "Challenges of serum thyroglobulin (Tg) measurement in the presence of Tg autoantibodies," *Journal of*

Clinical Endocrinology and Metabolism, vol. 89, no. 8, pp. 3702–3704, 2004.

[108] N. Panza, G. Lombardi, M. de Rosa, G. Pacilio, L. Lapenta, and M. Salvatore, "High serum thyroglobulin levels. Diagnostic indicators in patients with metastases from unknown primary sites," *Cancer*, vol. 60, no. 9, pp. 2233–2236, 1987.

[109] J. Hrafnkelsson, H. Tulinius, M. Kjeld, H. Sigvaldason, and J. G. Jónasson, "Serum thyroglobulin as a risk factor for thyroid carcinoma," *Acta Oncologica*, vol. 39, no. 8, pp. 973–977, 2000.

[110] N. Besic, G. Pilko, R. Petric, M. Hocevar, and J. Zgajnar, "Papillary thyroid microcarcinoma: prognostic factors and treatment," *Journal of Surgical Oncology*, vol. 97, no. 3, pp. 221–225, 2008.

[111] M. Maruyama, R. Kato, S. Kobayashi, and Y. Kasuga, "A method to differentiate between thyroglobulin derived from normal thyroid tissue and from thyroid carcinoma based on analysis of reactivity to lectins," *Archives of Pathology and Laboratory Medicine*, vol. 122, no. 8, pp. 715–720, 1998.

[112] K. Shimizu, K. Nakamura, S. Kobatake et al., "The clinical utility of *Lens culinaris* agglutinin-reactive thyroglobulin ratio in serum for distinguishing benign from malignant conditions of the thyroid," *Clinica Chimica Acta*, vol. 379, no. 1-2, pp. 101–104, 2007.

[113] T. Kanai, M. Amakawa, R. Kato et al., "Evaluation of a new method for the diagnosis of alterations of Lens culinaris agglutinin binding of thyroglobulin molecules in thyroid carcinoma," *Clinical Chemistry and Laboratory Medicine*, vol. 47, no. 10, pp. 1285–1290, 2009.

[114] U.-H. Stenman, H. Alfthan, and K. Hotakainen, "Human chorionic gonadotropin in cancer," *Clinical Biochemistry*, vol. 37, no. 7, pp. 549–561, 2004.

[115] H. O. Smith, C. Wiggins, C. F. Verschraegen et al., "Changing trends in gestational trophoblastic disease," *The Journal of Reproductive Medicine*, vol. 51, no. 10, pp. 777–784, 2006.

[116] L. A. Cole, D. Dai, S. A. Butler, K. K. Leslie, and E. I. Kohorn, "Gestational trophoblastic diseases: 1. Pathophysiology of hyperglycosylated hCG," *Gynecologic Oncology*, vol. 102, no. 2, pp. 145–150, 2006.

[117] H. Alfthan, C. Haglund, P. Roberts, and U.-H. Stenman, "Elevation of free beta subunit of human choriogonadotropin and core beta fragment of human choriogonadotropin in the serum and urine of patients with malignant pancreatic and biliary disease," *Cancer Research*, vol. 52, no. 17, pp. 4628–4633, 1992.

[118] A. Kobata and M. Takeuchi, "Structure, pathology and function of the N-linked sugar chains of human chorionic gonadotropin," *Biochimica et Biophysica Acta*, vol. 1455, no. 2-3, pp. 315–326, 1999.

[119] L. Valmu, H. Alfthan, K. Hotakainen, S. Birken, and U.-H. Stenman, "Site-specific glycan analysis of human chorionic gonadotropin beta-subunit from malignancies and pregnancy by liquid chromatography—electrospray mass spectrometry," *Glycobiology*, vol. 16, no. 12, pp. 1207–1218, 2006.

[120] J. R. Lurain, "Gestational trophoblastic disease II: classification and management of gestational trophoblastic neoplasia," *American Journal of Obstetrics and Gynecology*, vol. 204, no. 1, pp. 11–18, 2011.

[121] M. A. Rahman, S. Mitra, A. Sarkar, M. D. Wewers, and D. Hartl, "Alpha 1-antitrypsin does not inhibit human monocyte caspase-1," *PLOS ONE*, vol. 10, no. 2, Article ID e0117330, 2015.

[122] M. Guarino, "Epithelial-mesenchymal transition and tumour invasion," *The International Journal of Biochemistry & Cell Biology*, vol. 39, no. 12, pp. 2153–2160, 2007.

[123] J.-H. Rho, M. H. A. Roehrl, and J. Y. Wang, "Glycoproteomic analysis of human lung adenocarcinomas using glycoarrays and tandem mass spectrometry: differential expression and glycosylation patterns of vimentin and fetuin A isoforms," *Protein Journal*, vol. 28, no. 3-4, pp. 148–160, 2009.

[124] Y. Liang, T. Ma, A. Thakur et al., "Differentially expressed glycosylated patterns of α-1-antitrypsin as serum biomarkers for the diagnosis of lung cancer," *Glycobiology*, vol. 25, no. 3, pp. 331–340, 2015.

[125] E. Miyoshi and M. Nakano, "Fucosylated haptoglobin is a novel marker for pancreatic cancer: detailed analyses of oligosaccharide structures," *Proteomics*, vol. 8, no. 16, pp. 3257–3262, 2008.

[126] I. U. Song, Y. D. Kim, S. W. Chung, and H. J. Cho, "Association between serum haptoglobin and the pathogenesis of Alzheimer's disease," *Internal Medicine*, vol. 54, no. 5, pp. 453–457, 2015.

[127] K. Taketa, Y. Endo, C. Sekiya et al., "A collaborative study for the evaluation of lectin-reactive α- fetoproteins in early detection of hepatocellular carcinoma," *Cancer Research*, vol. 53, no. 22, pp. 5419–5423, 1993.

[128] T. Fujimura, Y. Shinohara, B. Tissot et al., "Glycosylation status of haptoglobin in sera of patients with prostate cancer vs. benign prostate disease or normal subjects," *International Journal of Cancer*, vol. 122, no. 1, pp. 39–49, 2008.

[129] Y. Kamada, N. Kinoshita, Y. Tsuchiya et al., "Reevaluation of a lectin antibody ELISA kit for measuring fucosylated haptoglobin in various conditions," *Clinica Chimica Acta*, vol. 417, pp. 48–53, 2013.

[130] Y. Takeda, S. Shinzaki, K. Okudo, K. Moriwaki, K. Murata, and E. Miyoshi, "Fucosylated haptoglobin is a novel type of cancer biomarker linked to the prognosis after an operation in colorectal cancer," *Cancer*, vol. 118, no. 12, pp. 3036–3043, 2012.

[131] K. Fujita, M. Shimomura, M. Uemura et al., "Serum fucosylated haptoglobin as a novel prognostic biomarker predicting high-Gleason prostate cancer," *Prostate*, vol. 74, no. 10, pp. 1052–1058, 2014.

[132] J. S. Johansen, B. V. Jensen, A. Roslind, D. Nielsen, and P. A. Price, "Serum YKL-40, a new prognostic biomarker in cancer patients?" *Cancer Epidemiology Biomarkers and Prevention*, vol. 15, no. 2, pp. 194–202, 2006.

[133] A. K. Mylin, T. Rasmussen, J. S. Johansen et al., "Serum YKL-40 concentrations in newly diagnosed multiple myeloma patients and YKL-40 expression in malignant plasma cells," *European Journal of Haematology*, vol. 77, no. 5, pp. 416–424, 2006.

[134] A. K. Mylin, N. Abildgaard, J. S. Johansen et al., "High serum YKL-40 concentration is associated with severe bone disease in newly diagnosed multiple myeloma patients," *European Journal of Haematology*, vol. 80, no. 4, pp. 310–317, 2008.

[135] A. K. Mylin, N. Abildgaard, J. S. Johansen et al., "Serum YKL-40: a new independent prognostic marker for skeletal complications in patients with multiple myeloma," *Leukemia & Lymphoma*, pp. 1–10, 2015.

[136] S.-E. Lee, J.-H. Yoon, S.-H. Shin et al., "Bone marrow plasma cell assessment before peripheral blood stem cell mobilization in patients with multiple myeloma undergoing autologous stem cell transplantation," *BioMed Research International*, vol. 2014, Article ID 982504, 8 pages, 2014.

[137] A. Mayampurath, E. Song, A. Mathur et al., "Label-free glycopeptide quantification for biomarker discovery in human sera," *Journal of Proteome Research*, vol. 13, no. 11, pp. 4821–4832, 2014.

[138] K. Biskup, E. I. Braicu, J. Sehouli, R. Tauber, and V. Blanchard, "The serum glycome to discriminate between early-stage epithelial ovarian cancer and benign ovarian diseases," *Disease Markers*, vol. 2014, Article ID 238197, 10 pages, 2014.

[139] S. Ozcan, D. A. Barkauskas, L. Renee Ruhaak et al., "Serum glycan signatures of gastric cancer," *Cancer Prevention Research*, vol. 7, no. 2, pp. 226–235, 2014.

[140] J.-H. Kim, C. W. Park, D. Um et al., "Mass spectrometric screening of ovarian cancer with serum glycans," *Disease Markers*, vol. 2014, Article ID 634289, 9 pages, 2014.

[141] D. H. Dube and C. R. Bertozzi, "Glycans in cancer and inflammation—potential for therapeutics and diagnostics," *Nature Reviews Drug Discovery*, vol. 4, no. 6, pp. 477–488, 2005.

[142] J. N. Arnold, R. Saldova, U. M. Abd Hamid, and P. M. Rudd, "Evaluation of the serum *N*-linked glycome for the diagnosis of cancer and chronic inflammation," *Proteomics*, vol. 8, no. 16, pp. 3284–3293, 2008.

[143] P. Niederhafner, M. Reiniš, J. Šebestík, and J. Ježek, "Glycopeptide dendrimers, Part III—a review: use of glycopeptide dendrimers in immunotherapy and diagnosis of cancer and viral diseases," *Journal of Peptide Science*, vol. 14, no. 5, pp. 556–587, 2008.

[144] P.-L. Li, X. Zhang, T. Li et al., "Combined detection of sialic acid and hydroxyproline in diagnosis of ovarian cancer and its comparison with human epididymis protein 4 and carbohydrate antigen 125," *Clinica Chimica Acta*, vol. 439, pp. 148–153, 2015.

[145] B. J. Marshall and J. R. Warren, "Unidentified curved bacilli in the stomach of patients with gastritis and peptic ulceration," *The Lancet*, vol. 1, no. 8390, pp. 1311–1315, 1984.

[146] N. Ohnishi, H. Yuasa, S. Tanaka et al., "Transgenic expression of Helicobacter pylori CagA induces gastrointestinal and hematopoietic neoplasms in mouse," *Proceedings of the National Academy of Sciences of the United States of America*, vol. 105, no. 3, pp. 1003–1008, 2008.

[147] T. Watanabe, M. Tada, H. Nagi, S. Sasaki, and M. Nakao, "*Helicobacter pylori* infection induces gastric cancer in Mongolian gerbils," *Gastroenterology*, vol. 115, no. 3, pp. 642–648, 1998.

[148] L. Fuccio, R. M. Zagari, L. H. Eusebi et al., "Meta-analysis: can *Helicobacter pylori* eradication treatment reduce the risk for gastric cancer?" *Annals of Internal Medicine*, vol. 151, no. 2, pp. 121–128, 2009.

[149] Helicobacter and Cancer Collaborative Group, "Gastric cancer and *Helicobacter pylori*: a combined analysis of 12 case control studies nested within prospective cohorts," *Gut*, vol. 49, no. 3, pp. 347–353, 2001.

[150] R. Siegel, D. Naishadham, and A. Jemal, "Cancer statistics, 2013," *CA: A Cancer Journal for Clinicians*, vol. 63, no. 1, pp. 11–30, 2013.

[151] F. Ceciliani and V. Pocacqua, "The acute phase protein α1-acid glycoprotein: a model for altered glycosylation during diseases," *Current Protein and Peptide Science*, vol. 8, no. 1, pp. 91–108, 2007.

[152] E. Giménez, M. Balmaña, J. Figueras et al., "Quantitative analysis of N-glycans from human alfa-acid-glycoprotein using stable isotope labeling and zwitterionic hydrophilic interaction capillary liquid chromatography electrospray mass spectrometry as tool for pancreatic disease diagnosis," *Analytica Chimica Acta*, vol. 866, pp. 59–68, 2015.

[153] R. S. Jabir, G. F. Ho, M. A. Anuar, and J. Stanslas, "Abstract 5563: docetaxel-induced mucositis in breast cancer patients: association with plasma alpha-1-acid glycoprotein level and SLCO1B3 genotype," *Cancer Research*, vol. 74, supplement 19, pp. 5563–5563, 2014.

[154] A. Harazono, N. Kawasaki, S. Itoh et al., "Site-specific N-glycosylation analysis of human plasma ceruloplasmin using liquid chromatography with electrospray ionization tandem mass spectrometry," *Analytical Biochemistry*, vol. 348, no. 2, pp. 259–268, 2006.

[155] M. Balmaña, A. Sarrats, E. Llop et al., "Identification of potential pancreatic cancer serum markers: Increased sialyl-Lewis X on ceruloplasmin," *Clinica Chimica Acta*, vol. 442, pp. 56–62, 2015.

[156] J.-H. Rho, J. R. Mead, W. S. Wright et al., "Discovery of sialyl Lewis A and Lewis X modified protein cancer biomarkers using high density antibody arrays," *Journal of Proteomics*, vol. 96, pp. 291–299, 2014.

[157] F. Hvid-Jensen, L. Pedersen, A. M. Drewes, H. T. Srøensen, and P. Funch-Jensen, "Incidence of adenocarcinoma among patients with Barrett's esophagus," *The New England Journal of Medicine*, vol. 365, no. 15, pp. 1375–1383, 2011.

[158] M. Titi, A. Overhiser, O. Ulusarac et al., "Development of subsquamous high-grade dysplasia and adenocarcinoma after successful radiofrequency ablation of Barrett's esophagus," *Gastroenterology*, vol. 143, no. 3, pp. 564–566.e1, 2012.

[159] A. Pierce, R. Saldova, U. M. Abd Hamid et al., "Levels of specific glycans significantly distinguish lymph node-positive from lymph node-negative breast cancer patients," *Glycobiology*, vol. 20, no. 10, pp. 1283–1288, 2010.

[160] P. J. Johnson, T. C. W. Poon, N. M. Hjelm, C. S. Ho, C. Blake, and S. K. W. Ho, "Structures of disease-specific serum alpha-fetoprotein isoforms," *British Journal of Cancer*, vol. 83, no. 10, pp. 1330–1337, 2000.

Hindawi Publishing Corporation
BioMed Research International
Volume 2015, Article ID 808531, 5 pages
http://dx.doi.org/10.1155/2015/808531

Research Article

Expression of Stem Cell Markers in Preinvasive Tubal Lesions of Ovarian Carcinoma

G. Chene,[1,2,3,4] V. Ouellet,[1,2] K. Rahimi,[1,2,5] V. Barres,[1,2] L. Meunier,[1,2] M. De Ladurantaye,[1,2] D. Provencher,[1,2,6] and A. M. Mes-Masson[1,2,7]

[1]*Centre de Recherche du Centre Hospitalier de l'Université de Montréal, Montreal, QC, Canada H2X 0A9*
[2]*Institut du Cancer de Montréal, Montreal, QC, Canada H2X 0A9*
[3]*Department of Gynecology, Hôpital Femme Mère Enfant, Hospices Civils de Lyon, 69677 Bron, France*
[4]*Université Claude Bernard Lyon 1, EMR 3738, 69000 Lyon, France*
[5]*Department of Pathology, Centre Hospitalier de l'Université de Montréal, Université de Montréal, Montreal, QC, Canada H2X 0A9*
[6]*Division of Gynecologic Oncology, Université de Montréal, Montreal, QC, Canada H2X 0A9*
[7]*Department of Medicine, Université de Montréal, Montreal, QC, Canada H2X 0A9*

Correspondence should be addressed to G. Chene; chenegautier@yahoo.fr

Received 2 April 2015; Accepted 28 July 2015

Academic Editor: Franco M. Buonaguro

In order to better understand the ovarian serous carcinogenic process with tubal origin, we investigated the expression of stem cell markers in premalignant tubal lesions (serous tubal intraepithelial carcinoma or STIC). We found an increased stem cell marker density in the normal fallopian tube followed by a high CD117 and a low ALDH and CD44 expression in STICs raising the question of the role of the stem cell markers in the serous carcinogenic process.

1. Introduction

The model of cancer genesis from stem cells is based on the principle of self-renewal of these cells, followed by their differentiation into multipotent progenitors and finally an evolution towards differentiated cancer cells. This population of cancer stem cells, probably representing less than 5% of all tumor cells, would be responsible for the degree of aggressiveness of the disease, the metastatic potential, and chemoresistance [1, 2].

Various ovarian cancer stem cell markers have been described, such as ALDH1, CD44, and CD117. ALDH1 (also known as ALDH1A1) is an enzyme involved in the metabolism of retinoic acids and probably plays a central role in cellular differentiation [3]. The retinoic acid system is involved in chromosome stability and epigenetic regulation and is probably a protective mechanism against alterations in stem cells related to oxidative stress [3]. ALDH1 is also involved in the modulation of various signalling pathways (e.g., AKT/β-catenin, WNT, and p21-p53...) which are in turn involved in the molecular regulation of cancer stem cells.

CD44 is a cell-surface glycoprotein involved in invasion and metastasis via the activation of the PI3K/AKT pathway [4, 5]. CD117 is a protooncogene (c-kit) that encodes for a tyrosine kinase receptor and plays an important role in oncogenic process such as cell proliferation and tumor development [6].

An ovarian serous carcinogenic sequence was recently described and it has been suggested that most high-grade serous ovarian cancers (HGSC) would have a tubal origin and a tubal precursor lesion called "serous tubal intraepithelial carcinomas (STICs)" could metastasize to the ovary and adjacent peritoneum [7]. We have previously demonstrated that there was an activation of the DNA damage response machinery in STICs which could consequently trigger the invasive carcinogenic process [8, 9]. Of note, little is known about the stem cell profile of STICs. A recent study has demonstrated that the loss of ALDH1A1 is associated with tumor progression from STIC to HGSC [10]. In order to further validate this finding, we have included additional stem cell-associated markers in a cohort of STICs and HGSC in order to describe their expression along the neoplastic continuum.

2. Material and Method

2.1. Patients and Clinical Data. Tissue samples were obtained from patients who underwent surgery between 1993 and 2012 for either prophylactic salpingo-oophorectomy or ovarian cancer at the Division of Gynecologic Oncology (Centre hospitalier de l'Université de Montréal (CHUM), Hôpital Notre-Dame). All patients gave consent for the banking and use of their tissue samples and clinical data (SARDO database). The ethic review board at the CHUM approved the study.

2.2. Tissue Microarray (TMA) Construction. A pathologist specialised in gynecologic oncology reviewed all cases. STICs were defined by presence of nonciliated cells exhibiting high immunohistochemical expression of TP53 and Ki67 and the presence of 3 or more of the following features: abnormal chromatin pattern, nuclear enlargement, marked nuclear pleomorphism, epithelial stratification, and/or loss of polarity or nuclear molding [7]. Areas of interest were circled on the H&E section and a representative core (0.6 mm) of each specimen was arrayed on a receiver paraffin block using the MArrayer (Pathology Devices). Due to the small size of STIC lesions, only one core was arrayed on the TMA. TMAs were cut at 5 μm thickness and sections were laid onto Superfrost + glass slides. Once completed, a TMA section was stained with hematoxylin-eosin to receive a final pathology review.

The TMA included 21 benign-appearing fallopian tubes, 21 STICs (from the same patients as the benign-appearing fallopian tubes), 17 HGSC from patients with STICs (associated ovarian cancer or AOC), and 30 HGSC without STICs (non-AOC). Only chemonaive cases from patients without any BRCA germline mutation were considered for this study.

2.3. Western Blot. The specificity of each antibody was assessed by Western blot using PC3, DU145, LNCaP, OVCAR 3 cell lines, benign prostatic (RWPE), and benign ovarian cells (BOV 2655G and BOV 2567D). Antibody conditions were defined using an optimisation TMA containing cell pellets of cancer cell lines from several origins including prostate (LNCaP, DU145, and PC3), ovary (OV90, SKOV3, TOV1946, and TOV81D), and breast (MCF-7), in addition to benign prostatic cells (RWPE), Hela cells (irradiated and nonirradiated cells), Jurkat cells, and benign tubal cores.

2.4. Immunohistochemistry. Staining of all antibodies was performed using the Benchmark XT autostainer (Ventana Medical System Inc.). Antigen retrieval was performed with Cell Conditioning 1 (Ventana Medical System Inc., number 950-124) during 30 or 60 minutes for most antibodies although the Cell Conditioning 2 (Ventana Medical System Inc., number 950-124) was used for TP53. Prediluted antibodies were manually added to the slides and incubated at 37°C for 20 to 60 minutes. The following antibodies and dilutions were used: Ki67 (1 : 500; Clone SP6, RM-9106, NeoMarkers), p53 (1 : 200; Clone DO-1, sc-126, Santa Cruz Biotechnologies), ALDH1 (1 : 400, Clone 44/ALDH, 611194, BD transduction lab), CD44 (1 : 100, Clone 2F10, BBA13, RD System), and CD117 (1 : 200, c-kit, Dako). Staining was revealed using the UltraView universal DAB detection kit (Ventana Medical System Inc., 760-500). Counterstaining was achieved with hematoxylin and bluing reagent (Ventana Medical System Inc., number 760-2021 and number 760-2037). Substitution of the primary antibody with phosphate-buffered saline served as a negative control. All sections were scanned using a VS-110 microscope with a 20x 0.75NA objective with a resolution of 0.3225 μm (Olympus). Images were analysed with the OlyVIA software (Olympus).

2.5. Scoring and Statistical Analysis. Protein expression was scored according to the extent (as a percentage of cells of interest) and intensity (value of 0 for absent, 1 for low, 2 for moderate, and 3 for high) of staining based on no-automated visualization and a previously described semiquantitative score was used [11]. All slides were independently scored in a blind manner by 2 observers and interrating agreement was >80%. In case of differences between the two scorings, the core was reevaluated to reach a consensus. Statistical analyses were performed using SPSS Statistics 20 software (IBM). The nonparametric Mann-Whitney U test was used to compare protein expression between groups. A p value below 0.05 was considered as statistically significant.

3. Results

As expected, CD117 and CD44 expression were cytoplasmic and membranous in epithelial tissues. Cytoplasmic staining was seen for ALDH1 protein in both epithelium and stroma. The uniform ALDH1 expression in stromal cells constituted an internal control. TP53 and Ki67 expression were nuclear and were used to confirm the diagnosis of STICs. Briefly, STICs were characterized by an intense and diffuse expression of TP53 with a moderate to high Ki67 proliferative index. Expression of TP53 and Ki67 was absent in benign-appearing fallopian tubes whereas it was intense and higher in AOC and non-AOC.

ALDH1A staining was detected in both secretory and ciliated cells of all the 21 benign-appearing fallopian tubes (long and discontinuous stretches of high immunoreactivity) whereas the level of expression of ALDH1 was significantly lower in STICs, AOC, and non-AOC ($p = 0.001$) (see Table 1 and Figure 1). Interestingly, there were rare positive cells with high ALDH1 expression in 3 STICs; there was also a CD117 and CD44 overexpression in these same cells (see Figure 2). CD117 expression level was as high as in benign tube (located in both secretory and ciliated cells) and AOC but significantly lower in non-AOC ($p = 0.01$). While there appeared to be an increase in the CD117 positive cells in the STICs compared to fallopian tube epithelium, this difference was not statistically significant (Table 1).

The expression level of CD44 was weak or absent in most specimens. However, expression was significantly lower in non-AOC as compared to benign tubes, STICs, and AOC ($p = 0.001$).

Finally, differences in immunohistochemical profiles between AOC and non-AOC were also noted (Table 1).

Table 1: Protein expression of ALDH1, CD44, and CD117 in the epithelial compartment of normal-appearing fallopian tubes, STICs, AOC (associated carcinoma with STICs), and non-AOC (ovarian carcinoma without STICs).

	Normal-appearing fallopian tube ($n = 21$)	STICs ($n = 21$)	AOC ($n = 17$)	Non-AOC ($n = 30$)
ALDH1 mean scores ± St error	47 ± 7.42	10.37 ± 5.01	7.41 ± 3.02	1.93 ± 0.88
CD117 mean scores ± St error	48.11 ± 9.33	58.29 ± 9.96	44.27 ± 10.95	16.08 ± 4.47
CD44 mean scores ± St error	23.63 ± 7.52	17.24 ± 8.23	13.33 ± 4.74	1.72 ± 4.19

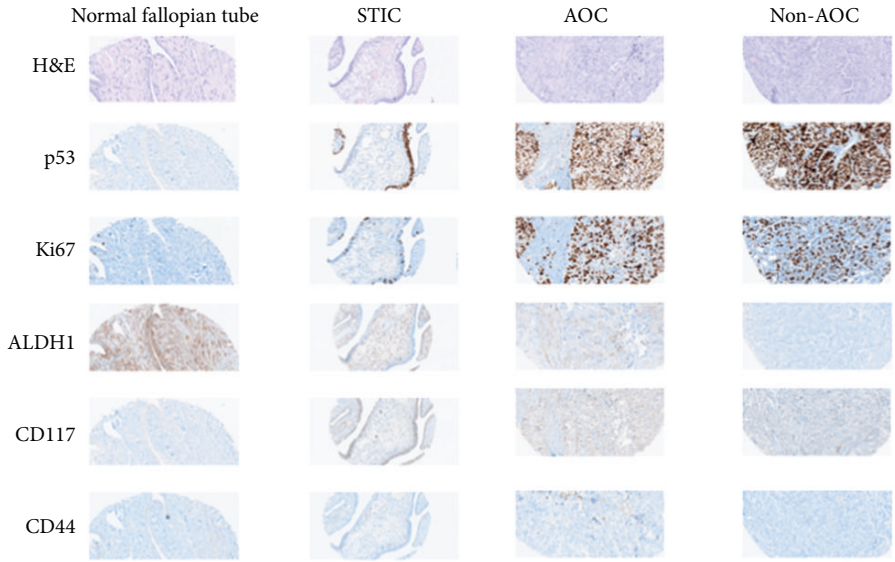

Figure 1: Immunoprofiles of p53, Ki67, ALDH1, CD44, and CD117 in normal-appearing fallopian tube, STIC, AOC (associated carcinoma with STICs), and non-AOC (carcinoma without STICs). STICs are defined by an intense and diffuse expression of TP53 with a moderate to high Ki67 proliferative index. Expression of TP53 and Ki67 is absent in benign-appearing fallopian tubes whereas it is intense and higher in AOC and non-AOC. ALDH1A and CD117 staining is detected in both secretory and ciliated cells of the benign-appearing fallopian tubes. The level of ALDH1 expression is significantly lower in STICs, AOC, and non-AOC than in normal fallopian tube. CD117 expression level is as high as in benign tube and AOC but significantly lower in non-AOC. There is also an increase in the CD117 positive cells in the STICs compared to fallopian tube epithelium. The expression level of CD44 was weak or absent in most specimens. However, expression is significantly lower in non-AOC than in benign tubes, STICs, and AOC.

4. Discussion

The recent establishment of STICs as precursor lesions for HGSC opens up new horizons in the understanding of ovarian carcinogenesis and could lead to the development of new screening and/or early prevention strategies [7]. Historically, the origin of ovarian cancer was thought to be ovarian from the ovarian surface epithelium. This was followed by a paradigm shift with the establishment of a tubal origin of most HGSC. Indeed, these cancers may originate in the epithelium of the fimbriae. A lesion named STICs (located almost always in the fimbriae) has recently been reported in prophylactic salpingo-oophorectomies for BRCA mutation as well as in the tubal fimbriae from women with sporadic nonhereditary HGSC. There is a molecular lesional continuity between STICs and ovarian cancer with identical mutations of TP53 [9, 12]. STICs are also characterised by an important genetic instability as shown by the overexpression of the marker of double-strand DNA breaks γH2AX [9]. In this new serous carcinogenic sequence, there may be metastasis exfoliation from STICs to the adjacent ovary and the peritoneum [12]. Little is known about the molecular pathways of STICs.

Regulation of noncancerous stem cells is a complex balance between cellular proliferation, cellular differentiation, and cell death via various signaling pathways including Sonic Hedgehog Shh, Notch, and Wnt. If a deregulation of these signalling pathways is associated with certain mutations, this could result in carcinogenesis due to the appearance of cancer stem and progenitor cells. Deregulation in these signalling pathways is associated with mutations providing the affected cell with stem/progenitor cells characteristics leading to carcinogenesis. Such mutations represent one of the major alterations that might explain the different histological types found in ovarian cancers. Indeed, cancer stem cells and progenitor cells bearing p53 mutations and BRCA (BRCA mutations in genetic cases or BRCA functional abnormalities in sporadic cases) would result in serous tumors and those with β-catenin and PTEN would lead to endometrioid tumors. Less is known in the mutations leading to mucinous and clear cell histotypes but p53 seems to be a trigger [2].

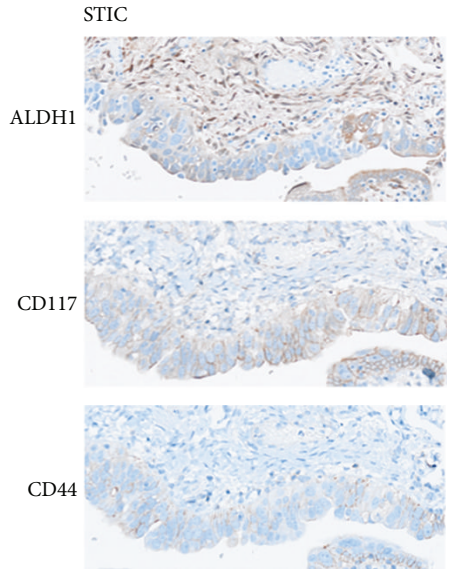

Figure 2: ALDH1, CD117, and CD44 overexpression in some cells of a STIC lesion, suggesting a possible and specific location for stem cells within these lesions and a possible stem cell niche.

The parallel with breast cancer could be suggestive because of the epidemiological and molecular relationship with the ovarian cancer. This type of association was also found in breast cancer where experimental and *in vitro* works demonstrate that BRCA1 is a mammary stem and progenitor cells regulator, allowing their differentiation into mature luminal and myoepithelial cells [13, 14]. BRCA1 mutations would result in overexpression of ALDH1 at mammary cell level and would prevent differentiation of these stem cells [14]. Since BRCA1 is also involved in DNA repair and genomic stability, it has been proposed that BRCA mutations or functional abnormalities would result in accumulation of genetically unstable mammary stem cells and thus a step towards breast cancer [15, 16].

The highest ALDH1 expression is found in the normal-appearing fallopian tube in our study. Auersperg [17] studied the stem cell profile of oviductal fimbriae with 5 stem cell markers (NANOG, SFRP1, LHX9, ALDH1A1, and ALDH1A2); the author found that the fimbriae express the stem cell markers (mainly ALDH1A1, also known as ALDH1) and concluded that the fallopian tube may be pluripotent with the capacity to generate cancer stem cells. Similarly, another study found that stemlike cells (epithelial cell adhesion molecule, CD44, and integrin $\alpha 6$) are concentrated in the fimbriated distal end of the tube [18]. The results indicate that STICs may express CD44 and KRT 5 suggesting that these cells may play a role in the initiation of HGSC. However, while we agree with the probable biological adaptation for repair (due to genotoxic stress during ovulation) in the normal fallopian tube, we and others [10] did not find an increase in expression of all the stem cells in STICs: ALDH1 and CD44 expressions were low in STICs whereas we found a more elevated CD117 expression in STICs compared with the normal-appearing fallopian tube (despite the absence of a statistical difference).

Our results are in line with those of Chui et al. [10] where high expression of ALDH1 was noted in normal tubal epithelial cells (29 cases), and then there was an absence of expression in STICs (17 cases). The authors concluded that loss of ALDH1 expression may be an early event in ovarian carcinogenesis which is subsequently turned off later in the process [19]. However, we found some cases with rare positive cells with high ALDH1, CD117, and CD44 expression in STICs, suggesting a possible and specific location for stem cells within these lesions and a possible stem cell niche.

In the other cases where ALDH1 expression is low in STICs, the explanation could be that ALDH1 is not directly involved in the development of STICs. On the contrary, the high expression of CD117 in STICs could mean that CD117 is specifically involved in the pathogenesis and the development of cancer stem cells in STICs. Because kinase inhibitors (such as imatinib mesylate, sunitinib, nilotinib, or dasatinib) target the CD117 positive tumors, other studies are still needed to explore the stem cell profile of the serous tubal carcinogenic sequence [6].

Finally, we have found some differences in the patterns of ALDH1, CD44, and CD117 staining between AOC and non-AOC. In our previous immunohistochemical study on DNA damage signalling and apoptosis in preinvasive tubal lesions, we also highlighted differences between AOC and non-AOC. We hypothesize that AOC and non-AOC may not represent the same lesions. Indeed, these results are intriguing as it can be argument that HGSC could have a dual origin (tubal or ovarian origin) that represents with distinct molecular profiles [9].

5. Conclusions

There is emerging evidence that most of HGSC arise from the fallopian tube, especially those associated with STIC lesions [7]. The clinical and pathological significance of stem cells in STICs remains unresolved. It seems that the increased stem cell marker density in the normal fallopian tube may contribute to the carcinogenic process resulting in a low ALDH and CD44 expression in STICs. There could be also an on-off effect of ALDH1 expression during the cancer disease process [19]. Our results hint at the presence of a specific stem cell niche in STICs. In clinical point of view, the higher CD117 expression and the AHDH1 extinction in STICs could be of interest as specific targets [19, 20].

Conflict of Interests

The authors have no conflict of interests regarding the publication of this paper.

Authors' Contribution

G. Chene, D. Provencher, and A. M. Mes-Masson conceived the study, participated in its design and coordination, and helped to draft the paper. G. Chene, V. Ouellet, K. Rahimi, V. Barres, L. Meunier, and M. De Ladurantaye carried out the immunohistochemical analysis and the construction of

the TMA. G. Chene validated all antibodies using Western blot. All authors read and approved the final paper.

Acknowledgments

This research was supported by funding through the Institut du cancer de Montreal and a grant by the Institut du cancer de Montreal (Spyder Defi Initiative). The Centre de Recherche du Centre Hospitalier de l'Université de Montréal received support from the Fonds de Recherche du Québec-Santé (FRQS). Tumor banking was supported by the Banque de Tissus et Données of the Réseau de Recherche Sur le Cancer of the FRQS associated with the Canadian Tumor Repository Network (CTRNet).

References

[1] M. P. Ponnusamy and S. K. Batra, "Ovarian cancer: emerging concept on cancer stem cells," *Journal of Ovarian Research*, vol. 4, pp. 1–9, 2008.

[2] S. Dyall, S. A. Gayther, and D. Dafou, "Cancer stem cells and epithelial ovarian cancer," *Journal of Oncology*, vol. 2010, Article ID 105269, 9 pages, 2010.

[3] C. Ginestier, J. Wicinski, N. Cervera et al., "Retinoid signaling regulates breast cancer stem cell differentiation," *Cell Cycle*, vol. 8, no. 20, pp. 3297–3302, 2009.

[4] M. M. Shah and C. N. Landen, "Ovarian cancer stem cells: are they real and why are they important?" *Gynecologic Oncology*, vol. 132, no. 2, pp. 483–489, 2014.

[5] J. Zhang, B. Chang, and J. Liu, "CD44 standard form expression is correlated with high-grade and advanced-stage ovarian carcinoma but not prognosis," *Human Pathology*, vol. 44, no. 9, pp. 1882–1889, 2013.

[6] M. Medinger, M. Kleinshmidt, K. Mross et al., "C-kit (CD117) expression in human tumors and its prognostic value: an immunohistochemical analysis," *Pathology and Oncology Research*, vol. 16, no. 3, pp. 295–301, 2010.

[7] G. Chene, J. Dauplat, N. Radosevic-Robin, A. Cayre, and F. Penault-Llorca, "Tu-be or not tu-be: that is the question… About serous ovarian carcinogenesis," *Critical Reviews in Oncology/Hematology*, vol. 88, no. 1, pp. 134–143, 2013.

[8] G. Chene, A. Tchirkov, E. Pierre-Eymard et al., "Early telomere shortening and genomic instability in tubo-ovarian preneoplastic lesions," *Clinical Cancer Research*, vol. 19, no. 11, pp. 2873–2882, 2013.

[9] G. Chene, V. Ouellet, K. Rahimi et al., "DNA damage signaling and apoptosis in preinvasive tubal lesions of ovarian carcinoma," *International Journal of Gynecological Cancer*, vol. 25, no. 5, pp. 761–769, 2015.

[10] M. H. Chui, Y. Wang, R.-C. Wu et al., "Loss of ALDH1A1 expression is an early event in the pathogenesis of ovarian high-grade serous carcinoma," *Modern Pathology*, vol. 28, pp. 437–445, 2015.

[11] V. Ouellet, M.-C. Guyot, C. Le Page et al., "Tissue array analysis of expression microarray candidates identifies markers associated with tumor grade and outcome in serous epithelial ovarian cancer," *International Journal of Cancer*, vol. 119, no. 3, pp. 599–607, 2006.

[12] E. Kuhn, R. J. Kurman, and I. M. Shih, "Ovarian cancer is an imported disease: fact or fiction?" *Current Obstetrics and Gynecology Reports*, vol. 1, no. 1, pp. 1–9, 2012.

[13] W. D. Foulkes, "BRCA1 functions as a breast stem cell regulator," *Journal of Medical Genetics*, vol. 41, no. 1, pp. 1–5, 2004.

[14] S. Liu, C. Ginestier, E. Charafe-Jauffret et al., "BRCA1 regulates human mammary stem/progenitor cell fate," *Proceedings of the National Academy of Sciences of the United States of America*, vol. 105, no. 5, pp. 1680–1685, 2008.

[15] M. R. H. van Voss, P. van der Groep, J. Bart, E. van der Wall, and P. J. van Diest, "Expression of the stem cell marker ALDH1 in the normal breast of BRCA1 mutation carriers," *Breast Cancer Research and Treatment*, vol. 123, no. 2, pp. 611–612, 2010.

[16] C. Ginestier, M. H. Hur, E. Charafe-Jauffret et al., "ALDH1 is a marker of normal and malignant human mammary sterm cells and a predictor of poor clinical outcome," *Cell Stem Cell*, vol. 1, no. 5, pp. 555–567, 2007.

[17] N. Auersperg, "The stem-cell profile of ovarian surface epithelium is reproduced in the oviductal fimbriae, with increased stem-cell marker density in distal parts of the fimbriae," *International Journal of Gynecological Pathology*, vol. 32, no. 5, pp. 444–453, 2013.

[18] D. Y. Paik, D. M. Janzen, A. M. Schafenacker et al., "Stem-like epithelial cells are concentrated in the distal end of the fallopian tube: a site for injury and serous cancer initiation," *Stem Cells*, vol. 30, no. 11, pp. 2487–2497, 2012.

[19] G. Chene, A. Cayre, I. Raoelfils, N. Lagarde, J. Dauplat, and F. Penault-Llorca, "Morphological and immunohistochemical pattern of tubo-ovarian dysplasia and serous tubal intraepithelial carcinoma," *European Journal of Obstetrics Gynecology and Reproductive Biology*, vol. 183, pp. 89–95, 2014.

[20] G. Chene, N. Radosevic-Robin, A. S. Tardieu et al., "Morphological and immunohistochemical study of ovarian and tubal dysplasia associated with tamoxifen," *European Journal of Histochemistry*, vol. 58, no. 2, pp. 112–119, 2014.

Hindawi Publishing Corporation
BioMed Research International
Volume 2015, Article ID 921435, 10 pages
http://dx.doi.org/10.1155/2015/921435

Review Article

Predictive Biomarkers to Chemoradiation in Locally Advanced Rectal Cancer

Raquel Conde-Muíño,[1] Marta Cuadros,[2] Natalia Zambudio,[1] Inmaculada Segura-Jiménez,[1] Carlos Cano,[3] and Pablo Palma[1]

[1]*Division of Colon & Rectal Surgery, University Hospital Virgen de las Nieves, Spain*
[2]*Department of Biochemistry, University of Granada, Spain*
[3]*Department of Computer Science and Artificial Intelligence, University of Granada, Spain*

Correspondence should be addressed to Pablo Palma; pablopalma@andaluciajunta.es

Received 1 April 2015; Accepted 10 August 2015

Academic Editor: Pierre Hainaut

There has been a high local recurrence rate in rectal cancer. Besides improvements in surgical techniques, both neoadjuvant short-course radiotherapy and long-course chemoradiation improve oncological results. Approximately 40–60% of rectal cancer patients treated with neoadjuvant chemoradiation achieve some degree of pathologic response. However, there is no effective method of predicting which patients will respond to neoadjuvant treatment. Recent studies have evaluated the potential of genetic biomarkers to predict outcome in locally advanced rectal adenocarcinoma treated with neoadjuvant chemoradiation. The articles produced by the PubMed search were reviewed for those specifically addressing a genetic profile's ability to predict response to neoadjuvant treatment in rectal cancer. Although tissue gene microarray profiling has led to promising data in cancer, to date, none of the identified signatures or molecular markers in locally advanced rectal cancer has been successfully validated as a diagnostic or prognostic tool applicable to routine clinical practice.

1. Introduction

Colorectal cancer is the third most frequent cancer and the second most frequent cause of cancer related death, both in Europe [1]. The proportion of rectal cancer cases is variable depending on the cancer registry and classification of rectosigmoid tumours, ranging from 27% to 58% [2]. The ideal treatment recommendations for rectal cancer are under permanent appraisal; nevertheless, studies have demonstrated that, for locally advanced rectal cancer (LARC) (stage T3, stage T4, or node-positive disease), preoperative (neoadjuvant) chemoradiation (CRT) significantly improves local control and reduces toxicity profiles compared with postoperative CRT but with similar survival rates [3, 4]. Furthermore, the ability to achieve pathologic downstaging, or a complete pathologic response (pCR), after neoadjuvant CRT is correlated with improved survival, decreased local recurrence, and a higher rate of sphincter-preserving surgeries [5]. Approximately 40–60% of LARC patients treated with neoadjuvant CRT achieve some degree of pathologic response. However, there is no effective method of predicting which patients will respond to neoadjuvant CRT [6]. Prospective identification of patients who have a higher likelihood of responding to preoperative CRT could be important in deceasing treatment morbidity and improving survival and local control in LARC. In addition, patients who are unlikely to respond could be offered alternative approaches to therapy. Recent studies have evaluated the potential of genetic biomarkers to predict outcome in LARC treated with neoadjuvant CRT [7, 8]. The goal of this review is to examine the current literature for the most commonly researched biomarkers for predicting outcome to neoadjuvant CRT in LARC patients.

2. Material and Methods

An exhaustive search of PubMed was performed on March, 2014, with combinations of the following terms: "rectal cancer," "response," "prediction," "microarray," "gene expression," "mi-RNA," and "ln- RNA." The articles produced by the PubMed search were reviewed for those specifically addressing a genetic profile's ability to predict response to neoadjuvant CRT in LARC (genes, microRNA, or long noncoding RNA). Articles analysing response prediction to CRT in colorectal cancer cell lines were excluded. Sixteen studies evaluating genetic profiles predicting outcome of neoadjuvant CRT in rectal cancer were found. Ten of them identified an over- or downregulated gene signature, 5 found microRNA (miRNA) signature. Only one screened long noncoding RNA (lncRNA) was associated with radiosensitivity but was made in colorectal cancer cell lines and was written in Chinese and therefore was excluded.

3. Results

3.1. Prediction of Response Based on DNA Microarrays in Tumor Tissue (prior to Neoadjuvant Treatment) (Table 1). The first study on the application of a genetic signature to predict response to neoadjuvant treatment in rectal cancer appeared in 2005 [9]. It included 30 patients from a data base pertaining to the German Group for the Study of Rectal Cancer [22] who received preoperative chemoradiation therapy (50.4 Gy of radiation, applied in 28 fractions and continuous infusion of 5FU). They underwent surgery 6 weeks following completion of the neoadjuvant therapy. Response to treatment was measured by the following: tumor shrinkage (when compared with a preoperative ultrasound scan, uT) and the stages of tumor remission under Dworak's regression grades (3-4 considered to be responders) [23]. Based on *downsizing* or tumor shrinkage they identified 54 genes expressed differently between responders versus nonresponders in tumor samples extracted prior to neoadjuvant therapy. By using these genes they attained 83% precision in the prediction, both for responders and nonresponders, thus proving that the study of genetic expression through *microarrays* was useful in predicting a reduction in tumor size (measured by the decrease of ypT in relation to uT) in response to preoperative CRT therapy. These 54 genes are involved in many biological functions, including repairing damage to cellular DNA (SMC1), organizing microtubules (CLMN and CDC42BPA), and cellular signaling (FLNB).

The following year a Japanese group with a similar objective, published a *microarray* analysis of DNA [10] that analyzed a total of 52 patients. Neoadjuvant therapy consisted of preoperative radiotherapy (50.4 Gy) without any chemotherapy, followed by a four-week rest period and then surgery. The evaluation of response was determined based on an anatomical pathological analysis of the surgical sample, employing a Japanese semiquantitative scale that identified stages 2-3 as responders and stages 0-1 as nonresponders. A group of 33 differentially expressed genes was established among responders and nonresponders: 20 were overexpressed genes related to apoptosis such as lumican (LUM), thrombospondin 2 (THBS2), and galectin-1 (LGALS1), while 13 were repressed in the responder-group, such as cyclophilin 40 (CYP40) and glutathione peroxidase 2 (GPX2). A protein structure prediction was then done on 33 genes from 17 patients included in the validation group, which found 82.4% exactness for determining class, 50% sensibility, 100% specificity, a positive predictive value of 100%, and a negative predictive value of 76.6%.

Kim and colleagues conducted a study in 2007 using samples from 46 patients (31 for the initial trial group and 15 for the validation) [11]. Neoadjuvant treatment included radiotherapy (50.4 Gy in 28 fractions) and chemotherapy (5FU + leucovorin, capecitabine or capecitabine + irinotecan). Patients underwent surgery 6 weeks after completion of treatment; tumor response was classified according to Dworak's tumor regression grade system. They identified a group of 95 genes and applied the *leave-one-out-cross-validation* (LOOCV) method to predict response and found that this group of genes enabled tumor response to be predicted with 84% precision, 64% sensibility, 95% specificity, an 88% positive predictive value and an 87% negative predictive value. The validation group reached 87% precision, 100% sensibility, and 82% specificity. Two of the 95 genes stood out: thymidylate synthase (TYMS, involved in DNA synthesis), which was highly expressed in responding tumors, and RAD23B (involved in nucleotide excision repair), which was elevated in nonresponders and has previously been associated with patients resistant to treatment with 5FU. These two genes could be used to evaluate response to treatment with 5FU.

Rimkus et al. [12] also studied the tumor biopsies of patients in stage T3. The therapeutic approach used involved radiation (45 Gy) and continuous infusion of 5FU. Surgery was done following a 4–6-week rest period. The anatomical pathological response was classified according to Becker's regression grade (responders in stage 1 and nonresponders in stages 2-3). They found 42 statistically significant genes that were expressed differently among responders and nonresponders. Five of them (FREM1, M-RIP, SDHC, TDE1, and USP42) had a reduced expression in the group of responders, while the rest of the genes were overexpressed and involved in apoptosis (CASP1), transport (SLC35E1), cellular signaling (STAT2 and ETS2), and cellular cycle (CCNK). Sensibility was 71%, specificity was 86%, positive predictive value was 71%, and negative predictive value was 86%.

More recently, a group formed by Nishioka and colleagues [13] included 20 patients (17 in a trial group and 3 in the validation unit) who received radiotherapy (40 Gy in fractions of 2 Gy), associated with S1, an oral chemotherapeutic agent whose action is similar to capecitabine, not currently authorized for use in Europe. They used a response scale from the Japanese Society for Cancer of the Colon and Rectumthat classified patients in groups 0-1 as nonresponders and those in groups 2-3 as responders. A *microarray* of 132 genes related to a response to 5FU was used in addition to other chemotherapeutics. Researchers identified 17 genes expressed differently among the two patient subgroups (responders versus nonresponders). Of them, five were metalloproteinases (MMP1, MMP7, MMP9, MMP14, and MMP16). In addition, they conducted an immunological and histological chemical

Table 1: Studies showing DNA microarray gene expression profile predictive of response to CRT in LARC.

Study	Specimen	*N* patients	Validation group	*Radiotherapy dose* Chemotherapy	Response assessment	Identified genes: more relevant genes	Outcome
Ghadimi et al. 2005 [9]	Tumor tissue biopsy	30	No	*50.4 Gy/28 fractions* 5FU	*Downsizing*	54 genes: SMC1, CLMN, CDC42BPA, and FLNB	Group prediction 83%
Watanabe et al. 2006 [10]	Tumor tissue biopsy	52	17	*50.4 Gy* —	Japanese Classification of Colorectal Carcinoma	33 genes (i) Overexpressed: LUM, THBS2, and LGALS1 (ii) Downregulated: CYP40 and GPX2	Class prediction 82.4%, sensitivity 50%, specificity 100%, PPV 100%, NPV 76.6%
Kim et al. 2007 [11]	Tumor tissue biopsy	31	15	*50.4 Gy/28 fractions* 5FU + LV/capecitabine/ capecitabine + irinotecan	Dworak regression grade	95 genes: TYMS and RAD23B	Precision 87%, sensitivity 100%, specificity 82%
Rimkus et al. 2008 [12]	Tumor tissue biopsy	43	No	*45 Gy* 5FU	Becker regression grade	42 genes (i) Overexpressed: CASP1, SLC35E1, CCNK, STAT2, and ETS2 (ii) Downregulated: TDE1, USP42, M-RIP, and FREM1	Accuracy 81%, sensitivity 71%, specificity 86%, PPV 71%, NPV 86%
Nishioka et al. 2011 [13]	Tumor tissue biopsy	17	3	*40 Gy/20 fractions* S1	Japanese Classification of Colorectal Carcinoma	17 genes: MMP7, MMP14, MMP9, MMP1, MMP16, and RRM1	
Casado et al. 2011 [14]	Tumor tissue biopsy formalin-fixed paraffin-embedded biopsies	25 94		*50.4 Gy/28 fractions* 25 oxaliplatin + raltitrexed 94 different treatment	Dworak regression grade	24 genes: genetic profile of 13: (i) 6 overexpressed: ALDH1A1, CDKN1 1, FOS, RELB, STAT3, and TFF3 (ii) 7 downregulated: BAK, MLH1, TYMS, CKB, GPX2, HIG2, and PH-4	Nonresponders: accuracy 86%, sensitivity 87%, specificity 82%
Palma et al. 2013 [8]	Blood sample	27	8	*50.4 Gy/28 fractions* Capecitabine/capecitabine + oxaliplatin	Mandard regression grade	8 genes: FALZ	
Palma et al. 2014 [7]	Tumor tissue biopsy	26	8	*50.4 Gy/28 fractions* Capecitabine/capecitabine + oxaliplatin	Mandard regression grade	257 genes: c-MYC, GNG4, POLA, and RRM1	Accuracy 85%, sensitivity 60%, specificity 100%, PPV 100%, NPV 80%
Gantt et al. 2014 [15]	Tumor tissue biopsy	36	10	*50.4 Gy/30 fractions* 5FU	American Joint Committee on Cancer	183 genes up- and downregulated: RAD50	No response: sensitivity 33%, specificity 100%
Watanabe et al. 2014 [16]	Tumor tissue biopsy	46	16	*50.4 Gy/28 fractions* Tegafur-uracil + leucovorin	Japanese Classification of Colorectal Carcinoma	22 probes (18 genes): signature LRRIQ3, FRMD3, SAMD5, and TMC7	Accuracy 81.3%, sensitivity 100%, specificity 62.5%, PPV 72.7%, NPV 100%

study to evaluate expression of the MMP7 protein, whose gene was the one most overexpressed in normal tissue. Among responders, four patients overexpressed MMP7 (4/10, 40%), while none in the group of nonresponders expressed that protein. These 17 genes were used to classify samples from the validation group and were correct in three cases. It is worth emphasizing that in the nonresponder case none of the genes were overexpressed.

Our group [7] identified a 4-gene profile (C-MYC, GNG4, POLA, and RRM1) associated with response to preoperative chemoradiotherapy in rectal cancer patients. The microarrays study included a total of 35 patients with LARC with additional 8 patients in the validation group. Tumor samples were prospectively obtained before treatment (total dose of 50.4 Gy of radiation in 28 fractions of 1.8 Gy associated with capecitabine alone or capecitabine combined with oxaliplatin). Tumor response was assessed in surgical specimens by pathological examination based on Mandard's tumor regression grading (TRG) system [24]: TRG 1 and TRG 2 scores were considered responders, whereas TRG 3, TRG 4, and TRG 5 scores were classified as nonresponders. To validate microarray experimental data, expression levels of 20 genes in rectal tumor patients were obtained by real-time quantitative reverse transcription PCR. 257 genes were overexpressed in responders, but only 4 were confirmed with PCR. High expression levels of the 4 genes (Gng4, c-Myc, Pola1, and Rrm1) were a significant prognostic factor for response to treatment in LARC patients. Using this gene set, a new model for predicting the response to CRT in rectal cancer was established with a sensitivity of 60% and 100% specificity. For each of the genes Gng4, c-Myc, Pola1, and Rrm1, receiver operating characteristic (ROC) curves were computed. The one with the higher AUC was c-Myc, with a sensitivity of 70% and a specificity of 100% at a cut-off point set at 64.45. Functional analysis showed that the encoding proteins were associated with several canonical pathways (pyrimidine and purine metabolism, colorectal cancer metastasis signalling). The most significant network consisting of 49 genes contained 24 focus genes directly or indirectly connected to a c-Myc network.

Granttet published a study in 2014 using high-throughput nucleotide *microarrays* to develop a genetic profile associated with CRT-resistant rectal cancer. Thirty-three patients were incorporated in the study [15]. Patients who met clinical criteria for neoadjuvant CRT underwent biopsy of the tumour. The treatment regimen included 50.4 Gy radiation in 30 fractions with 5-fluorouracil. Patients underwent curative surgery approximately 8–10 weeks after completion of CRT. Posttreatment responses were assessed according to the American Joint Committee on Cancer (AJCC) criteria considering patients with AJCC 0–2 as responders and those with AJCC 3 as nonresponders. They identified a unique gene expression profile composed of 812 genes associated with rectal cancer that had a poor response to CRT. This profile enabled the classification of nonresponders with 100% accuracy in a small validation group (sensitivity and specificity of 100% for predicting nonresponders). Using the 183-gene profile, specificity remained 100%, while sensitivity decreased to 33.3%. The top 10 upregulated genes included APOA2, AHSG, DBH, APOA1, APOB, APOC3, LMX1A, SOAT2, SLC7A9, and TF. The top 10 downregulated genes included LOC729399, SERINC5, SCNN1B, ZC3H6, SLC4A4, DTWD2, MS4A12, BEX5, MMRN1, and CLCA4. Functional analysis of differentially expressed genes with IPA software (Ingenuity Pathways Analysis) revealed "DNA repair by homologous recombination" as a statistically significant canonical pathway in this study with RAD50 as the most significant differentially expressed gene in this pathway. RAD50 is a member of the MRE11-RAD50-NBS1 (MRN) complex that detects double-stranded DNA breaks and regulates DNA damage repair primarily through homologous recombination. A number of apolipoprotein genes were upregulated in nonresponders (APOA2, APOA1, APOB, and APOC3). AHSG is a serum glycoprotein involved in endocytosis, brain development, and the formation of bone tissue previously associated with resistance to neoadjuvant chemotherapy in patients with advanced breast cancer. LMX1A is known to be involved in insulin gene transcription and the embryogenesis of dopamine-producing neurons. In cancer, LMX1A has been shown to be a poor prognostic indicator in ovarian and pancreatic tumors but LMX1A was also recently shown to inhibit cell proliferation, migration, invasion, and colony formation in vitro.

Recently, Watanabe conducted a new study to establish a prediction model for response to chemoradiotherapy in rectal cancer based on gene expression by RT-PCR analysis as it allows accurate and reproducible quantification of genes [16]. Biopsy specimens were collected before preoperative treatment (50.4 Gy in 28 fractions during 6 weeks concomitantly with tegafur-uracil and leucovorin). Standardized curative resection was performed 6 weeks after the completion of chemoradiotherapy. Response to chemoradiotherapy was determined by histopathological examination of surgically resected specimens based on a semiquantitative classification system defined by the Japanese Society for Cancer of the Colon and Rectum. Tumors were classified as "nonresponders" when assigned to grade 0 or grade 1 and "responders" when assigned to regression grade 2 or grade 3. First, gene expression profiles were determined by DNA microarray analysis on 46 training samples. They identified 24 probes that were differentially expressed between responders and nonresponders. Twenty genes showed higher and four genes showed lower expression in nonresponders compared with responders. Microarray expression levels were validated by quantitative RT-PCR of 18 genes (that were represented among the 24 probes) in the 46 training samples, showing significant differences in the expression levels of 16 of the 18 genes (20 probes) between responders and nonresponders. Based on the 16 genes and their combination, the predictive accuracies of the 2500 different sets of predictor genes were calculated. The highest accuracy rate (89.1%) was obtained with a 4-gene set including LRRIQ3, FRMD3, SAMD5, and TMC7. This 4-gene signature was validated in an independent cohort of 16 patients. Predictive accuracy rate was 81.3% and sensitivity, specificity, positive predictive value, and negative predictive value were 100%, 62.5%, 72.7%, and 100%, respectively.

3.2. Prediction of Response Based on Microarrays of Gene Expression in Peripheral Blood. Peripheral blood mononuclear cells have emerged recently as pathology markers of cancer and other diseases, making their use as therapy predictors possible. Furthermore, the importance of the immune response in radiosensitivity of solid organs led Palma et al. [8] to hypothesize that microarray gene expression profiling of peripheral blood mononuclear cells could identify patients with response to CRT in LARC. Thirty-five 35 patients with locally advanced rectal cancer were recruited initially to perform the study. Peripheral blood samples were obtained before neoadjuvant treatment. RNA was extracted and purified to obtain cDNA and cRNA for hybridization of microarrays included in Human WG CodeLink bioarrays. Quantitative real-time PCR was used to validate microarray experiment data. Results were correlated with pathological response, according to Mandard's criteria and final UICC Stage (patients with tumor regression grades 1-2 and downstaging being defined as responders and patients with grades 3–5 and no downstaging as nonresponders). The authors performed a multiple t-test using Significance Analysis of Microarrays to find those genes differing significantly in expression between responders ($n = 11$) and nonresponders ($n = 16$) to CRT. The differently expressed genes were BC 035656.1, CIR, PRDM2, CAPG, FALZ, HLA-DPB2, NUPL2, and ZFP36. The measurement of FALZ ($P = 0.029$) gene expression level determined by qRT-PCR showed statistically significant differences between the two groups. They postulated the idea that gene expression profiling reveals novel genes in peripheral blood samples of mononuclear cells that could predict responders and nonresponders to CRT in patients with LARC. The authors hypothesized the importance of mononuclear cells' mediated response in the neoadjuvant treatment of rectal cancer.

3.3. Prediction of Response Using Microarrays of MicroRNA (Table 2). MicroRNAs (miRNAs), discovered in 1993, represent a relatively new field in the rapidly developing world of genetics and the regulation of genetic expression. A miRNA is a small sequence of single-stranded RNA (normally between 18 and 25 nucleotides) that do not code proteins but do act as posttranscriptional regulators of genetic expression. They act by binding to complementary strands of messenger RNA, usually inhibiting expression and silencing the gene. Their function can be very similar to the function of oncogenes as well as tumor-suppressing genes [25]. The aberrant expression of miRNA is involved in numerous pathologies and some alterations in its regulation have been associated with colorectal cancer. Furthermore, it has been determined that CRT in LARC can induce alterations in the expression of miRNA in normal tissue samples and these have been associated with positive response to treatment [26].

Changes in miRNA expression can be induced as a consequence of various external stimuli such as hypoxia and gemcitabine. Svoboda and colleagues studied changes of selected microRNAs in rectal cancer biopsies from patients treated with chemoradiotherapy (50.4 Gy in 1.8 fractions concomitantly with capecitabine) and correlation with response [17]. Microexcision biopsies were taken from the same rectal cancers before therapy and subsequently two weeks after starting preoperative chemoradiotherapy treatment. Radical surgery was performed within the 6th week after completion of neoadjuvant treatment. Tumor response to therapy was assessed microscopically by the Dworak tumor regression grade system. Following a pilot study of normal mucosa biopsies researchers found that microRNAs mi-R125b and mi-R137 showed significant induction and exhibited the same expression trends in most samples two weeks after starting therapy, so they were chosen for further analysis in the total sample set. Real-time PCR was performed and relative expressions of microRNA were determined. Patients with early tumors have lower induction than patients with higher stage cancers. MiR125b is downregulated in several cancers and thought to act as a tumor suppressor. In this study, tumors with the highest upregulation of mi-R125b level two weeks after starting therapy showed no downstaging and less regression (poor response). Mi-R137 was significantly upregulated only in the most advanced T-stage. Researchers concluded that higher induced levels of mi-R125b and mi-R137 were associated with a worse response to the therapy.

In 2012 Della Vittoria Scarpati and colleagues published an article based on this technique which established a specific profile associated with response to treatment in the biopsies of patients with locally advanced rectal neoplasms who underwent neoadjuvant therapy [18]. The team took biopsies from 35 patients affected by rectal cancer T3-4/N+ prior to the initiation of radiotherapy (45 Gy) combined with capecitabine and oxaliplatin. Following a 6-to-8-week rest period a conventional surgical resection was performed. The anatomical pathological response was classified according to Mandard's tumor regression scale: responding patients (TRG 1) and nonresponders (TRG 2, TRG 3, TRG 4, and TRG 5). Results were then validated through quantitative RT-PCR. Researchers studied 373 miRNAs, 53 of which were overexpressed in the group of responders compared with 4 in the group of nonresponders. Of those, 14 were selected for validation by RT-PCR and 13 of them were confirmed. Two of the miRNAs involved in DNA repair mechanisms stood out (miR-622 and miR-630), possibly inhibiting the process and converging in the P53 pathway. These two miRNAs are not expressed in samples proceeding from responding patients and show 100% sensibility and sensitivity.

The authors of another recently published study [19] extracted 12 RNA samples from pretherapeutic biopsies embedded in paraffin and then compared their RNA expression profile with response to neoadjuvant chemoradiation. They identified three RNAs associated with complete response (miR-16, miR-153, and miR-590-5p), employing Mansard's tumor regression grade for quantification and two (miR-519c-3p and miR-561) that predicted good versus poor response, with exactness close to 100%. miRNA expression was analysed in formalin-fixed paraffin-embeddedsamples and in fresh-frozen samples using real-time PCR. The expression levels of miR-10b, miR-143, and miR-145 were downregulated in both FFPE and fresh-frozen tissues, while those for miR-21 were upregulated in tumors.

Table 2: Studies showing miRNA expression profile predictive of response to CRT in LARC.

Study	Specimen	*N* patients	Validation group	*Radiotherapy dose* Chemotherapy	Response assessment	Identified miRNA: more relevant miRNAs	Outcome
Svoboda et al. 2008 [17]	Tumor tissue biopsies	35		*50.4 Gy/28 fractions* Capecitabine	Dworak regression grade	Interpatient variability miR125b miR137 upregulated during treatment: poor response	
Della Vittoria Scarpati et al. 2012 [18]	Tumor tissue biopsy	35		*45 Gy* Capecitabine + oxaliplatin	Mandard regression grade	57 miRNAs: 13 confirmed by PCR miR-622 and miR-630	Sensitivity 100% Specificity 100%
Kheirelseid et al. 2013 [19]	Formalin-fixed paraffin-embedded biopsies Fresh-frozen biopsies	12		*Not specified* Not specified	Mandard regression grade	Downregulated: miR-10b, miR-143, and miR-145 Upregulated: miR-21 Signature: miR-519c-3p and miR-561	Accuracy 100%
Svoboda et al. 2012 [20]	Tumor tissue biopsy	20		*45 + 5.4 Gy* Capecitabine/5-FU	Mandard regression grade	Nonresponders: Overexpressed: miR-215, miR190b, and miR-29b-2 Lower expression: let7e, miR-196b, miR-450a, miR-450b-5p, and miR-99a	Accuracy 90%
Hotchi et al. 2013 [21]	Tumor tissue biopsy	43	21	*40 Gy/20 fractions* S1	Histopathological RECIST Downstaging	2 miRNAs: miR-223 9 miRNAs: miR-223 3 miRNAs: miR-223	AUC 0.768 Sensitivity 100% Specificity 78%

In another retrospective study large-scale miRNA expression analysis was performed on 20 samples of preoperative biopsies of rectal cancer tissues [20]. All patients underwent neoadjuvant treatment based on radiotherapy (45 Gy to the pelvis plus 5.4 Gy boost to tumor) and chemotherapy with capecitabine or 5FU followed 6 weeks later by standard radical surgery. Response was evaluated using a grading system adapted from Mandard and establishing an average and a maximal percentual representation of residual cancer cells in the cell population detected in 10 examined slices of formalin-fixed and paraffin-embedded primary tumors. Responders were classified as patients with tumors in TRG 1-2 and nonresponders were those with or without partial regression (TRG 3–5). Researchers identified eight miRNAs with different expression levels between the two groups. Three of them (miR-215, miR190b, and miR-29b-2) were overexpressed, while the other five (let7e, miR-196b, miR-450a, miR-450b-5p, and miR-99a) showed lower expression levels in nonresponders. Using these miRNAs, 90% of responders and 90% of nonresponders were correctly classified. Five of them (miR-215, miR-99a*, miR-196b, miR-450b-5p, and let-7e) were previously correlated with radioresistance or chemoresistance to thymidylate synthase inhibitors. There is evidence in previous studies that MiR-215 induces inhibition of cell proliferation and subsequent chemoresistance. The let-7 family of miRNAs (let-7a through let-7h) regulates expression of key oncogenes, such as RAS and MYC, and is specifically downregulated in many cancer types. Important proteins involved in DNA repair are among putative targets of miR-99a*, so upregulation of miR-99a* in tumors could be associated with lower DNA repair capacity through downregulation of these genes, which may lead to radiotherapy sensitization. Researchers concluded that miRNAs are part of the response mechanism involved in rectal cancer to chemoradiotherapy and that miRNAs could represent promising predictive biomarkers for patients undergoing such treatment.

Hotchi's group from Japan obtained rectal cancer samples during colonoscopy from 43 patients, prior to preoperative chemoradiotherapy (22 for training and 21 for testing the outcome prediction model) [21]. Samples were used for RNA extraction when paralleled biopsies contained at least 70% tumor cells. Neoadjuvant treatment consisted of 4,000 cGy of pelvic irradiation, five times a week, with a daily fraction of 200 cGy utilizing a four-field technique concomitantly with S1 on radiation days (a novel oral fluoropyrimidine inhibitory for dihydropyrimidine dehydrogenase with a potent radiosensitizing property). Surgery was performed 6–8 weeks following completion of preoperative CRT. Response to CRT was evaluated by three parameters:

(1) Histopathological examination of surgically resected specimens (based on a semiquantitative classification system). Tumors were classified as responders when assigned to regression grade 2 or grade 3 and nonresponders when assigned to grade 0 or grade 1.

(2) Response Evaluation Criteria in Solid Tumors (RECIST): tumors were classified as responders when assigned to complete response (CR) or partial response (PR) and nonresponders when stable disease (SD) or progressive disease (PD) was reported.

(3) Downstaging (yes/no): using real-time RT-PCR in a training set, a candidate miRNA detected by miRNA microarray analysis was evaluated.

With regard to the histopathological examination of surgically resected specimens, two genes are differentially expressed at significant levels in responders and nonresponders (miR-223 and miR-142-3p), with responders showing higher expression in comparison to nonresponders. Nine genes were differentially expressed at significant levels with regard to RECIST: one (miR-223) showed a higher expression, while eight showed a lower expression (miR-20b, miR-92a, let-7a*, miR-20a, miR-17*, miR-106a, miR-17, and miR-20a*) in responders compared to nonresponders. Three genes (miR-223, miR-630, and miR-126*) showed a higher expression in responders compared to nonresponders with regard to downstaging. A candidate gene, miR-223, showed a higher expression among responders than nonresponders in the three parameters evaluated using real-time RT-PCR. The miR-223 level was significantly higher in responders compared to nonresponders. ROC curve analyses showed that miR-223 might differentiate between responders and nonresponders with an area under the curve (AUC) of 0.768 (95% confidence internal (CI), 0.661–0.865). At the cut-off value of 0.4 for miR-223, the sensitivity and the specificity in the 21 testing samples were 100 and 78.0%, respectively.

3.4. Response Prediction Using SAGE (Serial Analysis of Gene Expression). In 2011 Casado and colleagues performed a serial analysis of genetic expression to identify a genetic profile that could predict response to chemoradiation therapy in locally advanced rectal cancer [14]. An initial selection of genes was made using SAGE analysis. They recruited 25 patients and applied a neoadjuvant therapy regimen composed of oxaliplatin and raltitrexed (130 mg/m^2 and 3 mg/m^2, days 1, 21, and 42) in three cycles, combined with radiotherapy (50.4 Gy in 28 fractions). Response was determined in the surgical sample following the scale used by Dworak and colleagues [23]. In contrast to studies presented to date, the goal here was to find genes predictive of a poor response. They identified 24 genes associated with a lack of response. Based on these results and available literature, the team selected 53 genes for a subsequent retrospective study in 94 patients with locally advanced rectal cancer that had received neoadjuvant treatment (under four different radiochemotherapy regimens). They used stored samples of those tumors embedded in paraffin and performed a qRT-PCR following the *TaqMan Low Density Array* (TLDA) protocol. This enabled them to identify a genetic profile composed of 13 genes that permitted the prediction of nonresponse with an exactness of 85%, sensibility of 87%, and specificity of 82%. This study's weakest point is the diversity of neoadjuvant treatments employed. Technology based on tumor samples embedded in paraffin to determine genetic profiles is more suitable to clinical practice than the use of *microarray* studies of gene expression.

Currently, a multicentric study backed by the *Grupo Español Multidisciplinar en Cancer Digestivo* (Multidisciplinary Spanish Group on Digestive Cancer, GEMCAD) is underway to confirm these results.

4. Discussion

There has been a high local recurrence rate in LARC. Besides improvements in surgical techniques, both neoadjuvant short-course radiotherapy and long-course chemoradiation improve oncological results [27]. After CRT, the ability to achieve tumor reduction or even a pCR is observed in up to 60% of the patients treated. This treatment also correlates with a decreasing local recurrence. Conversely patients with a poor response have a worse oncological outcome.

Modern oncological treatment decisions increasingly depend on so-called clinical and laboratory predictive and prognostic markers. While prognostic markers explain variability irrespective of treatment, our study intends to use predictive markers to explain outcome variability in response to treatment. Gene expression profile using the microarray technology has led to a series of promising results through tissue gene expression profiling of different malignancies, including cancer. Interestingly, gene signatures have been used successfully as prognostic predictor for patients with colorectal carcinomas [9, 28].

A successful biomarker should be able to predict a certain group of rectal cancer patients that would be likely to experience response or even a pCR. For this group of patients, the biomarker would be a useful prognostic factor that could indicate a more favorable outcome, and their management would not change from the standard treatment regimen. Those patients with biomarkers predicting a poor response to standard treatment could be offered adjusted therapy courses in terms of the agents used or sequence of treatments (e.g., induction chemotherapy, the addition of a targeted agent such as an EGFR antibody, or surgery without any delay, followed by adjuvant CRT).

The literature was reviewed for studies of biomarkers predicting response to neoadjuvant CRT for rectal cancer. Fifteen studies evaluating genetic profiles predicting outcome of neoadjuvant CRT in rectal cancer were analyzed. Ten of them identified an over- or downregulated gene signature; five studies found microRNA (miRNA) signature.

Although tissue gene microarray profiling has led to promising data in cancer, to date, none of the identified signatures or molecular markers in LARC has been successfully validated as a diagnostic or prognostic tool applicable to routine clinical practice. Moreover, there has been little agreement between signatures published, with scarce overlap in the reported genes [9–13]. Only two genes, MMP4 and FLNA, have been reported in more than one paper [10, 11, 13] and only one of the 257 genes reported by our research group, RRM1 (an important marker for chemotherapy resistance in colon tumors [29]), was also identified by Nishioka et al. [13].

Significant bias was found by analyzing the literature. The scant number of patients in the studies is one of them. The evaluated studies examined between 12 and 94 patients. Even if a significant correlation was determined between a biomarker and a measurement of outcome, the literature has failed to demonstrate reproducibility. Before the clinical use can be established, prospective studies, including a large number of patients should be performed in order to achieve reproducible results.

Furthermore, significant variability in the CRT course can hinder the interpretation of results. Neoadjuvant CRT for LARC typically consists of 5FU and 45–50.4 Gy of pelvic irradiation. By using alternative chemotherapeutic agents in the studies, the results are more difficult to interpret. For example, the addition of oxaliplatin or irinotecan to 5FU for a subset of patients could confound the outcome measurements by altering the baseline response. Variability in the response scoring system is also a debatable bias between the studies.

Despite this variability, our review underlines two main hypothesis: first, the elevated expression of c-Myc mRNA as an important marker of response to CRT in LARC as an essential component of the neoplastic phenotype in rectal tumors.

Second, miRNAs, highly conserved noncoding RNAs ranging between 21 and 24 nucleotides in size, play a major role in the posttranscriptional regulation of mRNA. The inhibition of translation after forming a complex similar to the RNA-interference-induced silencing complex (RISC), by downregulating the expression of their protein-coding gene targets, is the general mechanism of microRNA action in animal and human cells [30, 31]. Some miRNAs function as oncogenes, while others could function as tumor suppressors. miRNAs are considered to be master regulators of several important biological processes, such as cell growth, apoptosis, and cancer development [32–35]. miRNA expression profiles have been shown to be promising biomarkers for the classification or the outcome prediction of some human cancers [35, 36]. Moreover, miRNAs are involved in different stages of colorectal cancer pathogenesis by regulating the expression of oncogenes and tumor suppressor genes [37]. They are also known to be involved in the regulation of radioresistance [38, 39]. Due to their small size, miRNAs are more stable and resistant to environmental, physical, and chemical stresses compared to mRNAs. Therefore, their analysis as formalin-fixed paraffin-embedded tissue samples may provide more accurate replication of what would be observed in fresh tissues [19]. The analysis of formalin-fixed paraffin-embedded samples could be easily transferred to clinical practice.

In conclusion, the current literature does not lend enough support to any of the biomarkers to permit the clinical application in order to predict outcome to neoadjuvant CRT in rectal cancer.

In future clinical trials, assessing neoadjuvant CRT for rectal cancer, these biomarkers should be prospectively evaluated to determine their role as predictors of outcome. It is clear that there is a biological basis as to why some tumors respond to CRT and that biology could be related to the tumor, the patient, or both. In this context, the genes identified in Mononuclear Peripheral Blood Cells could offer new insights into the immune system's dysregulation in

LARC [8] and should be further investigated. Furthermore, the answer may not lie strictly in the genome of the tumor but could represent epigenetic factors, and these would also need to be explored. It is unlikely that any single factor will determine response characteristics; therefore a multifaceted approach will almost certainly be needed.

Conflict of Interests

The authors declare that there is no conflict of interests regarding the publication of this paper.

References

[1] H. Brenner, A. M. Bouvier, R. Foschi et al., "Progress in colorectal cancer survival in Europe from the late 1980s to the early 21st century: the EUROCARE study," *International Journal of Cancer*, vol. 131, no. 7, pp. 1649–1658, 2012.

[2] J. Ferlay, E. Steliarova-Foucher, J. Lortet-Tieulent et al., "Cancer incidence and mortality patterns in Europe: estimates for 40 countries in 2012," *European Journal of Cancer*, vol. 49, no. 6, pp. 1374–1403, 2013.

[3] R. Sauer, H. Becker, W. Hohenberger et al., "Preoperative versus postoperative chemoradiotherapy for rectal cancer," *The New England Journal of Medicine*, vol. 351, no. 17, pp. 1731–1740, 2004.

[4] R. Sauer, T. Liersch, S. Merkel et al., "Preoperative versus postoperative chemoradiotherapy for locally advanced rectal cancer: results of the German CAO/ARO/AIO-94 randomized phase III trial after a median follow-up of 11 years," *Journal of Clinical Oncology*, vol. 30, no. 16, pp. 1926–1933, 2012.

[5] W. H. Yoon, H. J. Kim, C. H. Kim, J. K. Joo, Y. J. Kim, and H. R. Kim, "Oncologic impact of pathologic response on clinical outcome after preoperative chemoradiotherapy in locally advanced rectal cancer," *Annals of Surgical Treatment and Research*, vol. 88, no. 1, pp. 15–20, 2015.

[6] P. Palma, R. Conde-Muíño, A. Rodríguez-Fernández et al., "The value of metabolic imaging to predict tumour response after chemoradiation in locally advanced rectal cancer," *Radiation Oncology*, vol. 5, article 119, 2010.

[7] P. Palma, C. Cano, R. Conde-Muiño et al., "Expression profiling of rectal tumors defines response to neoadjuvant treatment related genes," *PLoS ONE*, vol. 9, no. 11, Article ID e112189, 2014.

[8] P. Palma, M. Cuadros, R. Conde-Muíño et al., "Microarray profiling of mononuclear peripheral blood cells identifies novel candidate genes related to chemoradiation response in rectal cancer," *PLoS ONE*, vol. 8, no. 9, Article ID e74034, 2013.

[9] B. M. Ghadimi, M. Grade, M. J. Difilippantonio et al., "Effectiveness of gene expression profiling for response prediction of rectal adenocarcinomas to preoperative chemoradiotherapy," *Journal of Clinical Oncology*, vol. 23, no. 9, pp. 1826–1838, 2005.

[10] T. Watanabe, Y. Komuro, T. Kiyomatsu et al., "Prediction of sensitivity of rectal cancer cells in response to preoperative radiotherapy by DNA microarray analysis of gene expression profiles," *Cancer Research*, vol. 66, no. 7, pp. 3370–3374, 2006.

[11] I.-J. Kim, S.-B. Lim, H. C. Kang et al., "Microarray gene expression profiling for predicting complete response to preoperative chemoradiotherapy in patients with advanced rectal cancer," *Diseases of the Colon and Rectum*, vol. 50, no. 9, pp. 1342–1353, 2007.

[12] C. Rimkus, J. Friederichs, A.-L. Boulesteix et al., "Microarray-based prediction of tumor response to neoadjuvantradiochemotherapy of patients with locally advanced rectal cancer," *Clinical Gastroenterology and Hepatology*, vol. 6, no. 1, pp. 53–61, 2008.

[13] M. Nishioka, M. Shimada, N. Kurita et al., "Gene expression profile can predict pathological response to preoperative chemoradiotherapy in rectal cancer," *Cancer Genomics & Proteomics*, vol. 8, no. 2, pp. 87–92, 2011.

[14] E. Casado, V. M. García, J. J. Sánchez et al., "A combined strategy of SAGE and quantitative PCR provides a 13-gene signature that predicts preoperative chemoradiotherapy response and outcome in rectal cancer," *Clinical Cancer Research*, vol. 17, no. 12, pp. 4145–4154, 2011.

[15] G. A. Gantt, Y. Chen, K. Dejulius, A. G. Mace, J. Barnholtz-Sloan, and M. F. Kalady, "Gene expression profile is associated with chemoradiation resistance in rectal cancer," *Colorectal Disease*, vol. 16, no. 1, pp. 57–66, 2014.

[16] T. Watanabe, T. Kobunai, T. Akiyoshi, K. Matsuda, S. Ishihara, and K. Nozawa, "Prediction of response to preoperative chemoradiotherapy in rectal cancer by using reverse transcriptase polymerase chain reaction analysis of four genes," *Diseases of the Colon and Rectum*, vol. 57, no. 1, pp. 23–31, 2014.

[17] M. Svoboda, L. I. Holla, R. Sefr et al., "Micro-RNAs miR125b and miR137 are frequently upregulated in response to capecitabine chemoradiotherapy of rectal cancer," *International Journal of Oncology*, vol. 33, no. 3, pp. 541–547, 2008.

[18] G. Della Vittoria Scarpati, F. Falcetta, C. Carlomagno et al., "A specific miRNA signature correlates with complete pathological response to neoadjuvant chemoradiotherapy in locally advanced rectal cancer," *International Journal of Radiation Oncology Biology Physics*, vol. 83, no. 4, pp. 1113–1119, 2012.

[19] E. A. H. Kheirelseid, N. Miller, K. H. Chang et al., "miRNA expressions in rectal cancer as predictors of response to neoadjuvant chemoradiation therapy," *International Journal of Colorectal Disease*, vol. 28, no. 2, pp. 247–260, 2013.

[20] M. Svoboda, J. Sana, P. Fabian et al., "MicroRNA expression profile associated with response to neoadjuvant chemoradiotherapy in locally advanced rectal cancer patients," *Radiation Oncology*, vol. 7, article 195, 2012.

[21] M. Hotchi, M. Shimada, N. Kurita et al., "microRNA expression is able to predict response to chemoradiotherapy in rectal cancer," *Molecular and Clinical Oncology*, vol. 1, no. 1, pp. 137–142, 2013.

[22] R. Sauer, R. Fietkau, C. Wittekind et al., "Adjuvant versus neoadjuvantradiochemotherapy for locally advanced rectal cancer. A progress report of a phase-III randomized trial (protocol CAO/ARO/AIO-94)," *Strahlentherapie und Onkologie: Organ der Deutschen Rontgengesellschaft*, vol. 177, no. 4, pp. 173–181, 2001.

[23] O. Dworak, L. Keilholz, and A. Hoffmann, "Pathological features of rectal cancer after preoperative radiochemotherapy," *International Journal of Colorectal Disease*, vol. 12, no. 1, pp. 19–23, 1997.

[24] A.-M. Mandard, F. Dalibard, J.-C. Mandard et al., "Pathologic assessment of tumor regression after preoperative chemoradiotherapy of esophageal carcinoma. Clinicopathologic correlations," *Cancer*, vol. 73, no. 11, pp. 2680–2686, 1994.

[25] S. K. Shenouda and S. K. Alahari, "MicroRNA function in cancer: oncogene or a tumor suppressor?" *Cancer and Metastasis Reviews*, vol. 28, no. 3-4, pp. 369–378, 2009.

[26] U. Drebber, M. Lay, I. Wedemeyer et al., "Altered levels of the onco-microRNA 21 and the tumor-supressor microRNAs 143

and 145 in advanced rectal cancer indicate successful neoadjuvant chemoradiotherapy," *International Journal of Oncology*, vol. 39, no. 2, pp. 409–415, 2011.

[27] R. Glynne-Jones and M. Kronfli, "Locally advanced rectal cancer: a comparison of management strategies," *Drugs*, vol. 71, no. 9, pp. 1153–1177, 2011.

[28] E. Bandrés, R. Malumbres, E. Cubedo et al., "A gene signature of 8 genes could identify the risk of recurrence and progression in Dukes' B colon cancer patients," *Oncology Reports*, vol. 17, no. 5, pp. 1089–1094, 2007.

[29] M. A. van de Wiel, J. L. Costa, K. Smid et al., "Expression microarray analysis and oligo array comparative genomic hybridization of acquired gemcitabine resistance in mouse colon reveals selection for chromosomal aberrations," *Cancer Research*, vol. 65, no. 22, pp. 10208–10213, 2005.

[30] L. P. Lim, N. C. Lau, P. Garrett-Engele et al., "Microarray analysis shows that some microRNAs downregulate large numbers of target mRNAs," *Nature*, vol. 433, no. 7027, pp. 769–773, 2005.

[31] R. I. Gregory and R. Shiekhattar, "MicroRNA biogenesis and cancer," *Cancer Research*, vol. 65, no. 9, pp. 3509–3512, 2005.

[32] V. Ambros, "The functions of animal microRNAs," *Nature*, vol. 431, no. 7006, pp. 350–355, 2004.

[33] G. A. Calin and C. M. Croce, "MicroRNA signatures in human cancers," *Nature Reviews Cancer*, vol. 6, no. 11, pp. 857–866, 2006.

[34] E. A. Miska, "How microRNAs control cell division, differentiation and death," *Current Opinion in Genetics and Development*, vol. 15, no. 5, pp. 563–568, 2005.

[35] C. Jay, J. Nemunaitis, P. Chen, P. Fulgham, and A. W. Tong, "miRNA profiling for diagnosis and prognosis of human cancer," *DNA and Cell Biology*, vol. 26, no. 5, pp. 293–300, 2007.

[36] S.-L. Yu, H.-Y. Chen, P.-C. Yang, and J. J. W. Chen, "Unique MicroRNA signature and clinical outcome of cancers," *DNA and Cell Biology*, vol. 26, no. 5, pp. 283–292, 2007.

[37] O. Slaby, M. Svoboda, J. Michalek, and R. Vyzula, "MicroRNAs in colorectal cancer: translation of molecular biology into clinical application," *Molecular Cancer*, vol. 8, article 102, 2009.

[38] K. M. Lee, E. J. Choi, and I. A. Kim, "MicroRNA-7 increases radiosensitivity of human cancer cells with activated EGFR-associated signaling," *Radiotherapy and Oncology*, vol. 101, no. 1, pp. 171–176, 2011.

[39] W. Y. Mansour, N. V. Bogdanova, U. Kasten-Pisula et al., "Aberrant overexpression of miR-421 downregulates ATM and leads to a pronounced DSB repair defect and clinical hypersensitivity in SKX squamous cell carcinoma," *Radiotherapy and Oncology*, vol. 106, no. 1, pp. 147–154, 2013.

Hindawi Publishing Corporation
BioMed Research International
Volume 2015, Article ID 365273, 10 pages
http://dx.doi.org/10.1155/2015/365273

Research Article

miR-125b Suppresses Proliferation and Invasion by Targeting MCL1 in Gastric Cancer

Shihua Wu,[1,2] Feng Liu,[3] Liming Xie,[1] Yaling Peng,[2] Xiaoyuan Lv,[2] Yaping Zhu,[2] Zhiwei Zhang,[1] and Xiusheng He[1]

[1]*Cancer Research Institute, Key Laboratory of Cancer Cellular and Molecular Pathology of Hunan Provincial University, University of South China, Hengyang 421001, China*
[2]*Department of Pathology, Shaoyang Medical College, Shaoyang 422000, China*
[3]*Graduate Department, University of South China, Hengyang 421001, China*

Correspondence should be addressed to Zhiwei Zhang; nhdxzzw@qq.com and Xiusheng He; hexiusheng@hotmail.com

Received 24 January 2015; Revised 8 May 2015; Accepted 18 May 2015

Academic Editor: Franco M. Buonaguro

Understanding the molecular mechanisms underlying gastric cancer progression contributes to the development of novel targeted therapies. In this study, we found that the expression levels of miR-125b were strongly downregulated in gastric cancer and associated with clinical stage and the presence of lymph node metastases. Additionally, miR-125b could independently predict OS and DFS in gastric cancer. We further found that upregulation of miR-125b inhibited the proliferation and metastasis of gastric cancer cells in vitro and in vivo. miR-125b elicits these responses by directly targeting MCL1 (myeloid cell leukemia 1), which results in a marked reduction in MCL1 expression. Transfection of miR-125b sensitizes gastric cancer cells to 5-FU-induced apoptosis. By understanding the function and molecular mechanisms of miR-125b in gastric cancer, we may learn that miR-125b has the therapeutic potential to suppress gastric cancer progression and increase drug sensitivity to gastric cancer.

1. Introduction

Despite achieving significant progress in therapeutic strategies, gastric cancer remains the second most frequent cause of global cancer mortality [1, 2]. Understanding the precise molecular mechanisms underlying the development and progression of gastric cancer is urgently needed and can provide the basis for molecular treatment strategies [3]. MicroRNAs (miRNAs) are a group of endogenously expressed, noncoding small RNAs. miRNAs negatively regulate the expression of target mRNAs by suppressing translation or decreasing the stability of mRNAs [4]. It has been found that miRNAs play crucial roles in various biological processes, including development, differentiation, apoptosis, and cell proliferation [5–7]. An increasing number of studies have demonstrated that miRNAs can function as oncogenes or tumor suppressors and that they are often dysregulated in tumors [8, 9]. miR-125b has been identified as a tumor suppressor in many tumors, including bladder cancer, breast cancer, and oral squamous cell carcinoma [10–13]. Fassan et al. reported that both miR-125a-5p and miR-125b levels were significantly downregulated throughout the gastric and esophageal carcinogenic cascades [14]. However, a recent study found that miR-125b promotes cell migration and invasion by targeting the PPP1CA-Rb signal pathway in gastric cancer, resulting in a poor prognosis [15], which means that miR-125b could be regarded as oncogene in gastric cancer. To date, the role of miR-125b in gastric cancer has been undefined.

In this study, we found that miR-125b expression is downregulated in 36 stomach tumor specimens and gastric cell lines. miR-125b expression was detected by in situ hybridization on tissue microarrays, and the association between miR-125b levels and clinicopathological factors and prognoses were analyzed. The results indicated that decreased miR-125b levels correlate with advanced clinical stage lymph node metastases and poor clinical outcomes. Additionally, luciferase assay results confirmed *MCL1* (myeloid cell leukemia 1) as a direct target gene of miR-125b. Ectopic overexpression of miR-125b dramatically repressed proliferation, induced apoptosis in vitro, and suppressed tumorigenicity

in vivo. Furthermore, miR-125b increased 5-FU-sensitivity through *MCL1*.

2. Materials and Methods

2.1. Cell Culture. The gastric epithelial cell line GES-1 was purchased from the Beijing Institute for Cancer Research (Beijing, China). The gastric cancer cell lines MGC-803, BGC-823, MKN-28, SGC-7901, HGC-27, AGS, and MKN-45 were obtained from the American Type Culture Collection (ATCC, Rockville, MD). These cells were maintained at 37°C in a 5% CO_2 atmosphere in RPMI-1640 medium supplemented with 10% fetal bovine serum, penicillin, and streptomycin (Gibco BRL, NY, USA).

2.2. Clinical Samples. All of the tissue samples used in this study were collected from the Hunan Provincial Tumor Hospital (Changsha, Hunan, China). Written informed consent was obtained from all of the study participants [9]. This study was approved by the Ethics Committee of the University of South China Health Authority. The collection and use of tissues followed procedures that are in accordance with ethical standards as formulated in the Helsinki Declaration. Tissue samples from 36 gastric cancer patients were used for quantitative real-time PCR (qRT-PCR) analysis. Resected cancerous tissues (tumor) and paired matched normal gastric tissues (normal) were immediately cut and stored in RNAlater solution (Ambion). The tissue microarrays (TMAs) consisted of 126 cases of gastric carcinomas. All of the data, including age, sex, histological grade, tumor size, invasion depth (T stage), and lymph node metastasis, were obtained from clinical and pathological records.

2.3. In Situ Hybridization. Tissue microarray slides were deparaffinized and rehydrated [8]. The miR-125b miRCURY LNA custom detection probe (Exiqon, Vedbaek, Denmark) was used for in situ hybridization (ISH). The sequence 5′-3′ (enhanced with LNA) was UCCCUGAGACCCUAACUUGUGA with digoxigenin (DIG) at the 5′ and 3′ ends. Hybridization, washing, and scanning were carried out according to the manuals and protocols provided by the Exiqon Life Science Department. The intensities of miR-125b staining were scored by 0–4, according to the standards of 0-1 (no staining), 1-2 (weak staining), 2-3 (medium staining), and 3-4 (strong staining). The percentages of miR-125b cells in three representative high-power fields of individual samples were analyzed. Those expression scores were equal to scores of the intensities × the percentages of positive cells, and the maximum was 4 and the minimum was 0. Individual samples were evaluated by at least two pathologists in a blinded manner, and those expression scores greater than or equal to 2 were defined as high expression, less than 2 being low expression.

2.4. Overall Survival (OS) and Disease-Free Survival (DFS). DFS was defined as the interval between surgery and the date of diagnosis of the first recurrence or the date of the last follow-up. OS was calculated from diagnosis to the date of death for any cause, and patients who were alive were censored at date of last follow-up visit.

2.5. Bioinformatics. Target prediction was performed by online software Targetscan 6.2.

2.6. Quantitative RT-PCR Analysis (qRT-PCR). Total RNAs were extracted from cells with TRIzol reagent (Invitrogen, Carlsbad, USA). Reverse transcription and qRT-PCR reactions were performed by means of a qSYBR-green-containing PCR kit (Qiagen, Germantown, USA). Fold change was determined as $2^{-\Delta\Delta Ct}$. The Ct is the fractional cycle number at which the fluorescence of each sample passes the fixed threshold. The ΔCt was calculated by subtracting the Ct of snRNA U6 from the Ct of the miRNA of interest. The ΔΔCt was calculated by subtracting the ΔCt of the reference sample (paired nontumourous tissue for surgical samples) from the ΔCt of each sample. The primers for qRT-PCR detection of *MCL1* mRNA (F: TAAGGACAAAACGGGACTGG; R: CCTCTTGCCACTTGCTTTTC) were synthesized by Invitrogen. All qRT-PCR was performed with the Bio-Rad C1000 Multicolor Real-Time PCR Detection System (USA).

2.7. Dual Luciferase Reporter Assay and 3′UTR Binding Site Mutagenesis. MGC-803 cells (6×10^4) were seeded in 24-well plates immediately prior to transfection. The pMIR-MCL1 plasmids were transfected into MGC-803 cells using Lipofectamine 2000 (Invitrogen) according to the manufacturer's instructions. We also generated several inserts with deletions of 4 bp from the site of perfect complementarity of the *MCL1* gene using the QIAGEN XL-site directed Mutagenesis Kit (QIAGEN, Valencia, CA). The miR-125b mimics and pMIR-*MCL1* plasmids were cotransfected where indicated. Forty-eight hours after transfection, cells were assayed for both firefly and Renilla luciferase using the dual luciferase glow assay (Promega). Transfection experiments were performed in duplicate and repeated at least three times in independent experiments.

2.8. Lentivirus Production and Infection. Lentivirus plasmids were cotransfected with pLP1, pLP2, and pLP/VSVG (Invitrogen) into 293T cells (Invitrogen), and virus-containing supernatants were prepared according to the manufacturer's instructions. For lentiviral infection, cells were incubated with virus-containing supernatants in the presence of 6 μg/mL polybrene. Infected cells were selected in the presence of 2 μg/mL puromycin to generate two paired stable monoclonal cell lines. For infection with the GFP-expressing viruses for miRNA expression, flow cytometry analyses (FacsCalibur, Becton Dickinson) were performed to confirm that 90% of cells were infected.

2.9. In Vivo Gastric Tumor Model. Male BALB/c nude mice (4–6 weeks old) were purchased from the Hunan Province Laboratory Animal Co., Ltd. (Changsha, China). All of the animal studies were conducted according to protocols approved by the Institutional Animal Care and Use Committee. Briefly, nude mice were inoculated subcutaneously with

either MGC-803-control or MGC-803-miR-125b cells (n = 5 per group). The formation and growth of human gastric tumors in the recipients were monitored every four days, and the tumor volumes were estimated by measuring two dimensions of the tumors using a digital caliper in a blinded manner. The animal handling and all experimental procedures were approved by the Animal Ethics Committee of the University of South China. Strict sterility was maintained throughout the procedure.

2.10. Cell Invasion Assays. Cells were seeded onto the basement membrane matrix in the insert of a 24-well culture plate (EC matrix, Chemicon, Temecula, CA) and fetal bovine serum was added to the lower chamber as a chemoattractant. After 48 hours, the noninvading cells and EC matrix were gently removed with a cotton swab. Invasive cells located on the lower side of the chamber were stained with crystal violet, counted, and imaged.

2.11. Western Blot Analysis. Protein lysates from cells were subjected to sodium dodecyl sulfate polyacrylamide gel electrophoresis (SDS-PAGE) and target proteins were detected with primary antibodies recognizing MCL1 (Santa Cruz, USA), cleaved caspase-3, cleaved PARP, and GAPDH (Cell Signaling), respectively. Following incubation with the appropriate horseradish peroxidase- (HRP-) conjugated secondary antibodies (Jackson ImmunoResearch), protein bands were visualized using enhanced chemiluminescence (ECL) plus western blotting detection reagents and exposed in a Bio Image Intelligent Quantifier 1D.

2.12. Statistical Analysis. Data were expressed as the mean ± standard error of the mean (SEM) from at least three independent experiments. Comparisons between the groups were analyzed by the t-test and χ^2 test. All differences were considered statistically significant when $P \leq 0.05$. Statistical analyses were performed using the SPSS16.0 software.

3. Results

3.1. miR-125b Is Downregulated in Gastric Cancer. First, a series of human gastric cancer cell lines were analyzed to assess the expression profile of miR-125b in gastric cancer using qRT-PCR (Figure 1(a)). Compared with the nonmalignant gastric cell line GES-1, seven of the gastric cancer cell lines showed reduced miR-125b expression, especially the MGC-803 and SGC-7901 cells. We also compared miR-125b expression levels in a series of 36 pairs of gastric cancer tissues and their matched adjacent tissues. Among the 36 gastric cancer patients, significant downregulation of miR-125b was observed in 80.1% of the tumors (29/36, Figure 1(b)), and miR-125b levels decreased (2.5-fold) relative to the adjacent nontumor tissues (Figure 1(b)).

3.2. Decreased miR-125b Correlates with Advanced Clinical Stage, Lymph Node Metastases, and Poor Clinical Outcomes. To further verify the results concerning the biological role of miR-125b in gastric cancer, we used in situ hybridization to evaluate miR-125b levels in tissue microarrays (TMAs) consisting of 126 gastric tumor tissues. Our results found that miR-125b levels inversely correlated with invasion depth, clinical stage, and lymph node metastasis (P = 0.031, P = 0.002, and P = 0.001, resp.) (Table 1). However, no significant correlations between miR-125b expression and age, gender, tumor size, or cell differentiation were identified. Our results suggest that miR-125b could play critical roles in progression of gastric cancer. To further examine the significance of miR-125b in terms of clinical prognosis, Kaplan-Meier survival analyses were performed using patient overall survival and relapse-free survival. The results demonstrated that patients with low miR-125b expression had shorter mean months of OS ($P < 0.001$) (Figure 1(c)) and DFS ($P < 0.001$) (Figure 1(d)) than patients with high miR-125b expression.

Table 1: Analysis of the correlation between expression of miR-125b in primary gastric cancer and its clinicopathological parameters.

Viable	Cases	miR-125b		P value
		Low	High	
Age (years)				
<60	73	40	33	0.858
≥60	53	28	25	
Gender				
Male	70	35	35	0.370
Female	56	33	23	
Histological grade				
Well and moderate	32	22	10	0.065
Poor and other	94	46	48	
T stage				
T1-T2	71	32	39	0.031
T3-T4	55	36	19	
TNM stage				
I-II	51	19	32	0.002
III-IV	75	49	26	
Lymph node metastasis				
Present	88	56	32	0.001
Absent	38	12	26	

3.3. MCL1 Is a Target of miR-125b in Breast Cancer Cells. miR-125 target sites were predicted using online software Targetscan 6.2. The algorithm predicted *MCL1* from the candidate target genes (Figure 2(a)). miR-125b mimics, but not miR-ctr, specifically decreased luciferase expression in the *MCL1*-wt reporter cells. In contrast, no change in relative luciferase expression was observed in cells transfected with the *MCL1*-mut reporter (Figure 2(b)). These results suggest that *MCL1* is a direct target gene of miR-125b. The results from qPCR and western blots showed that enhanced expression of miR-125b by miR-125b mimics in the MGC-803 cells leads to downregulation of endogenous *MCL1* mRNAs and decreased protein levels (Figures 2(c) and 2(d)). Taken together, these results indicate that MCL1 is a direct target gene of miR-125b and can be negatively regulated by miR-125b.

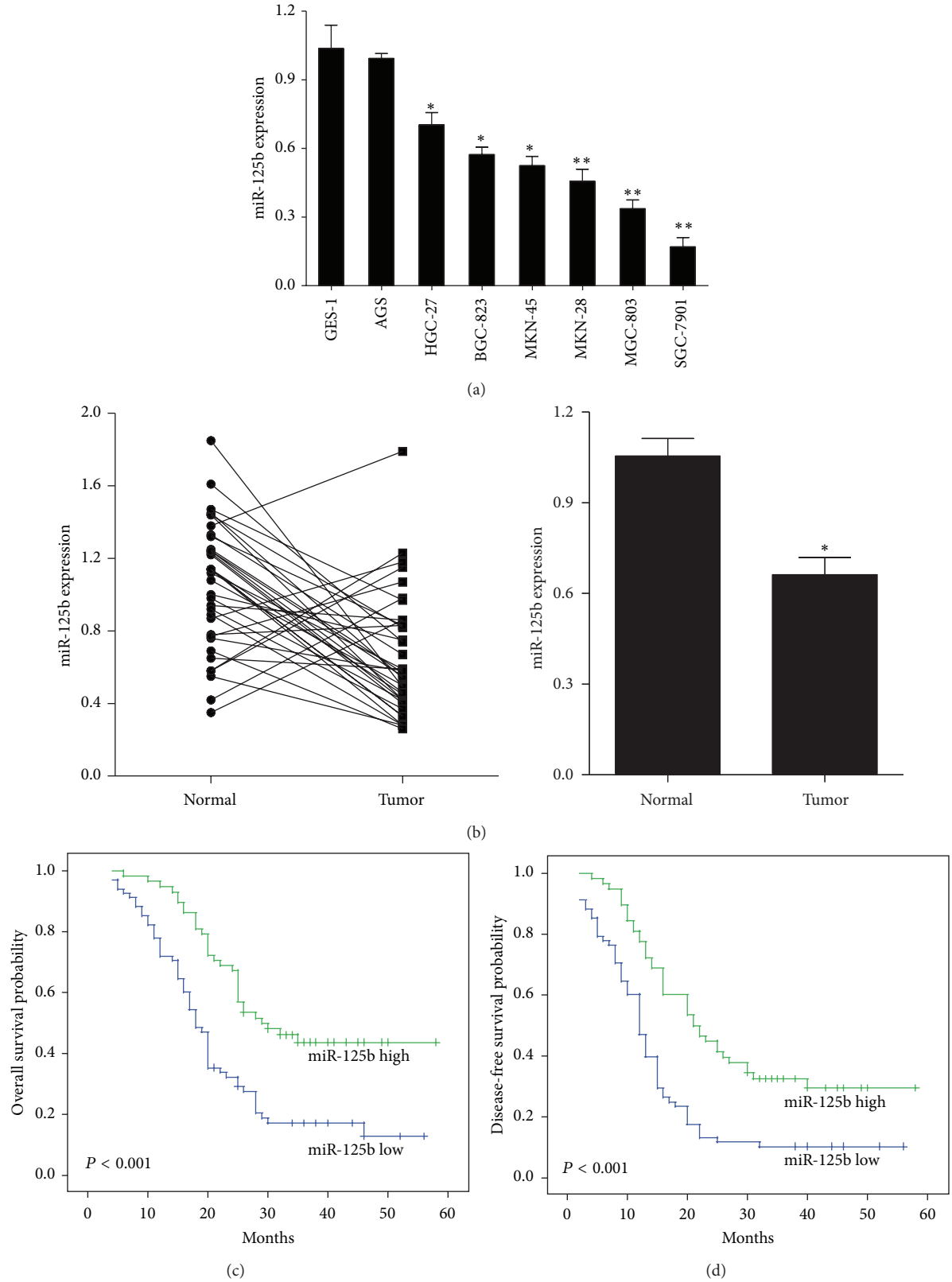

FIGURE 1: miR-125b expression levels are frequently downregulated in human gastric cancer. (a) Relative expression of miR-125b in 7 cell lines derived from gastric cancer and one nonmalignant gastric cell line (GES-1) was determined by qRT-PCR. The error bars represent the standard deviations (SD) from triplicates of one representative experiment. $^{*}P < 0.05$ and $^{**}P < 0.01$. (b) miR-125b expression was detected in 36 gastric cancer patient tumors by qRT-PCR. The error bars represent the standard deviations (SD) from triplicates of one representative experiment. $^{*}P < 0.05$. Survival curves of (c) OS and (d) DFS according to miR-125b expression. Whether miR-125b expression levels were high or low was determined using the Kaplan-Meier method and evaluated using the log-rank test.

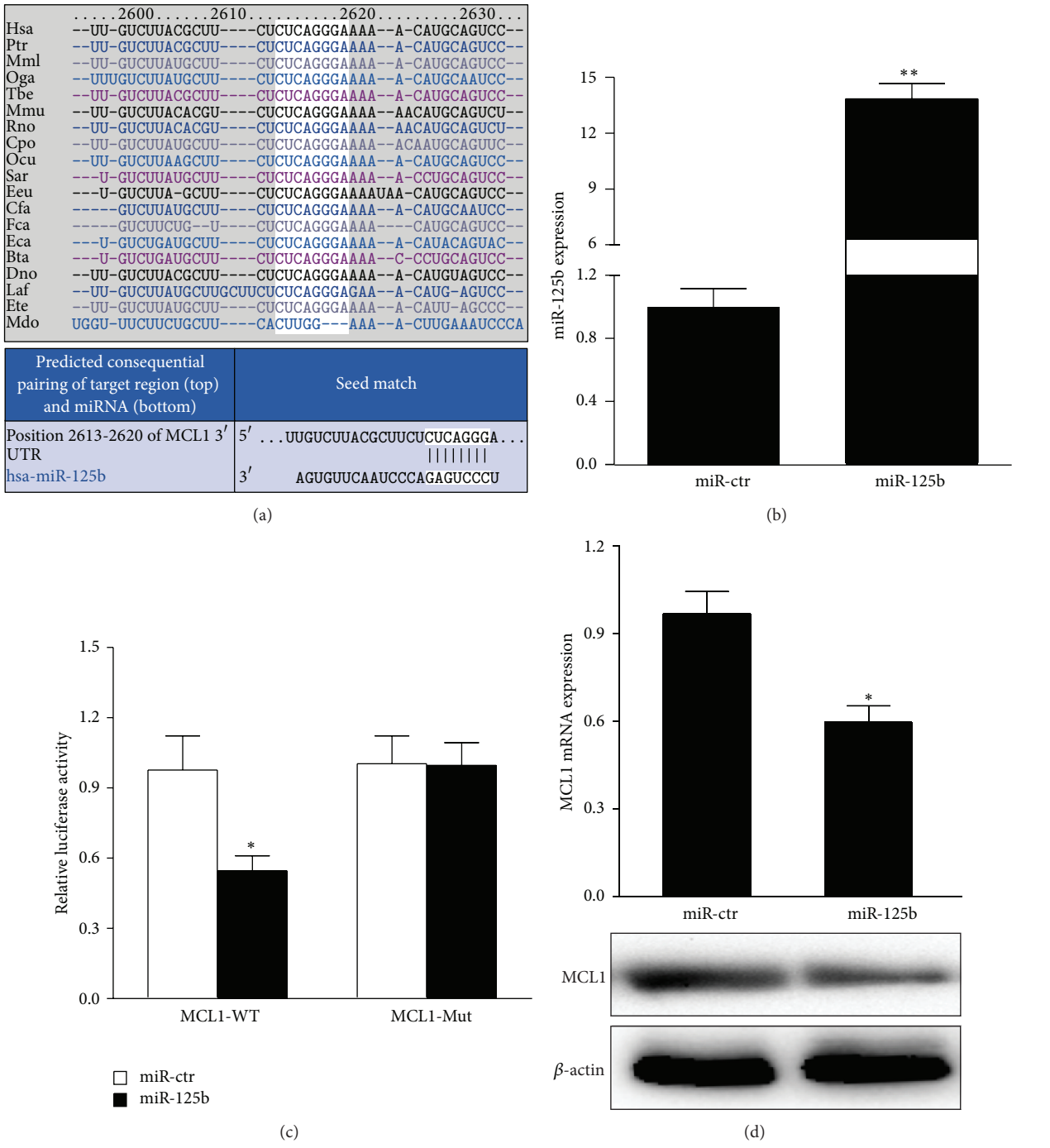

FIGURE 2: *MCL1* is a target of miR-125b in breast cancer cells. (a) Schematic of the predicted miR-125b site in the 3′UTR of *MCL1* mRNA, which is broadly conserved among vertebrates. (b) miR-125b expression was detected in MGC-803 cells transfected with either miR-125b mimics or the miR-ctr control by qRT-PCR. The error bars represent the standard deviations (SD) from triplicates of one representative experiment. $^{**}P < 0.01$. (c) Luciferase reporter assays were performed after transfection of the indicated pMIR-Report plasmids, a Renilla transfection control plasmid, and with either miR-34a or the relevant scrambled controls. The data shown are the means ± SD of three replicates and are representative of three independent experiments. $^{*}P < 0.05$. (d) MCL1 mRNA and protein expression levels were much lower in MGC-803 cells transfected with miR-125b mimics compared to cells transfected with miR-ctr. The data shown are the means ± SD of three replicates and are representative of three independent experiments. $^{*}P < 0.05$.

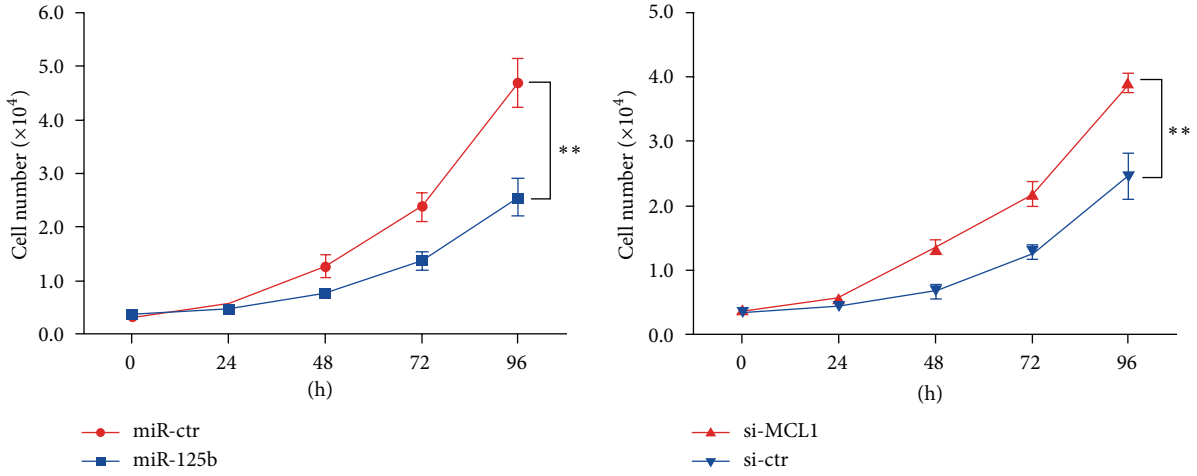

(a)

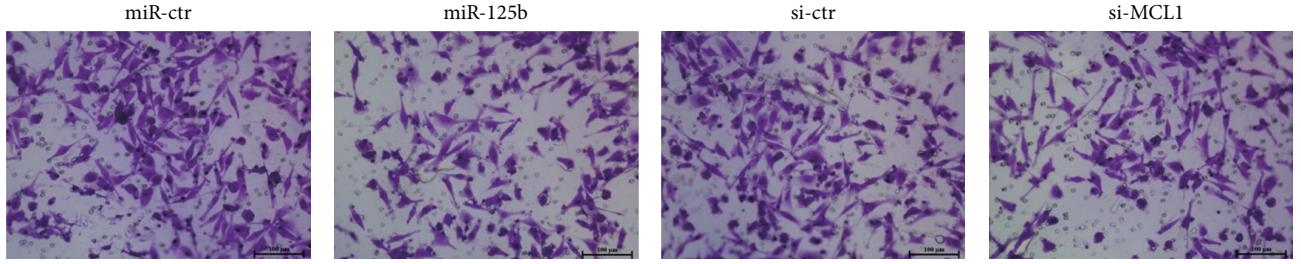

(b)

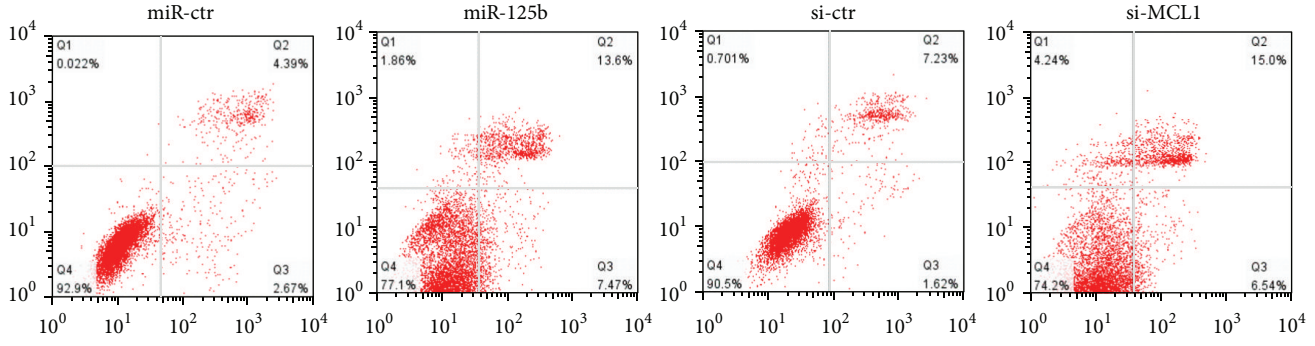

(c)

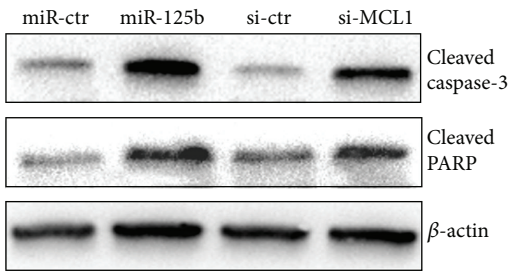

(d)

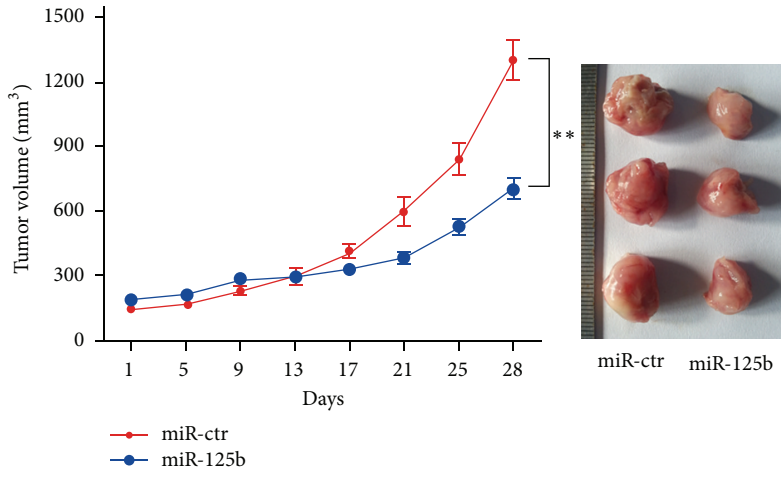

(e)

Figure 3: Continued.

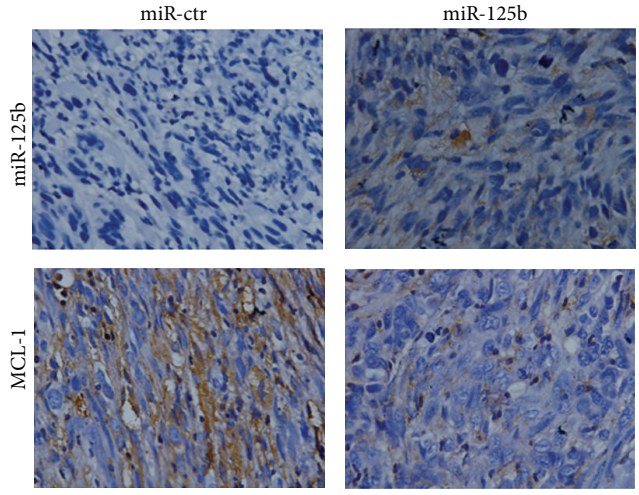

(f)

Figure 3: miR-125b represses gastric cancer progression. (a) MGC-803 cells transfected with either miR-125b or miR-ctr (left) and either si-*MCL1* or si-ctr were seeded in 12-well plates at the desired cell concentrations and maintained in medium containing 10% FBS. The cells were counted at the indicated time points in triplicate and their growth rates were recorded. $^{**}P < 0.01$. (b) The invasion assay of the MGC-803 cells transfected with either miR-125b or miR-ctr and either si-*MCL1* or si-ctr. (c) MGC-803 cells were transfected with either miR-125b, miR-ctr, si-*MCL1*, or si-ctr. The apoptotic cells were evaluated with Annexin V-FITC and propidium iodine staining and analyzed by FACS. (d) MGC-803 cells were transfected with either miR-125b, miR-ctr, si-*MCL1*, or si-ctr. The levels of cleaved caspase-3 and cleaved PRAP were evaluated by western blot analysis. (e) MGC-803 cells were subcutaneously injected into nude mice. Then, the effect of an intratumoral injection of 40 μL of either miR-ctr or miR-125b mimic in PBS on tumor volume was examined. Average tumor volumes are shown ($n = 5$ for both experimental groups) from the first injection and continue until after the mice were killed at 28 days (left). After 32 days, the mice were euthanized, necropsies were performed, and tumors were weighed. All data are shown as the mean ± SEM, $^{**}P < 0.01$ (right). (f) In situ hybridization was used to detect the expression of miR-125b, and immunohistochemistry was used to detect the expression of MCL1 in transplanted tumor tissues injected with either miR-125b mimics or the control.

3.4. miR-125b Represses Gastric Cancer Progression. While exploring the functional effect of miR-125b and MCL1 on gastric cancer by cell proliferation, we found that upregulation of miR-125b inhibited the proliferation capacity of MGC-803 cells via functional downregulation of MCL1 expression (Figure 3(a)). The rate of cell survival was considerably lower in cells transfected with miR-125b mimics or *MCL1* siRNA compared to the respective controls. These results indicated that either transfection of miR-125b or knockdown of *MCL1* significantly suppressed gastric cancer cell proliferation in vitro. Furthermore, we found that overexpression of miR-125b or knockdown of *MCL1* significantly inhibited the invasion capacity of MGC-803 cells (Figure 3(b)). Flow cytometry was performed to assess whether this effect was mediated through the induction of apoptosis. The apoptosis rate of MGC-803 cells was increased by transfection with miR-125b mimics or MCL1 siRNA (Figure 3(c)). Western blot analysis of miR-125b mimics/*MCL1*-siRNA-transfected gastric cancer cells indicated a higher expression of cleaved caspase-3 and PARP, which coincide with apoptosis, compared to controls (Figure 3(d)). These data indicate that miR-125b not only inhibited proliferation and invasion but also induced gastric cancer cell apoptosis by directly targeting *MCL1*. To directly evaluate the role of miR-125b in tumour formation and growth in vivo, the xenograft model of human MGC-803 cells in nude mice was adopted. MGC-803 cells infected with miR-125b or miR-ctr lentivirus were injected subcutaneously into each nude mice. After the cells were injected, the tumour volume was monitored every four days. Twenty-eight days after injection, the mean volume and weight of the tumors generated from the MGC-803 cells treated with the miR-125b mimics were significantly lower than those of tumors from mice in the control groups (Figure 3(e)). miR-125b was able to inhibit the expression of MCL1 in vivo (Figure 3(f)). These observations provide strong evidence that overexpression of miR-125b significantly inhibits gastric cancer proliferation in vitro and in vivo.

3.5. Transfection of miR-125b Sensitizes Gastric Cancer Cells to 5-FU-Induced Apoptosis. Novel cancer treatment strategies are often composed of conventional chemotherapies and biotherapies, and increasing amounts of evidence indicate that miRNAs are associated with sensitivity to chemotherapeutic drugs, such as 5-fluorouracil in various cancer types. To further assess the synergistic antitumor effects of miR-125b or decreased *MCL1* expression, MGC-803 cells were treated with 5-FU (10 ng/mL) combined with overexpression of miR-125b or *MCL1* silencing. MGC-803 cells with enhanced expression of miR-125b or decreased expression of *MCL1* exhibited greater inhibition of cell proliferation (Figure 4(a)), invasion (Figure 4(b)), and an increase in apoptotic rate (Figure 4(c)) after Taxol treatment. These results suggest that miR-125b is able to sensitize gastric cancer cells to 5-FU-induced apoptosis by targeting *MCL1*.

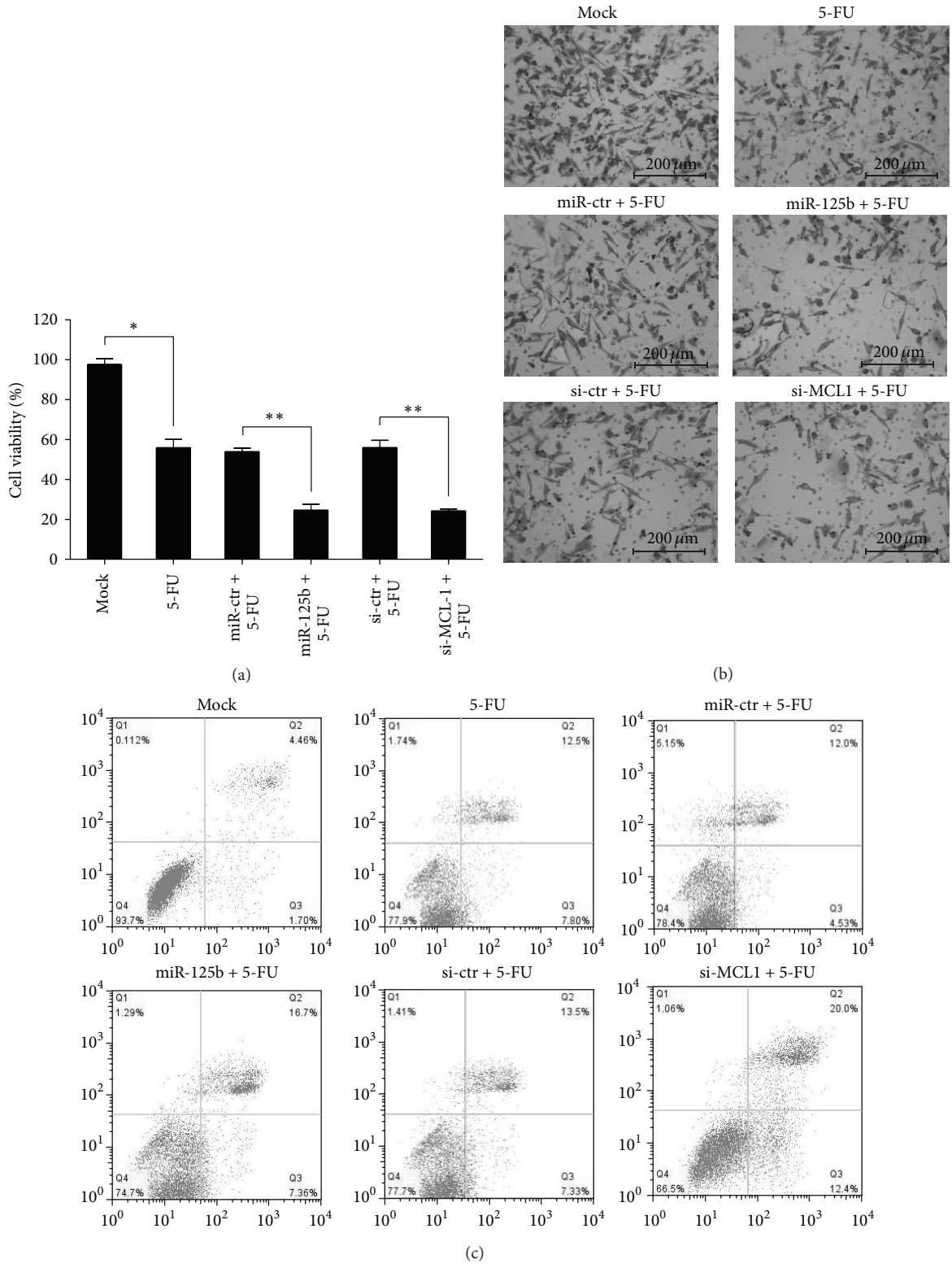

FIGURE 4: miR-125b inhibited the gastric cancer invasion ability in vitro by targeting Rhoc. (a) MGC-803 were transfected with 5-FU, miR-125b mimics, si-*MCL1*, or combinations of the reagents. MTT assays were performed in MGC-803 cells 48 h after treatment. miR-125b, miR-ctr, si-*MCL1*, or si-ctr was transiently transfected at a concentration of 40 nM. The work concentration of 5-FU was 10 ng/mL. All data are shown as the mean ± SEM, $^{*}P < 0.05$, $^{**}P < 0.01$. (b) MGC-803 were transfected with 5-FU, miR-125b mimics, si-*MCL1*, or combinations of the reagents. Invasion assays were evaluated by the Transwell assay. (c) MGC-803 were transfected with 5-FU, miR-125b mimics, si-*MCL1*, or combinations of the reagents. The apoptotic cells were evaluated by Annexin V-FITC and propidium iodine staining and analyzed with FACS.

4. Discussion

MicroRNA represents approximately 1% of the genome in different species, each of which has hundreds of different conserved or nonconserved targets, making them key players in various cellular processes [16]. Thus, we believe that more effort should be made to identify relevant miRNAs and to understand the specific mechanisms by which they accomplish their specific functions, particularly their role in the oncogenesis of different tumor types [17–19]. In this study, we used qRT-PCR and ISH to show that miR-125b was frequently downregulated in gastric cancers. Furthermore, we found that miR-125b levels inversely correlated with invasion depth, clinical stage, and lymph node metastasis, suggesting that low expression of miR-125b is associated with gastric cancer progression. Kaplan-Meier survival analyses revealed that patients whose primary tumors displayed a low expression of miR-125b had a shorter OS and DFS in gastric cancer. Further studies showed that overexpression of miR-125b suppressed proliferation and promoted apoptosis capacity in MGC-803 cells. The data from this study suggests that the miR-125b is important for gastric cancer initiation and progression.

We next explored the possible targets of miR-125b in gastric cancer using different computational algorithms. In silico analysis revealed *MCL1* as a candidate target of miR-125b. MCL1 (myeloid cell leukemia 1), a prosurvival member of the Bcl-2 family, was expected to be important due to the association between the aberrant expression of prosurvival Bcl-2 family proteins, tumorigenesis, and resistance to chemotherapeutics [20]. MCL1 is overexpressed in glioma cells. Downregulation of *MCL1* promotes temozolomide-induced apoptosis in gliomas [21]. It has also been demonstrated that several miRNAs induce apoptosis by targeting MCL1 in acute myeloid leukemia [22], lung cancer [23], breast cancer [24], and ovarian cancer [25]. In our study, *MCL1* was further confirmed to be a direct target of miR-125b via luciferase activity assays in gastric cancer cells. We showed that overexpression of miR-125b or downregulation of MCL1 significantly inhibited proliferation and invasion and induced apoptosis in vitro. Due to the heterogeneity and complexity of the mechanisms of tumor progression, it is necessary to develop a new method for modeling the integrated action of these complex relationships and their impact on cancer [26].

Apoptosis is involved in progression and it has been reported that miRNAs play important roles in inducing apoptosis [27] and sensitizing tumor cells to chemotherapeutic agents [28]. In our previous study, we showed that miR-124 could sensitize human gastric cancer cells to 5-FU-induced apoptosis by downregulating EZH2 expression [3]. In this study, we demonstrated that overexpression of miR-125b upregulated apoptosis-related cleaved caspase-3 and PARP and that downregulating MCL1 could enhance the expression of 5-FU-induced cleaved caspase-3 and PARP in gastric cancer cells. These results highlight the ability of miR-125b transfection to increase chemotherapeutic drug-induced apoptosis in gastric cancer.

In summary, we observed downregulation of miR-125b in gastric cancer cells and tissues. We further found that miR-125b is an important tumor suppressor miRNA capable of inhibiting cell proliferation and invasion and promoting cell apoptosis by targeting MCL1 in gastric cancer. Our findings demonstrate that the miR-125b is important for gastric cancer initiation and progression and can be used as a potential therapeutic to suppress gastric cancer proliferation and invasion.

Disclaimer

The funders had no role in study design, data collection and analysis, decision to publish, or preparation of the paper.

Conflict of Interests

No conflict of interests is disclosed. And there are no financial or other relationships that might lead to a conflict of interests.

Authors' Contribution

Shihua Wu and Feng Liu contributed equally to this work.

Acknowledgment

This work was supported by grants from National Natural Science Foundation of China (81172575).

References

[1] J. G. Misleh, P. Santoro, J. F. Strasser, and J. J. Bennett, "Multidisciplinary management of gastric cancer," *Surgical Oncology Clinics of North America*, vol. 22, no. 2, pp. 247–264, 2013.

[2] H. Tang, Y. Kong, J. Guo et al., "Diallyl disulfide suppresses proliferation and induces apoptosis in human gastric cancer through Wnt-1 signaling pathway by up-regulation of miR-200b and miR-22," *Cancer Letters*, vol. 340, no. 1, pp. 72–81, 2013.

[3] L. Xie, Z. Zhang, Z. Tan et al., "MicroRNA-124 inhibits proliferation and induces apoptosis by directly repressing EZH2 in gastric cancer," *Molecular and Cellular Biochemistry*, vol. 392, pp. 153–159, 2014.

[4] I. Slezak-Prochazka, D. Selvi, B.-J. Kroesen, and A. van den Berg, "MicroRNAs, macrocontrol: regulation of miRNA processing," *RNA*, vol. 16, no. 6, pp. 1087–1095, 2010.

[5] T. Kunej, I. Godnic, J. Ferdin, S. Horvat, P. Dovc, and G. A. Calin, "Epigenetic regulation of microRNAs in cancer: an integrated review of literature," *Mutation Research: Fundamental and Molecular Mechanisms of Mutagenesis*, vol. 717, no. 1-2, pp. 77–84, 2011.

[6] F. E. Nicolas and A. F. Lopez-Martinez, "MicroRNAs in human diseases," *Recent Patents on DNA and Gene Sequences*, vol. 4, no. 3, pp. 142–154, 2010.

[7] H. Tang, P. Liu, L. Yang et al., "miR-185 suppresses tumor proliferation by directly targeting E2F6 and DNMT1 and indirectly up-regulating BRCA1 in triple negative breast cancer," *Molecular Cancer Therapeutics*, vol. 13, no. 12, pp. 3185–3197, 2014.

[8] H. Tang, M. Deng, Y. Tang et al., "MiR-200b and miR-200c as prognostic factors and mediators of gastric cancer cell progression," *Clinical Cancer Research*, vol. 19, no. 20, pp. 5602–5612, 2013.

[9] Z. Tan, H. Jiang, Y. Wu et al., "MiR-185 is an independent prognosis factor and suppresses tumor metastasis in gastric cancer," *Molecular and Cellular Biochemistry*, vol. 386, no. 1-2, pp. 223–231, 2014.

[10] Y. Han, Y. Liu, H. Zhang et al., "Hsa-miR-125b suppresses bladder cancer development by down-regulating oncogene SIRT7 and oncogenic long non-coding RNA MALAT1," *FEBS Letters*, vol. 587, no. 23, pp. 3875–3882, 2013.

[11] A. Feliciano, J. Castellvi, A. Artero-Castro et al., "miR-125b acts as a tumor suppressor in breast tumorigenesis via its novel direct targets ENPEP, CK2-α, CCNJ, and MEGF9," *PLoS ONE*, vol. 8, no. 10, Article ID e76247, 2013.

[12] M. Shiiba, K. Shinozuka, K. Saito et al., "MicroRNA-125b regulates proliferation and radioresistance of oral squamous cell carcinoma," *British Journal of Cancer*, vol. 108, no. 9, pp. 1817–1821, 2013.

[13] M. Ferracin, C. Bassi, M. Pedriali et al., "miR-125b targets erythropoietin and its receptor and their expression correlates with metastatic potential and ERBB2/HER2 expression," *Molecular Cancer*, vol. 12, no. 1, article 130, 2013.

[14] M. Fassan, M. Pizzi, S. Realdon et al., "The HER2-miR125a5p/miR125b loop in gastric and esophageal carcinogenesis," *Human Pathology*, vol. 44, no. 9, pp. 1804–1810, 2013.

[15] J. G. Wu, J. J. Wang, X. Jiang et al., "MiR-125b promotes cell migration and invasion by targeting PPP1CA-Rb signal pathways in gastric cancer, resulting in a poor prognosis," *Gastric Cancer*, 2014.

[16] B. Zhang and M. A. Farwell, "MicroRNAs: a new emerging class of players for disease diagnostics and gene therapy: translational Medicine," *Journal of Cellular and Molecular Medicine*, vol. 12, no. 1, pp. 3–21, 2008.

[17] Z.-X. Yang, C.-Y. Lu, Y.-L. Yang, K.-F. Dou, and K.-S. Tao, "MicroRNA-125b expression in gastric adenocarcinoma and its effect on the proliferation of gastric cancer cells," *Molecular Medicine Reports*, vol. 7, no. 1, pp. 229–232, 2013.

[18] J. Zhang, Y. Zhang, S. Liu et al., "Metadherin confers chemoresistance of cervical cancer cells by inducing autophagy and activating ERK/NF-κB pathway," *Tumor Biology*, vol. 34, no. 4, pp. 2433–2440, 2013.

[19] K. Zhu, Z. Dai, Q. Pan et al., "Metadherin promotes hepatocellular carcinoma metastasis through induction of epithelial-mesenchymal transition," *Clinical Cancer Research*, vol. 17, no. 23, pp. 7294–7302, 2011.

[20] R. J. Youle and A. Strasser, "The BCL-2 protein family: opposing activities that mediate cell death," *Nature Reviews Molecular Cell Biology*, vol. 9, no. 1, pp. 47–59, 2008.

[21] R.-Y. Li, L.-C. Chen, H.-Y. Zhang et al., "MiR-139 inhibits Mcl-1 expression and potentiates TMZ-induced apoptosis in glioma," *CNS Neuroscience and Therapeutics*, vol. 19, no. 7, pp. 477–483, 2013.

[22] F. Lu, J. Zhang, M. Ji et al., "miR-181b increases drug sensitivity in acute myeloid leukemia via targeting HMGB1 and MCL-1," *International Journal of Oncology*, vol. 45, no. 1, pp. 383–392, 2014.

[23] H. Huang, K. Shah, N. A. Bradbury, C. Li, and C. White, "Mcl-1 promotes lung cancer cell migration by directly interacting with VDAC to increase mitochondrial Ca^{2+} uptake and reactive oxygen species generation," *Cell Death and Disease*, vol. 5, no. 10, Article ID e1482, 2014.

[24] J. Gao, L. Li, M. Wu et al., "MiR-26a inhibits proliferation and migration of breast cancer through repression of MCL-1," *PLoS ONE*, vol. 8, no. 6, Article ID e65138, 2013.

[25] Y.-M. Rao, H.-R. Shi, M. Ji, and C.-H. Chen, "MiR-106a targets Mcl-1 to suppress cisplatin resistance of ovarian cancer A2780 cells," *Journal of Huazhong University of Science and Technology—Medical Science*, vol. 33, no. 4, pp. 567–572, 2013.

[26] F. Ye, H. Tang, Q. Liu et al., "miR-200b as a prognostic factor in breast cancer targets multiple members of RAB family," *Journal of Translational Medicine*, vol. 12, article 17, 2014.

[27] G. Di Leva, M. Garofalo, and C. M. Croce, "MicroRNAs in cancer," *Annual Review of Pathology*, vol. 9, pp. 287–314, 2014.

[28] C. K. Kontos, M.-I. Christodoulou, and A. Scorilas, "Apoptosis-related BCL2-family members: key players in chemotherapy," *Anti-Cancer Agents in Medicinal Chemistry*, vol. 14, no. 3, pp. 353–374, 2014.

Hindawi Publishing Corporation
BioMed Research International
Volume 2015, Article ID 359392, 14 pages
http://dx.doi.org/10.1155/2015/359392

Research Article

Prognostic Value of Homotypic Cell Internalization by Nonprofessional Phagocytic Cancer Cells

Manuela Schwegler,[1] Anna M. Wirsing,[1] Hannah M. Schenker,[1] Laura Ott,[1] Johannes M. Ries,[1] Maike Büttner-Herold,[2] Rainer Fietkau,[1] Florian Putz,[1] and Luitpold V. Distel[1]

[1]*Department of Radiation Oncology, University Hospital Erlangen, 91054 Erlangen, Germany*
[2]*Department of Pathology, University Hospital Erlangen, 91054 Erlangen, Germany*

Correspondence should be addressed to Luitpold V. Distel; luitpold.distel@uk-erlangen.de

Received 13 February 2015; Accepted 17 June 2015

Academic Editor: Franco M. Buonaguro

Background. In this study, we investigated the prognostic role of homotypic tumor cell cannibalism in different cancer types. *Methods*. The phenomenon of one cell being internalized into another, which we refer to as "cell-in-cell event," was assessed in 416 cases from five head and neck cancer cohorts, as well as one anal and one rectal cancer cohort. The samples were processed into tissue microarrays and immunohistochemically stained for E-cadherin and cleaved caspase-3 to visualize cell membranes and apoptotic cell death. *Results*. Cell-in-cell events were found in all of the cohorts. The frequency ranged from 0.7 to 17.3 cell-in-cell events per mm^2. Hardly any apoptotic cells were found within the cell-in-cell structures, although apoptotic cell rates were about 1.6 to two times as high as cell-in-cell rates of the same tissue sample. High numbers of cell-in-cell events showed adverse effects on patients' survival in the head and neck and in the rectal cancer cohorts. In multivariate analysis, high frequency was an adverse prognostic factor for overall survival in patients with head and neck cancer ($p = 0.008$). *Conclusion*. Cell-in-cell events were found to predict patient outcomes in various types of cancer better than apoptosis and proliferation and might therefore be used to guide treatment strategies.

1. Background

The mechanism by which a cell becomes internalized into another is the definition of the term "cell-in-cell formation" [1]. Cell-in-cell (CIC) formation includes the internalization of living lymphocytes into nonphagocytic cells (emperipolesis), the homotypic and heterotypic phagocytosis-like uptake of living or dead cells, and the invasion of one tumor cell into the host cell (entosis). The definition also covers the fate of the included cells, which can undergo cell death, remain in the host cell, undertake cell division, or pass out of the cell. In this context the term cell cannibalism arose that describes the uptake of alive and dead tumor cells as well as of lymphocytes by tumor cells and is restricted to cancer cells [2]. Cannibalism was suggested as a marker of malignancy [3] and reported to provide an advantage for survival. Lugini et al. reported that cannibalistic malignant metastatic melanoma cells engulf autologous live $CD8^+$ T-lymphocytes as a source of nutrients under starvation conditions [4]. Reports on homotypic cannibalism are conflicting, proposing a tumor-promoting and metastasis-protecting role. This discrepancy complicates the use of homotypic cannibalism as a prognostic factor [5–7] and highlights that further studies are necessary to shed light on this phenomenon and its impact on eventual cancer type-specific prognosis. Investigation on the phagocytic activity of cancer cells and normal fibroblasts may contribute to providing new insights into this issue [8, 9]. The use of in vivo experiments to identify the triggering factors and underlying mechanisms of cell cannibalism may facilitate a prognosis-relevant examination of CIC formation in association with specific proteins in tumor tissue sections.

Here, we present data on the prognostic relevance of CIC structures and their divergent effects on patient prognosis in

three different tumor entities. Additionally, the impact of CIC rates was compared to those of apoptosis and proliferation.

2. Methods

2.1. Human Specimens. Cancer tissue samples from 416 patients were evaluated for the presence of CIC structures. Patients originated from seven different cohorts. (i) One cohort of anal carcinomas ($n = 23$) and (ii) one rectal cancer cohort ($n = 83$) were studied. Five head and neck squamous cell carcinoma (HNSCC) cohorts were compared, including (iii) an early disease, low-risk group ($n = 62$); (iv) an advanced disease, high-risk group ($n = 52$); (v) cancer biopsies with affected lymph nodes ($n = 29$); (vi) pretherapeutic biopsies with posttherapeutic tumor resections ($n = 35$); and (vii) pretherapeutic tumor resections of the central tumor area and the invasion front ($n = 143$). All patients were treated by definitive, adjuvant, or neoadjuvant radiotherapy or radiochemotherapy. Patients characteristics are described in Tables 1 and 2. Patient characteristics of five of the cohorts were previously published [10–13]. All samples were processed into tissue microarrays (TMAs) of 1.6–2 mm diameter cores [14]. Clinical data were obtained from the Erlangen Tumour Centre Database. All patients signed a "front door" informed consent allowing collection of their tissue and clinical data. The study was approved by the Ethics Review Committee of the University Hospital Erlangen, Erlangen, Germany.

2.2. Antibodies and Immunohistochemistry. Immunohistochemistry was performed for detection of specific proteins in tissue sections using several antibodies including Ki-67 (DakoCytomation, Hamburg, Germany), cleaved caspase-3 (Cell Signaling, Danvers, MA, USA), E-cadherin (BD, Heidelberg, Germany), CD68 (DakoCytomation), and Alexa Fluor 488, 555, 594, and 647 conjugated secondary antibodies (all from Invitrogen, Darmstadt, Germany).

Double staining was performed with Ki-67 and cleaved caspase-3-specific antibodies. Briefly, sections were incubated overnight with a cleaved caspase-3-specific antibody and then a biotin-labeled secondary antibody. Biotin was visualized using streptavidin-biotinylated alkaline phosphatase complex (DakoCytomation). Fast Red was used as a chromogen. A double staining enhancer (Zymed, San Francisco, California, USA) was used followed by an avidin and biotin block (Avidin/Biotin Blocking Kit, Vector Laboratories, Peterborough, UK). Slides were incubated with Ki-67-specific primary antibodies after application of a postblock solution. Secondary antibodies covalently linked with an AP-Polymer (ZytoChem-Plus, Berlin, Germany) were used with Fast Blue (Sigma-Aldrich, Taufkirchen, Germany) as a chromogen. E-cadherin labeling was performed on a Ventana BenchMark Ultra stainer (Roche, Grenzach-Wyhlen, Germany) using CC1 buffer (Benchmark ULTRA CC1, Roche) for antigen retrieval. Cell nuclei were stained with hematoxylin.

In a quadruple immunofluorescence approach, four antigens were labeled successively in HNSCC tumor specimens. Antigen retrieval was performed in a steam cooker (Biocarta Europe, Hamburg, Germany) for 5 min at 120°C using a target retrieval solution (pH 6) (TRS6, DakoCytomation) or 0.01 M Na-citrate buffer (pH 6). Cells were stained with primary and secondary antibodies, nuclei were counterstained with 4′,6-diamidino-2-phenylindole (DAPI) (Roche), and slides were mounted with Vectashield medium (Vector Laboratories).

2.3. Imaging and Image Analysis. Stained TMAs were scanned with a high throughput scanner (Mirax MIDI Scan, Zeiss, Göttingen, Germany) equipped with a Plan-Apochromat objective (20x; NA: 0.8, Zeiss) and a camera (Stingray F146C, AVT, Stadtroda, Germany). Images were converted into TIF format and each TMA spot was saved separately. CIC structures were counted using Biomas image processing software (MSAB, Erlangen, Germany). A minimum of two TMA core sections with tumor areas of 0.75 mm^2 was evaluated per patient. Apoptotic cells, proliferating cells, and CIC structures were counted in the same area. To achieve this, the E-cadherin TMA spot was precisely aligned with Ki-67/cleaved caspase-3 double-stained spot using the image analysis system. The region of interest was selected in the E-cadherin spot and transferred to the Ki-67/cleaved caspase-3 spot, and events were counted.

2.4. Statistical Analysis. IBM SPSS Statistics version 19 was used. The Kolmogorov-Smirnov test and Lilliefors test were applied for testing normality. The local failure-free, metastasis-free, and overall survival was calculated according to Kaplan Meier. The log-rank test was used to compare survival curves between subgroups of patients. Univariate and multivariate regression analyses of overall survival were performed using Cox's proportional hazards model (Table 3, additional file 2, Tables A2-A3 in Supplementary Material available online at http://dx.doi.org/10.1155/2015/359392). The proportional hazards assumption was tested through plotting log-minus-log curves. p values < 0.05 were considered to be significant.

3. Results

3.1. Study Groups. The frequency and prognostic relevance of CIC structures in tumor tissue were investigated. A total of 416 tumor tissue samples from five cohorts of HNSCC and one (i) anal and one (ii) rectal cancer cohort were analyzed for the presence of CIC structures. The five HNSCC cohorts consisted of the following: (iii) a low-risk, early disease, treated by adjuvant radiochemotherapy (RCT); (iv) a high-risk, advanced disease, treated by definitive radiotherapy (RT) [10]; (v) metastatic disease, treated by adjuvant RT or RCT [11]; (vi) no distant metastasis, treated by neoadjuvant RCT [12]; and (vii) tumors treated by adjuvant RT or RCT having tissue samples of the central tumor area and the invasion front. The patients' clinical and histological characteristics are depicted in Tables 1 and 2. Overall survival in the head and neck and rectal and anal cancer cohort were 60.3%, 75.0%, and 68.5% at 5 years, respectively. The median follow-up in the head and neck and rectal and anal cancer cohort were 4.6, 7.2, and 3.8 years, respectively. Median and mean local failure-free, metastasis-free, and overall survival time are presented in additional file 2, Table A1.

Table 1: Clinical characteristics of the head and neck squamous cell carcinoma cohorts.

	All HNSCC		Early disease Adjuvant RCT			Advanced disease Definitive RT			Metastatic disease			Neoadjuvant RCT			Adjuvant RCT Center/invasion front		
n	321		62			52			29			35			143		
Gender (*n*)																	
Male	274	(85.4)	51	(82.3)	(15.9)	43	(82.7)	(13.4)	28	(96.6)	(8.7)	32	(91.4)	(10)	120	(83.9)	(37.4)
Female	47	(14.6)	11	(17.7)	(3.4)	9	(17.3)	(2.8)	1	(3.4)	(0.3)	3	(8.6)	(0.9)	23	(16.1)	(7.2)
Age (years)																	
Median (95% C.I.)	54.3	(53.9–55.7)	51.0	(49.4–53.3)		56.0	(53.2–58)		53.0	(49.3–55)		52.5	(51.3–54.5)		58.0	(56.2–59.2)	
Local failure time (months)																	
Median (95% C.I.)	50.0	(58.3–69.4)	67.0	(72.1–111)		42.0	(44.9–72.4)		51.0	(48.8–83.9)		87.0	(74.1–96.6)		32.0	(34.5–46.1)	
Time to metastatic disease (months)																	
Median (95% C.I.)	53.0	(61.7–73)	81.5	(82–121.7)		42.0	(44.7–72.4)		61.0	(51.3–85.7)		90.0	(77.2–99.6)		37.5	(37–48.3)	
Overall survival time (months)																	
Median (95% C.I.)	54.0	(63.5–74.6)	81.5	(82–121.7)		44.0	(47.6–74.2)		61.0	(53.8–89.3)		90.0	(77.5–99.8)		41.0	(39.9–51)	
T stage (*n*)																	
T1	59	(18.4)	13	(21)	(4)	0	0	(0)	7	(24.1)	(2.2)	3	(8.6)	(0.9)	36	(25.2)	(11.2)
T2	105	(32.7)	30	(48.4)	(9.3)	2	(3.8)	(0.6)	8	(27.6)	(2.5)	9	(25.7)	(2.8)	56	(39.2)	(17.4)
T3	78	(24.3)	14	(22.6)	(4.4)	25	(48.1)	(7.8)	6	(20.7)	(1.9)	6	(17.1)	(1.9)	27	(18.9)	(8.4)
T4	79	(24.6)	5	(8.1)	(1.6)	25	(48.1)	(7.8)	8	(27.6)	(2.5)	17	(48.6)	(5.3)	24	(16.8)	(7.5)
N stage (*n*)																	
N0	68	(21.2)	23	(37.1)	(7.2)	5	(9.6)	(1.6)	0	(0)	(0)	7	(20.0)	(2.2)	38	(26.6)	(11.8)
N1	55	(17.1)	17	(27.4)	(5.3)	4	(7.7)	(1.2)	4	(13.8)	(1.2)	2	(5.7)	(0.6)	29	(20.3)	(9)
N2	186	(57.9)	22	(35.5)	(6.9)	41	(78.8)	(12.8)	23	(79.3)	(7.2)	25	(71.4)	(7.8)	69	(48.3)	(21.5)
N3	12	(3.7)	0	(0)	(0)	2	(3.8)	(0.6)	2	(6.9)	(0.6)	1	(2.9)	(0.3)	7	(4.9)	(2.2)
M stage (*n*)																	
M0	237	(73.8)	62	(100.0)	(19.3)	39	(75.0)	(12.1)	6	(20.7)	(1.9)	32	(91.4)	(10)	98	(68.5)	(30.5)
M1	84	(26.2)	0	(0.0)	(0)	13	(25.0)	(4)	23	(79.3)	(7.2)	3	(8.6)	(0.9)	45	(31.5)	(14)
Grading (*n*)																	
G1/2	176	(54.8)	37	(59.7)	(11.5)	37	(71.2)	(11.5)	15	(51.7)	(4.7)	27	(77.1)	(8.4)	60	(42)	(18.7)
G3/4	145	(45.2)	25	(40.3)	(7.8)	15	(28.8)	(4.7)	14	(48.3)	(4.4)	8	(22.9)	(2.5)	83	(58)	(25.9)
UICC97 (*n*)																	
1	15	(4.7)	6	(9.7)	(1.9)	0	(0)	(0)	0	(0)	(0)	1	(2.9)	(0.3)	8	(5.6)	(2.5)
2	30	(9.3)	13	(21)	(4)	0	(0)	(0)	1	(3.4)	(0.3)	2	(5.7)	(0.6)	14	(9.8)	(4.4)
3	61	(19)	17	(27.4)	(5.3)	7	(13.5)	(2.2)	2	(6.9)	(0.6)	2	(5.7)	(0.6)	33	(23.1)	(10.3)
4	215	(67)	26	(41.9)	(8.1)	45	(86.5)	(14)	26	(89.7)	(8.1)	30	(85.7)	(9.3)	88	(61.5)	(27.4)

Values behind the first bracket are relative values within the subcohort and values behind the second bracket are relative values of the total cohort. Confidence interval: C.I.

Table 2: Clinical characteristics of the rectal and anal cancer cohorts.

	Rectal cancer, clinical	Rectal cancer, pathological	Anal cancer
All	83	83	23
Male	59 (71.1)		9 (39.1)
Female	24 (28.9)		14 (60.9)
Age (years)			
Median (95% C.I.)	64.0 (59.7–65.2)		59.0 (48.7–64.2)
Local failure time (months)			
Median (95% C.I.)	39.0 (35.7–44.1)		71.0 (53.3–98.8)
Time to metastatic disease (months)			
Median (95% C.I.)	38.0 (29.9–40.5)		82.0 (62–113.5)
Overall survival time (months)			
Median (95% C.I.)	44.0 (41.9–48.6)		86.5 (65.9–115.6)
T stage (*n*)			
T0	—	11 (13.3)	—
T1	0 (0)	2 (2.4)	1 (4.3)
T2	7 (8.4)	25 (30.1)	13 (56.5)
T3	64 (77.1)	32 (38.6)	7 (30.4)
T4	12 (14.5)	13 (15.7)	2 (8.7)
N stage (*n*)			
N0	18 (21.7)	53 (63.9)	10 (43.5)
N1	52 (62.7)	30 (36.1)	5 (21.7)
N2	13 (15.7)	0 (0.0)	8 (34.8)
M stage (*n*)			
M0	53 (63.9)	—	20 (87)
M1	30 (36.1)	—	3 (13)
Grading (*n*)			
G1/2	73 (88.0)		16 (69.6)
G3/4	10 (12.0)		7 (30.4)
UICC97 (*n*)			
1	22 (26.5)		3 (13)
2	28 (33.7)		7 (30.4)
3	21 (25.3)		13 (56.5)
4	12 (14.5)		0 (0)

3.2. Criteria of CIC Structures. All tumor tissues were processed into TMAs and were stained for the adhesion molecule E-cadherin to visualize cell membranes. Nuclei were counterstained with hematoxylin (Figure 1(a)). Stained TMA spots were analyzed for the presence of CIC events per mm^2 using an image analysis system. Three criteria were used to define homotypic CICs: total encirclement of the inner cell by the host cell membrane, a semilunar host cell nucleus, and a round shape of the inner cell (Figure 1(b)).

3.3. CIC Structures Are Found in Various Tumor Tissues with Varying Frequencies. CIC structures were found in all of the cancer cohorts. The average frequency ranged from 0.7 CICs/mm^2 in the (iii) low-risk, early disease HNSCC to 17.3 CICs/mm^2 in the (ii) rectal cancer group (Figure 1(c)). The percentage of CIC-positive cancer tissues varied from 25.0% in the (vi) posttherapeutic HNSSC collection to 95.7% in the (i) anal cancer cohort (Figure 1(d) (A)–(E)). The pretherapeutic biopsies from the anal cancer cohort showed a high frequency of CIC-positive samples, with an average frequency of 10.7 CICs/mm^2. However, the highest single values of up to 200 CICs/mm^2 were observed in the (ii) posttherapeutic rectal cancer cohort.

In HNSCC tumor samples, we grouped the patients cohorts according to low- and high-risk characteristics and treatment modalities for separate analyses and comparison. We found that (iv) high-risk, inoperable patients with advanced disease had significantly more CIC than (iii) low-risk patients with early disease (Figures 1(c) and 1(d) (B)). In (v) lymph nodes, the average CIC numbers were significantly lower than in the corresponding primary tumors, while the number of CIC-positive patients differed only slightly (Figures 1(c) and 1(d) (C)). In a HNSCC cohort with (vi) pretherapeutic biopsy and tumor resections six weeks after RCT, both the frequency of CIC-positive patients and the average CIC number decreased significantly (Figures 1(c) and 1(d) (D)). We also compared CIC numbers in the (vii) central tumor area and at the invasive front. In the central tumor

Table 3: Univariate and multivariate overall survival analyses according to Cox's proportional hazards model and HNSCC adjuvant radiochemotherapy central tumor area collectively.

HNSCC central tumor area; $n = 143$	Univariate analysis			Multivariate analysis		
Variable	Hazard ratio	95% C.I.	p	Hazard ratio	95% C.I.	p
Age, years (younger than 58 years [$n = 72$] versus older than 58 years [$n = 71$])	1.853	1.007–3.41	**0.048**	1.559	0.901–2.697	0.113
Gender (male [$n = 120$] versus female [$n = 23$])	1.275	0.566–2.871	0.558	—	—	—
T category (T1/T2 [$n = 92$] versus T3/T4 [$n = 51$])	0.748	0.36–1.554	0.436	—	—	—
N category (N0 [$n = 38$] versus N+ [$n = 105$])	1.080	0.333–3.5	0.899	—	—	—
M-category (M0 [$n = 98$] versus M+ [$n = 45$])	8.094	1.59–41.214	**0.012**	4.660	1.377–15.767	**0.013**
Stage (UICC I [$n = 22$] versus UICC II and higher [$n = 121$])	0.971	0.309–3.053	0.960	—	—	—
Grade (1 + 2 [$n = 60$] versus 3 + 4 [$n = 83$])	0.987	0.526–1.851	0.967	—	—	—
CIC ($0/mm^2$ [$n = 74$] versus $>0/mm^2$ [$n = 69$])	2.555	1.334–4.894	**0.005**	2.139	1.215–3.764	**0.008**
Apoptotic cells ($<9.5/mm^2$ [$n = 71$] versus $\geq 9.5/mm^2$ [$n = 72$])	1.037	0.329–3.266	0.950	—	—	—
Proliferating cells ($<122/mm^2$ [$n = 71$] versus $\geq 122/mm^2$ [$n = 72$])	0.689	0.358–1.325	0.264	0.686	0.39–1.208	0.192

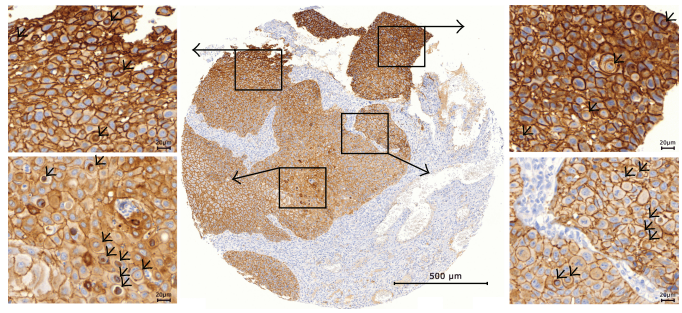

(a)

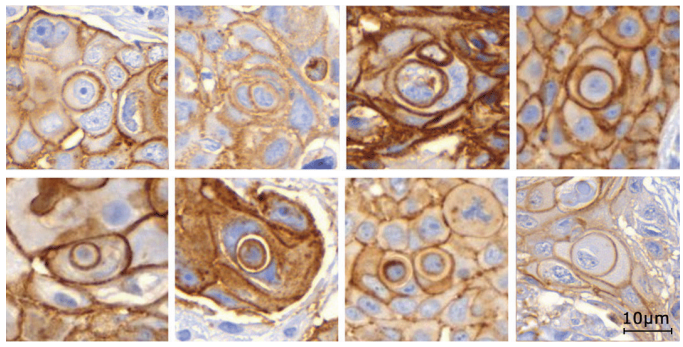

(b)

Tissue										
n =	23	83	62	52	29	29	35	32	143	102
with CIC (%) =	95.7	72.2	67.7	69.2	82.6	75.9	80.0	25.0	49.7	27.5

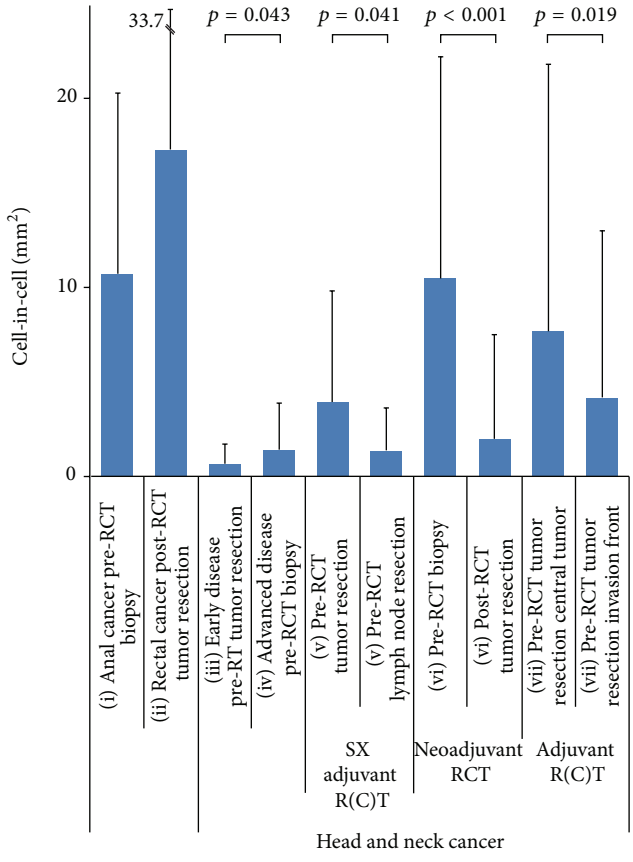

(c)

Figure 1: Continued.

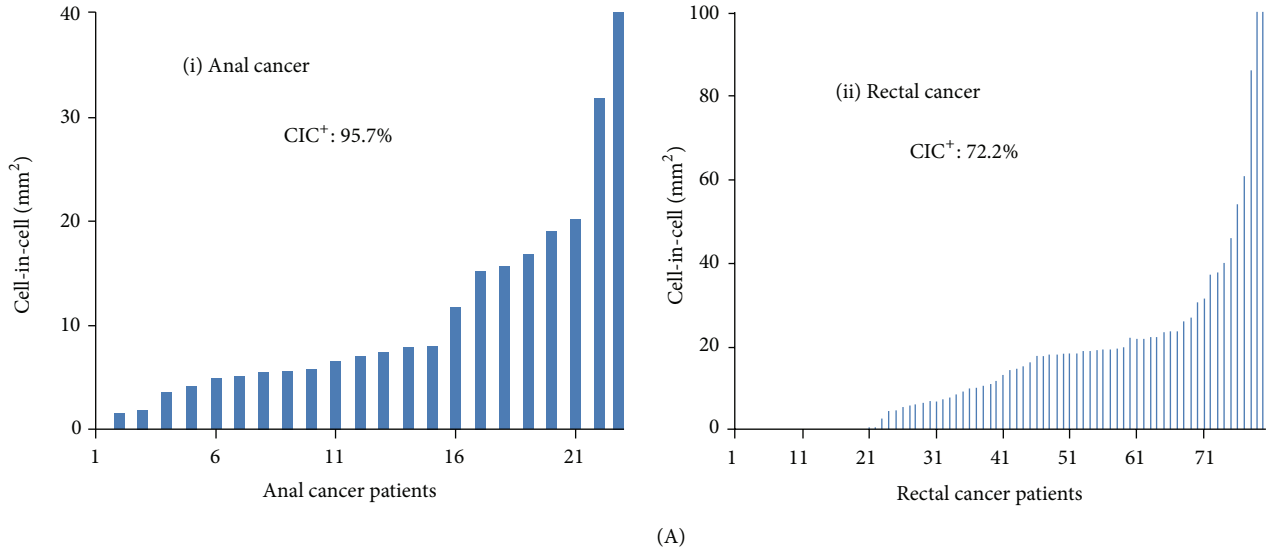

(A)

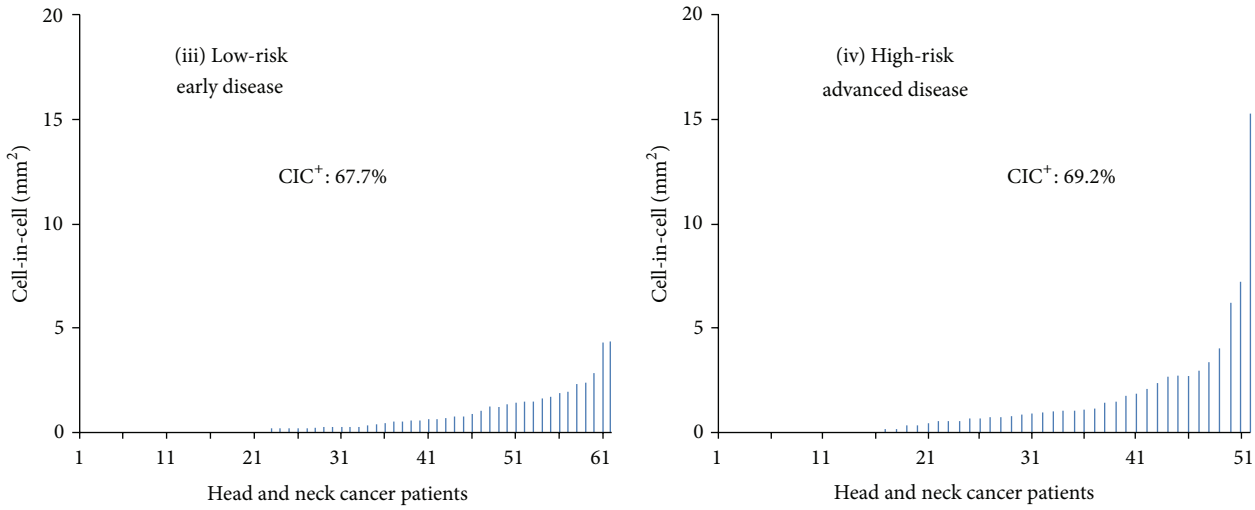

(B)

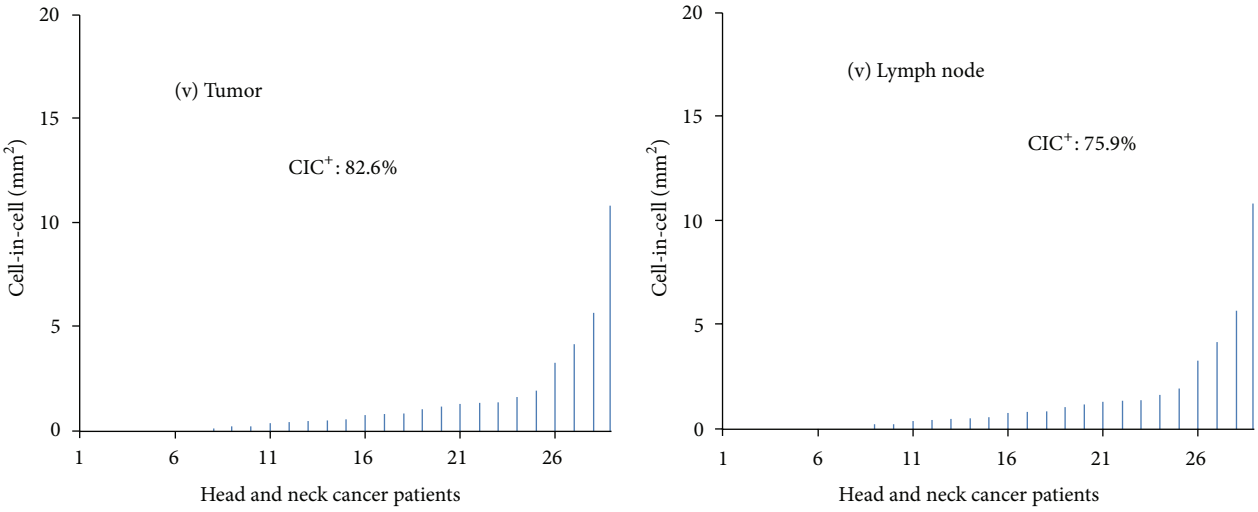

(C)

Figure 1: Continued.

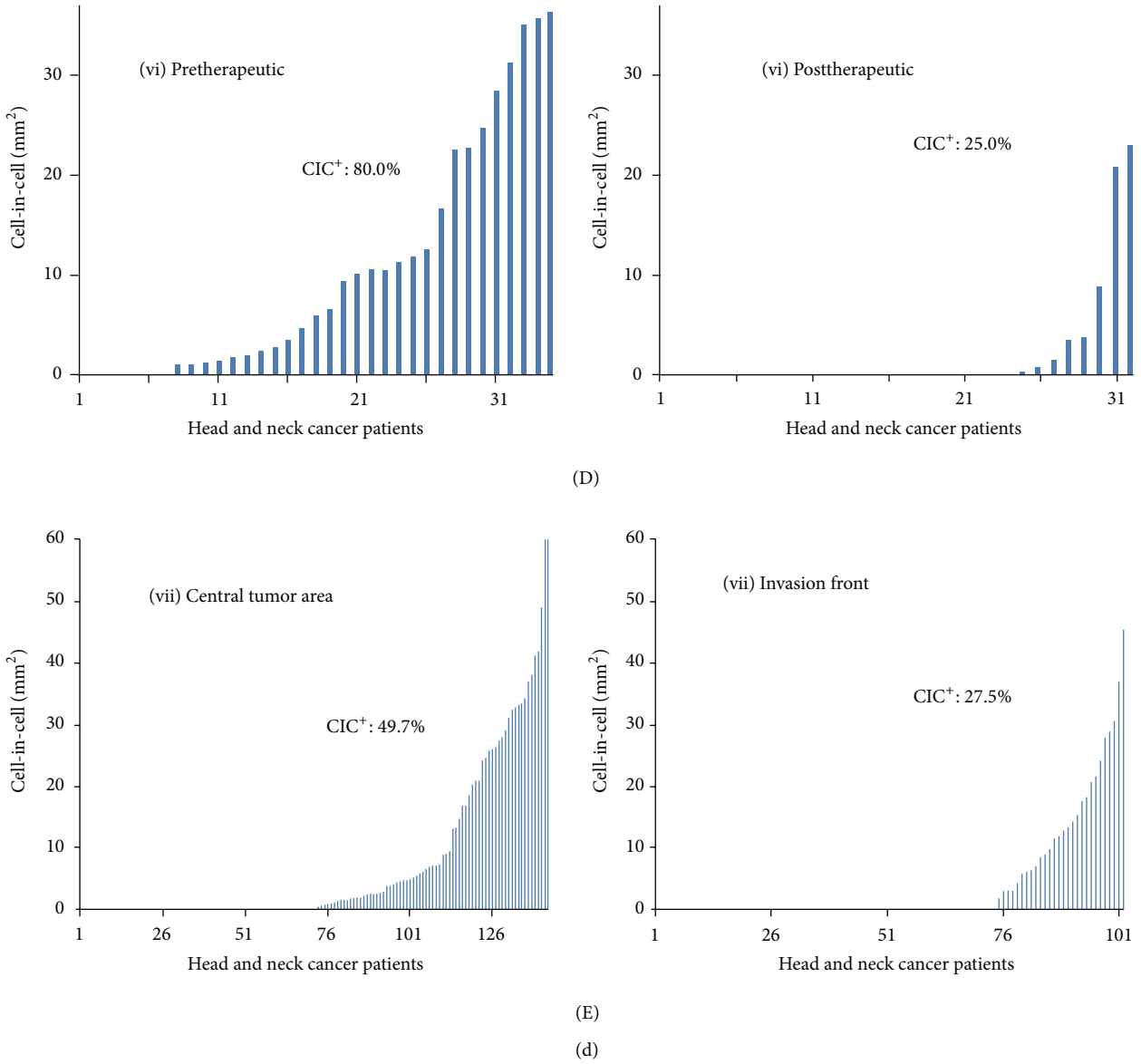

Figure 1: Cell-in-cell structures are found in different tumor tissues. (a) Representative image of an E-cadherin-labeled head and neck squamous cell carcinoma tissue microarray spot with numerous CIC structures and magnifications of indicated regions. (b) Representative images of E-cadherin-labeled head and neck cancer CIC structures. (c) Frequency of CIC structures in different cancer types. (d) Comparative frequency of CIC (A) in the tumor tissue of rectal and anal cancer patients, (B) in low-risk and high-risk HNSCC patients, (C) in the primary tumor of HNSCC tumors and the affected regional lymph nodes, (D) before and after neoadjuvant radiochemotherapy, and (E) in the central tumor area and invasive front of HNSCC. R(C)T: radiochemotherapy or radiotherapy.

area, more samples were CIC-positive and the overall average value of CIC structures was higher than in the invasive front (Figures 1(c) and 1(d) (E)).

3.4. CIC Rate Compared to Apoptotic Cell Death and Proliferation. We then compared CIC frequency to apoptotic cell death and proliferation by quantifying apoptotic and proliferating cells in HNSCC samples stained for cleaved caspase-3 and Ki-67. In total, we studied 143 central tumor samples and 102 invasive front samples. Compared to invasive front samples, significantly more CIC structures and apoptotic cells were identified in samples from cancer centers. In the central tumor area, the portion of apoptotic cells was 1.6 times higher than that of CIC structures, and the number of apoptotic cells in the invasive front was two times higher (Figures 2(a) and 2(b)). The proportion of proliferating cells was much higher than that of CIC and apoptosis, with similar frequencies in the central tumor area and the invasive front (Figures 2(a) and 2(c)).

3.5. CIC Rate and Cell Death Events in Tumor Sections. We were particularly interested in whether the inner cells of

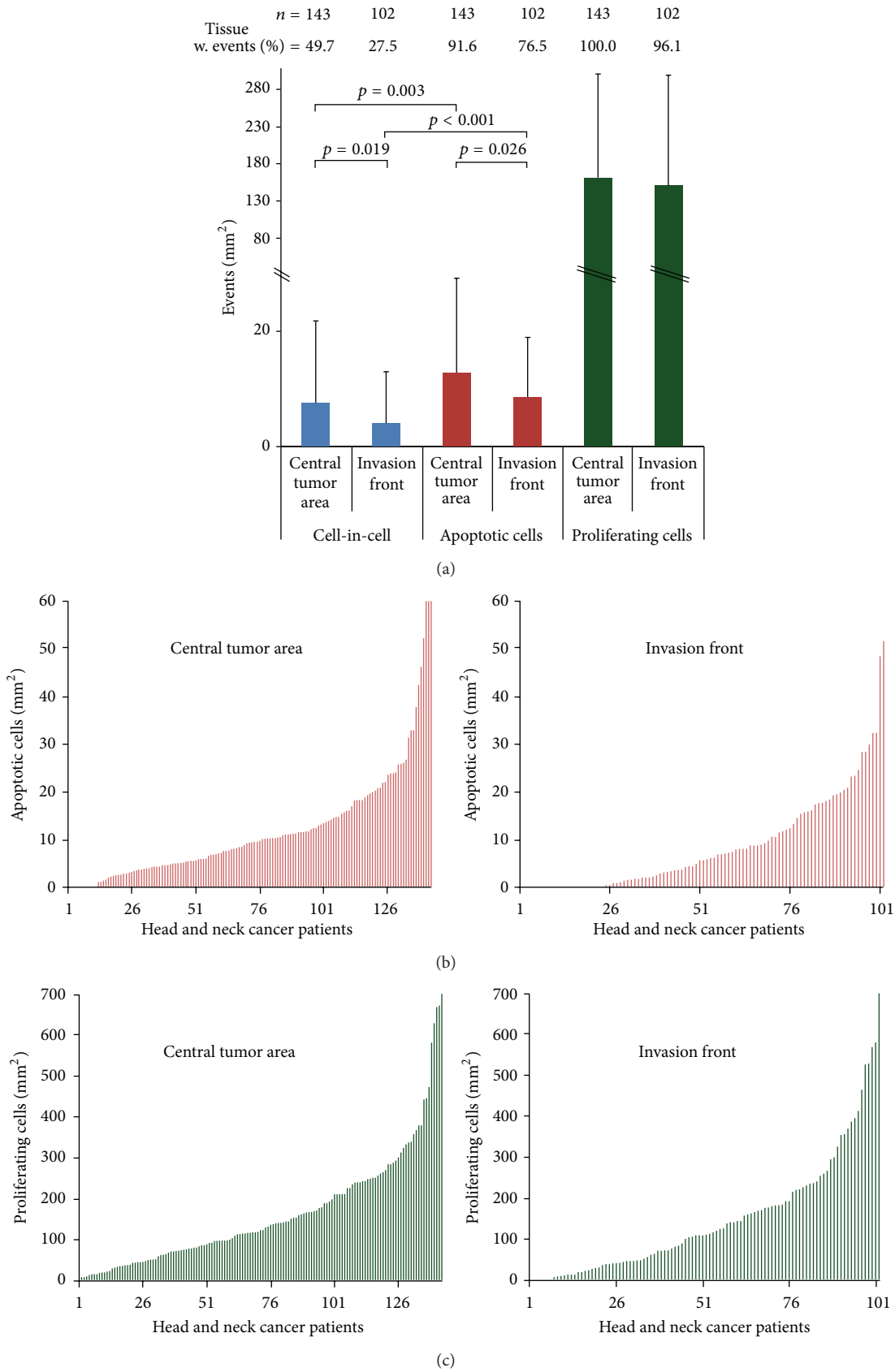

FIGURE 2: Apoptotic and proliferating cell rates. (a) CIC events, apoptotic cells, and proliferating cells in the central tumor area and invasive front of HNSCC. Frequency of (b) apoptotic and (c) proliferating cells in the central tumor area compared to the invasive front of individual HNSCC patients.

CIC structures in tumor tissue were apoptotic. Thus, we stained the HNSCC tumor samples with cleaved caspase-3 to determine whether CIC structures in tumor tissue sections contained apoptotic cells. We counted 572 CIC events and found three cleaved caspase-3-positive cells; thus 99.5% of CIC structures were negative for cleaved caspase-3 (Figure 3(a)).

To determine whether there is a relationship between the frequency of CIC formation and apoptotic cells, we correlated both events in the pre- and posttherapeutic tissue samples from central tumor areas and invasion fronts. There was no correlation between these events, indicating that high numbers of apoptotic cells do not promote CIC formation (Figures 3(b) and 3(c)).

Additionally, we used multicolor immunofluorescence imaging of anal and HNSCC cancer in order to stain the tissue with DAPI, E-cadherin, cleaved caspase-3, Ki-67, and the phagocytic marker CD68. A recent report on homotypic cell cannibalism in pancreatic adenocarcinoma suggested ectopic expression of the scavenger receptor gene CD68 as a marker of cannibalistic cells in pancreatic adenocarcinoma [7]. Our histological study did not reveal expression of CD68 indicating that this molecule is not necessary for CIC formation in these tissues. We visualized rare CIC structures (green arrows) with inner apoptotic cells (red arrows), high numbers of not-engulfed Ki-67-positive proliferating cells (yellow arrow), and CD68-positive cells (orange arrows) that were presumably macrophages (Figure 3(d), additional file 1, Figure A1).

3.6. CIC Rates as Prognostic Factor for Different Tumor Entities. In total, 23 anal cancer patients, 83 rectal cancer patients, and 234 HNSCC patients were included in this analysis. Kaplan-Meier plot analysis was based on the elapsed time from the date of diagnosis, and this method revealed that more than 10 CICs/mm^2 had a positive impact on local failure-free survival for anal cancer ($p = 0.007$). The correlation for metastasis-free, tumor-specific survival (additional file 1, Figure A2) and overall survival was weaker. By contrast, either low numbers or the absence of CIC structures had a beneficial prognostic value in rectal cancer and HNSCC. In these cohorts, low CIC rates were associated with longer local failure-free and metastasis-free survival ($p = 0.032$, for rectal cancer). Low numbers or the absence of CIC structures was significantly correlated to an improved overall survival in HNSCC ($p = 0.005$) (Figure 4).

A multivariate analysis of the HNSCC adjuvant therapy subgroup with samples of the central tumor area was performed. Age, M-category, CIC/mm^2, and proliferating cells/mm^2 were included. Only CIC/mm^2 and M-category were independent significant variables with impact on overall survival (Table 2). Neither apoptotic rates nor proliferating cells had an impact on overall survival. The five HNSCC cohorts were grouped and a multivariate analysis was performed; for those cases all clinical data, patient's characteristics, and immunohistological data were available. 234 patients were included and gender, M-category, grading, and CIC/mm^2 were analyzed in a multivariate way. Again only CIC/mm^2 and M-category were independent significant variables with impact on overall survival (additional file 2, Table A2). In multivariate analysis of rectal cancer patients distance of tumor from anal verge, grading, and CIC/mm^2 were included. Only grading was an independent significant variable with impact on overall survival (additional file 2, Table A3).

4. Discussion

4.1. CIC Frequency in Tissue Correlates with Patient Outcomes. CIC events were observed in all of the cohorts, but the number of CIC-positive patients and the CIC rates vary considerably, depending on the cancer type, stage, previous therapeutic intervention, and localization of CIC events within the tumor. Compared to apoptotic cell rates, CIC rates are half to two-thirds as frequent. Though CICs are frequent events they have been nearly completely disregarded in the last 100 years [15]. We studied the possible correlation between CIC structures found in tumor tissues and patients' prognosis and confirmed that engulfed tumor cells in HNSCC and rectal and anal carcinoma tissues have a clear impact on the prognosis of these patients. In the anal cancer cohort, high numbers of CIC events led to an improved prognosis, whereas, in the HNSCC and rectal cancer cohorts, low numbers were associated with a good prognosis. Previously, a relationship between the occurrence of homotypic CIC structures and low risk for metastasis was observed in pancreatic adenocarcinoma patients [7]. In contrast, several studies have proposed a relationship between poor prognosis and the presence of homotypic cannibalism in breast carcinoma [6], bladder cancer [16], and medulloblastoma [5], as well as the presence of heterotypic cannibalism in gastric carcinoma [17]. Consistent with these heterogeneous studies, our results indicate that existence of CIC structures affects patient outcomes in different ways. The discrepancy observed in the correlation of CIC frequency and patient outcomes in different tumor entities might be explained by tissue and cell type-specific properties regarding tumor-specific metastatic potential and immune cell infiltration.

It was shown that homotypic CIC structures normally undergo cell death [7] regardless of whether alive cells or dead cells are internalized [4, 18]. Therefore, CIC seems to be a kind of cell death. However, the Nomenclature Committee on Cell Death (NCCD) demands the approval of CIC to be degraded within the cell as a result of homotypic interactions and that it should not be dependent on apoptotic cell [19]. Thus, we compared the frequency of apoptotic cells to CIC rates. We found CIC rates, which were half to two-thirds as frequent as apoptotic rates. However, only very rarely the engulfed cells were apoptotic and there was no correlation between the frequency of apoptotic and CIC rates. We hypothesize that the conditions of the NCCD are met. We would speculate that the engulfed cells were alive and matrix-deprived cells similar to metastatic cells and were phagocytized by cancer cells. Further, after engulfment cells lacked the chance to develop an apoptotic phenotype due to internalization and metabolic degradation.

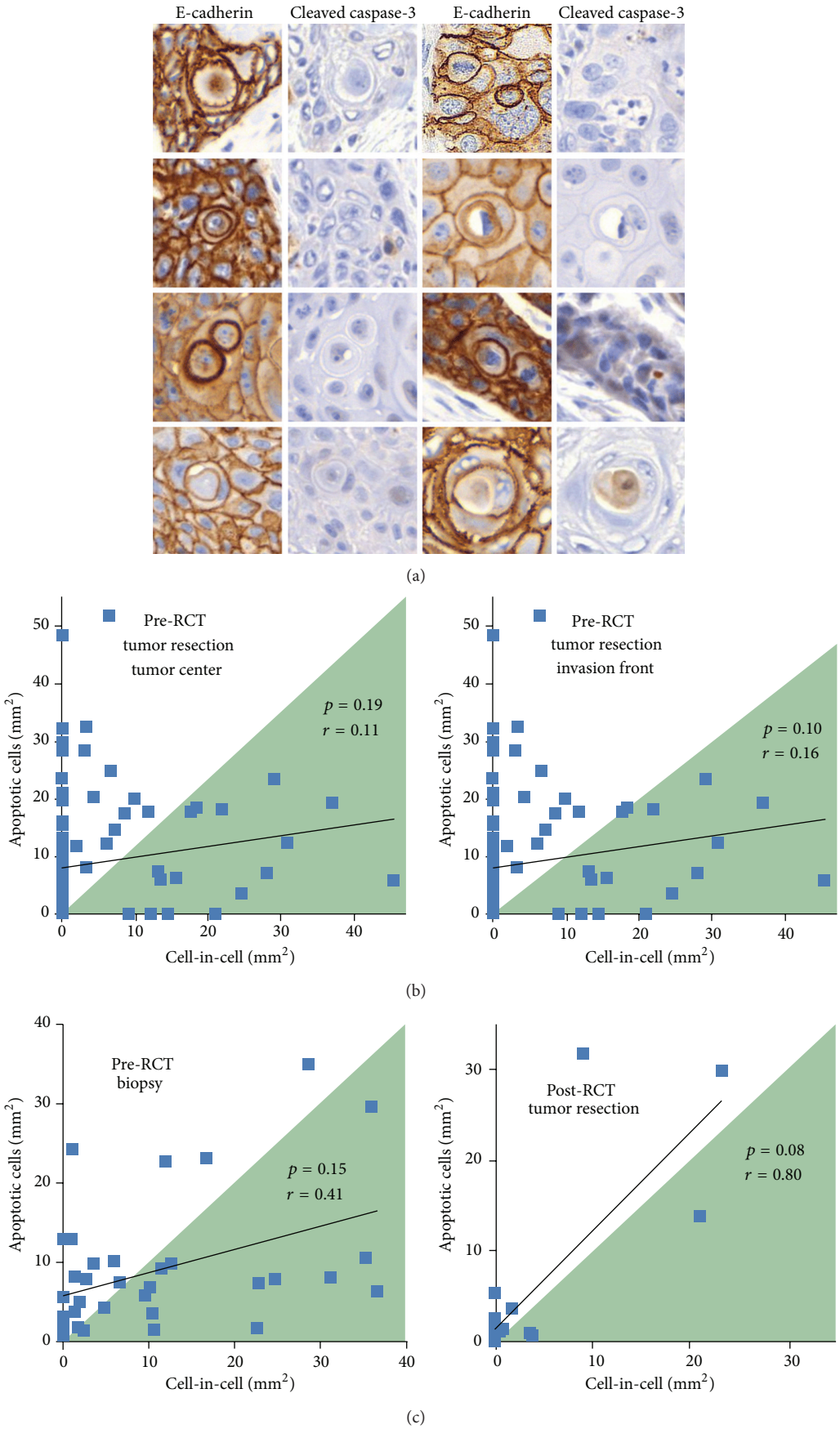

Figure 3: Continued.

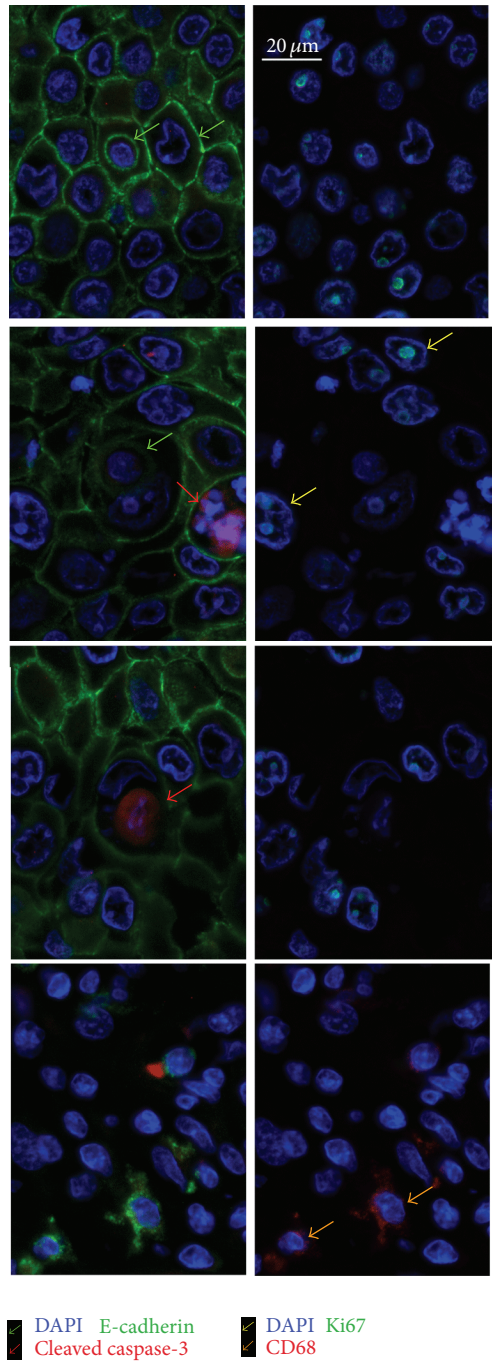

(d)

Figure 3: Cell-in-cell events compared to apoptotic events and prognostic impact of cell-in-cell events. (a) E-cadherin and cleaved caspase-3-labeled tumor sections containing CIC structures. (b) Frequency of CIC structures compared with the frequency of apoptotic cells in the central tumor area and invasive front of HNSCC. (c) CIC frequency compared to apoptotic cells in pretherapeutic biopsies and in posttherapeutic tumor resections of HNSCC. The shaded area marks tissues containing more CIC/mm^2 than apoptotic cells/mm^2. (d) Immunofluorescence staining for E-cadherin and cleaved caspase-3 in the left panel and Ki-67 and CD68 in the right panel. Nuclei were stained with DAPI.

Alternatively, it is possible that necrotic dying cells were phagocytized. Nevertheless, CIC frequency was an independent prognostic factor in multivariate analyses of the HNSCC cohorts, whereas apoptotic and proliferating rates did not reach a comparable impact. Maybe CICs have a similar high importance in prognosis as apoptosis and proliferation. Furthermore it could be speculated that CIC structure formation impacts tumor patient outcomes by elimination

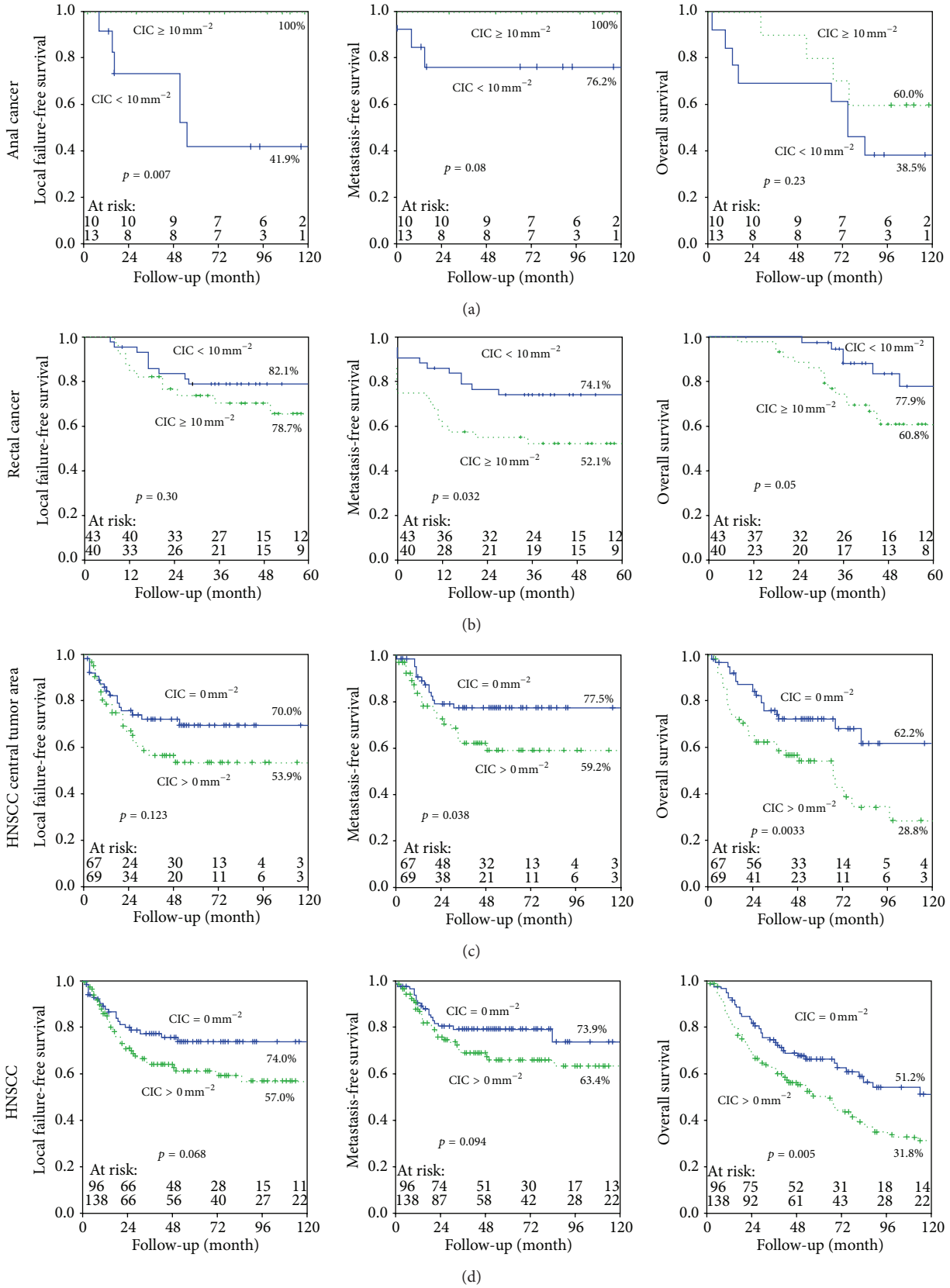

FIGURE 4: Kaplan-Meier analyses. (a) Kaplan-Meier curves depicting anal and (b) rectal cancer patients with fewer than 10 CIC structures per 10 mm^2 (blue solid lines) and with equal or more than 10 CIC structures per 10 mm^2 (green dotted lines). HNSCC patients with CIC structures (green dotted lines) and without CIC structures (blue solid lines) (c) in the central tumor area and (d) from all five HNSCC patient cohorts; from those patients the clinical data, patients' characteristics, and immunohistological data were completely available.

of detached cells that might form metastasis or suppression of the immune response by prohibition of emanation of immunogenic signals by nonapoptotic dying cells.

5. Conclusion

Our histological analyses showed that tumor cells containing incorporated, nonapoptotic tumor cells are commonly observed in many tumor tissue samples. Furthermore, we demonstrated that CIC structures correspond with clinical outcome depending on the cancer type and may have opposing effects on prognosis. CIC frequency is a valuable independent prognostic factor which should be considered in the same way as proliferation or apoptosis. Future work should also focus on functional studies in order to gain more insights into the mechanisms of CIC formation and to evaluate its potential value as a prognostic marker in other types of cancer.

Conflict of Interests

The authors declare that they have no conflict of interests in the research.

Acknowledgments

The authors thank the Tumour Centre at the Friedrich-Alexander University Erlangen-Nürnberg, Erlangen, Germany, for providing them with patient data. They especially thank Christa Winkelmann for excellent technical assistance. The authors thank Carol Geppert for assistance with the "Whole Slide Imaging."

References

[1] National Library of Medicine (US), "Medical Subject Headings," National Library of Medicine (US), Bethesda, Md, USA, 2011, http://www.nlm.nih.gov/cgi/mesh/2014/MB_cgi?mode=&index=25547&field=all&HM=&II=&PA=&form=&input.

[2] S. Fais, "Cannibalism: a way to feed on metastatic tumors," *Cancer Letters*, vol. 258, no. 2, pp. 155–164, 2007.

[3] K. Gupta and P. Dey, "Cell cannibalism: diagnostic marker of malignancy," *Diagnostic Cytopathology*, vol. 28, no. 2, pp. 86–87, 2003.

[4] L. Lugini, P. Matarrese, A. Tinari et al., "Cannibalism of live lymphocytes by human metastatic but not primary melanoma cells," *Cancer Research*, vol. 66, no. 7, pp. 3629–3638, 2006.

[5] P. V. Kumar, M. Hosseinzadeh, and G. R. Bedayat, "Cytologic findings of medulloblastoma in crush smears," *Acta Cytologica*, vol. 45, no. 4, pp. 542–546, 2001.

[6] W. T. Abodief, P. Dey, and O. Al-Hattab, "Cell cannibalism in ductal carcinoma of breast," *Cytopathology*, vol. 17, no. 5, pp. 304–305, 2006.

[7] C. E. Cano, M. J. Sandí, T. Hamidi et al., "Homotypic cell cannibalism, a cell-death process regulated by the nuclear protein 1, opposes to metastasis in pancreatic cancer," *EMBO Molecular Medicine*, vol. 4, no. 9, pp. 964–979, 2012.

[8] M. Schwegler, A. M. Wirsing, A. J. Dollinger et al., "Clearance of primary necrotic cells by non-professional phagocytes," *Biology of the Cell*, 2015.

[9] F. Lozupone, M. Perdicchio, D. Brambilla et al., "The human homologue of *Dictyostelium discoideum* phg1A is expressed by human metastatic melanoma cells," *EMBO Reports*, vol. 10, no. 12, pp. 1348–1354, 2009.

[10] L. V. Distel, R. Fickenscher, K. Dietel et al., "Tumour infiltrating lymphocytes in squamous cell carcinoma of the oro- and hypopharynx: prognostic impact may depend on type of treatment and stage of disease," *Oral Oncology*, vol. 45, no. 10, pp. e167–e174, 2009.

[11] D. Pretscher, L. V. Distel, G. G. Grabenbauer, M. Wittlinger, M. Buettner, and G. Niedobitek, "Distribution of immune cells in head and neck cancer: $CD8^+$ T-cells and $CD20^+$ B-cells in metastatic lymph nodes are associated with favourable outcome in patients with oro- and hypopharyngeal carcinoma," *BMC Cancer*, vol. 9, article 292, 2009.

[12] M. Tabachnyk, L. V. R. Distel, M. Büttner et al., "Radiochemotherapy induces a favourable tumour infiltrating inflammatory cell profile in head and neck cancer," *Oral Oncology*, vol. 48, no. 7, pp. 594–601, 2012.

[13] G. G. Grabenbauer, G. Lahmer, L. Distel, and G. Niedobitek, "Tumor-infiltrating cytotoxic T cells but not regulatory T cells predict outcome in anal squamous cell carcinoma," *Clinical Cancer Research*, vol. 12, no. 11, pp. 3355–3360, 2006.

[14] N. Tehrany, J. Kitz, M. Rave-Frank et al., "High-grade acute organ toxicity and p16 expression as positive prognostic factors in primary radio(chemo)therapy for patients with head and neck squamous cell carcinoma," *Strahlentherapie und Onkologie*, vol. 191, no. 7, pp. 566–572, 2015.

[15] Y. Wang and X. N. Wang, "Cell-in-cell: a virgin land of cell biology," *OncoImmunology*, vol. 2, no. 10, Article ID e25988, 2014.

[16] S. Kojima, H. Sekine, I. Fukui, and H. Ohshima, "Clinical significance of 'cannibalism' in urinary cytology of bladder cancer," *Acta Cytologica*, vol. 42, no. 6, pp. 1365–1369, 1998.

[17] R. A. Caruso, A. O. Muda, A. Bersiga, L. Rigoli, and C. Inferrera, "Morphological evidence of neutrophil-tumor cell phagocytosis (cannibalism) in human gastric adenocarcinomas," *Ultrastructural Pathology*, vol. 26, no. 5, pp. 315–321, 2002.

[18] L. Lugini, F. Lozupone, P. Matarrese et al., "Potent phagocytic activity discriminates metastatic and primary human malignant melanomas: a key role of ezrin," *Laboratory Investigation*, vol. 83, no. 11, pp. 1555–1567, 2003.

[19] L. Galluzzi, I. Vitale, J. M. Abrams et al., "Molecular definitions of cell death subroutines: recommendations of the Nomenclature Committee on Cell Death 2012," *Cell Death & Differentiation*, vol. 19, no. 1, pp. 107–120, 2012.

Hindawi Publishing Corporation
BioMed Research International
Volume 2015, Article ID 158682, 10 pages
http://dx.doi.org/10.1155/2015/158682

Research Article

Prognostic Value of Cancer Stem Cells Markers in Triple-Negative Breast Cancer

Francesca Collina,[1] Maurizio Di Bonito,[1] Valeria Li Bergolis,[1] Michelino De Laurentiis,[2] Carlo Vitagliano,[1] Margherita Cerrone,[1] Francesco Nuzzo,[2] Monica Cantile,[1] and Gerardo Botti[1]

[1] *Pathology Unit, Istituto Nazionale Tumori Fondazione "G. Pascale", IRCCS, 80131 Napoli, Italy*
[2] *Department of Breast Surgery and Cancer Prevention, Istituto Nazionale Tumori Fondazione "G. Pascale", IRCCS, 80131 Napoli, Italy*

Correspondence should be addressed to Monica Cantile; monicantile@libero.it

Received 18 December 2014; Revised 1 April 2015; Accepted 18 May 2015

Academic Editor: Pierre Hainaut

Triple-negative breast cancer (TNBC) has a significant clinical relevance of being associated with a shorter median time to relapse and death and does not respond to endocrine therapy or other available targeted agents. Increased aggressiveness of this tumor, as well as resistance to standard drug therapies, may be associated with the presence of stem cell populations within the tumor. Several stemness markers have been described for the various histological subtypes of breast cancer, such as CD44, CD24, CD133, ALDH1, and ABCG2. The role of these markers in breast cancer is not clear yet and above all there are conflicting opinions about their real prognostic value. To investigate the role of CSCs markers in TNBC cancerogenesis and tumor progression, we selected 160 TNBCs samples on which we detected protein expression of CD44, CD24, CD133, ALDH1, and ABCG2 by immunohistochemistry. Our results highlighted a real prognostic role only for CD44 in TNBCs. All other CSCs markers do not appear to be related to the survival of TNBC patients. In conclusion, despite the fact that the presence of the cancer stem cells in the tumor provides important information on its potential aggressiveness, today their detection by immunohistochemistry is not sufficient to confirm their role in carcinogenesis, because specific markers probably are not yet identified.

1. Introduction

Triple-negative breast cancer (TNBC) (tumors that do not express estrogen receptor (ER) and progesterone receptor (PR) genes and with nonoverexpressed/nonamplified HER-2 gene) accounts for 10%–24% of invasive breast cancers, and it is typically high-grade tumor with different histological types. The TNBC occurs predominantly in young African or African American women in premenopausal period and tends to display aggressive behavior demonstrating a great propensity to metastasize. The main metastatic locations are the bones and the central nervous system [1, 2]. Usually, patients with TNBC tend to have a higher recurrence rate after diagnosis, a short disease-free interval, and reduced overall survival, especially for the lack of targeted therapies [3]. Originally, several studies have shown that TNBC can be grouped into two main immunophenotypically and clinically distinct subgroups: (I) basal-like subtype that accounts for approximately 70% of TNBCs (expressing basal markers) and (II) the nonbasal subtype [4, 5].

Recently, Lehmann et al., by gene expression profiles studies, have further stratified the TNBCs into 6 subtypes, expressing many different molecular markers specific for the different groups [6]. However, more recently, another RNA and DNA genomic profiles study showed that TNBCs can be divided into four fundamental subtypes with molecular characteristics even more specific, often targets of biological therapies, with differential potentiality of aggressiveness [7]. In both studies, the molecular more aggressive subtypes were those associated with the expression of immunomodulatory and stem-like molecules.

Recent acquisitions on human carcinogenesis suggest that small populations of tumor stem cells can influence and

modify neoplastic cells behavior and aggressiveness as well as therapeutic response. Many observations suggest that breast cancer ability to proliferate, progress, and spread is also based on a limited subpopulation of cells with properties similar to stem cells, defined as "breast cancer stem cells" (BCSCs) [8, 9].

Several stemness markers have been described for identification of BCSCs in cancer subtypes, such as CD44, CD24, CD133, EpCAM, CD166, Lgr5, CD47, ALDH1, and ABCG2 [9, 10].

CD44/CD24 expression profiles showed a large variability within breast cancer subtypes [11] especially for TNBCs. In fact, Idowu et al. [12] showed that $CD44^{+}CD24^{-/low}$ phenotype was associated with a worse prognosis in TNBCs patients, while Giatromanolaki et al. [13] described that $CD44^{-}CD24^{-}$ phenotype was associated with a worse prognosis also in TNBCs. Finally, Ahmed et al. observed that $CD44^{-}CD24^{+}$ phenotype was the only one associated with poor prognosis in breast cancer [14].

Other studies suggested that ABCG2 alone can be considered a suitable marker for breast cancer, in particular for TNBC phenotype, but this observation was limited to cellular models [15]. ALDH1 expression was described to be higher in TNBC than non-TNBC cell [16], and in a small case series of TNBC patients its expression was associated with poor clinical outcomes [17].

Recently, CD133 proved to be suitable also in the identification of CSCs in TNBC, as shown in several in vitro [18, 19] and in vivo studies [20]. In addition, the recent use of CD133 to detect circulating tumor cells in TNBC patients [21, 22] has increased attention to this marker highlighting its role in establishing prognostic and predictive value in TNBCs.

However, the role of these markers in breast cancer progression is not clearly defined and, above in TNBC phenotype, the most suitable for the characterization of the niches of tumor stem cells have not been determined. Most studies, in fact, were carried out on small series of TNBCs or on cellular models [15, 17, 20] and aimed at understanding the molecular mechanisms related to the single markers.

In this study we analyzed protein expression of CD133, CD24, CD44, ABCG2, and ALDH1 in a case series of TNBCs, included in a Tissue Microarray, to correlate their expression to clinic-pathological features and survival of TNBC patients and identify the CSCs marker with the best prognostic value.

2. Materials and Methods

2.1. Patients and Specimens. One hundred sixty patients who underwent mastectomy or quadrantectomy from 2003 to 2009 at the National Cancer Institute "Giovanni Pascale" of Naples were enrolled in this study. All cases were reviewed according to WHO classification criteria, using standard tissue sections and appropriate immunohistochemical slides.

Medical records were reviewed for clinical information; histologic parameters were determined from the H&E-stained slides. Clinicopathologic parameters evaluated for each tumor included patient age at initial diagnosis, tumor size, histologic subtype, nuclear grade, number of positive lymph nodes, tumor stage, tumor recurrence, distant metastasis, and type of surgery. Moreover, all specimens were characterized for all routine diagnostic immunophenotypic parameters.

2.2. TMA Building. Tissue Microarray (TMA) was built using the most representative areas from each single case with one replicate. All tumours and controls were reviewed by two experienced pathologists (MDB/GB). Discrepancies between two pathologists from the same case were resolved in a joint analysis of the cases. Tissue cylinders with a diameter of 1 mm were punched from morphologically representative tissue areas of each "donor" tissue block and brought into one recipient paraffin block (3 × 2.5 cm) using a semiautomated tissue arrayer (Galileo TMA).

2.3. Immunohistochemistry Analysis. Before the preparation of the TMA on whole sections breast tumor samples were characterized for routinely immunophenotypical parameters, including ER, PgR, HER2, and Ki67. All samples which were negative for ER, PgR, and ErbB2 (TNBCs subtype) were included in the study. To confirm the diagnosis, all three markers were again analyzed on TMA slides.

Immunohistochemical staining was done on 9 TMA slides from formalin-fixed, paraffin embedded tissues to evaluate the expression of CD133, ER, PgR, c-erbB2, Ki67, CD24, CD44, ALDH1A1, and ABCG2 markers. Paraffin slides were then deparaffinized in xylene and rehydrated through graded alcohols. Antigen retrieval was performed with slides heated in 0.01 M citrate buffer (pH 6.0 for CD133, ABCG2, PgR, c-erbB2, Ki67, CD24, and CD44) or Tris-EDTA (pH 9 for ER and ALDH) in a bath for 20 min at 97°C. After antigen retrieval, the slides were allowed to cool. The slides were rinsed with TBS and the endogenous peroxidase was inactivated with 3% hydrogen peroxide. After protein block (BSA 5% in PBS 1x), the slides were incubated with primary antibody to human CD133 (Miltenyi Biotec Monoclonal Mouse CD133/1 (AC 133) pure 1 : 150) and CD24 (Abcam Rabbit Polyclonal Anti-CD24 ab110448 1 : 100) for one hour, to human ERα (DAKO Monoclonal Mouse Anti-Human ERα Clone ID5 1 : 35), PR (DAKO Monoclonal Mouse Anti-Human PR Clone 636 1 : 50), c-erbB2 (DAKO Polyclonal Rabbit Anti-Human Oncoprotein 1 : 300), Ki67 (DAKO Monoclonal Mouse Anti-Human Ki67 Ab Clone MIB-1 1 : 75), CD44 (Novocastra Lyophilized Mouse Monoclonal Antibody CD44 Variant 3 1 : 35) for 30 minutes, and to ABCG2 (Abcam Mouse Monoclonal Anti-BCRP/ABCG2 antibody ab3380 1 : 30) and ALDH1A1 (Abcam Rabbit Monoclonal Anti-ALDH1A1 antibody (ab52492), 1 : 100) overnight. The sections were rinsed in TBS and incubated for 20 min with Novocastra Biotinylated Secondary Antibody (RE7103), a biotin-conjugated secondary antibody formulation that recognized mouse and rabbit immunoglobulins. Then the sections were rinsed in TBS and incubated for 20 min with Novocastra Streptavidin-HRP (RE7104) and then peroxidase reactivity was visualized using a 3,3′-diaminobenzidine (DAB). Finally, the sections were counterstained with hematoxylin and mounted. Results are interpreted using a light microscope.

2.4. Evaluation of Immunohistochemistry. Antigen expression was evaluated independently by two pathologists using light microscopy. Observer was unaware of the clinical outcome. For each sample, two cores (inside the tumor) were analyzed. Using a semiquantitative scoring system microscopically and referring to each antigen scoring method in other studies, an observer evaluated the intensity, extent, and subcellular distribution of CD133, ER, PR, c-erbB2, Ki67, ABCG2, ALDH1A1, CD24, and CD44. The cutoff used to distinguish "positive" from "negative" cases was ≥1% ER/PR positive tumor cells. Immunohistochemical analyses of c-erbB2 expression describe the intensity and staining pattern of tumor cells. Only membrane staining intensity and pattern were evaluated using the 0 to 3+ score as illustrated in the HercepTest kit scoring guidelines. The ASCO/CAP 2013 describes a new HER2 Testing Algorithms identifying 4 categories: no staining or incomplete and faint/barely perceptible membrane staining within ≤10% of tumor cells (0 negative); incomplete and faint/barely perceptible membrane staining within >10% of tumor (1+ negative); incomplete and circumferential weak/moderate membrane staining within >10% of tumor cells or complete and circumferential intense membrane staining within ≤10% of tumor cells (2+ equivocal); and complete and circumferential intense membrane staining within >10% of tumor cells (3+ positive). Cases with score 2+ underwent fluorescence in situ hybridization analysis. The proliferative index Ki67 was defined as the percentage of immunoreactive tumour cells out of the total number of cells (low = ≤20%; high = >20%). In scoring CD133, CD44, and ABCG2 proteins expression, both the extent and intensity of immunopositivity in the cell membrane and cytoplasm were considered, while, for CD24 and ALDHA1, we have considered only the cytoplasmic staining.

There are not standardized criteria for CD133, CD44, CD24, and ALDHA1 markers staining evaluation; thus we schematized our score evaluation as follows: for CD133 we considered the positivity or negativity of the staining; for CD24 staining we evaluated cell percentage positivity (low = <50%/high = ≥50%); for ALDHA1 staining we evaluated cell percentage positivity (low = <25%/high = ≥25%); for cytoplasmic CD44 we considered the expression as high when the cell positivity percentage was >50% with intermediate-high intensity and considered the expression as low when it was ≤50%; for membrane CD44 we considered the expression as high when the cell positivity percentage was ≥25% with intermediate-high intensity and considered the expression as low when it was <25%.

The ABCG2 score was determined by combining the proportion of positively stained tumor cells and the intensity of staining as previously described [23].

2.5. Statistical Analysis. The association between CD133, CD44, CD24, ALDH, and ABCG2 with each other and with the clinicopathological data was conducted using χ^2 or Spearman correlation test when appropriate. Pearson's χ^2 test was used to determine whether a relationship exists between the variables included in the study. The level of significance was defined as $p < 0.05$. Overall Survival (OS) and Disease-Free Survival (DFS) curves were calculated using Kaplan-Meier method.

OS was defined as the time from diagnosis (first biopsy) to death by any cause or until the most recent follow-up. DFS was measured as the time from diagnosis to the occurrence of progression, relapse after complete remission, or death from any cause.

All the statistical analyses were carried out using the Statistical Package for Social Science v. 20 software (SPSS Inc., Chicago, IL, USA).

3. Results

3.1. Clinicopathological Characteristics of TNBC Patients. In our cohort, we have included 160 TNBC samples of breast cancers 12 lobular, 4 mixed, 9 medullary, 1 mucinous, 6 metaplastic, and 128 invasive ductal breast carcinomas (including 5 TNBC metastases).

The age of patients ranged from 24 to 93 years, with an average age of 57 years. Tumor sizes were lower than 2 cm in 47.1% (73/155) of the samples, between 2 and 5 cm in 44.5% (69/155) of the samples, and larger than 5 cm in 8.4% (13/155) of the samples. These data were not available for the five cases of metastases that have been included in the study. Metastatic lymph nodes were found in 43.1% (66/153) of patients at surgery (this information for 7 patients was lost), while distant metastases were found in 24.4% (39/155). 5 cases were unable to recover this information. The percentages of tumor grading were 86.5% (134/155) grade 3, 12.2% (19/155) grade 2, and 1.3% (2/155) grade 1. The expression of proliferation factor Ki67 was high (>20%) in 121/153 cases (79.1%) and low (≤20%) in 32/153 cases (20.9%). This information for 7 patients was lost. All clinicopathological characteristics are shown in Tables 1 and 2.

3.2. CD44 Expression in TNBC Patients. CD44 protein expression was detected, excluding the samples that could not be assessed, in 143/160 samples. In 108 samples, there was a low cytoplasmic CD44 expression, while, in 35 samples, there was a high expression (Figure 1). The membrane expression was low in 133 cases and high in 10 cases, while only 4/143 cases showed cytoplasmic and membrane expression.

Based on statistical elaboration of CD44 protein expression analysis with the other clinicopathological parameters in TNBC, considering only cytoplasmic expression, we showed that CD44 was significantly associated with metastases ($p = 0.011$) (Table 1) and with DFS ($p = 0.051$) (Figure 2). No statistical association with OS was present. Moreover, there was a trend of statistical association with proliferation index Ki67 ($p = 0.078$).

If we consider only membrane positivity, a trend of inverse association with distant metastases ($p = 0.085$) was present (Table 1). Considering membrane and cytoplasmic positive immunostaining, a direct association with age of patients (>40 ≤60) ($p = 0.051$) and a trend of inverse association with lymph node metastases were present ($p = 0.087$) (Table 1). In these cases, there were no statistical associations with DFS ($p = 0.462$ and $p = 0.609$, resp.) or OS.

Table 1: Relation between CD133 and CD44 (cytoplasmic, membranous, and cytoplasmic/membranous positivity) markers with clinical pathological features in TNBC patients.

	CD133		p value	CD44C		p value	CD44M		p value	CD44CM		p value
	Negative	Positive		Low	High		Low	High		Low	High	
Age												
<40	11 (63,1%)	4 (36,9%)		15 (78,9%)	4 (21,1%)		18 (94,7%)	1 (5,3%)		19 (100%)	0 (0%)	
>40 ≤ 60	49 (84,6%)	13 (15,4%)	0,806	42 (72,4%)	16 (27,6%)	0,783	52 (89,7%)	6 (10,3%)	0,440	54 (93,1%)	4 (6,9%)	0,051
>60	55 (75,7%)	13 (24,3%)		50 (80,6%)	15 (19,4%)		62 (95,4%)	3 (4,6%)		65 (100%)	0 (0%)	
Missed data	1	0		1	0		1	0		1	0	
Histotype												
IDC	93 (76,9%)	28 (23,1%)		88 (75,2%)	29 (24,8%)		107 (91,5%)	10 (8,5%)		114 (97,4%)	3 (2,6%)	
NIDC	23 (92%)	2 (8%)	0,088	20 (76,9%)	6 (23,1%)	0,855	26 (100%)	0 (0%)	0,122	25 (96,2%)	1 (3,8%)	0,720
Missed data	0	0		0	0		0	0		0	0	
Size												
≤2 cm	55 (79,7%)	14 (20,3%)		48 (75%)	16 (25%)		60 (93,8%)	4 (6,2%)		63 (98,4%)	1 (1,6%)	
>2 ≤ 5	49 (79%)	13 (21%)	0,934	47 (73,4%)	17 (26,6%)	0,768	60 (93,8%)	4 (6,2%)	0,408	61 (95,3%)	3 (4,7%)	0,470
>5	9 (75%)	3 (25%)		10 (83,3%)	2 (16,7%)		10 (83,3%)	2 (16,7%)		12 (100%)	0 (0%)	
Missed data	3	0		3	0		3	0		3	0	
LNM												
Negative	63 (80,5%)	19 (19,5%)		62 (77,5%)	18 (22,5%)		73 (91,3%)	7 (8,7%)		76 (95%)	4 (5%)	
Positive	48 (90,6%)	11 (9,4%)	0,517	40 (70,2%)	17 (29,8%)	0,333	54 (94,7%)	3 (5,3%)	0,439	57 (100%)	0 (0%)	0,087
Missed data	5	0		6	0		6	0		6	0	
Metastasis												
Negative	89 (77,4%)	26 (25,6%)		90 (80,4%)	22 (19,8%)		102 (91%)	10 (9%)		108 (96,4%)	4 (3,6%)	
Positive	27 (87%)	4 (13%)	0,235	18 (58,1%)	13 (41,9%)	0,011	31 (100%)	0 (0%)	0,085	31 (100%)	0 (42%)	0,286
Missed data	0	0		0	0		0	0		0	0	
Grading												
G1	2 (100%)	0 (0%)		1 (100%)	0 (0%)		1 (100%)	0 (0%)		1 (100%)	0 (0%)	
G2	15 (93,7%)	1 (6,3%)	0,223	12 (75%)	4 (25%)	0,844	16 (100%)	0 (0%)	0,463	16 (100%)	0 (0%)	0,751
G3	96 (76,8%)	29 (23,2%)		91 (74,6%)	31 (25,4%)		112 (91,8%)	10 (8,2%)		118 (96,7%)	4 (3,3%)	
Missed data	3	0		4	0		4	0		4	0	
Ki67												
≤20%	24 (85,7%)	4 (14,3%)		23 (92%)	3 (8%)		24 (92,3%)	2 (7,7%)		26 (100%)	0 (0%)	
>20%	88 (77,9%)	25 (22,1%)	0,358	79 (71,8%)	31 (28,2%)	0,078	102 (92,7%)	8 (7,3%)	0,941	106 (96,4%)	4 (3,6%)	0,324
Missed data	4	1		6	1		6	0		7	0	

IDC = infiltrant ductal carcinoma; NIDC = noninfiltrant ductal carcinoma; LNM = lymph node metastasis.

Table 2: Relation between CD24, ALD1A1, and ABCG2 with clinical pathological features in TNBC patients.

	CD24		*P* value	ALDH		*P* value	ABCG2			*P* value
	Low	High		Low	High		Negative	Low	High	
Age										
<40	1 (5,6%)	17 (94,4%)		13 (68,4%)	6 (28,6%)		2 (11,1%)	7 (38,9%)	9 (50%)	
>40 ≤ 60	7 (12,3%)	50 (87,7%)	0,706	39 (65%)	21 (35%)	0,559	9 (15,8%)	8 (14%)	40 (70,2%)	0,132
>60	6 (9,8%)	55 (90,2%)		48 (73,8%)	17 (26,2%)		15 (23%)	12 (18,5%)	38 (58,5%)	
Missed data	0	1		0	1		0	0	1	
Histotype										
IDC	9 (8%)	104 (92%)		85 (70,8%)	35 (29,2%)		23 (19,5%)	21 (17,8%)	74 (62,7%)	
NIDC	5 (20,8%)	19 (79,2%)	0,059	15 (60%)	10 (40%)	0,427	3 (13%)	6 (26%)	14 (61%)	0,567
Missed data	0	0		0	0		0	0	0	
Size										
≤2 cm	4 (6,6%)	57 (93,4%)		43 (67,2%)	21 (32,8%)		14 (21,5%)	12 (18,5%)	39 (60%)	
>2 ≤ 5	9 (14,8%)	52 (85,2%)	0,314	46 (69,7%)	20 (30,3%)	0,946	10 (16,1%)	10 (16,1%)	42 (67,8%)	0,599
>5	1 (7,7%)	12 (92,3%)		8 (66,6%)	4 (33,4%)		2 (16,6%)	4 (33,4%)	6 (50%)	
Missed data	0	2		3	0		0	1	1	
LNM										
Negative	8 (10,4%)	69 (89,6%)		58 (74,4%)	20 (25,6%)		13 (17,3%)	15 (20%)	47 (62,7%)	
Positive	6 (11,1%)	48 (88,9%)	0,895	38 (62,3%)	23 (37,7%)	0,127	13 (21,6%)	10 (16,7%)	37 (61,7%)	0,767
Missed data	0	6		4	2		0	2	4	
Metastasis										
Negative	11 (10,4%)	95 (89,6%)		80 (70,2%)	34 (29,8%)		20 (18,5%)	21 (19,4%)	67 (62%)	
Positive	3 (9,7%)	28 (90,3%)	0,910	20 (64,5%)	11 (35,5%)	0,546	6 (18,2%)	6 (18,2%)	21 (63,6%)	0,982
Missed data	0	0		0	0		0	0	0	
Grading										
G1	0 (0%)	2 (100%)		1 (100%)	0 (0%)		0 (0%)	1 (100%)	0 (0%)	
G2	1 (9%)	10 (91%)	0,875	7 (53,8%)	6 (46,2%)	0,386	4 (36,4%)	2 (18,2%)	5 (45,4%)	0,145
G3	13 (10,7%)	108 (89,3%)		89 (70,1%)	38 (29,9%)		22 (17,5%)	23 (18,2%)	81 (64,3%)	
Missed data	0	3		3	1		0	1	2	
Ki67										
≤20%	2 (8,3%)	22 (91,7%)		21 (91,3%)	3 (8,7%)		8 (32%)	7 (28%)	10 (40%)	
>20%	9 (8,5%)	97 (91,5%)	0,980	76 (66,7%)	38 (33,3%)	0,042	16 (14,4%)	19 (17,1%)	76 (68,5%)	0,024
Missed data	3	4		3	4		2	1	2	

IDC = infiltrant ductal carcinoma; NIDC = noninfiltrant ductal carcinoma; LNM = lymph node metastasis.

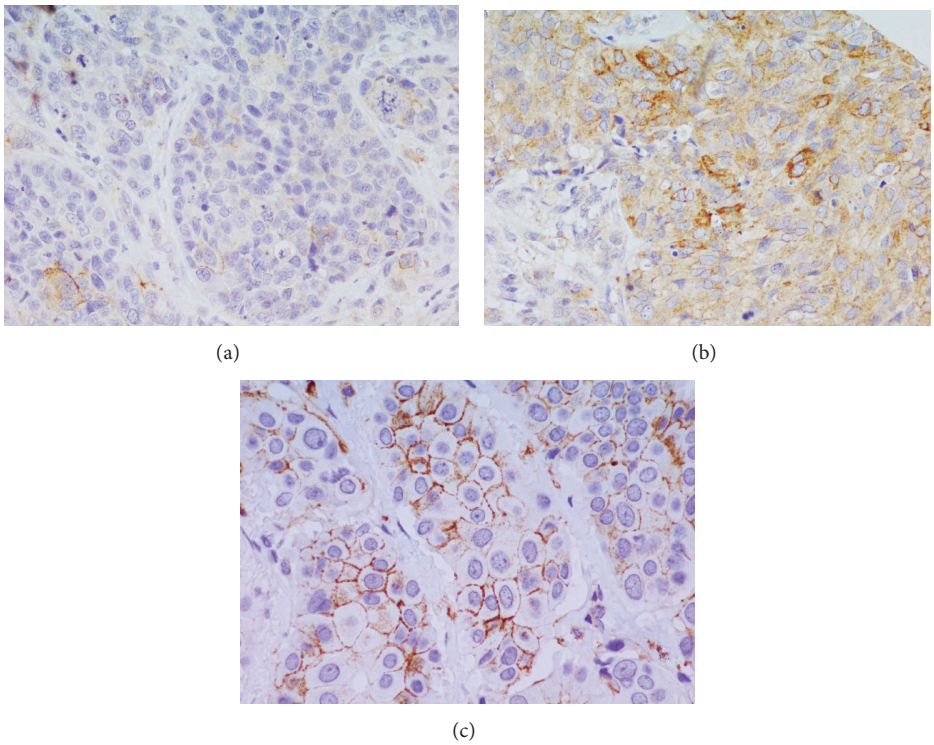

Figure 1: CD44 immunostaining in TNBC. (a) Low membrane and cytoplasmic expression (40x). (b) High membrane and cytoplasmic expression (40x). (c) High membrane expression (40x).

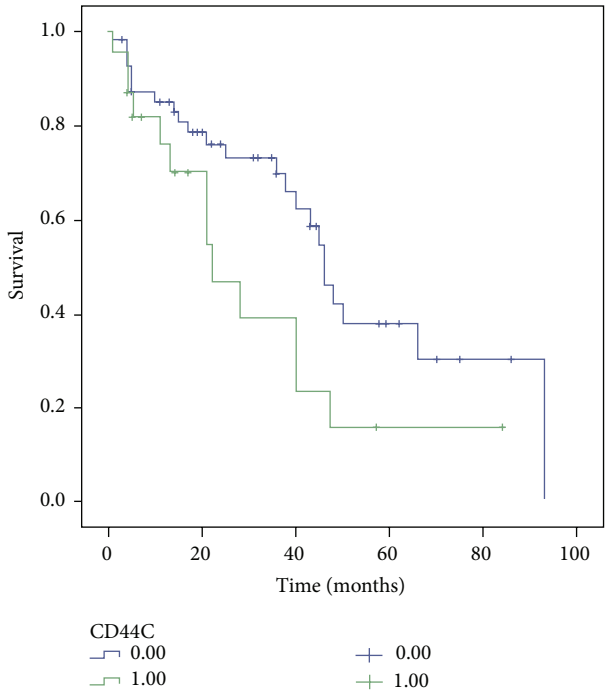

Figure 2: CD44 Disease-Free Survival Kaplan-Meier curve. The patients with high expression of cytoplasmic CD44 have worse prognosis than those with low expression of CD44.

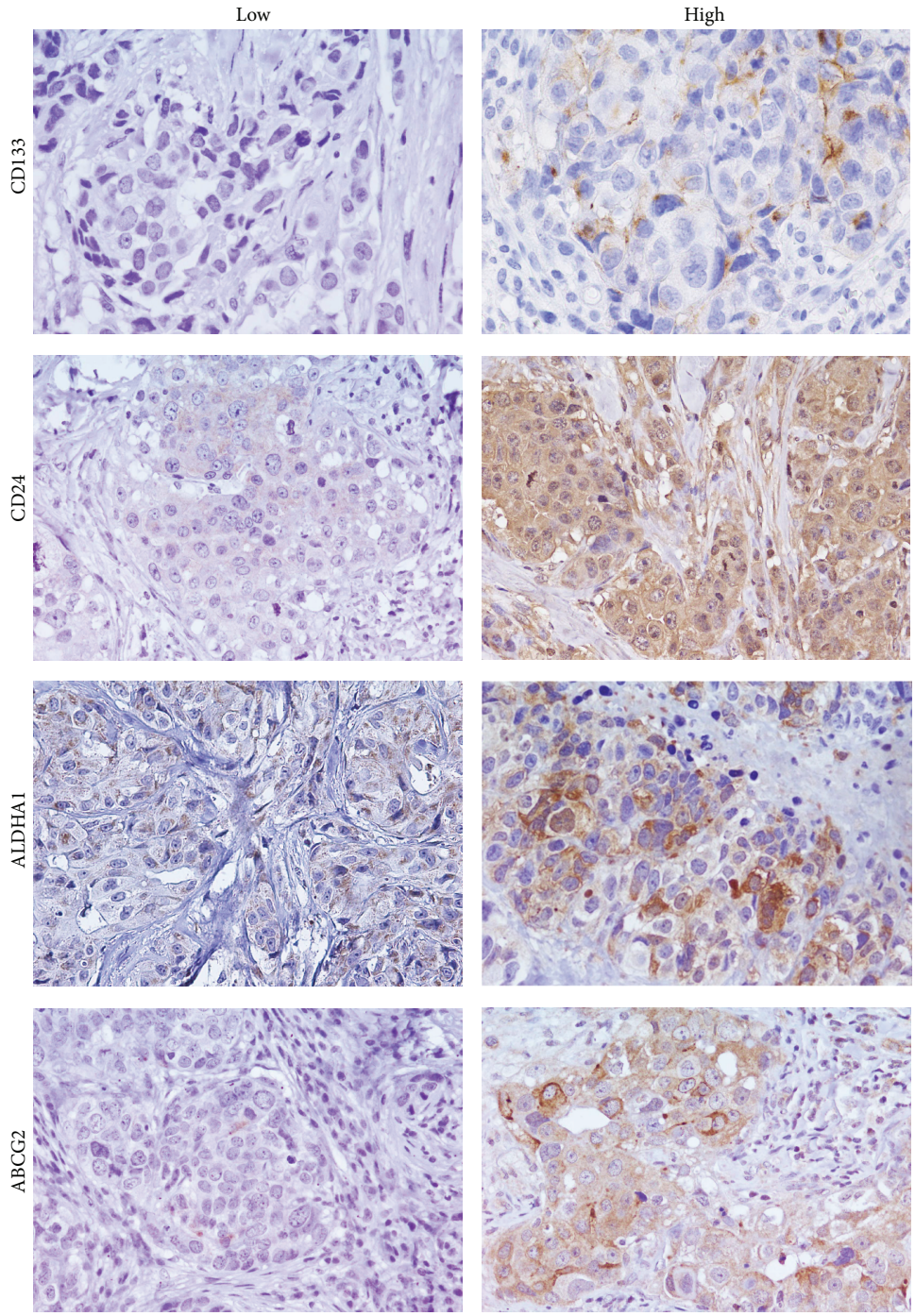

Figure 3: CD133, CD24, ALDH1A1, and ABCG2 immunostaining in TNBC (40x).

3.3. CD133 Expression in TNBC Patients. 146/160 samples were stained for CD133. 116/146 samples were negative and 30/146 samples were positive (Figure 3). 14/160 samples are missing data.

Based on statistical elaboration of CD133 protein expression analysis with the clinicopathological parameters in TNBCs, we showed that only a trend of statistical association with the ductal histotype ($p = 0.088$) (Table 1) was present. No statistical association with OS and DFS was present.

3.4. CD24 Expression in TNBC Patients. CD24 protein expression was detected, excluding the samples that could not be assessed, in 137/160 samples. In 123 samples there

was a high CD24 expression; in 14 samples there was a low expression (Figure 3).

Statistical analysis showed only a direct association with invasive ductal histotype ($p = 0.059$) (Table 2). No statistical association with DFS and OS was present.

3.5. ABCG2 Expression in TNBC Patients. ABCG2 protein expression was detected, excluding the samples that could not be assessed, in 141/160 samples. In 88 cases there was a high ABCG2 expression; in 27 cases there was a low expression and 26 cases were negative (Figure 3).

Statistical analysis showed a significant association only with proliferative index Ki67 ($p = 0.024$) (Table 2). No statistical association with DFS was present. An inverse trend of statistical association with OS was present ($p = 0.081$) (see Figure S1 in Supplementary Material available online at http://dx.doi.org/10.1155/2015/158682).

3.6. ALDHA1 Expression in TNBC Patients. ALDHA1 protein expression was detected, excluding the samples that could not be assessed, in 145/160 samples. In 45 cases there was a high ALDHA1 expression; in 100 cases there was a low expression (Figure 3).

Following the statistical analysis, a direct statistical association with Ki67 was found ($p = 0.042$) (Table 2). No statistical association with DFS and OS was present.

3.7. Relation between All CSCs Markers. Statistical analysis showed no significant associations between all cancer stem cell markers considered (data not shown).

4. Discussion

Breast tumors are a heterogeneous group of malignancies, which differ in morphology, gene profiling, prognosis, and therapeutic response [24].

Immunophenotypic analysis identify a particular breast tumor subtype, defined TNBC, because it do not express ER and PgR hormone receptors and shows non-overxepressed/amplified HER-2 oncogene. Its incidence is particularly high in younger women and the clinical course of the disease is often very aggressive [1, 2].

For this reason, the search for new molecular markers that can better explain the biology of this disease and especially its progression is becoming essential for the development of new and more appropriate therapeutic strategies.

Recently, the identification of cancer stem cell niches in tumor tissues is acquiring a great prognostic value, mainly because breast carcinogenesis may be the result of deregulation of molecular pathways controlling self-renewal of mammary epithelial cells [9].

Numerous cell surface markers have been used for the identification of stem cell clones in several tumors, but, for breast cancers, CSCs detection appears much more complex because of the extreme heterogeneity of histotypes/phenotypes that characterize these tumors [24].

The main objective of this study was the use of a panel of stem cell markers, selected on the basis of the recent experimental evidences found in literature, to evaluate their expression in TNBCs and verify their potential prognostic value.

Primarily, our data showed a very heterogeneous distribution of the selected markers expression. CD24 showed an association with IDC histotype and a strong statistical association with proliferation index ki67 but no association with patients' survival. Review of the literature shows that the role of CD24 in breast cancer and specifically in TNBC has been extensively investigated.

However, the evaluation of this marker has always been associated with the prognosis combined to the CD44 expression [11–13]. In our study, the combination of the two markers showed no association with the survival of TNBCs patients.

Regarding ABCG2, its expression appeared very high in most of TNBCs and also was the only marker which showed a strong association with Ki67.

In literature, there are no data on the expression of ABCG2 in TNBCs samples as they exist only on cellular models as MDA-MB-231 cell lines [15]. Thus, our data showed for the first time the expression of ABCG2 on a cohort of TNBCs patients.

ALDHA1 appeared also expressed in the majority of TNBCs but its overexpression was detected only in 28% of cases. This marker showed only an association with Ki67, while no association with other clinicopathological features and survival of TNBCs patients were highlighted.

These observations appeared to contrast with those reported in the literature, where ALDHA1 is described as an independent prognostic factor in TNBC patients [25]. Ohi et al. showed ALDH1 expression in 51% of TNBC cases with a heterogeneous immunoreactivity in the cytoplasm of carcinoma cells as well as in macrophages, stromal fibroblasts, peripheral nerves, and vascular smooth muscle cells. We detected ALDH1 only in tumor cells and in some TNBC samples. We suppose that discordance in the ALDH1 staining can be associated with the different clones of antibodies used for staining and the subjective definition of the IHC score for evaluation.

CD133 expression in TNBC patients was detected only in 20% of cases. Its expression appeared to be associated with ductal histotype but it showed no statistical association with other clinicopathological parameters and survival.

Recent and numerous studies showed that positivity for CD133 allows identifying CSCs in breast cancer [26]. CD133 is expressed by several solid tumors, including invasive TNBC, with very low levels of expression compared to other CSCs markers previously reported, like CD44 and ALDH1 [27]. In early-onset breast cancers, associated with mutations on BRCA1, CD133+ cells show CSCs properties [26]. The employment of this tumour stemness marker in breast cancers has become popular more recently and its expression is often described as being associated with a worse prognosis [20, 28]. In TNBCs patients the role of CD133 was previously documented, showing that this marker expression was correlated with prognosis [28].

However, our data showed no strong statistical association with TNBCs patients' survival in contrast to all the experimental evidences in the literature. Zhao et al.

investigated CD133 expression in 67 TNBCs patients showing its expression in 43.3% of cases with a predominant expression in the membrane and minimally in the cytoplasm of the tumor cell. We described CD133 positivity in 20% of samples and with a prevalent cytoplasmic expression. Even in this case the discordant date may be associated with the different clones of antibodies used for staining and the subjective definition of the IHC score for evaluation. In fact, for all of these markers, there are not standardized criteria of evaluation that make doubt their real prognostic value.

Finally, regarding CD44 protein expression, detection revealed a heterogeneous distribution of membranous end cytoplasmic positivity, which we have separately correlated with clinicopathological parameters and survival of patients. The results seem to be opposite to cytoplasmic staining strongly correlated with metastasis and disease-free survival, while the membrane staining showed a trend of inverse association with metastases. Cytoplasmic positivity for CD44 may be associated with its cytoplasmic domain [29] and it can be considered as an independent parameter during cancer progression [30, 31], although in this case the association with Ki67 appears to be evident.

Moreover, during normal cell physiology, several isoforms of CD44, by alternatively splicing, can be generated. The mechanisms by which CD44 controls signaling events are not clear. Many evidences showed that CD44 is assembled in a regulated manner into membrane-cytoskeletal junctional complexes and, through both direct and indirect interactions, serves to focus on downstream signal transduction events [32]. The role of CD44 in breast cancer was abundantly described in literature, in particular its duality in cancer progression [29]. Some studies showed a protumorigenic role for CD44 [33], while others showed a protective role for CD44 in breast cancer [34], suggesting that CD44 may influence tumor growth or metastasis differently at different phases of tumor progression. Variability in CD44-mediated biology could be due to the expression of alternatively spliced isoforms. In fact, the expression of CD44 variants has produced conflicting results with no definitive association between expression and clinical outcomes [29].

For identification of stem cell phenotype, many studies showed that high levels of CD44 associated to low levels of CD24 (CD44(+)/CD24(−/low)) would characterize stem populations in breast cancer [12]. However, this acquisition is not sufficiently clarified at least in breast cancer disease, where the combination of expression between the two markers can be very variable [11–14]. Our data on TNBCs suggest that their expressions would not be sufficiently selective for the identification of CSCs and their prognostic value contrasts with that reported in the literature [11–14]. CD44 alone seems to be a potential prognostic marker being statistically associated with the DFS of patients when its expression was cytoplasmic, while CD24low/CD44high not highligthed a prognostic role for TNBCs.

In conclusion, our data showed that all CSC markers selected seem to be associated only with the proliferative index in TNBCs, while the only marker significantly associated with the prognosis of TNBCs was CD44.

Despite the fact that the prognostic value of these markers has been thoroughly described in breast cancer, probably the use of these markers by immunohistochemistry not only fails to identify niches of stem cells, showing an abundant and heterogeneous expression in tumor samples, but also does not seem to have a real prognostic value in TNBC.

This could be due to the limit of the technique and the extreme heterogeneity and specificity of commercial antibodies and could also be due to TNBCs being no longer a homogeneous tumor class. Lehmann et al., by gene expression profiles studies, have further stratified the TNBCs into 6 subtypes, expressing many different molecular markers specific for the different groups [6]. However, more recently, another genomic profiles study showed that TNBCs can be divided into four fundamental subtypes with molecular characteristics even more specific, often targets of biological therapies, with differential potentiality of aggressiveness [7].

In both studies, Basal-Like Immune Activated (BLIA) (with upregulation of genes controlling B cell, T cell, natural killer cell functions and inflammatory cytokines) and mesenchymal stem like (MSL) subtypes represent the more aggressive molecular subtypes.

Perhaps these markers may manifest a stronger prognostic value if we were capable of subtyping TNBCs evaluating their expression in MSL subtype.

In conclusion, our data supported the idea that it is necessary to identify more specific CSCs markers for prognostic stratification of TNBCs by immunohistochemistry.

Conflict of Interests

The authors declare that there is no conflict of interests regarding the publication of this paper.

Authors' Contribution

Francesca Collina and Maurizio Di Bonito contributed equally to this paper.

References

[1] R. Schmadeka, B. E. Harmon, and M. Singh, "Triple-negative breast carcinoma: current and emerging concepts," *American Journal of Clinical Pathology*, vol. 141, no. 4, pp. 462–477, 2014.

[2] S. Elsamany and S. Abdullah, "Triple-negative breast cancer: future prospects in diagnosis and management," *Medical Oncology*, vol. 31, no. 2, article 834, 2014.

[3] H. J. Burstein, "Patients with triple negative breast cancer: is there an optimal adjuvant treatment?" *Breast*, vol. 22, no. 2, pp. S147–S148, 2013.

[4] W. D. Foulkes, I. E. Smith, and J. S. Reis-Filho, "Triple-negative breast cancer," *The New England Journal of Medicine*, vol. 363, no. 20, pp. 1938–1948, 2010.

[5] A. Prat, B. Adamo, M. C. U. Cheang, C. K. Anders, L. A. Carey, and C. M. Perou, "Molecular characterization of basal-like and non-basal-like triple-negative breast cancer," *Oncologist*, vol. 18, no. 2, pp. 123–133, 2013.

[6] B. D. Lehmann, J. A. Bauer, X. Chen et al., "Identification of human triple-negative breast cancer subtypes and preclinical

models for selection of targeted therapies," *The Journal of Clinical Investigation*, vol. 121, no. 7, pp. 2750–2767, 2011.

[7] M. D. Burstein, A. Tsimelzon, G. M. Poage et al., "Comprehensive genomic analysis identifies novel subtypes and targets of triple-negative breast cancer," *Clinical Cancer Research*, vol. 21, no. 7, pp. 1688–1698, 2015.

[8] E. Charafe-Jauffret, C. Ginestier, F. Iovino et al., "Breast cancer cell lines contain functional cancer stem sells with metastatic capacity and a distinct molecular signature," *Cancer Research*, vol. 69, no. 4, pp. 1302–1313, 2009.

[9] S.-Q. Geng, A. T. Alexandrou, and J. J. Li, "Breast cancer stem cells: Multiple capacities in tumor metastasis," *Cancer Letters*, vol. 349, no. 1, pp. 1–7, 2014.

[10] N. Kagara, K. T. Huynh, C. Kuo et al., "Epigenetic regulation of cancer stem cell genes in triple-negative breast cancer," *American Journal of Pathology*, vol. 181, no. 1, pp. 257–267, 2012.

[11] H. J. Kim, M.-J. Kim, S. H. Ahn et al., "Different prognostic significance of CD24 and CD44 expression in breast cancer according to hormone receptor status," *Breast*, vol. 20, no. 1, pp. 78–85, 2011.

[12] M. O. Idowu, M. Kmieciak, C. Dumur et al., "$CD44^+/CD24^{-/low}$ cancer stem/progenitor cells are more abundant in triple-negative invasive breast carcinoma phenotype and are associated with poor outcome," *Human Pathology*, vol. 43, no. 3, pp. 364–373, 2012.

[13] A. Giatromanolaki, E. Sivridis, A. Fiska, and M. I. Koukourakis, "The $CD44^+/CD24^-$ phenotype relates to 'triple-negative' state and unfavorable prognosis in breast cancer patients," *Medical Oncology*, vol. 28, no. 3, pp. 745–752, 2011.

[14] M. A. H. Ahmed, M. A. Aleskandarany, E. A. Rakha et al., "A $CD44^-/CD24^+$ phenotype is a poor prognostic marker in early invasive breast cancer," *Breast Cancer Research and Treatment*, vol. 133, no. 3, pp. 979–995, 2012.

[15] K. M. Britton, R. Eyre, I. J. Harvey et al., "Breast cancer, side population cells and ABCG2 expression," *Cancer Letters*, vol. 323, no. 1, pp. 97–105, 2012.

[16] H. Li, F. Ma, H. Wang et al., "Stem cell marker aldehyde dehydrogenase 1 (ALDH1)-expressing cells are enriched in triple-negative breast cancer," *International Journal of Biological Markers*, vol. 28, no. 4, pp. e357–e364, 2013.

[17] Y. S. Kim, M. J. Jung, D. W. Ryu, and C. H. Lee, "Clinicopathologic characteristics of breast cancer stem cells identified on the basis of aldehyde dehydrogenase 1 expression," *Journal of Breast Cancer*, vol. 17, no. 2, pp. 121–128, 2014.

[18] T. J. Liu, B. C. Sun, X. L. Zhao et al., "CD133+ cells with cancer stem cell characteristics associates with vasculogenic mimicry in triple-negative breast cancer," *Oncogene*, vol. 32, no. 5, pp. 544–553, 2013.

[19] F. Brugnoli, S. Grassilli, M. Piazzi et al., "In triple negative breast tumor cells, PLC-β2 promotes the conversion of $CD133^{high}$ to $CD133^{low}$ phenotype and reduces the CD133-related invasiveness," *Molecular Cancer*, vol. 12, no. 1, article 165, 2013.

[20] P. Zhao, Y. Lu, X. Jiang, and X. Li, "Clinicopathological significance and prognostic value of CD133 expression in triple-negative breast carcinoma," *Cancer Science*, vol. 102, no. 5, pp. 1107–1111, 2011.

[21] R. Nadal, F. G. Ortega, M. Salido et al., "CD133 expression in circulating tumor cells from breast cancer patients: potential role in resistance to chemotherapy," *International Journal of Cancer*, vol. 133, no. 10, pp. 2398–2407, 2013.

[22] C. Bock, B. Rack, J. Huober, U. Andergassen, U. Jeschke, and S. Doisneau-Sixou, "Distinct expression of cytokeratin, N-cadherin and CD133 in circulating tumor cells of metastatic breast cancer patients," *Future Oncology*, vol. 10, no. 10, pp. 1751–1765, 2014.

[23] L. Xiang, P. Su, S. Xia et al., "ABCG2 is associated with HER-2 Expression, lymph node metastasis and clinical stage in breast invasive ductal carcinoma," *Diagnostic Pathology*, vol. 6, article 90, 2011.

[24] K. Polyak, "Heterogeneity in breast cancer," *Journal of Clinical Investigation*, vol. 121, no. 10, pp. 3786–3788, 2011.

[25] Y. Ohi, Y. Umekita, T. Yoshioka et al., "Aldehyde dehydrogenase 1 expression predicts poor prognosis in triple-negative breast cancer," *Histopathology*, vol. 59, no. 4, pp. 776–780, 2011.

[26] M. H. Wright, A. Calcagno, C. D. Salcido, M. D. Carlson, S. V. Ambudkar, and L. Varticovski, "Brca1 breast tumors contain distinct $CD44^+/CD24^-$ and $CD133^+$ cells with cancer stem cell characteristics," *Breast Cancer Research*, vol. 10, article R10, 2008.

[27] Y. Wu and P. Y. Wu, "CD133 as a marker for cancer stem cells: progresses and concerns," *Stem Cells and Development*, vol. 18, no. 8, pp. 1127–1134, 2009.

[28] A. Ieni, G. Giuffrè, V. Adamo, and G. Tuccari, "Prognostic impact of CD133 immunoexpression in node-negative invasive breast carcinomas," *Anticancer Research*, vol. 31, no. 4, pp. 1315–1320, 2011.

[29] J. M. V. Louderbough and J. A. Schroeder, "Understanding the dual nature of CD44 in breast cancer progression," *Molecular Cancer Research*, vol. 9, no. 12, pp. 1573–1586, 2011.

[30] H. S. Berner, Z. Suo, B. Risberg, K. Villman, M. G. Karlsson, and J. M. Nesland, "Clinicopathological associations of CD44 mRNA and protein expression in primary breast carcinomas," *Histopathology*, vol. 42, no. 6, pp. 546–554, 2003.

[31] B. D. Gun, B. Bahadir, S. Bektas et al., "Clinicopathological significance of fascin and CD44v6 expression in endometrioid carcinoma," *Diagnostic Pathology*, vol. 7, no. 1, article 80, 2012.

[32] R. F. Thorne, J. W. Legg, and C. M. Isacke, "The role of the CD44 transmembrane and cytoplasmic domains in co-ordinating adhesive and signalling events," *Journal of Cell Science*, vol. 117, no. 3, pp. 373–380, 2004.

[33] A. Ouhtit, Z. Y. Abd Elmageed, M. E. Abdraboh, T. F. Lioe, and M. H. G. Raj, "In vivo evidence for the role of CD44s in promoting breast cancer metastasis to the liver," *American Journal of Pathology*, vol. 171, no. 6, pp. 2033–2039, 2007.

[34] J. I. Lopez, T. D. Camenisch, M. V. Stevens, B. J. Sands, J. McDonald, and J. A. Schroeder, "CD44 attenuates metastatic invasion during breast cancer progression," *Cancer Research*, vol. 65, no. 15, pp. 6755–6763, 2005.

Hindawi Publishing Corporation
BioMed Research International
Volume 2015, Article ID 756359, 6 pages
http://dx.doi.org/10.1155/2015/756359

Research Article

A Pyrosequencing Assay for the Quantitative Methylation Analysis of *GALR1* in Endometrial Samples: Preliminary Results

Christine Kottaridi,[1] Nikolaos Koureas,[2] Niki Margari,[1] Emmanouil Terzakis,[2] Evripidis Bilirakis,[3] Asimakis Pappas,[4] Charalampos Chrelias,[4] Aris Spathis,[1] Evangelia Aga,[1] Abraham Pouliakis,[1] Ioannis Panayiotides,[5] and Petros Karakitsos[1]

[1] *Department of Cytopathology, "ATTIKON" University Hospital, University of Athens Medical School, 1 Rimini, Haidari, 12462 Athens, Greece*
[2] *2nd Department of Gynecology, St. Savas Cancer Hospital, 171 Alexandras Avenue, 11522 Athens, Greece*
[3] *Department of Obstetrics and Gynecology, IASO Hospital, 37-39 Kifisias Avenue, Maroussi, 15123 Athens, Greece*
[4] *3rd Department of Obstetrics and Gynecology, "ATTIKON" University Hospital, 1 Rimini, Haidari, 12462 Athens, Greece*
[5] *2nd Department of Pathology, "ATTIKON" University Hospital, University of Athens Medical School, 1 Rimini, Haidari, 12462 Athens, Greece*

Correspondence should be addressed to Christine Kottaridi; ckottaridi@gmail.com

Received 26 March 2015; Revised 3 June 2015; Accepted 4 June 2015

Academic Editor: Maria Lina Tornesello

Endometrial cancer is the most common malignancy of the female genital tract while aberrant DNA methylation seems to play a critical role in endometrial carcinogenesis. Galanin's expression has been involved in many cancers. We developed a new pyrosequencing assay that quantifies DNA methylation of galanin's receptor-1 (*GALR1*). In this study, the preliminary results indicate that pyrosequencing methylation analysis of *GALR1* promoter can be a useful ancillary marker to cytology as the histological status can successfully predict. This marker has the potential to lead towards better management of women with endometrial lesions and eventually reduce unnecessary interventions. In addition it can provide early warning for women with negative cytological result.

1. Introduction

Endometrial cancer is the most common malignancy of the female genital tract. 80% of endometrial cancers occur in postmenopausal women with a mean of age 61 years at diagnosis [1]. According to already published data, the background incidence of endometrial cancer ranges from 0.6 to 6/1000 [2, 3]; thus endometrial cancer may potentially be a serious problem of public health, especially for postmenopausal women. Additionally, the duration of endometrial intraepithelial carcinoma can be of 8–12 years and of occult disease more than 5 years, thus providing plenty of time for detection in early stage. Endometrium is an easy to access organ, providing adequate and representative cytological material for examinations. Thus this material plays an important role for endometrial cancer detection and prevention.

One of the most important cancer hallmarks is aberrant DNA methylation [4]. However, it remains unclear when these changes take place and what is their precise role in the development of cancer. DNA methylation occurs when a methyl group is transferred to the 5′ position of a cytosine nucleotide adjacent to guanine (CpG). Usually CpGs are clustered in CpG islands and those that reside at gene's promoter region are normally unmethylated allowing the active transcription of the gene. In cancer cells a transcriptional silencing is observed due to methylation that is targeting the promoters of genes [5–7]. As far as endometrial carcinogenesis is concerned, there is accumulating evidence that except from the environment [8, 9] aberrant DNA methylation plays a critical role [10–12].

Galanin is a neuropeptide which belongs in a family of peptides whose expression has been involved in many cancers

[13]. It regulates many biological and pathological functions through three different receptor subtypes (*GALR1*, *GALR2*, and *GALR3*) [14]. Loss of *GALR1* expression is associated with its promoter hypermethylation supporting the hypothesis that *GALR1* acts as a tumor suppressor gene [14–16].

In the present study, a new pyrosequencing approach was developed. The purpose was to assess this method and evaluate its utility to identify possible differences of DNA methylation status in *GALR1* promoter genomic region between normal and malignant endometrial samples.

2. Materials and Methods

2.1. Samples and DNA Extraction. *GALR1* DNA methylation was investigated in 61 specimens, coming from the sample that has been collected with the EndoGyn device. Samples were collected from women who were admitted to the 3rd Department of Obstetrics and Gynecology "ATTIKON" University Hospital, "Saint Savvas" Anticancer Hospital, Athens, Greece. All patients signed an informed consent form, while the study was approved by the bioethics committee of the hospitals.

The samples' analysis was performed at cytopathology Department and the histological evaluation at the 2nd department of pathology, "ATTIKON" University Hospital. The histological material was from dilation and curettage and/or hysterectomy. The mean age of women was 61.2 years ± 12.7 (minimum 33, maximum 86). For the histologically benign cases the mean age was 54.7 years ± 7.0 (minimum 47, maximum 72) and for the histologically malignant cases the mean age was 64.0 years ± 13.6 (minimum 33, maximum 86). The pooled t-test was used for the comparison of the histologically benign and malignant group ages; it gave $t = -2.74$, $p = 0.0080 < 0.05$, meaning that the two groups have statistically significant different ages. The studied cases were selected as follows: from the files of the cytopathology laboratory we extracted all cases that had histological correlation and available biological material for further analysis. From these cases we randomly selected 61.

The cytological material was collected by gynecologists using the EndoGyn device especially designed for endometrial sampling. After the collection of endometrial material, the EndoGyn device was withdrawn and immersed into a vial containing 30 mL of appropriate hemolytic, mucolytic, and proteinolytic solution (CytoLyt, Cytyc Corporation), removing the unwanted background which limits cytological diagnosis [17]. LBC ThinPrep methodology was performed as described in detail in our previous work [18, 19]. In the cytopathology laboratory liquid-based cytology is applied as routine because it allows standardized and reproducible endometrial preparations and additional material remains for ancillary tests. For each case we prepared one slide stained with the Papanicolaou technique using an automated staining machine (Varistain; Thermo Electron Corporation [formerly Shandon], Runcorn, UK) and the remaining material was used for ancillary techniques including quantification of DNA methylation in *GALR1*.

The routine diagnostic procedure of the lab for reporting endometrial cytology was conformant to the 1994 World Health Organization (WHO) classification scheme [19, 20]. Thus, in this study the cytological diagnosis was provided as follows: benign, polyp, hyperplasia without cytological atypia (subsequently referred as hyperplasia WoA), atypical, and malignant. Cases diagnosed as atypical were subject to differential diagnosis between hyperplasia with atypia and well differentiated adenocarcinoma. In terms of increasing severity, the cytological categories in this study formed four groups: benign, hyperplasias WoA and polyp (subsequently referred to as HWoA-P) atypical, and malignant.

The histological material included cases diagnosed as benign, polyp, hyperplasia without atypia (hyperplasias WoA), and malignant, the last category includes endometrioid, mucinous, clear cell carcinoma (subsequently referred as CCC), serous carcinomas, and mixed and carcinosarcoma.

Concerning DNA methylation tests, DNA was extracted from 1.5 mL preserved cells using the PureLink Genomic DNA Mini Kit (Invitrogen, USA) according to manufacturer instructions. At the end of DNA extraction method, 100 μL of eluted DNA was recovered and stored at −20°C.

2.2. Sodium Bisulfate Treatment and Pyrosequencing. All DNAs were bisulfite converted using the EpiTect Bisulfite Kit (Qiagen, Hilden, Germany), according the manufacturer's instructions. All bisulfite converted samples were checked with β-actin (ACTB) and their concentration was adjusted to be the same as control's (10 ng/μL). The housekeeping gene ACTB was chosen as an internal reference [21]. Primers were designed using PyroMark Assay design SW 2.0 (Qiagen, Hilden, Germany). Assays were designed to target a region within the CpG island located around the transcription start site of the gene coding for *GALR1*. The selection of this region was based on Doufekas et al. [15] where it is shown that there is an increase of mean methylation in cancerous endometrium when it is compared with normal. PCRs were performed using the following primers: sense-GALFd GTTTAGGGGGAAGTTTAGATTT, antisense-GALRd BTN- ACCCCCAACTCCATAACCC, and sequencing forward-sGALd GGGGGAAGTTTAGATTTT. All PCRs were performed with the PyroMark PCR kit (Qiagen, Hilden, Germany). The conditions for PCR amplifications were as follows: A 15-minute incubation at 95°C was followed by 45 cycles of 30 seconds at 94°C, 30 seconds at 56°C, and 30 seconds at 72°C. A ten-minute elongation step at 72°C completed the PCR amplification.

A total of thirteen CpGs were analyzed. The pyrosequencing reactions were conducted using PyroMark Q24 Advanced CpG reagents and a PyroMark Q24 Instrument upgraded with the PyroMark Q24 Advanced software (Qiagen, Hilden, Germany). The pyrograms were analyzed using the CpG mode of the PyroMark Q24 Advanced software, to determine the methylation percentage of each site as well as the overall mean methylation. Every PCR and methylation run included H_2O, an EpiTect methylated and bisulfite converted, and an EpiTect unmethylated and bisulfite converted control human DNA (Qiagen, Hilden, Germany).

2.3. Statistical Analysis. The statistical analysis was performed by SAS 9.3 for Windows (SAS Institute Inc., NC, USA)

Table 1: Cytology/Histology correlation.

		Histology								
		Benign	Polyp	Hyperplasia WoA	Endometrioid	Carcinosarcoma	CCC	Serous	Mixed	Grand total
Cytology	Benign	10	2							12
	Polyp		1							1
	Hyperplasia WoA			5						5
	Atypical				2			1	1	4
	Malignant				32	1	2		4	39
	Grand total	10	3	5	34	1	2	1	5	61

[22, 23]. Within the analysis we have included an additional variable, namely, the mean methylation level calculated as the total of methylation levels for all positions divided by the number of positions that methylation measurement was successful (see Supplementary Information in Supplementary Material available online at http://dx.doi.org/10.1155/2015/756359 for the variables involved in the study).

The first step of the analysis was to examine the correlation of methylation percentages for each individual position; this analysis was performed by calculating the Pearson correlation coefficients for all possible pairs.

The second step was to examine if the mean methylation level is different for the cytological category groups and for this reason we produced boxplots of the mean methylation and performed regression analysis in order identify if there is a relation governing the mean methylation percentage and the disease severity as this is expressed in the cytological result.

The next step of the analysis was to extract the receiver operating characteristics curves (ROC) for each methylation position and identify if there are individual methylation positions that can be used as discriminators for the detection of endometrial malignancies. We used as cut-off level the histological categories benign and malignant.

Finally we tried to identify a cut-off value of the mean methylation level in order to characterize a sample as histologically benign or malignant. For this purpose the data were separated into two sets: the training set used to identify the threshold and the test set used to test the performance of the method on unknown data. Comparison with the cytological approach was performed as well. The algorithms for the determination of the optimum threshold values were calculated with in-house developed software for the MATLAB environment (The MathWorks, Inc., Natick, Massachusetts, USA).

Within our measurements, there were positions that were assigned as unsuccessful by the PyroMark Advanced software. Specifically from the 61 cases it was possible to measure methylation in all 13 positions in 43 cases (70.49%), in 14 cases (22.95%) in 12 positions, and in 4 cases (6.56%) in 12 positions.

3. Results

We developed a pyrosequencing assay that recognizes part of the CpG island near the transcription start site of *GALR1*. To design a set of primers we used as target sequence a region that was previously shown as being highly methylated in endometrial cancer using a MethyLight assay [15]. The reproducibility of the assay was checked when different runs were performed by testing two samples characterized as unmethylated and two samples characterized as methylated when compared with the negative control, in previous runs. The level of the methylation that was observed was almost similar. All raw pyrograms were evaluated. The quantitative methylation levels of the CpG sites in the region sequenced were analyzed by the Advanced PyroMark software.

The correlation of the cytological with the histological diagnosis is presented in Table 1. Cytologically 12 (19.67%) cases were negative: one case was secretory endometrium, one case was proliferative, and the remaining ten cases atrophic endometrium. One case was characterized cytologically as polyp (1.64%) and five cases (8.20%) were characterized as hyperplasias without atypia, four cases (8.20%) were found cytologically as atypical, and 39 (63.93) as malignant. From the 39 cytologically malignant cases 36 were diagnosed in cytology as adenocarcinomas, one case as squamous cell carcinoma, and two cases as malignant unless otherwise specified. In our material there were no cases of hyperplasia with atypia.

A plot indicating methylation percentages for each CpG position on the x-axis and methylation percentage on the y-axis for all involved samples is provided in Figure 1. The red solid lines representing the malignant cases are mostly concentrated on the upper part in contrast to the benign cases. This figure depicts as well that methylation is highly correlated in various positions; the correlation analysis via the Pearson correlation coefficient is presented in the supplement.

In relation to the lesion severity as this is depicted by the cytological result (expressed in numeric form; see Supplement, CytologyNumeric variable) we performed regression analysis (see Figure 2) and this produced a linear relation between the mean methylation and the cytological outcome: mean methylation $= 0.10 + 0.13 * \text{CytologyNumeric}$. The line fit is almost perfect as $R^2 = 98.41\%$. The positive slope (0.13) indicates that from one cytological category to the other the mean methylation percentage increases by 13%.

Subsequently we calculated the ROC curve for mean methylation, in order to evaluate the potential value of the mean methylation percentage as a predictor of the status of malignancy as this is defined by the histological golden

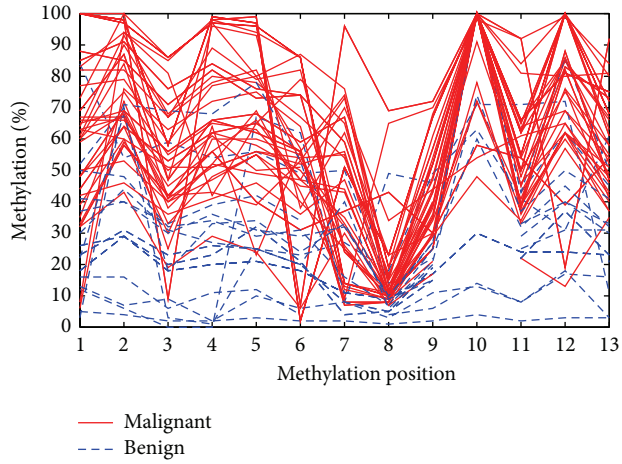

Figure 1: Methylation percentages for each methylation position for the studied samples.

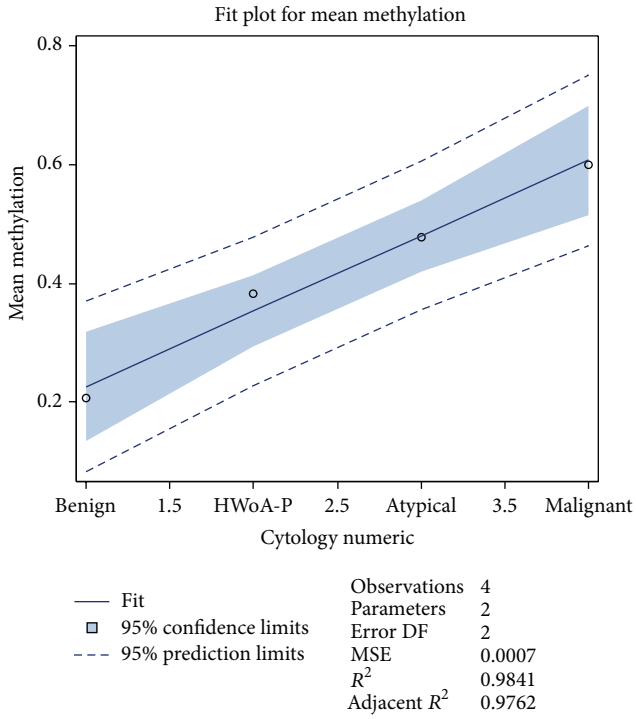

Figure 2: Fit plot for mean methylation in relation to the severity of the cytological diagnosis.

standard. The ROC curve appears in Figure 3. A more detailed ROC analysis for all methylation positions appears in the Supplement.

As the mean methylation has the best performance, in terms of ROC curve analysis, the next step was to identify a threshold and separate the histologically benign from histologically malignant cases. About 50% (9 histologically benign and 22 malignant cases) were randomly selected and used to identify the optimum threshold. This was determined using a procedure already described in the bibliography [24]; specifically a broad range of thresholds was used starting

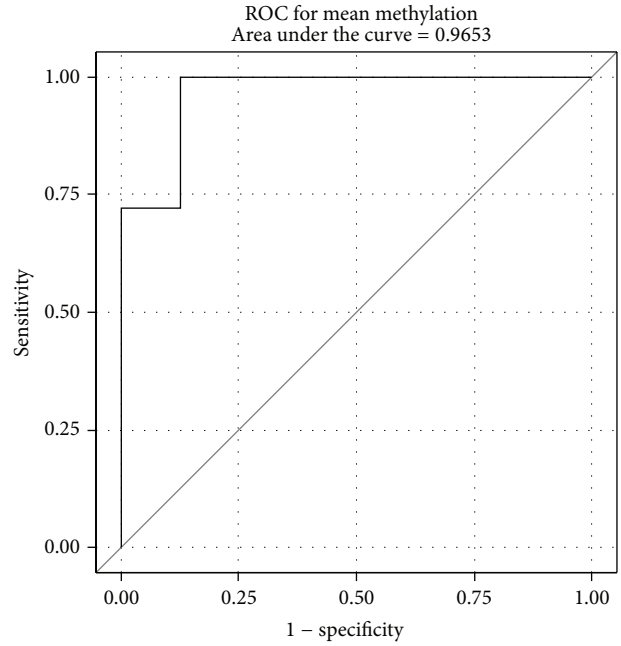

Figure 3: ROC curves of the mean methylation in relation to the histological outcome using as categories benign and malignant.

from 20% and increasing up to 100% with an increment step of 1%; for each threshold value we calculated the percentage of the cases that were correctly classified (overall accuracy). As most suitable threshold, the threshold that maximized the overall accuracy on the training set was selected. The optimal threshold using this approach was 37%. Thus an algorithm was able to be produced: "if the mean methylation level is higher than 37% then the sample is considered as histologically malignant and otherwise as benign."

Using this threshold from the 9 benign cases of the training set, 8 were classified as benign while all malignant cases (22) were classified correctly; this results in an overall accuracy of 96.77%, sensitivity of 100.00%, and specificity of 88.89%. By applying the same threshold on the test set (9 histologically benign and 21 malignant cases) it was possible to classify correctly 8 out of the 9 benign cases and 20 out of the 21 malignant cases. Overall accuracy = 93.33%, sensitivity = 95.24%, and specificity = 88.89%. The comparison of the overall accuracy percentages via the χ-square test proved that the two values are not statistically different ($\chi^2 = 0.00084$, $p = 0.98 > 0.05$) and thus the proposed method was stable on unknown data (despite the small sample number).

A figure depicting the overall accuracy for the training set, test set, and the complete data set for the various threshold values appears in the Supplement.

In this study all cytological cases were by design in agreement with the histological result (see Table 1); thus the overall accuracy of the cytological examination was by design 100%; however the comparison of the overall accuracy of the proposed method on the complete data set (overall accuracy = 95.08, sensitivity = 97.67, and specificity = 88.89%) via the χ-square test proved that there was no statistically

significant difference ($\chi^2 = 1.368$, $p = 0.24 > 0.05$). Thus statistically the proposed mean methylation thresholding method may be considered equivalent to cytology.

4. Discussion

Epigenetics are changes in gene expression which are not a result of altered nucleotide sequence [25]. As it was previously described, the definition of methylation levels could identify patients with different clinical characteristics [26]. Having the advantage of calculating the mean methylation of each CpG during pyrosequencing and expressing it as an absolute value, this method is featured as gold standard technology for quantitative methylation studies.

The neuropeptide galanin elicits a range of biological effects by interaction with specific G-protein-coupled receptors. Galanin receptors are seven-transmembrane proteins shown to activate a variety of intracellular second-messenger pathways. *GALR1* inhibits adenylyl cyclase via a G protein of the Gi/Go family [27]. According to Rauch and Kofler [13], the galanin peptide expression is studied in pheochromocytoma, pituitary adenoma, neuroblastic tumors, gastrointestinal cancer, squamous cell carcinoma, brain tumors, melanoma, breast cancer, and embryonal carcinoma. In another study it is highlighted that the galanin promoter methylation profile could be an important marker predicting the clinical outcome of head and neck squamous cell carcinoma [16].

As far as the endometrium is concerned, the biological function of the galanin system is not studied extensively. According to Doufekas et al. [15], there is an evidence that *GALR1* suppression possibly plays a role in endometrial cancer development. The authors found that *GALR1* methylation is among the most frequent and consistent methylation differences between benign and cancerous endometrium.

In our study we found that the methylation percentage was increased from the benign lesions to the HWoA-P as well as to atypical and malignant lesions (see Figure 2 related to the mean methylation), a fact that indicates that methylation of *GALR1* may play a role in carcinogenesis. This finding led to subsequent analysis using the histological outcome as gold standard; the high percentages of the areas under the ROC for almost all measured positions (see Supplement) and especially for the mean methylation level proved that this test is not only reliable but accurate as well. A strong correlation of the methylation percentages in numerous positions was observed during the analysis of the results of the present study. This could be an indication for retaining accuracy in the overall mean methylation percentage; even if for laboratory reagents consuming or for time saving purposes, this method has to analyze less positions in a massive application.

A recent study describes that DNA hypermethylation in endometrial tissues quantified by pyrosequencing can also be identified in vaginal pool DNA collected via intravaginal tampon, combining thus a minimally invasive collection method with a high-throughput methodology for the early detection of endometrial cancer [28]. Although our present work discusses a possible role of the described pyrosequencing technology in the future as an indicator of malignancy, additional studies with larger series may in the future be substantiated and provide more evidence and confirm these preliminary results. It is important that methylation can be measured on cytological material by applying a sampling method that is well tolerated, easy to use, less painful than biopsy, and cost-effective. It additionally provides a generous and adequate material as long as endometrium is an easy to access organ for sampling which is representative of the lesion for cytological evaluation and the application of ancillary techniques [19].

The detailed analysis of the mean methylation for the two major histologically malignant subgroups (see Table 1), specifically for endometrioid carcinomas (34 cases, mean methylation = 59.99%, min = 39.56%, max = 82.86%, S.D. = 12.24%) versus nonendometrioid carcinomas (9 cases, mean methylation = 52.24%, min = 23.06%, max = 70.48%, S.D. = 14.13%), revealed that the mean methylation levels of the two groups do not differ significantly ($\chi^2 = 0.048$, $p = 0.94 > 0.05$). Thus in the small data set the conclusion is that the mean methylation measurements do have potential to discriminate endometrioid from nonendometrioid carcinomas.

Similar analysis in the histologically benign subgroups which is negative (10 cases, mean methylation = 19.70%, min = 2.36%, max = 36.16%, S.D. = 10.77%) versus the group including polyp or hyperplasias without atypia (8 cases, mean methylation = 35.15%, min = 20.13%, max = 51.32%, S.D. = 10.62%) revealed that the mean methylation levels of these two groups are not different ($\chi^2 = 0.040$, $p = 0.84 > 0.05$). Therefore the mean methylation level of a case seems not to have the potential to discriminate cases that may harbor a polyp or hyperplasia without atypia from healthy subjects.

According to the results, it is possible to define a reliable cut-off level (37%) in the mean methylation in order to discriminate histologically benign from malignant lesions. As the comparison of the cut-off method proved that there is no statistically significant difference compared to cytology alone, the pyrosequencing methylation analysis of *GALR1* promoter has the potential to be used in the future as an additional marker (or even single test) to the cytological examination, for better management of women with endometrial lesions, either towards a follow-up or for referral to dilatation and curettage. Eventually it could reduce unnecessary interventions and provide an early warning for women with negative cytology or borderline lesions with high methylation percentages.

Conflict of Interests

The authors declare that there is no conflict of interests regarding the publication of this paper.

Acknowledgments

The authors would like to thank the reviewers for their comments, providing ideas to radically enhance the original paper.

References

[1] D. G. Gallup and R. J. Stock, "Adenocarcinoma of the endometrium in women 40 years of age or younger," *Obstetrics & Gynecology*, vol. 64, no. 3, pp. 417–420, 1984.

[2] L. G. Koss, K. Schreiber, S. G. Oberlander, M. Moukhtar, H. S. Levine, and H. F. Moussouris, "Screening of asymptomatic women for endometrial cancer," *CA: A Cancer Journal for Clinicians*, vol. 31, no. 5, pp. 300–317, 1981.

[3] R. I. Horwitz, A. R. Feinstein, S. M. Horwitz, and S. J. Robboy, "Necropsy diagnosis of endometrial cancer and detection-bias in case/control studies," *The Lancet*, vol. 2, no. 8237, pp. 66–68, 1981.

[4] P. A. Jones and S. B. Baylin, "The epigenomics of Cancer," *Cell*, vol. 128, no. 4, pp. 683–692, 2007.

[5] J. G. Herman and S. B. Baylin, "Gene silencing in cancer in association with promoter hypermethylation," *The New England Journal of Medicine*, vol. 349, no. 21, pp. 2042–2054, 2003.

[6] M. L. Suvà, N. Riggi, and B. E. Bernstein, "Epigenetic reprogramming in cancer," *Science*, vol. 340, no. 6127, pp. 1567–1570, 2013.

[7] H. Shen and P. W. Laird, "Interplay between the cancer genome and epigenome," *Cell*, vol. 153, no. 1, pp. 38–55, 2013.

[8] P. Lichtenstein, N. V. Holm, P. K. Verkasalo et al., "Environmental and heritable factors in the causation of cancer: analyses of cohorts of twins from Sweden, Denmark, and Finland," *The New England Journal of Medicine*, vol. 343, no. 2, pp. 78–85, 2000.

[9] L. J. Schouten, R. A. Goldbohm, and P. A. van den Brandt, "Anthropometry, physical activity, and endometrial cancer risk: results from the Netherlands cohort study," *International Journal of Gynecological Cancer*, vol. 16, no. supplement 2, p. 492, 2006.

[10] S. B. Baylin and P. A. Jones, "A decade of exploring the cancer epigenome—biological and translational implications," *Nature Reviews Cancer*, vol. 11, no. 10, pp. 726–734, 2011.

[11] A. Jones, A. E. Teschendorff, Q. Li et al., "Role of DNA methylation and epigenetic silencing of HAND2 in endometrial cancer development," *PLoS Medicine*, vol. 10, no. 11, Article ID e1001551, 2013.

[12] X. C. Zhou, S. C. Dowdy, K. C. Podratz, and S.-W. Jiang, "Epigenetic considerations for endometrial cancer prevention, diagnosis and treatment," *Gynecologic Oncology*, vol. 107, no. 1, pp. 143–153, 2007.

[13] I. Rauch and B. Kofler, "The galanin system in cancer," *EXS*, vol. 102, pp. 223–241, 2010.

[14] B. S. Henson, R. R. Neubig, I. Jang et al., "Galanin receptor 1 has anti-proliferative effects in oral squamous cell carcinoma," *The Journal of Biological Chemistry*, vol. 280, no. 24, pp. 22564–22571, 2005.

[15] K. Doufekas, R. Hadwin, R. Kandimalla et al., "GALR1 methylation in vaginal swabs is highly accurate in identifying women with endometrial cancer," *International Journal of Gynecological Cancer*, vol. 23, no. 6, pp. 1050–1055, 2013.

[16] K. Misawa, T. Kanazawa, Y. Misawa et al., "Galanin has tumor suppressor activity and is frequently inactivated by aberrant promoter methylation in head and neck cancer," *Translational Oncology*, vol. 6, no. 3, pp. 338–346, 2013.

[17] A. M. Buccoliero, F. Castiglione, C. F. Gheri et al., "Liquid-based endometrial cytology: its possible value in postmenopausal asymptomatic women," *International Journal of Gynecological Cancer*, vol. 17, no. 1, pp. 182–187, 2007.

[18] M. Papaefthimiou, H. Symiakaki, P. Mentzelopoulou et al., "The role of liquid-based cytology associated with curettage in the investigation of endometrial lesions from postmenopausal women," *Cytopathology*, vol. 16, no. 1, pp. 32–39, 2005.

[19] M. Papaefthimiou, H. Symiakaki, P. Mentzelopoulou et al., "Study on the morphology and reproducibility of the diagnosis of endometrial lesions utilizing liquid-based cytology," *Cancer*, vol. 105, no. 2, pp. 56–64, 2005.

[20] R. E. Scully and H. E. Poulsen, *Histological Typing of Female Genital Tract Tumours*, Springer, Berlin, Germany, 2nd edition, 1994.

[21] R. M. Overmeer, J. A. Louwers, C. J. L. M. Meijer et al., "Combined CADM1 and MAL promoter methylation analysis to detect (pre-)malignant cervical lesions in high-risk HPV-positive women," *International Journal of Cancer*, vol. 129, no. 9, pp. 2218–2225, 2011.

[22] C. DiMaggio, *SAS for Epidemiologists: Applications and Methods*, Springer, New York, NY, USA, 2013.

[23] SAS Institute, "SAS Home Page," Ed., 2014.

[24] D. Zygouris, A. Pouliakis, N. Margari et al., "Classification of endometrial lesions by nuclear morphometry features extracted from liquid-based cytology samples: a system based on logistic regression model," *Analytical and Quantitative Cytopathology and Histopathology*, vol. 36, no. 4, pp. 189–198, 2014.

[25] R. Holliday, "The inheritance of epigenetic defects," *Science*, vol. 238, no. 4824, pp. 163–170, 1987.

[26] B. Banelli, S. Bonassi, I. Casciano et al., "Outcome prediction and risk assessment by quantitative pyrosequencing methylation analysis of the SFN gene in advanced stage, high-risk, neuroblastic tumor patients," *International Journal of Cancer*, vol. 126, no. 3, pp. 656–668, 2010.

[27] J. S. Gutkind, "Cell growth control by G protein-coupled receptors: from signal transduction to signal integration," *Oncogene*, vol. 17, no. 11, pp. 1331–1342, 1998.

[28] J. N. Bakkum-Gamez, N. Wentzensen, M. J. Maurer et al., "Detection of endometrial cancer via molecular analysis of DNA collected with vaginal tampons," *Gynecologic Oncology*, vol. 137, no. 1, pp. 14–22, 2015.

Hindawi Publishing Corporation
BioMed Research International
Volume 2015, Article ID 238757, 9 pages
http://dx.doi.org/10.1155/2015/238757

Review Article

Genomic and Histopathological Tissue Biomarkers That Predict Radiotherapy Response in Localised Prostate Cancer

Anna Wilkins,[1,2] David Dearnaley,[2] and Navita Somaiah[2,3]

[1]*Division of Clinical Studies, The Institute of Cancer Research, London SM2 5NG, UK*
[2]*Division of Radiotherapy and Imaging, The Institute of Cancer Research, London SM2 5NG, UK*
[3]*Division of Cancer Biology, The Institute of Cancer Research, London SM2 5NG, UK*

Correspondence should be addressed to Anna Wilkins; anna.wilkins@icr.ac.uk

Received 1 April 2015; Accepted 24 May 2015

Academic Editor: Franco M. Buonaguro

Localised prostate cancer, in particular, intermediate risk disease, has varied survival outcomes that cannot be predicted accurately using current clinical risk factors. External beam radiotherapy (EBRT) is one of the standard curative treatment options for localised disease and its efficacy is related to wide ranging aspects of tumour biology. Histopathological techniques including immunohistochemistry and a variety of genomic assays have been used to identify biomarkers of tumour proliferation, cell cycle checkpoints, hypoxia, DNA repair, apoptosis, and androgen synthesis, which predict response to radiotherapy. Global measures of genomic instability also show exciting capacity to predict survival outcomes following EBRT. There is also an urgent clinical need for biomarkers to predict the radiotherapy fraction sensitivity of different prostate tumours and preclinical studies point to possible candidates. Finally, the increased resolution of next generation sequencing (NGS) is likely to enable yet more precise molecular predictions of radiotherapy response and fraction sensitivity.

1. Introduction

Heterogeneity in tumour biology between prostate tumours results in a varied response to radiotherapy. At present no molecular tissue biomarkers are in routine clinical use to risk-stratify patients with localised prostate cancer. Instead, current management of localised prostate cancer is based upon established clinical risk factors including presenting PSA, clinical or radiological T (tumour) stage, and the total Gleason score. However, estimates of recurrence and survival vary considerably; for example, in the National Comprehensive Cancer Network (NCCN) intermediate risk group biochemical failure at five years following definitive local therapy varies from 2% to 70% [1]. Although new clinical factors have been identified including percentage core positivity and the primary Gleason score [2], there remains an urgent need to incorporate molecular biomarkers predicting radioresistance into treatment decisions. Such biomarkers would enable a personalised prediction of radiotherapy efficacy. If combined with personalised predictors of radiation toxicity including radiogenomic markers [3], both sides of the therapeutic ratio of radiotherapy for localised prostate cancer would be improved.

The lethality of radiotherapy is centred on the creation of chromosomal lesions including DNA double strand breaks (DSB), which are particularly lethal when they cluster in close physical proximity to each other [4]. Cells that are unable to repair this radiation induced DNA damage are likely to undergo programmed cell death via apoptosis or autophagy or alternatively death via mitotic catastrophe [5, 6]. Hypoxia has traditionally been viewed as an important contributor to radioresistance as oxygen reacts with damaged DNA bases created by free radicals thus creating a stable adduct and fixing the damage [7]. More recently, the hypoxic state has also been associated with reduced capacity for DNA repair, increasing genomic instability, and creation of a mutator phenotype [8]. Whilst biomarkers of DNA repair and hypoxia have been shown to predict radioresistance, much broader aspects of tumour biology including cell proliferation, apoptosis, and androgen synthesis have been implicated in treatment failure following radiotherapy. All of these offer considerable potential for improving treatment

precision, for example, with personalised dose escalation or concomitant use of systemic agents such as abiraterone.

Another important radiobiological question at present is the radiotherapy fraction size sensitivity of prostate cancer, as measured by the alpha/beta ratio. An expanding body of evidence points to the alpha/beta ratio of prostate adenocarcinoma being as low as 1.5 [9], suggesting that tumours are more sensitive to fraction size than neighbouring normal tissues. The results of randomised clinical trials testing this hypothesis are currently awaited [10]. However, it is highly likely that the alpha/beta ratio and therefore fraction size sensitivity differ between individual prostate tumours, especially as we know that cellular proliferation, DNA repair, hypoxia, and other relevant biological parameters vary considerably. Although an exciting area of research, once again no molecular biomarkers are in clinical use to assess fraction size sensitivity of tumours prior to radiotherapy treatment.

Recent rapid progress in next generation sequencing techniques offers huge potential for personalisation of radiotherapy treatment, despite some of the required technological expertise being currently beyond the scope of most routine pathology laboratories. Other routinely available histopathological techniques such as immunohistochemistry (IHC) or genomic techniques such as fluorescent in situ hybridisation (FISH), comparative genomic hybridisation (CGH), and polymerase chain reaction (PCR) have identified many candidate biomarkers which with further validation could rapidly enter the clinic.

Molecular biomarker development following prostatectomy has progressed at an accelerated pace compared to following radiotherapy due to limited tissue availability with the latter treatment [11]. Critics suggest that diagnostic biopsies do not represent the true biological heterogeneity within the entire prostate gland. However, as image-guided template biopsies become more commonly used, tumour representation in prostate biopsies continues to increase in accuracy. Furthermore, for the foreseeable future, diagnostic biopsies will continue to be the main tumour tissue available to guide radiotherapy stratification. It is important that the above differences in tissue availability do not hinder the development and validation of predictive biomarkers that distinguish benefit from different local treatments for early prostate cancer as this remains a clinical priority.

This paper aims to review biomarkers predicting radiotherapy response in prostate cancer incorporating genomic signatures and individual candidates as well as biomarkers identified by longer established techniques. It does not address microRNA or biomarkers involved in the diagnosis of prostate cancer or prognostication outside of radiotherapy treatment; these were comprehensively reviewed in a recent paper in this journal [12].

2. Biomarkers of Radiosensitivity Identified Using Immunohistochemistry (IHC)

IHC enables direct evaluation of protein expression, which is advantageous as proteins are determinants of cellular function. Recent comprehensive genomic and proteomic work suggests that changes in nucleic acid do not necessarily translate to corresponding changes in protein expression [13]. IHC is a technique that is readily available in routine pathology laboratories; tumour histopathology can be correlated with protein expression; hence, tumour dissection is not required. For bulky prostate tumours, sufficient tissue may be present to construct tissue microarrays which facilitates high throughput analysis [14, 15]; however, in intermediate risk localised prostate tumours this approach has recently been shown to be unfeasible due to inadequate numbers of tumour cells [16].

The Radiation Therapy Oncology Group (RTOG) 8610 and 9202 clinical trials of radiotherapy and varying lengths of androgen deprivation for localised prostate cancer have reported several biomarkers predicting outcome using IHC (Table 1). A consistent prediction of survival outcomes has been shown for some candidates and the second trial has validated earlier findings. For example, Ki-67, a well-established marker of cellular proliferation, has consistently predicted biochemical-free survival, local recurrence, and overall survival [17–21]. p53, one of the most commonly mutated tumour suppressor genes with a central role in checkpoint activation, is regulated by the oncogene MDM2. Both genes have shown prediction of prostate cancer outcome in the RTOG studies and elsewhere [17, 22–27]. Low expression of the cyclin dependent kinase inhibitor p16 has also been consistently associated with poor survival outcomes following radiotherapy [28, 29]. As poor outcomes following surgery are predicted by high expression, p16 is one of very few true predictive biomarkers identified to date [11]. Finally increased expression of COX2, a gene with cell cycle modulatory effects as well as antiapoptotic, proangiogenic, and proliferative effects via prostaglandin E2 [30, 31], has also been repeatedly associated with poor survival outcomes [32].

Pollack et al. recently modelled the risk of distant metastases using expression of the above 5 candidates plus the apoptotic proteins Bcl-2 and Bax with competing risks hazard regression, adjusting for age, PSA, the Gleason score, T-stage, and treatment [33]. The resulting model included 4 tissue biomarkers (Ki-67, MDM2, p16, and COX2) and showed a concordance index of 0.77 versus 0.70 without molecular biomarkers, meaning a relative improvement in prediction of distant metastases of 10%. This "immunopanel" is the first known multiplex panel of biomarkers developed using IHC to date in prostate cancer.

The role of hypoxia markers in prognostication following radiotherapy is more controversial. VEGF and HIF1-alpha were not included in the RTOG modelling of risk of distant metastases because an earlier RTOG study failed to demonstrate a significant association of VEGF with any survival outcomes following radiotherapy [34]. However, in two British studies of VEGF and HIF1-alpha, increased expression independently predicted biochemical recurrence [35, 36]. Furthermore, lactate dehydrogenase (LDH), a marker of anaerobic metabolism and an indirect marker of hypoxia, has also been associated with inferior radiotherapy response [37]. Osteopontin (OPN) is a small integrin-binding ligand N-linked glycoprotein (SIBLING) that is thought to be induced by hypoxia [38]. OPN has been associated with reduced

Table 1: Predictive tissue biomarkers for radiotherapy response identified using immunohistochemistry (IHC).

Tissue biomarkers for radiotherapy response identified using IHC			
Marker	Function	Technique	IHC cut point used
p53 [22, 23, 25, 27]	Cell cycle checkpoints	IHC	0 versus 1–4* [22], ≤30% nuclei versus >30% nuclei [23], <20% nuclei versus ≥20% nuclei [25], and 0 versus 1 versus 2–4 [27]
p16 [28, 29]	Cell cycle checkpoints	IHC	≤25% versus >25% [28], ≤81.3% versus >81.3% [29]
Rb1 [28]	Cell cycle checkpoints	IHC	≤20% versus >20%
MDM2 [17, 24]	Cell cycle checkpoints	IHC	≤184 versus >184 AU (IA) [17], ≤3% versus >3% ACIS [24]
Ki67 [17–21]	Cell proliferation	IHC	≤11.3% nuclei versus >11.3% nuclei [17], SI ≤3.5% versus >3.5% [18, 19], continuous and SI ≤7.1% versus >7.1% [20], and SI <6.2% versus ≥6.2% [21]
PKA [39]	Cell proliferation	IHC	Manual: 0, 1, and 2 versus 3 and 0, 1 versus 2, 3* IA: median of 111.8, Q3 of 128.0 and 135.5
STAT3 (activated) [40]	Cell proliferation/apoptosis	IHC	Continuous and ACIS ≤29% versus >29%
Her2/neu [41]	Growth receptor	IHC	Membrane positivity ≤10% versus >10%
EGFR [42]	Growth receptor	IHC	Negative versus weak or strong membranous staining
Bcl2 [22, 23, 43]	Apoptosis	IHC	Nil versus any cytoplasmic staining [22, 23], ≤20% versus >20% cytoplasmic staining [43]
Bax [44]	Apoptosis	IHC	Greater or lesser cytoplasm staining intensity relative to normal prostate
E-cadherin [15]	Cell adhesion	PCR array, IHC validation	Absent or weak (0/1+) versus moderate or strong (2+/3+)
COX2 [32]	Prostaglandin synthesis	IHC	134 AU (median) and continuous variable [32]
LDH5 [37]	Anaerobic metabolism and hypoxia	IHC	<50% cytoplasmic expression and/or <10% nuclear expression versus >50% and >10%
HIF1a [35, 42]	Hypoxia	IHC	0% versus <1% versus 1–10% versus 10–33% versus 34–67% versus >67% cytoplasmic staining [35], ≤50% versus >50% nuclear and cytoplasm staining [42]
VEGF [35, 36]	Hypoxia	IHC	0% versus <1% versus 1–10% versus 10–50% versus >50% cytoplasmic staining [35], IRS score* 0–4 versus 5–8 [36]
DNA PKcs [45]	NHEJ	IHC	Nil versus any nuclear staining

NHEJ: nonhomologous end joining; PCR: polymerase chain reaction; IA: image analysis; IRS: immunoreactive score; AU: arbitrary units; ACIS: automated cellular imaging system; *cut point refers to semiquantitative scoring system incorporating staining intensity and percentage of tumour cells positive; SI: staining index.

survival times in prostate cancer [38], however, was only significant in predicting radiotherapy response on univariate analysis, not when modelling adjusted for other clinical factors [35]. A study of plasma OPN levels in localised prostate cancer indicated that OPN levels did not change in response to radiotherapy [46].

There are several possible reasons for conflicting data regarding hypoxic biomarkers and prediction of radiotherapy response. These include differences in the size of patient cohorts, NCCN risk group, and IHC cut points used to determine high expression of VEGF and HIF1-alpha. Furthermore, our understanding of how hypoxia impacts DNA repair is evolving rapidly. Recent studies suggest that hypoxia induces downregulation of proteins within the DNA double strand break repair pathways of homologous recombination (HR) and nonhomologous end joining (NHEJ) [47–49]. This has implications for radiosensitivity and also provides a mechanism for hypoxia inducing a mutator phenotype as DNA repair downregulation could permit survival and subsequent clonal selection of unrepaired unstable mutant tumour cells [8]. Further work to clarify the role of hypoxic markers in treatment stratification would be of considerable value.

With regard to DNA repair, error prone NHEJ operates in all phases of the cell cycle to repair DNA DSB; DNA PKcs has a key role in NHEJ by forming a synaptic complex bringing the free broken ends of DNA together with other ligating enzymes. Nuclear expression of DNA PKcs using IHC showed an independent association with biochemical recurrence after radiotherapy. However, other NHEJ proteins, also evaluated with IHC, such as Ku70, Ku80, and XRCC4 were not predictive of relapse [45].

The TMPRSS2/ERG fusion is an important cellular rearrangement occurring in 50% of localised prostate tumours and ERG protein expression using IHC has been shown to be a robust surrogate for detecting the gene fusion [50]. Preclinical studies have suggested that the gene fusion may be a biomarker of inferior double stranded DNA break repair capacity with important clinical implications [51]. However, the gene fusion was not prognostic for recurrence after radiotherapy when assessed with either IHC or CGH suggesting that it does not affect prostate tumour radiosensitivity [16] (Table 3).

There is thought to be direct cross talk between the EGFR cellular proliferation pathway and DNA repair. This provides

Table 2: Predictive tissue biomarkers for radiotherapy response identified using genomic techniques.

Marker/signature	Function	Technique
DNA ploidy [52]	Genomic instability	Image analysis (Feulgen) and DNA/protein flow cytometry
Nuclear DNA content [53]	Genomic instability	Static DNA cytometry
c-myc [54]	Cell proliferation	Array CGH validated by FISH
PTEN [54]	Cell survival	Array CGH validated by FISH
E-cadherin [15]	Cell adhesion	PCR array, IHC validation
NKX3.1 [55]	Androgen related homeobox gene, DNA repair	Array CGH
NBN [56]	DNA damage response	Array CGH
StAR [57]	Androgen synthesis	Array CGH
HSD17B2 [57]	Androgen synthesis	Array CGH
Cell cycle progression score [58]	Cell cycle progression	RT-PCR (RNA expression)
CAN_RF [59]	Genomic and microenvironment heterogeneity	Array CGH, intraglandular hypoxia with piezoelectrode

FISH: fluorescent in situ hybridisation; CGH: comparative genomic hybridisation; RT-PCR: reverse transcription polymerase chain reaction.

a possible biological rationale for the observed correlation between high EGFR expression and poor prognosis following prostate radiotherapy [42]. However, the aetiology of poor survival outcomes with increased EGFR expression is likely to be multifactorial and includes increased cellular proliferation. Protein kinase A type 1 and STAT3 also function in cell proliferation and malignant transformation and have been studied in the RTOG trials where overexpression has been associated with poorer outcomes [39, 40]. However, STAT3 expression only correlated with distant metastases and not with other survival outcomes such as local failure. For protein kinase A, overexpression was associated with a diminished response to long term androgen deprivation therapy (LTAD) and radiation, relative to short term androgen deprivation and radiotherapy suggesting that these patients require alternative treatment escalation to LTAD.

The antiapoptotic protein Bcl-2 and proapoptotic Bax both have key roles in determining cell fate following radiotherapy. Independent prediction of survival outcomes has been demonstrated in some [22, 23, 43], but not all [44, 60], studies to date and further work to clarify their prognostic role is needed. Androgen deprivation is known to cause apoptotic cell death so different use of androgen deprivation within treatment arms of RTOG 8610 and 9202 is likely to have impacted predictive outcomes [44]. Some of the observed discrepancies may have arisen due to high numbers of patients with locally advanced versus early prostate cancer, a lack of standardised IHC protocol and antibody, as well as use of different cut points defining high or low expression between studies.

Identifying biomarkers of radiotherapy fraction size sensitivity is another area of unmet need. There is a tight association between proliferative indices and fraction size sensitivity of normal tissues [61]. Normal tissues that respond early (within days of radiotherapy) have high proliferative indices and low sensitivity to fraction size and vice versa for those that respond late (years later). The association is so tight as to offer clues to mechanisms [62–64]. Published literature also suggests that the choice of DNA DSB repair pathway (homologous recombination (HR) versus NHEJ) between rapidly proliferating and slowly proliferating cells may influence fraction size sensitivity. Using *in vitro* clonogenic assays rodent cell lines with defects in NHEJ showed loss of fraction size sensitivity [65, 66]. In addition, IHC on *in vivo* irradiated human skin showed that a 10-fold increase in the use of HR to repair radiation-induced DNA DSB towards the end of radiotherapy correlated with loss of fractionation sensitivity seen clinically [67]. On average, prostate tumours are thought to have a low alpha/beta ratio and hence are sensitive to both fraction size and total dose of radiation [9]. However, biological heterogeneity means that fraction size sensitivity is likely to vary between prostate tumours and therefore there is a need to identify tissue biomarkers to guide individualised fractionation.

3. Biomarkers of Radiosensitivity Identified Using Genomic Techniques

3.1. Fluorescent In Situ Hybridisation (FISH). Use of a fluorogen with FISH, rather than a chromogen as in IHC, means that interpreting expression can be more straightforward than with IHC [68]. In addition, multiple fluorophores can be combined on a single slide which is particularly advantageous with the limited tissue available from pre-radiotherapy biopsies [69]. FISH is routinely available in histopathology laboratories where it is particularly useful for confirming HER2 status in breast tumours and therefore the technique offers considerable potential for development of predictive biomarkers.

FISH has been used to demonstrate a role for biomarkers of cell proliferation such as PTEN and c-myc in predicting radiotherapy response. Loss of the tumour suppressor gene PTEN and amplification of the oncogene c-myc have both been associated with inferior outcomes following radiotherapy [54] (Table 2). In combination, these biomarkers were more strongly associated with increased biochemical recurrence than either in isolation.

Table 3: Negative predictive studies in EBRT.

Marker	Function	Technique	IHC cut point used
VEGF [34]	Hypoxia	IHC	0-1 versus 2-3 cytoplasmic staining intensity
Bcl-2 [44, 60, 70]	Apoptosis	IHC	Nil versus any cytoplasmic staining [44, 60], <10% versus >10% cell staining [70]
Bax [60]	Apoptosis	IHC	Greater or lesser cytoplasm staining intensity relative to normal prostate
AR [15]	Androgen receptor	PCR array	
PCA3 [15]	Prostate marker	PCR array	
PTEN [15]	Cell survival	PCR array	
EZH2 [15]	Transcriptional control	PCR array	
EGFR [15]	Growth receptor	PCR array	
PSMA [15]	Prostate marker	PCR array	
MSMB [15]	Tumour suppression	PCR array	
CAG repeats [71]		Genotyping (PCR)	
CYP3A4 polymorphisms [72]		Genotyping	
TMPRSS2/ERG (or ETV1) [16]	Androgen regulated/cell proliferation gene fusion	Array CGH, IHC	Any positive staining versus negative
Osteopontin [46]	SIBLING, tumour associated protein	ELISA	
Ku70 and Ku80 [45]	NHEJ	IHC	Ku70 ≤50% versus >50% nuclear staining, Ku80 ≤60% versus >60% nuclear staining
MRE11 [56]	DNA damage response	Array CGH	
RAD50 [56]	DNA damage response	Array CGH	
ATM [56]	DNA damage response	Array CGH	
ATR [56]	DNA damage response	Array CGH	
PRKDC (DNA PKcs) [56]	NHEJ	Array CGH	

SIBLING: small integrin-binding ligand: N-linked glycoprotein.

3.2. Polymerase Chain Reaction (PCR) Array. PCR array involves synthesis and amplification of complimentary DNA (cDNA) prior to expression profiling. Although amplification can introduce bias, this multiplex technique is particularly useful when tissue and hence nucleic acid quantity is limited. A reduction in mRNA (messenger RNA) of the cell-cell adhesion molecule E-cadherin has recently been associated with poor outcome after radiotherapy, but not after primary androgen deprivation therapy alone using PCR array [15]. The authors validated the predictive ability of E-cadherin in an independent dataset by demonstrating that reduced protein expression using IHC was significantly and independently associated with early biochemical recurrence. A number of other candidates were simultaneously assessed including previously discussed EGFR and PTEN, as well as EZH2, PSMA, and MSMB, all of which have shown prognostic ability following surgery; however, they were non-prognostic after radiotherapy in this study. However, the study cohort size was modest at 60 patients which may have contributed to negative findings [15]. The fact that AR also showed no prognostic ability after EBRT illustrates the differences in tumour biology between castration resistant and castration sensitive tumours.

3.3. Comparative Genomic Hybridisation (CGH). CGH differs from Reverse Transcription Polymerase Chain Reaction (RT-PCR) in that it measures DNA copy number variations rather than messenger RNA expression. It thus enables a measure of genomic instability and can calculate the percentage of genomic alteration (PGA) per tumour sample. Today CGH arrays are able to evaluate global copy number variations with as little as 100 ng of DNA [73]. This is highly relevant to localised prostate tumours treated with radiotherapy, not only because there is limited tissue available but also because progression of prostate cancer is known to be characterised by increased chromosomal and subchromosomal alterations characteristic of genomic instability [73]. Some of the earliest prognostic molecular biomarkers identified over two decades ago were based on detection of genomic instability in the form of polyploidy or nondiploidy assessed using flow cytometry and nuclear DNA content measured by static DNA cytometry [52, 53].

Using CGH, copy number loss of several novel biomarkers with diverse functions has been proposed, as well as further validation of previously identified candidates including PTEN [54] (Table 3). These include two genes involved in androgen synthesis, namely, androgen synthesis genes

steroidogenic acute regulatory protein (StAR) and hydroxysteroid (17-beta) dehydrogenase 2 HSD17B2 [57]. NKX3.1 is a tumour suppressor gene with a role in prostate stem cell maintenance. It interacts with topoisomerase I and is thought to facilitate recruitment of phosphorylated ATM and gamma H2AX to sites of DNA double strand breaks, both highly relevant to the DNA damage response [55]. NKX3.1 allelic loss alone independently predicted failure from image-guided radiotherapy (IGRT) in a model adjusting for relevant clinical parameters, androgen treatment, radiotherapy dose, and PGA [55]. When allelic gain in c-myc was combined with NKX3.1 loss, the combination showed further predictive capacity [55]. Nibrin (NBN), also known as Nijmegen Breakage Syndrome- (NBS-) 1, forms part of the MRN complex which is central to initiation of the DNA damage response (DDR). In a study of 6 important genes in the DDR (also including MRE11A, RAD50, ATM, ATR, and PRKDC) NBN gain was the only copy number variation significantly predicting biochemical recurrence after IGRT [56]. As it did not predict outcome after radical prostatectomy, NBN may have a role as a predictive biomarker guiding local treatment decisions.

3.4. RNA Expression Profiles. A number of RNA expression signatures have been proposed to risk-stratify in localised prostate cancer [74, 75]. The majority have not been evaluated in a radiotherapy cohort due to inadequate tissue quantity, although the oncotype DX for prostate has been tested on needle biopsy specimens [76]. The cell cycle progression score is a 31-gene signature based on RNA expression which was developed using quantitative RT-PCR [77]. The 31 genes were selected from a larger panel of 126 candidate genes known to be involved in cell cycle progression within the Gene Expression Omnibus database. The score includes genes with central roles in DNA repair such as RAD51. Initially developed using radical prostatectomy and TURP specimens [77], the signature has subsequently shown significant prediction of biochemical recurrence following image-guided radiotherapy on multivariate analysis that adjusted for known clinical predictive factors [58].

3.5. DNA Signatures. The first known DNA based signature to predict recurrence after EBRT has recently been reported [59] and was developed in a radiotherapy cohort by the use of a customised array to detect copy number alterations together with measurement of partial oxygen pressure using an intraglandular piezoelectrode. Four unique genomic subtypes were identified using unsupervised hierarchical clustering. Information on PGA and hypoxia was then integrated into the genomic subtypes. Finally, supervised machine learning was used to develop a 100-loci 276-gene DNA signature which was validated in a surgically treated cohort. The new signature outperformed a clinical model and 23 previously published RNA signatures in predicting biochemical relapse-free survival. Intriguingly several genes involved in lipid biology were included in the signature; the association of the local cholesterol metabolism of prostate tumours with disease progression has been demonstrated previously [78].

3.6. Next Generation Sequencing. Next generation sequencing (NGS) offers enormous potential for personalisation of treatment. It enables assessment of genomic events usually affecting more than 1 kbp such as structural copy number alterations and chromosomal rearrangements including translocations, inversions, and recombination events. In addition, the powerful resolution of NGS also enables detection of events affecting less than 1 kbp such as substitutions, insertions, and deletions [79]. To our knowledge, biomarker signatures using NGS predicting response to radiotherapy are not yet available, and limited tissue availability may be an explanation for this. However, this is likely to change soon with studies involving combined DNA, RNA, and epigenetic analyses ongoing as part of the International Cancer Genome Consortium and The Cancer Genome Atlas [59]. NGS technology continues to evolve rapidly and recently targeted DNA sequencing of prostate tumours using the Illumina platform has been possible with as little as 30 ng of DNA [80] and using the PGM Ion Torrent platform with as little as 6 ng [81].

4. Conclusion

Fundamental aspects of cancer biology including DNA repair and hypoxia are intimately related to the efficacy of radiotherapy. It is therefore not surprising that over recent decades a number of promising tissue biomarkers have been developed using a range of molecular techniques. Whilst the majority of biomarker candidates are protein markers developed using IHC, markers of genomic instability using more quantitative techniques have shown excellent prognostic capability. Validation of these biomarkers is a priority so that the added benefit to standard clinical parameters can be clearly quantified and existing inconsistencies resolved. Development of predictive biomarkers that differentiate benefit from different local treatments and active surveillance would further enhance personalised management of early prostate cancer. Challenges include the need for standardised reproducible protocols and antibodies for IHC, together with the technical limitations of using very small biopsies for genomic techniques. However, technology continues to advance rapidly and the potential for molecular biomarkers to improve prediction of both sides of the therapeutic ratio of radiotherapy for localised prostate cancer is hugely promising.

Conflict of Interests

The authors declare that there is no conflict of interests regarding the publication of this paper.

Acknowledgments

The authors acknowledge NHS funding to the NIHR Biomedical Research Centre at The Royal Marsden and The Institute of Cancer Research (ICR), London. Anna Wilkins is supported by a Cancer Research UK Ph.D. Training Fellowship at the CRUK Centre at The Institute of Cancer Research and The Royal Marsden; David Dearnaley is Joint Lead Applicant of

Cancer Research UK Programme Grant A19727 and Principal Investigator of CRUK (BIDD Project Award) A12518. Navita Somaiah has a Clinician Scientist Fellowship supported by ICR/CRUK funding.

References

[1] G. D. Grossfeld, D. M. Latini, D. P. Lubeck et al., "Predicting disease recurrence in intermediate and high-risk patients undergoing radical prostatectomy using percent positive biopsies: results from CaPSURE," *Urology*, vol. 59, no. 4, pp. 560–565, 2002.

[2] Z. S. Zumsteg, D. E. Spratt, I. Pei et al., "A new risk classification system for therapeutic decision making with intermediate-risk prostate cancer patients undergoing dose-escalated external-beam radiation therapy," *European Urology*, vol. 64, no. 6, pp. 895–902, 2013.

[3] C. West, B. S. Rosenstein, J. Alsner et al., "Establishment of a radiogenomics consortium," *International Journal of Radiation Oncology Biology Physics*, vol. 76, no. 5, pp. 1295–1296, 2010.

[4] D. T. Goodhead, "Energy deposition stochastics and track structure: what about the target?" *Radiation Protection Dosimetry*, vol. 122, no. 1–4, pp. 3–15, 2006.

[5] R. C. Taylor, S. P. Cullen, and S. J. Martin, "Apoptosis: controlled demolition at the cellular level," *Nature Reviews Molecular Cell Biology*, vol. 9, no. 3, pp. 231–241, 2008.

[6] K. Chu, N. Teele, M. W. Dewey, N. Albright, and W. C. Dewey, "Computerized video time lapse study of cell cycle delay and arrest, mitotic catastrophe, apoptosis and clonogenic survival in irradiated 14-3-3sigma and CDKN1A (p21) knockout cell lines," *Radiation Research*, vol. 162, no. 3, pp. 270–286, 2004.

[7] K. R. Luoto, R. Kumareswaran, and R. G. Bristow, "Tumor hypoxia as a driving force in genetic instability," *Genome Integrity*, vol. 4, no. 1, article 5, 2013.

[8] R. Bristow, A. Berlin, and A. Dal Pra, "An arranged marriage for precision medicine: hypoxia and genomic assays in localized prostate cancer radiotherapy," *The British Journal of Radiology*, vol. 87, no. 1035, 2014.

[9] D. J. Brenner and E. J. Hall, "Fractionation and protraction for radiotherapy of prostate carcinoma," *International Journal of Radiation Oncology, Biology, Physics*, vol. 43, no. 5, pp. 1095–1101, 1999.

[10] D. Dearnaley, I. Syndikus, G. Sumo et al., "Conventional versus hypofractionated high-dose intensity-modulated radiotherapy for prostate cancer: preliminary safety results from the CHHiP randomised controlled trial," *The Lancet Oncology*, vol. 13, no. 1, pp. 43–54, 2012.

[11] V. J. Gnanapragasam, "Molecular markers to guide primary radical treatment selection in localized prostate cancer," *Expert Review of Molecular Diagnostics*, vol. 14, no. 7, pp. 871–881, 2014.

[12] T. Sequeiros, M. García, M. Montes et al., "Molecular markers for prostate cancer in formalin-fixed paraffin-embedded tissues," *BioMed Research International*, vol. 2013, Article ID 283635, 15 pages, 2013.

[13] B. Zhang, J. Wang, X. Wang et al., "Proteogenomic characterization of human colon and rectal cancer," *Nature*, vol. 513, no. 7518, pp. 382–387, 2014.

[14] F. McCarthy, N. Dennis, P. Flohr, S. Jhavar, C. Parker, and C. S. Cooper, "High-density tissue microarrays from prostate needle biopsies," *Journal of Clinical Pathology*, vol. 64, no. 1, pp. 88–90, 2011.

[15] N. Kachroo, A. Y. Warren, and V. J. Gnanapragasam, "Multi-transcript profiling in archival diagnostic prostate cancer needle biopsies to evaluate biomarkers in non-surgically treated men," *BMC Cancer*, vol. 14, no. 1, article 673, 2014.

[16] A. D. Pra, E. Lalonde, J. Sykes et al., "TMPRSS2-ERG status is not prognostic following prostate cancer radiotherapy: implications for fusion status and DSB repair," *Clinical Cancer Research*, vol. 19, no. 18, pp. 5202–5209, 2013.

[17] L.-Y. Khor, K. Bae, R. Paulus et al., "MDM2 and Ki-67 predict for distant metastasis and mortality in men treated with radiotherapy and androgen deprivation for prostate cancer: RTOG 92-02," *Journal of Clinical Oncology*, vol. 27, no. 19, pp. 3177–3184, 2009.

[18] D. Cowen, P. Troncoso, V. S. Khoo et al., "Ki-67 staining is an independent correlate of biochemical failure in prostate cancer treated with radiotherapy," *Clinical Cancer Research*, vol. 8, no. 5, pp. 1148–1154, 2002.

[19] R. Li, K. Heydon, M. E. Hammond et al., "Ki-67 staining index predicts distant metastasis and survival in locally advanced prostate cancer treated with radiotherapy: an analysis of patients in Radiation Therapy Oncology Group Protocol 86-10," *Clinical Cancer Research*, vol. 10, no. 12, part 1, pp. 4118–4124, 2004.

[20] A. Pollack, M. Desilvio, L.-Y. Khor et al., "Ki-67 staining is a strong predictor of distant metastasis and mortality for men with prostate cancer treated with radiotherapy plus androgen deprivation: Radiation Therapy Oncology Group trial 92-02," *Journal of Clinical Oncology*, vol. 22, no. 11, pp. 2133–2140, 2004.

[21] B. Verhoven, Y. Yan, M. Ritter et al., "Ki-67 is an independent predictor of metastasis and cause-specific mortality for prostate cancer patients treated on Radiation Therapy Oncology Group (RTOG) 94-08," *International Journal of Radiation Oncology Biology Physics*, vol. 86, no. 2, pp. 317–323, 2013.

[22] R. Vergis, C. M. Corbishley, K. Thomas et al., "Expression of Bcl-2, p53, and MDM2 in localized prostate cancer with respect to the outcome of radical radiotherapy dose escalation," *International Journal of Radiation Oncology, Biology, Physics*, vol. 78, no. 1, pp. 35–41, 2010.

[23] D. S. Scherr, E. D. Vaughan Jr., J. Wei et al., "bcl-2 and p53 expression in clinically localized prostate cancer predicts response to external beam radiotherapy," *Journal of Urology*, vol. 162, no. 1, pp. 12–17, 1999.

[24] L.-Y. Khor, M. DeSilvio, T. Al-Saleem et al., "MDM2 as a predictor of prostate carcinoma outcome: an analysis of Radiation Therapy Oncology Group protocol 8610," *Cancer*, vol. 104, no. 5, pp. 962–967, 2005.

[25] D. J. Grignon, R. Caplan, F. H. Sarkar et al., "p53 status and prognosis of locally advanced prostatic adenocarcinoma: a study based on RTOG 8610," *Journal of the National Cancer Institute*, vol. 89, no. 2, pp. 158–165, 1997.

[26] M. Che, M. DeSilvio, A. Pollack et al., "Prognostic value of abnormal p53 expression in locally advanced prostate cancer treated with androgen deprivation and radiotherapy: a study based on RTOG 9202," *International Journal of Radiation Oncology Biology Physics*, vol. 69, no. 4, pp. 1117–1123, 2007.

[27] M. A. Ritter, K. W. Gilchrist, M. Voytovich, R. J. Chappell, and B. M. Verhoven, "The role of p53 in radiation therapy outcomes for favorable-to-intermediate-risk prostate cancer," *International Journal of Radiation Oncology, Biology, Physics*, vol. 53, no. 3, pp. 574–580, 2002.

[28] A. Chakravarti, K. Heydon, C. L. Wu et al., "Loss of p16 expression is of prognostic significance in locally advanced

prostate cancer: an analysis from the Radiation Therapy Oncology Group protocol 86-10," *Journal of Clinical Oncology*, vol. 21, no. 17, pp. 3328–3334, 2003.

[29] A. Chakravarti, M. DeSilvio, M. Zhang et al., "Prognostic value of p16 in locally advanced prostate cancer: a study based on Radiation Therapy Oncology Group protocol 9202," *Journal of Clinical Oncology*, vol. 25, no. 21, pp. 3082–3089, 2007.

[30] A. Kirschenbaum, X.-H. Liu, S. Yao, and A. C. Levine, "The role of cyclooxygenase-2 in prostate cancer," *Urology*, vol. 58, no. 2, supplement 1, pp. 127–131, 2001.

[31] Y.-M. Kim, Y. K. Shin, H. J. Jun, S. Y. Rha, and H. Pyo, "Systematic analyses of genes associated with radio sensitizing effect by celecoxib, a specific cyclooxygenase-2 inhibitor," *Journal of Radiation Research*, vol. 52, no. 6, pp. 752–765, 2011.

[32] L.-Y. Khor, K. Bae, A. Pollack et al., "COX-2 expression predicts prostate-cancer outcome: analysis of data from the RTOG 92-02 trial," *The Lancet Oncology*, vol. 8, no. 10, pp. 912–920, 2007.

[33] A. Pollack, J. J. Dignam, D. A. Diaz et al., "A tissue biomarker-based model that identifies patients with a high risk of distant metastasis and differential survival by length of androgen deprivation therapy in RTOG protocol 92-02," *Clinical Cancer Research*, vol. 20, no. 24, pp. 6379–6388, 2014.

[34] L. Pan, S. Baek, P. R. Edmonds et al., "Vascular endothelial growth factor (VEGF) expression in locally advanced prostate cancer: secondary analysis of Radiation Therapy Oncology Group (RTOG) 8610," *Radiation Oncology*, vol. 8, no. 1, article 100, 2013.

[35] R. Vergis, C. M. Corbishley, A. R. Norman et al., "Intrinsic markers of tumour hypoxia and angiogenesis in localised prostate cancer and outcome of radical treatment: a retrospective analysis of two randomised radiotherapy trials and one surgical cohort study," *The Lancet Oncology*, vol. 9, no. 4, pp. 342–351, 2008.

[36] M. M. L. Green, C. T. Hiley, J. H. Shanks et al., "Expression of vascular endothelial growth factor (VEGF) in locally invasive prostate cancer is prognostic for radiotherapy outcome," *International Journal of Radiation Oncology Biology Physics*, vol. 67, no. 1, pp. 84–90, 2007.

[37] M. I. Koukourakis, A. Giatromanolaki, M. Panteliadou et al., "Lactate dehydrogenase 5 isoenzyme overexpression defines resistance of prostate cancer to radiotherapy," *British Journal of Cancer*, vol. 110, no. 9, pp. 2217–2223, 2014.

[38] D. T. Denhardt and X. Guo, "Osteopontin: a protein with diverse functions," *The FASEB Journal*, vol. 7, no. 15, pp. 1475–1482, 1993.

[39] L.-Y. Khor, K. Bae, T. Al-Saleem et al., "Protein kinase A RI-α predicts for prostate cancer outcome: analysis of Radiation Therapy Oncology Group trial 86-10," *International Journal of Radiation Oncology, Biology, Physics*, vol. 71, no. 5, pp. 1309–1315, 2008.

[40] J. F. Torres-Roca, M. DeSilvio, L. B. Mora et al., "Activated STAT3 as a correlate of distant metastasis in prostate cancer: a secondary analysis of Radiation Therapy Oncology Group 86-10," *Urology*, vol. 69, no. 3, pp. 505–509, 2007.

[41] A. Fosså, W. Lilleby, S. D. Fosså, G. Gaudernack, G. Torlakovic, and A. Berner, "Independent prognostic significance of Her-2 oncoprotein expression in pN0 prostate cancer undergoing curative radiotherapy," *International Journal of Cancer*, vol. 99, no. 1, pp. 100–105, 2002.

[42] D. C. Weber, J.-C. Tille, C. Combescure et al., "The prognostic value of expression of HIF1α, EGFR and VEGF-A, in localized prostate cancer for intermediate- and high-risk patients treated with radiation therapy with or without androgen deprivation therapy," *Radiation Oncology*, vol. 7, no. 1, article 66, 2012.

[43] A. Pollack, D. Cowen, P. Troncoso et al., "Molecular markers of outcome after radiotherapy in patients with prostate carcinoma: Ki-67, bcl-2, bax, and bcl-x," *Cancer*, vol. 97, no. 7, pp. 1630–1638, 2003.

[44] L. Y. Khor, J. Moughan, T. Al-Saleem et al., "Bcl-2 and bax expression predict prostate cancer outcome in men treated with androgen deprivation and radiotherapy on Radiation Therapy Oncology Group protocol 92–02," *Clinical Cancer Research*, vol. 13, no. 12, pp. 3585–3590, 2007.

[45] P. Bouchaert, S. Guerif, C. Debiais, J. Irani, and G. Fromont, "DNA-PKcs expression predicts response to radiotherapy in prostate cancer," *International Journal of Radiation Oncology Biology Physics*, vol. 84, no. 5, pp. 1179–1185, 2012.

[46] J. W. Thoms, A. dal Pra, P. H. Anborgh et al., "Plasma osteopontin as a biomarker of prostate cancer aggression: relationship to risk category and treatment response," *British Journal of Cancer*, vol. 107, no. 5, pp. 840–846, 2012.

[47] A. X. Meng, F. Jalali, A. Cuddihy et al., "Hypoxia down-regulates DNA double strand break repair gene expression in prostate cancer cells," *Radiotherapy and Oncology*, vol. 76, no. 2, pp. 168–176, 2005.

[48] R. Kumareswaran, O. Ludkovski, A. Meng, J. Sykes, M. Pintilie, and R. G. Bristow, "Chronic hypoxia compromises repair of DNA double-strand breaks to drive genetic instability," *Journal of Cell Science*, vol. 125, no. 1, pp. 189–199, 2012.

[49] N. Chan, M. Koritzinsky, H. Zhao et al., "Chronic hypoxia decreases synthesis of homologous recombination proteins to offset chemoresistance and radioresistance," *Cancer Research*, vol. 68, no. 2, pp. 605–614, 2008.

[50] S. M. Falzarano, M. Zhou, P. Carver et al., "ERG gene rearrangement status in prostate cancer detected by immunohistochemistry," *Virchows Archiv*, vol. 459, no. 4, pp. 441–447, 2011.

[51] T. A. Swanson, S. A. Krueger, S. Galoforo et al., "TMPRSS2/ERG fusion gene expression alters chemo- and radio-responsiveness in cell culture models of androgen independent prostate cancer," *The Prostate*, vol. 71, no. 14, pp. 1548–1558, 2011.

[52] A. Pollack, G. K. Zagars, A. K. El-Naggar, M. D. Gauwitz, and N. H. A. Terry, "Near-diploidy: a new prognostic factor for clinically localized prostate cancer treated with external beam radiation therapy," *Cancer*, vol. 73, no. 7, pp. 1895–1903, 1994.

[53] J. Song, W. S. Cheng, R. E. Cupps, J. D. Earle, G. M. Farrow, and M. M. Lieber, "Nuclear deoxyribonucleic acid content measured by static cytometry: important prognostic association for patients with clinically localized prostate carcinoma treated by external beam radiotherapy," *The Journal of Urology*, vol. 147, no. 3, pp. 794–797, 1992.

[54] G. Zafarana, A. S. Ishkanian, C. A. Malloff et al., "Copy number alterations of c-MYC and PTEN are prognostic factors for relapse after prostate cancer radiotherapy," *Cancer*, vol. 118, no. 16, pp. 4053–4062, 2012.

[55] J. A. Locke, G. Zafarana, A. S. Ishkanian et al., "NKX3.1 haploinsufficiency is prognostic for prostate cancer relapse following surgery or image-guided radiotherapy," *Clinical Cancer Research*, vol. 18, no. 1, pp. 308–316, 2012.

[56] A. Berlin, E. Lalonde, J. Sykes et al., "NBN gain is predictive for adverse outcome following image-guided radiotherapy for localized prostate cancer," *Oncotarget*, vol. 5, no. 22, pp. 11081–11090, 2014.

[57] J. A. Locke, G. Zafarana, C. A. Malloff et al., "Allelic loss of the loci containing the androgen synthesis gene, StAR, is prognostic

for relapse in intermediate-risk prostate cancer," *The Prostate*, vol. 72, no. 12, pp. 1295–1305, 2012.

[58] S. J. Freedland, L. Gerber, J. Reid et al., "Prognostic utility of cell cycle progression score in men with prostate cancer after primary external beam radiation therapy," *International Journal of Radiation Oncology, Biology, Physics*, vol. 86, no. 5, pp. 848–853, 2013.

[59] E. Lalonde, A. S. Ishkanian, J. Sykes et al., "Tumour genomic and microenvironmental heterogeneity for integrated prediction of 5-year biochemical recurrence of prostate cancer: a retrospective cohort study," *The Lancet Oncology*, vol. 15, no. 13, pp. 1521–1532, 2014.

[60] L.-Y. Khor, M. Desilvio, R. Li et al., "Bcl-2 and bax expression and prostate cancer outcome in men treated with radiotherapy in Radiation Therapy Oncology Group protocol 86-10," *International Journal of Radiation Oncology Biology Physics*, vol. 66, no. 1, pp. 25–30, 2006.

[61] F. A. Stewart and A. van der Kogel, "Proliferative and cellular organization of normal tissues," in *Basic Clinical Radiobiology*, G. G. Steel, Ed., pp. 23–29, Arnold, London, UK, 2002.

[62] J. W. Hopewell, J. Nyman, and I. Turesson, "Time factor for acute tissue reactions following fractionated irradiation: a balance between repopulation and enhanced radiosensitivity," *International Journal of Radiation Biology*, vol. 79, no. 7, pp. 513–524, 2003.

[63] G. M. Morris and J. W. Hopewell, "Changes in the cell kinetics of pig epidermis after repeated daily doses of X rays," *British Journal of Radiology. Supplement*, vol. 19, pp. 34–38, 1986.

[64] I. Turesson and H. D. Thames, "Repair capacity and kinetics of human skin during fractionated radiotherapy: erythema, desquamation, and telangiectasia after 3 and 5 year's follow-up," *Radiotherapy and Oncology*, vol. 15, no. 2, pp. 169–188, 1989.

[65] J. Thacker and R. E. Wilkinson, "The genetic basis of cellular recovery from radiation damage: response of the radiosensitive irs lines to low-dose-rate irradiation," *Radiation Research*, vol. 144, no. 3, pp. 294–300, 1995.

[66] N. Somaiah, J. Yarnold, A. Lagerqvist, K. Rothkamm, and T. Helleday, "Homologous recombination mediates cellular resistance and fraction size sensitivity to radiation therapy," *Radiotherapy and Oncology*, vol. 108, no. 1, pp. 155–161, 2013.

[67] N. Somaiah, J. Yarnold, F. Daley et al., "The relationship between homologous recombination repair and the sensitivity of human epidermis to the size of daily doses over a 5-week course of breast radiotherapy," *Clinical Cancer Research*, vol. 18, no. 19, pp. 5479–5488, 2012.

[68] D. L. Rimm, "What brown cannot do for you," *Nature Biotechnology*, vol. 24, no. 8, pp. 914–916, 2006.

[69] D. Trudel, G. Zafarana, J. Sykes, C. L. Have, R. G. Bristow, and T. van der Kwast, "4FISH-IF, a four-color dual-gene FISH combined with p63 immunofluorescence to evaluate NKX3.1 and MYC status in prostate cancer," *The Journal of Histochemistry and Cytochemistry*, vol. 61, no. 7, pp. 500–509, 2013.

[70] A. Bylund, P. Stattin, A. Widmark, and A. Bergh, "Predictive value of bcl-2 immunoreactivity in prostate cancer patients treated with radiotherapy," *Radiotherapy and Oncology*, vol. 49, no. 2, pp. 143–148, 1998.

[71] M. Abdel-Wahab, B. A. Berkey, A. Krishan et al., "Influence of number of CAG repeats on local control in the RTOG 86-10 protocol," *American Journal of Clinical Oncology*, vol. 29, no. 1, pp. 14–20, 2006.

[72] M. Roach III, M. De Silvio, T. Rebbick et al., "Racial differences in CYP3A4 genotype and survival among men treated on Radiation Therapy Oncology Group (RTOG) 9202: a phase III randomized trial," *International Journal of Radiation Oncology, Biology, Physics*, vol. 69, no. 1, pp. 79–87, 2007.

[73] A. S. Ishkanian, G. Zafarana, J. Thoms, and R. G. Bristow, "Array CGH as a potential predictor of radiocurability in intermediate risk prostate cancer," *Acta Oncologica*, vol. 49, no. 7, pp. 888–894, 2010.

[74] N. Erho, A. Crisan, I. A. Vergara et al., "Discovery and validation of a prostate cancer genomic classifier that predicts early metastasis following radical prostatectomy," *PLoS ONE*, vol. 8, no. 6, Article ID e66855, 2013.

[75] C.-L. Wu, B. E. Schroeder, X.-J. Ma et al., "Development and validation of a 32-gene prognostic index for prostate cancer progression," *Proceedings of the National Academy of Sciences of the United States of America*, vol. 110, no. 15, pp. 6121–6126, 2013.

[76] D. Knezevic, A. D. Goddard, N. Natraj et al., "Analytical validation of the Oncotype DX prostate cancer assay—a clinical RT-PCR assay optimized for prostate needle biopsies," *BMC Genomics*, vol. 14, article 690, 2013.

[77] J. Cuzick, G. P. Swanson, G. Fisher et al., "Prognostic value of an RNA expression signature derived from cell cycle proliferation genes in patients with prostate cancer: a retrospective study," *The Lancet Oncology*, vol. 12, no. 3, pp. 245–255, 2011.

[78] S. Yue, J. Li, S. Lee et al., "Cholesteryl ester accumulation induced by PTEN loss and PI3K/AKT activation underlies human prostate cancer aggressiveness," *Cell Metabolism*, vol. 19, no. 3, pp. 393–406, 2014.

[79] J. A. Watkins, S. Irshad, A. Grigoriadis, and A. N. J. Tutt, "Genomic scars as biomarkers of homologous recombination deficiency and drug response in breast and ovarian cancers," *Breast Cancer Research*, vol. 16, no. 3, article 211, 2014.

[80] D. Manson-Bahr, R. Ball, G. Gundem et al., "Mutation detection in formalin-fixed prostate cancer biopsies taken at the time of diagnosis using next-generation DNA sequencing," *Journal of Clinical Pathology*, vol. 68, no. 3, pp. 212–217, 2015.

[81] S. Carreira, A. Romanel, J. Goodall et al., "Tumor clone dynamics in lethal prostate cancer," *Science Translational Medicine*, vol. 6, no. 254, Article ID 254ra125, 2014.

Hindawi Publishing Corporation
BioMed Research International
Volume 2015, Article ID 186904, 10 pages
http://dx.doi.org/10.1155/2015/186904

Review Article

MicroRNAs as Important Players and Biomarkers in Oral Carcinogenesis

Anjie Min,[1] Chao Zhu,[1,2] Shuping Peng,[3] Saroj Rajthala,[4,5] Daniela Elena Costea,[4,5,6] and Dipak Sapkota[4,5,7]

[1]*Department of Oral and Maxillofacial Surgery, Xiangya Hospital, Central South University, Changsha, China*
[2]*School of Stomatology, Central South University, Changsha, China*
[3]*Cancer Research Institute, Central South University, Changsha, China*
[4]*The Gade Laboratory for Pathology, Department of Clinical Medicine, Faculty of Medicine and Dentistry, University of Bergen, 5021 Bergen, Norway*
[5]*Centre for Cancer Biomarkers (CCBIO), Faculty of Medicine and Dentistry, University of Bergen, 5021 Bergen, Norway*
[6]*Department of Pathology, Haukeland University Hospital, 5021 Bergen, Norway*
[7]*Department of Oncology and Medical Physics, Haukeland University Hospital, 5021 Bergen, Norway*

Correspondence should be addressed to Dipak Sapkota; dipak.sapkota@k1.uib.no

Received 6 February 2015; Revised 14 May 2015; Accepted 18 May 2015

Academic Editor: David Pauza

Oral cancer, represented mainly by oral squamous cell carcinoma (OSCC), is the eighth most common type of human cancer worldwide. The number of new OSCC cases is increasing worldwide, especially in the low-income countries, and the prognosis remains poor in spite of recent advances in the diagnostic and therapeutic modalities. MicroRNAs (miRNAs), 18–25 nucleotides long noncoding RNA molecules, have recently gained significant attention as potential regulators and biomarkers for carcinogenesis. Recent data show that several miRNAs are deregulated in OSCC, and they have either a tumor suppressive or an oncogenic role in oral carcinogenesis. This review summarizes current knowledge on the role of miRNAs as tumor promotors or tumor suppressors in OSCC development and discusses their potential value as diagnostic and prognostic markers in OSCC.

1. Introduction

Head and neck squamous cell carcinoma (HNSCC) consists of a heterogeneous group of malignancies arising from oral cavity, nasal cavity, paranasal sinuses, pharynx, larynx, and salivary glands. Oral cancer, represented mainly by oral squamous cell carcinoma (OSCC), is the most common type of HNSCC. OSCC is the eighth most common cancer worldwide accounting for more than 300,000 new cases and 145,000 deaths in 2012 [1]. Usually, OSCC detection depends on the clinical examination of oral cavity, followed by a biopsy for histological analysis. However, despite the easy access for visual examination, OSCC is often detected at advanced stages leading to severely reduced patient survival. In spite of the recent advances in diagnosis and treatment modalities, less than 50% of OSCC patients survive for 5 years [2]. Late diagnosis, regional lymph node metastasis, and recurrences are the major causes related to the poor prognosis and reduced survival for OSCC patients [3, 4]. Thus, reliable molecular markers that can (i) provide earlier and more precise OSCC diagnosis, (ii) predict prognosis, and (ii) assign patients to the best-targeted treatment available are urgently needed.

For almost three to four decades, changes in protein coding tumor suppressor genes and/or oncogenes have been thought to be the main drivers of tumor development [5, 6]. However, the recent discovery of thousands of genes that transcribe noncoding RNAs (including miRNAs) makes it obvious that cancer biology is even more complex than initially expected. Several layers of molecular regulators (e.g., mRNA, miRNA, and protein) are involved in the development and maintenance of cancerous phenotypes.

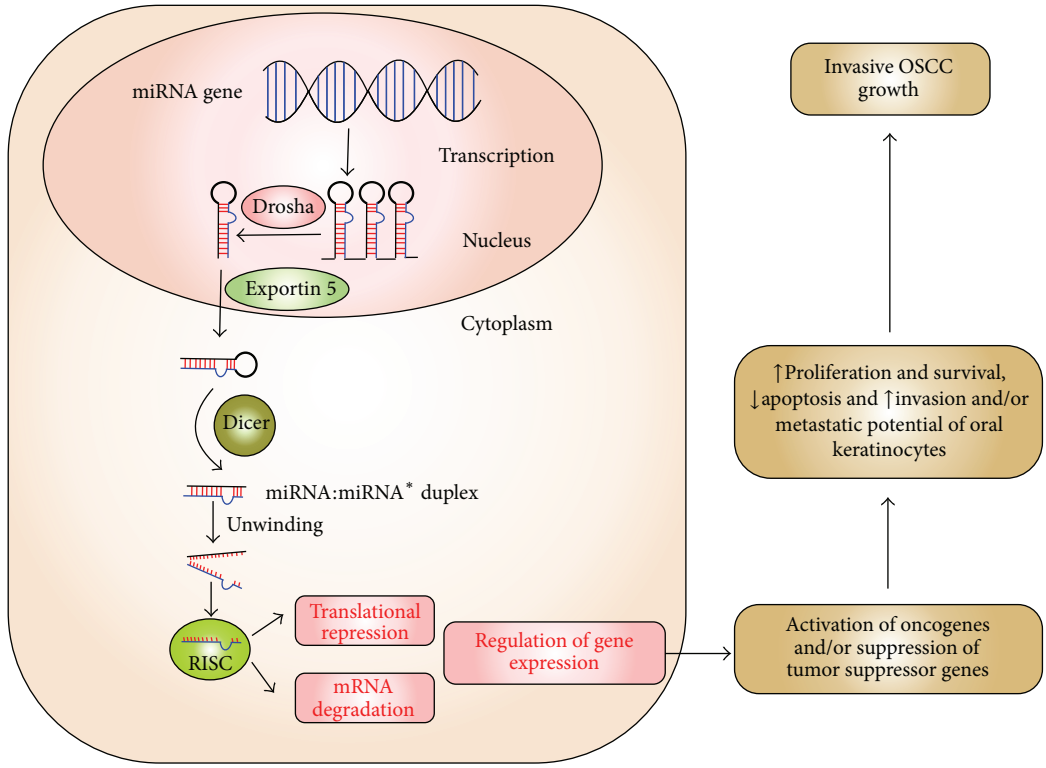

Figure 1: Schematic illustration demonstrating biogenesis and function of miRNA. miRNA genes are transcribed into primary miRNA (pri-miRNA) by RNA polymerase III. These miRNAs are further converted into second precursors (pre-miRNA) by Drosha and are exported into cytoplasm by Exportin 5. Additional processing by Dicer produces miRNA:miRNA* duplex. Only one strand of miRNA:miRNA* duplex is preferentially assembled into the RNA-induced silencing complex (RISC). RISC acts on target mRNA(s) and leads to either translational repression or mRNA cleavage. Suppression of tumor suppressive genes and/or activation of oncogenes by miRNA lead to excessive cell proliferation and survival, increased antiapoptosis, and enhanced invasive and metastatic potential of oral keratinocytes, resulting into invasive cancerous growth.

Among them, miRNAs, 18–25 nucleotides long, noncoding RNA molecules [7–9], have recently gained significant attention as potential regulators and biomarkers for human carcinogenesis. At the molecular level, miRNA binds to 3′-untranslated region (3′-UTR) of target mRNA(s) and suppresses its expression by either translational repression or mRNA cleavage [10] (Figure 1). A single miRNA can regulate expression and/or function of hundreds of target mRNAs and proteins and regulates several biological processes (e.g., cell proliferation, differentiation, migration, apoptosis, and signal transduction) important for cancer development [8, 11–13] (Figure 1).

Many recent studies have shown deregulated expression of miRNAs in OSCC and OSCC-derived cell-lines compared to their normal counterparts, indicating their potential role in oral cancer development. Accordingly, several miRNAs have been shown to function either as tumor suppressors or as tumor promoters in OSCCs (reviewed in [14, 15]). In addition to their key biological functions in OSCC tumorigenesis, expression levels of several of miRNAs have been shown to correlate with clinicopathological variables [16] and to have a diagnostic and prognostic value in OSCC [15, 17]. For these reasons, miRNA has been a hot topic in cancer research for the last few years and several studies about miRNAs in OSCC have been published recently, as summarized in Table 1. The current review aims to highlight the oncogenic and tumor suppressive roles of miRNAs in OSCC development and discusses their potential value as diagnostic and prognostic markers for OSCC management.

2. Methods

Literature search was performed by using the PubMed database. Following key words were used for the literature search: "oral cancer and miRNA," "oral cancer and microRNA," "oral squamous cell carcinoma and miRNA," and "oral squamous cell carcinoma and microRNA." Exclusion criteria were articles not related to OSCC/HNSCC and/or miRNA, purely descriptive articles, articles lacking clinical pathological correlation, and/or articles for which full texts were not available in English. Only clinically relevant articles published within April 2015 were included in this review. Additionally, individual articles retrieved manually from the reference list of the relevant papers were also included.

3. miRNAs as Oncogenes in OSCC

A number of miRNAs have been shown to be upregulated in OSCC and to function as oncogenes. A well-studied

Table 1: Summary of miRNAs and associated signal pathways/target genes in OSCC/HNSCC.

miRNA	Up/downregulation	Target genes/associated pathways	Ref.
miR-21	Up	PDCD4	[23]
		TPMI	[16]
		RECK	[26]
		CLU	[22]
		DKK2-Wnt/β-catenin	[18]
		Smad7-TGFβ1	[27]
		HA/CD44-Nanog/Stat3-PDCD4, IAPs	[24]
miR-31	Up	FIH-HIF-EVGF	[28]
miR-31*	Up	FGF3	[29]
		RhoA	[32]
miR-134	Up	WWOX	[36]
miR-146a	Up	IRK1, TRAF6, and NUMB	[33]
miR-155	Up	CDC73	[39]
miR-7	Up	RECK	[26]
		IGF1R-Akt	[45]
miR-9	Down	CXCR4-Wnt/β-catenin	[50]
miR-17/20a	Down	ITGβ8	[60]
miR-29a	Down	MMP2	[57]
miR-34	Down	E2F3, survivin, and VEGF	[64]
		SIRT6	[89]
miR-99a	Down	IGF1R	[46]
miR-124	Down	ITGB1	[58]
miR-125b	Down	ICAM2	[65]
miR-138	Down	FOSL1	[52]
		VIM, ZEB2, EZH2	[53]
		RhoC, and RoCK2	[54]
miR-140-5p	Down	ADAM10, ERBB4, PAX6, and LAMC1	[90]
miR-145	Down	c-Myc, Cdk6	[67]
miR-181a	Down	K-ras	[91]
		Twist1	[56]
miR-205	Down	IL-24, caspase-3/-7,	[92]
		and Axin-2	[93]
miR-218	Down	mTOR-Rictor-Akt	[48]
miR-320	Down	HIF-1α-NRP1-VEGF	[41]
miR-357	Down	CIP2A-MYC	[61]
		AEG-1/MTDH	[62]
miR-419-5p	Down	GIT1	[59]
		EGFR-ERK1/2-MMP2/9	
miR-483-3p	—	API5, BRIC5, and RAN	[94]
miR-196a	Up	MAMDC2	[95]
miR-26a/b	Down	TMEM184B	[96]

miRNA, the miR-21, has been shown to be overexpressed and to regulate several biological functions in OSCC [16, 18–20]. Overexpression of miR-21 has also been observed in oral premalignant lesions (oral leukoplakia) compared to normal oral mucosa, indicating that alteration in miR-21 could be an earlier event in OSCC progression [21]. A number of *in vitro* and *in vivo* experimental data have demonstrated an oncogenic role of miR-21 in OSCC by promoting cell proliferation [22], invasion [18, 23], antiapoptosis [16], and chemoresistance [24]. These oncogenic functions were shown to be regulated by miR-21-mediated downregulation of several established tumor suppressor molecules, including PTEN [25], programmed cell death 4 (PDCD4) [23], tropomyosin [16], reversion-inducing cysteine-rich protein with kazal motifs (RECK) [26], and dickkopf 2 (DKK2) [18]. In addition to the functional roles in OSCC cells, a growing

body of evidence suggests that miR-21 might be important in the regulation of carcinoma associated fibroblasts (CAFs) induction and their activity [20, 27]. miR-21 was shown to be predominately localized in OSCC stroma and colocalized with α-smooth muscle actin positive CAFs. Additionally, higher stromal expression of miR-21 was associated with poor prognosis in OSCC [20].

miR-31 and its passenger strand miRNA (miR-31*) have been shown to be upregulated in oral leukoplakia (OLP) and OSCC and to have an oncogenic role in OSCC tumorigenesis [28–31]. Liu et al. demonstrated that ectopic expression of miR-31 repressed its target factor-inhibiting hypoxia-inducible factor (FIH) expression to activate hypoxia-inducible factor (HIF) under normoxic conditions, both *in vitro* and *in vivo*. Additionally, miR-31-FIH-HIF-VEGF regulatory cascade was found to affect several biological processes such as cell proliferation, migration, and epithelial-mesenchymal transition (EMT) in OSCC cells [28]. Moreover, miR-31 was shown to collaborate with human telomerase reverse transcriptase (hTERT) to immortalize normal oral keratinocytes (NOKs), indicating that it might contribute to early stage oral carcinogenesis [31]. Similarly, miR-31* regulated apoptosis, cell proliferation, migration, and invasion in OSCC cells [29]. These miR-31* regulated functional effects were mediated by the regulation of fibroblast growth factor 3 (FGF3) [29] and RhoA [32] expression levels.

miR-146a has been demonstrated to be overexpressed in OSCC and to enhance OSCC tumorigenesis both in the *in vitro* and *in vivo* mouse xenograft model [33, 34]. The oncogenic functions of miR-146a were found to be associated with concomitant downregulation of IL-1 receptor-associated kinase 1 (IRAK1), TNF receptor-associated factor 6 (TRAF6), and NUMB [33]. A previous study from the same group suggested an association between a higher OSCC miR-146a expression and nodal involvement in patients carrying C polymorphism (rs2910164) [34]. However, findings from Palmieri et al. indicated that the rs2910164 polymorphism is not associated with OSCC progression [35]. Further investigations are needed to clarify a possible role of the variant allele or rs2910164 in OSCC progression.

miR-134 expression was upregulated in HNSCC tissue specimens and cells (HSC-3, OECM-1, and SAS cell-lines) compared to the corresponding normal controls. Functional analysis revealed that miR-134 expression enhanced the oncogenicity of HNSCC cells *in vitro* as well as tumor growth and metastasis of HNSCC cells *in vivo* via targeting WW domain-containing oxidoreductase (WWOX) [36]. In another study, miR-155 was found to be overexpressed in OSCC cells and tissues compared to the controls [37, 38]. Oncogenic effects of miR-155 were suggested to be due to downregulation of a tumor suppressor CDC73 in OSCC [39]. Similarly, miR-27a was shown to downregulate expression of and to inhibit tumor suppressor function of microcephalin 1 (MCPH1) in OSCC cells [40].

4. miRNAs as Tumor Suppressors in OSCC

Several miRNAs have been shown to be downregulated in OSCC. Accordingly, functional studies have demonstrated tumor suppressive roles for these miRNAs in OSCC tumorigenesis. miR-320 was downregulated in OSCC-derived cell-lines and tissue specimens, with its expression correlating inversely with the vascularity. Hypoxia suppressed miR-320 expression through HIF-1α and increased the expression of neuropilin 1 (NRP1) and promoted the motility and tube formation ability of endothelial cells via vascular endothelial growth factor (VEGF) signaling pathway, resulting in tumor angiogenesis [41].

The function of miR-7 has been characterized as a tumor suppressor in several human cancers, including glioblastoma, breast cancer, and OSCC among others. A number of protooncogenes were experimentally confirmed as its target genes, including insulin receptor substrate 1 (IRS1), insulin receptor substrate 2 (IRS2), epidermal growth factor receptor (EGFR), v-raf-1 murine leukaemia viral oncogene homologue 1 (RAF1), and p21/CDC42/RAC1-activated kinase 1 (PAK1) [42–44]. Jiang et al. showed that miR-7 regulated IGF1R/IRS/PI3K/Akt signaling pathway by posttranscriptional regulation of insulin-like growth factor 1 receptor (IGF1R) in cells derived from tongue squamous cell carcinoma (TSCC, the most common subtype of OSCC) cells [45]. Similarly, studies have demonstrated that IGF1R and mammalian target of rapamycin (mTOR), components of IGF1R signaling pathway, are target genes of another tumor suppressor miRNA, the miR-99a [46, 47]. Downregulation of miR-99a was observed in OSCC patient specimens and cell-lines [46, 47], especially in OSCC patients with lymphovascular invasion [46], suggesting a role for miR-99a in lymphovascular invasion. In addition, miR-99a induced apoptosis and inhibited OSCC cell proliferation, migration, and invasion *in vitro* as well as lung colonization *in vivo* [46, 47].

miR-218 has been shown to be epigenetically (DNA hypermethylation) silenced in OSCC tissue specimens and to have a tumor suppressive function by regulating the expression of rapamycin-insensitive component of mTOR, Rictor [48]. DNA hypermethylation has been suggested as one of the mechanisms for the downregulation of miR-9 in OSCC and oropharyngeal carcinoma [49]. Lentivirus-mediated miR-9 overexpression in highly aggressive tumor cells led to significant inhibition of proliferation *in vitro* and *in vivo*. These tumor suppressive functions were suggested to be mediated via targeting CXC chemokine receptor 4 (CXCR4) gene and Wnt/β-catenin signaling pathway [50].

Accumulating evidence suggests a critical role for EMT in tumor progression, invasion, and metastasis and acquisition of stem-like phenotype [51]. Findings from a number of studies point towards a role of miRNAs in the regulation of EMT and EMT-related malignant phenotypes in OSCC cells. Different studies have shown a role for miR-138 in the suppression of EMT, cell proliferation, migration, and invasion in HNSCC-derived cells. At the molecular level, miR-138 regulated the expression of key EMT-related molecules like Fos-like antigen 1 (FOSL1), vimentin (VIM), zinc finger E-box-binding homeobox 2 (ZEB2), enhancer of zeste homologue 2 (EZH2), RhoC, and ROCK2 [52–54]. Furthermore, miR-138 was suggested to suppress the expression of prometastatic RhoC and other downstream signaling molecules FAK, Src,

and Erk1/2 in HNSCC-derived cells [55]. Likewise, miR-181a was shown to inhibit Twist1 mediated EMT, metastatic potential and cisplatin induced chemoresistance in TSCC cells [56].

Recent studies have shown that miRNAs play a crucial role in the regulation of extracellular matrix (ECM) components, such as matrix metalloproteinases (MMPs) and integrins. Lu and coworkers reported that miR-29a was underexpressed in OSCC tissues and inhibited the expression of MMP2 by directly binding to the MMP2 3′-UTR. Functionally, miR-29a inhibited invasion and antiapoptosis of OSCC-derived cells [57]. Further functional studies revealed that transfection with miRNA-29a mimics attenuated invasive potential, increased apoptosis rate, and enhanced chemosensitivity of OSCC cell-lines to cis-platinum (CDDP) [57]. miR-124 was found to be downregulated in OSCC and its forced expression suppressed OSCC cell migration and invasion through downregulation of ITGB1 expression [58]. Furthermore, miR-491-5p was shown to suppress invasion and metastatic potential of OSCC cells *in vitro* and *in vivo* by targeting the expression of G-protein-coupled receptor kinase-interacting protein 1 (GIT1), which further regulated the expression of focal adhesions, steady-state levels of paxillin, phospho-paxillin, phospho-FAK, EGF/EGFR-mediated extracellular signal-regulated kinase (ERK1/2) activation, and MMP2/9 levels and activities [59].

A miRNA cluster, miR-17-92, including miR-17, miR-19b, miR-20a, and miR-92a, was found to be significantly downregulated in a more migratory OSCC-derived TW2.6 MS-10 cells as compared to the less migratory TW2.6 cells. Overexpression of this cluster was found to decrease the migratory ability of OSCC cell-lines. Through a bioinformatics screening analysis and 3′-UTR reporter assay, integrin (ITG) β8 was identified to be a direct target of miR-17/20a in OSCC cells [60]. Likewise, miR-375 was shown to be downregulated in HNSCC and to function as a tumor suppressor by regulating the expression of AEG-1/MTDH, CIP2A (cancerous inhibitor of protein phosphatase 2A). Transient transfection of miR-375 in HNSCC-derived cells reduced the expression of CIP2A (cancerous inhibitor of protein phosphatase 2A) [61, 62]. Furthermore, miR375 sensitized TNF-α-induced apoptosis probably through inhibiting NF-κB activation *in vitro* [63]. Previous studies have suggested miR-34a, which was frequently downregulated in a number of tumor types, to function as a tumor suppressor. Ectopic expression of miR-34a suppressed proliferation and colony formation of HNSCC cells by downregulation of E2F transcription factor 3 (E2F3) and survivin in the *in vitro* and *in vivo* models [64]. miR-34a further led to the inhibition of tumor angiogenesis by blocking VEGF production as well as by directly inhibiting endothelial cell functions [64]. miR-125b, another downregulated miRNA in OSCC, was able to inhibit proliferation rate and to enhance radiosensitivity to X-ray irradiation via downregulation of ICAM2 mRNA expression in OSCC-derived cells [65]. Likewise, miR-145 was found to be frequently downregulated in OSCCs [66] and to inhibit OSCC cell proliferation and colony formation [67].

5. Diagnostic and Prognostic Value of miRNAs in OSCC

Distinct expression profile of miRNA in OSCC and oral prelalignant tissue specimens compared to the normal controls offers the use of specific miRNA(s) signature for early stage diagnosis and prediction of OSCC prognosis [16, 17]. In addition, miRNAs possess the following unique properties which make them attractive diagnostic and prognostic tool in OSCC. Firstly, they are abundantly expressed in OSCC and control tissues and hence their isolation and quantification are convenient and reproducible. Secondly, several OSCC-related miRNAs are secreted in bodily fluids such as serum, plasma, and saliva [68] making them very useful for noninvasive clinical application. Candidate miRNAs reported to be relevant for OSCC diagnostics and prognosis are summarized in Table 2.

5.1. miRNA as Diagnostic Biomarkers. The use of a specific miRNA signature as a diagnostic tool in OSCC has been suggested by a number of recent studies. miR-16 and let-7b were highly upregulated in sera from patients with OSCC and oral carcinoma *in situ*, while miR-338-3p, miR-223, and miR-29a were highly downregulated as compared to the matched controls. ROC analysis indicated that the signature of five miRNAs (miR-16, let-7b, miR-338-3p, miR-223, and miR-29a) might be useful as a biomarker for oral cancer detection (AUC > 0.8) [69]. Lin et al. showed that the plasma levels of miR-24 in OSCC patients were significantly higher than in the control individuals [70]. Likewise, the elevated plasma levels of miR-21 and miR-146a were suggested to have a diagnostic value in OSCC [33, 71]. Expression level of miR-31 in saliva was found to be significantly increased in patients with OSCC of all clinical stages as compared to that of the healthy controls. The high salivary level was significantly reduced after excision of OSCC lesion, indicating that the main contributor for miR-31 upregulation was OSCC lesion [72]. In addition, increased expression of miR-27b in saliva of OSCC patients was suggested as a valuable biomarker to identify OSCC patients by ROC curve analyses [73]. However, another study showed a downregulated expression of miR-27b in both the tumor tissues and the plasma of OSCC patients [74]. Further research is therefore required to validate the above findings and elucidate the molecular mechanism of different levels of miR-27b in saliva and plasma in OSCC.

In addition to their potential use in OSCC diagnosis, several miRNAs were suggested to be important in the earlier diagnosis and prediction of malignant transformation of oral premalignant lesions/conditions. Dang et al. showed a significantly higher methylation frequency of miR-137 promotor in patients with oral lichen planus (35%) and OSCC (58.3%) as compared to the absence of methylation in normal controls, suggesting that the methylation status of miR-137 might be a valuable biomarker in the prediction of malignant transformation of OLP [75]. In saliva, significantly different expressions of miR-10b, miR-145, miR-99b, miR-708, and miR-181c were observed in progressive low grade dysplasia

Table 2: miRNA deregulation and relevance to OSCC diagnosis and prognosis.

miRNA(s)	Source	Up/downregulation (OSCC versus normal control)	Diagnostic/prognostic relevance	Ref.
miR-16, Let-7b	Serum	Up	Yes/ND	[69][a]
miR-223, miR-29a, and miR-338-3p	Serum	Down		
miR-24	Plasma	Up	Yes/ND	[70]
miR-146a	Tissue/plasma	Up	Yes/ND	[33]
miR-21	Tissue	Up	Yes/ND	[71][b]
	Plasma	Up	Yes/yes	
	Tissue	Up	ND/yes	[16][c]
	Tissue	Up	ND/yes	[26]
	Tissue	Up	Yes/yes	[17, 80][b]
	Tissue	Up	ND/yes	[20][d]
miR-31	Saliva	Up	Yes/ND	[72]
miR-27b	Saliva	Up	Yes/ND	[73]
miR-125b	Tissue	Down	ND/yes	[65]
miR-491-5p	Tissue	Down	ND/yes	[59]
miR-181	Plasma/tissue	Up	Yes/yes	[77]
miR-375	Tissue	Down	ND/yes	[78][b]
miR-205 and Let-7d	Tissue	Down	ND/yes	[79][b]
miR-155	Tissue	Up	ND/yes	[38]
	Tissue	Up	Yes/yes	[37]
miR-21-3p miR-141-3p miR-96-5p miR-130b-3p	Tissue	Up	ND/yes	[97]
miR-196a/b	Tissue	Up	Yes/yes	[98]
miR-196a	Plasma	Up	Yes/yes	
miR-211	Tissue	Down	ND/yes	[99]

[a]OSCC group also consists of lesions with carcinoma *in situ*; [b]HNSCC specimens; [c]TSCC; [d]expression examined in the tumor stroma; Ref.: references; ND: not determined.

(LGD) as compared to nonprogressive LGD leukoplakia patients [76].

5.2. miRNA as Prognostic Biomarkers. The expression patterns of certain miRNAs have been found to correlate with clinical stage, lymph node metastasis, and patient survival, indicating that these miRNAs can act as prognostic predictors in OSCC. Higher expression levels of miR-21 in TSCC correlated with advanced clinical stage, poor differentiation, and lymph node metastasis [16]. Moreover, multivariate analysis showed that expression level of miR-21 could be used as an independent prognostic factor for TSCC patients' survival [16]. Similarly, prognostic value of miR-21 in OSCC/HNSCC was reported in another study [26]. miR-31, miR-17/20a, miR-125b, miR-155, miR-181, miR-375 and miR-491-5p, miR-205, and miR-let7d were found to be associated with lymph node metastasis and poor OSCC patient survival [38, 59, 60, 65, 72, 77–80].

5.3. miRNA as Target for OSCC Therapy. The ability to manipulate miRNAs expression and function by local and systemic delivery of miRNA inhibitors (anti-miRNA oligonucleotides or miRNA sponges [81, 82]) or miRNA mimics [82] has recently gained immense interest as novel therapeutic approach. This treatment approach came into light after the first successful anti-miRNA oligonucleotides based human clinical trial in 2011 for the treatment of hepatitis C virus infection (reviewed in [83]). Recent identification of key miRNAs with either oncogenic or tumor suppressive functions in OSCC has opened up new possibilities for miRNA based OSCC therapy. The advantage of miRNA based cancer therapy lies in the ability of miRNAs to concurrently target multiple effectors of pathways involved in cell proliferation, differentiation, and survival [82]. Accordingly, several *in vitro* and *in vivo* studies, employing strategies to suppress the function of oncogenic miRNA and/or restore the tumor suppressive miRNAs, have reported significant inhibition of aggressive OSCC phenotypes. For example, inhibiting miR-21

by anti-miRNA oligonucleotides has been shown to inhibit survival, anchorage-independent growth [16], and invasion [18] of OSCC cells. Likewise, restoration of miR-99a level by miR mimic transfection markedly suppressed proliferation and induced apoptosis of TSCC cells [47].

Resistance to chemotherapy and resistance to radiotherapy are major challenges in the management of OSCC patients as significantly high proportions of OSCC lesions fail to respond to these treatment modalities. Recent studies have linked resistance to chemotherapy and radiotherapy in OSCC to altered miRNA expression and function. Dai et al. have correlated a miRNA signature (downregulation of miR-100, miR-130a, and miR-197 and upregulation of miR-181b, miR-181d, miR-101, and miR-195) in HNSCC cells with multiple drug resistance phenotypes *in vitro* [84]. In another study, low expression of miR-200b and miR-15b in TSCC was associated with chemotherapeutic resistance and poor patient prognosis [85]. Similarly, higher expression of miR-196a was reported to be associated with recurrent disease and resistance to radiotherapy in HNSCC [86]. The miRNA signature(s) related to therapeutic resistance has also been used experimentally to revert the resistance phenotypes. For example, inhibition of miR-21 by anti-miRNA oligonucleotides has been shown to inhibit chemoresistance in OSCC cells [24, 87]. Likewise, forced expression of miR-125b has been reported to enhance radiosensitivity in OSCC cells [65]. Recently, nanoparticle based delivery of miRNAs was suggested as a promising approach in the treatment of HNSCC [88]. Despite these promising results, more in-depth studies are necessary to better understand the effective delivery system for optimal uptake and to minimize degradation of miRNA based drugs in the *in vivo* situation.

6. Conclusions

Alteration in the expression pattern of miRNA is a common finding in OSCC tumorigenesis. Several altered miRNAs seem to play critical roles in the initiation and progression of OSCC by functioning either as oncogenes or as tumor suppressors. Specific miRNA signatures identified from tumor specimens, serum/plasma, or saliva from OSCC patients have a potential to be clinically useful in the diagnosis, prognosis, and therapeutic targets in OSCC. Nevertheless, it will be a big challenge ahead to translate these promising findings to clinic before the following issues will be fully addressed. Firstly, findings from several studies are based on limited number of patient materials from different sublocations of oral cavity, which lead to more heterogeneous data and reduced statistical power. Additionally, use of different expression profiling platforms (such as microarray or PCR) with different normalizing strategies leads to inconsistent miRNA expression results. Hence, a comprehensive miRNA profiling including larger number of paired tissue specimens of oral premalignant lesions/conditions, primary OSCC, and metastasis will enable us to identify miRNAs involved in stepwise tumorigenesis and metastatic process of OSCC. The identified miRNAs will pave the way for their future clinical use in the diagnosis, prognosis and therapy of OSCC.

Conflict of Interests

The authors declare that there is no conflict of interests regarding the publication of this paper.

Acknowledgments

The authors would like to thank Professor Anne Christine Johannessen for her assistance during the revision process of this paper. This work was supported by the Grants from National Natural Science Foundation for young scholar of China (no. 81102045), Clinical Key Subject Foundation of Health Ministry of China, Bergen Medical Research Foundation (2010/2011, DEC), The Western Norway Regional Health Authority, Norway (no. 911902), and University of Bergen (postdoctoral fund, DS).

References

[1] J. Ferlay, I. Soerjomataram, R. Dikshit et al., "Cancer incidence and mortality worldwide: sources, methods and major patterns in GLOBOCAN 2012," *International Journal of Cancer*, vol. 136, no. 5, pp. E359–E386, 2015.

[2] R. Siegel, D. Naishadham, and A. Jemal, "Cancer statistics, 2013," *CA Cancer Journal for Clinicians*, vol. 63, no. 1, pp. 11–30, 2013.

[3] J. Massano, F. S. Regateiro, G. Januário, and A. Ferreira, "Oral squamous cell carcinoma: review of prognostic and predictive factors," *Oral Surgery, Oral Medicine, Oral Pathology, Oral Radiology and Endodontology*, vol. 102, no. 1, pp. 67–76, 2006.

[4] K. D. C. B. Ribeiro, L. P. Kowalski, and M. D. R. D. D. O. Latorre, "Perioperative complications, comorbidities, and survival in oral or oropharyngeal cancer," *Archives of Otolaryngology—Head & Neck Surgery*, vol. 129, no. 2, pp. 219–228, 2003.

[5] T. Hunter, "Cooperation between oncogenes," *Cell*, vol. 64, no. 2, pp. 249–270, 1991.

[6] J. M. Bishop, "Molecular themes in oncogenesis," *Cell*, vol. 64, no. 2, pp. 235–248, 1991.

[7] D. P. Bartel, "MicroRNAs: genomics, biogenesis, mechanism, and function," *Cell*, vol. 116, no. 2, pp. 281–297, 2004.

[8] V. Ambros, "The functions of animal microRNAs," *Nature*, vol. 431, no. 7006, pp. 350–355, 2004.

[9] A. E. Pasquinelli, S. Hunter, and J. Bracht, "MicroRNAs: a developing story," *Current Opinion in Genetics and Development*, vol. 15, no. 2, pp. 200–205, 2005.

[10] L. P. Lim, N. C. Lau, P. Garrett-Engele et al., "Microarray analysis shows that some microRNAs downregulate large numbers of-target mRNAs," *Nature*, vol. 433, no. 7027, pp. 769–773, 2005.

[11] B. D. Harfe, "MicroRNAs in vertebrate development," *Current Opinion in Genetics & Development*, vol. 15, no. 4, pp. 410–415, 2005.

[12] D. P. Bartel and C.-Z. Chen, "Micromanagers of gene expression: the potentially widespread influence of metazoan microRNAs," *Nature Reviews Genetics*, vol. 5, no. 5, pp. 396–400, 2004.

[13] N. Rajewsky, "microRNA target predictions in animals," *Nature Genetics*, vol. 38, pp. S8–S13, 2006.

[14] N. Tran, C. J. O'Brien, J. Clark, and B. Rose, "Potential role of micro-RNAs in head and neck tumorigenesis," *Head & Neck*, vol. 32, no. 8, pp. 1099–1111, 2010.

[15] N. Sethi, A. Wright, H. Wood, and P. Rabbitts, "MicroRNAs and head and neck cancer: reviewing the first decade of research," *European Journal of Cancer*, vol. 50, no. 15, pp. 2619–2635, 2014.

[16] J. Li, H. Huang, L. Sun et al., "MiR-21 indicates poor prognosis in tongue squamous cell carcinomas as an apoptosis inhibitor," *Clinical Cancer Research*, vol. 15, no. 12, pp. 3998–4008, 2009.

[17] M. Avissar, B. C. Christensen, K. T. Kelsey, and C. J. Marsit, "MicroRNA expression ratio is predictive of head and neck squamous cell carcinoma," *Clinical Cancer Research*, vol. 15, no. 8, pp. 2850–2855, 2009.

[18] A. Kawakita, S. Yanamoto, S.-I. Yamada et al., "MicroRNA-21 promotes oral cancer invasion via the wnt/β-catenin pathway by targeting DKK2," *Pathology & Oncology Research*, vol. 20, no. 2, pp. 253–261, 2014.

[19] D. Chen, R. J. Cabay, Y. Jin et al., "MicroRNA deregulations in head and neck squamous cell carcinomas," *Journal of Oral & Maxillofacial Research*, vol. 4, no. 1, article e2, 2013.

[20] N. Hedbäck, D. H. Jensen, L. Specht et al., "miR-21 expression in the tumor stroma of oral squamous cell carcinoma: an independent biomarker of disease free survival," *PLoS ONE*, vol. 9, no. 4, Article ID e95193, 2014.

[21] J. A. R. Brito, C. C. Gomes, A. L. S. Guimarães, K. Campos, and R. S. Gomez, "Relationship between microRNA expression levels and histopathological features of dysplasia in oral leukoplakia," *Journal of Oral Pathology and Medicine*, vol. 43, no. 3, pp. 211–216, 2014.

[22] W. Mydlarz, M. Uemura, S. Ahn et al., "Clusterin is a gene-specific target of microRNA-21 in head and neck squamous cell carcinoma," *Clinical Cancer Research*, vol. 20, no. 4, pp. 868–877, 2014.

[23] P. P. Reis, M. Tomenson, N. K. Cervigne et al., "Programmed cell death 4 loss increases tumor cell invasion and is regulated by miR-21 in oral squamous cell carcinoma," *Molecular Cancer*, vol. 9, article 238, 2010.

[24] L. Y. W. Bourguignon, C. Earle, G. Wong, C. C. Spevak, and K. Krueger, "Stem cell marker (Nanog) and Stat-3 signaling promote MicroRNA-21 expression and chemoresistance in hyaluronan/CD44-activated head and neck squamous cell carcinoma cells," *Oncogene*, vol. 31, no. 2, pp. 149–160, 2012.

[25] F. Meng, R. Henson, H. Wehbe-Janek, K. Ghoshal, S. T. Jacob, and T. Patel, "MicroRNA-21 regulates expression of the PTEN tumor suppressor gene in human hepatocellular cancer," *Gastroenterology*, vol. 133, no. 2, pp. 647–658, 2007.

[26] H. M. Jung, B. L. Phillips, R. S. Patel et al., "Keratinization-associated miR-7 and miR-21 regulate tumor suppressor reversion-inducing cysteine-rich protein with kazal motifs (RECK) in oral cancer," *The Journal of Biological Chemistry*, vol. 287, no. 35, pp. 29261–29272, 2012.

[27] Q. Li, D. Zhang, Y. Wang et al., "MiR-21/Smad 7 signaling determines TGF-β1-induced CAF formation," *Scientific Reports*, vol. 3, article 2038, 2013.

[28] C.-J. Liu, M.-M. Tsai, P.-S. Hung et al., "miR-31 ablates expression of the HIF regulatory factor FIH to activate the HIF pathway in head and neck carcinoma," *Cancer Research*, vol. 70, no. 4, pp. 1635–1644, 2010.

[29] W. Xiao, Z.-X. Bao, C.-Y. Zhang et al., "Upregulation of miR-31* is negatively associated with recurrent/newly formed oral leukoplakia," *PLoS ONE*, vol. 7, no. 6, Article ID e38648, 2012.

[30] S.-B. Ouyang, J. Wang, Z.-K. Huang, and L. Liao, "Expression of microRNA-31 and its clinicopathologic significance in oral squamous cell carcinoma," *Zhonghua Kou Qiang Yi Xue Za Zhi*, vol. 48, no. 8, pp. 481–484, 2013.

[31] P.-S. Hung, H.-F. Tu, S.-Y. Kao et al., "miR-31 is upregulated in oral premalignant epithelium and contributes to the immortalization of normal oral keratinocytes," *Carcinogenesis*, vol. 35, no. 5, pp. 1162–1171, 2014.

[32] K.-W. Chang, S.-Y. Kao, Y.-H. Wu et al., "Passenger strand miRNA *miR*-31 regulates the phenotypes of oral cancer cells by targeting RhoA," *Oral Oncology*, vol. 49, no. 1, pp. 27–33, 2013.

[33] P.-S. Hung, C.-J. Liu, C.-S. Chou et al., "miR-146a enhances the oncogenicity of oral carcinoma by concomitant targeting of the IRAK1, TRAF6 and NUMB genes," *PLoS ONE*, vol. 8, no. 11, Article ID e79926, 2013.

[34] P.-S. Hung, K.-W. Chang, S.-Y. Kao, T.-H. Chu, C.-J. Liu, and S.-C. Lin, "Association between the rs2910164 polymorphism in pre-mir-146a and oral carcinoma progression," *Oral Oncology*, vol. 48, no. 5, pp. 404–408, 2012.

[35] A. Palmieri, F. Carinci, M. Martinelli et al., "Role of the MIR146A polymorphism in the origin and progression of oral squamous cell carcinoma," *European Journal of Oral Sciences*, vol. 122, no. 3, pp. 198–201, 2014.

[36] C.-J. Liu, W. G. Shen, S.-Y. Peng et al., "MiR-134 induces oncogenicity and metastasis in head and neck carcinoma through targeting WWOX gene," *International Journal of Cancer*, vol. 134, no. 4, pp. 811–821, 2014.

[37] Y.-H. Ni, X.-F. Huang, Z.-Y. Wang et al., "Upregulation of a potential prognostic biomarker, miR-155, enhances cell proliferation in patients with oral squamous cell carcinoma," *Oral Surgery, Oral Medicine, Oral Pathology and Oral Radiology*, vol. 117, no. 2, pp. 227–233, 2014.

[38] L. J. Shi, C. Y. Zhang, Z. T. Zhou et al., "MicroRNA-155 in oral squamous cell carcinoma: overexpression, localization, and prognostic potential," *Head & Neck*, 2014.

[39] M. I. Rather, M. N. Nagashri, S. S. Swamy, K. S. Gopinath, and A. Kumar, "Oncogenic microRNA-155 down-regulates tumor suppressor CDC73 and promotes oral squamous cell carcinoma cell proliferation: implications for cancer therapeutics," *Journal of Biological Chemistry*, vol. 288, no. 1, pp. 608–618, 2013.

[40] T. Venkatesh, M. N. Nagashri, S. S. Swamy, S. M. A. Mohiyuddin, K. S. Gopinath, and A. Kumar, "Primary microcephaly gene MCPH1 shows signatures of tumor suppressors and is regulated by miR-27a in oral squamous cell carcinoma," *PLoS ONE*, vol. 8, no. 3, Article ID e54643, 2013.

[41] Y.-Y. Wu, Y.-L. Chen, Y.-C. Jao, I.-S. Hsieh, K.-C. Chang, and T.-M. Hong, "MiR-320 regulates tumor angiogenesis driven by vascular endothelial cells in oral cancer by silencing neuropilin 1," *Angiogenesis*, vol. 17, no. 1, pp. 247–260, 2014.

[42] B. Kefas, J. Godlewski, L. Comeau et al., "microRNA-7 inhibits the epidermal growth factor receptor and the akt pathway and is down-regulated in glioblastoma," *Cancer Research*, vol. 68, no. 10, pp. 3566–3572, 2008.

[43] S. D. N. Reddy, K. Ohshiro, S. K. Rayala, and R. Kumar, "MicroRNA-7, a homeobox D10 target, inhibits p21-activated kinase 1 and regulates its functions," *Cancer Research*, vol. 68, no. 20, pp. 8195–8200, 2008.

[44] R. J. Webster, K. M. Giles, K. J. Price, P. M. Zhang, J. S. Mattick, and P. J. Leedman, "Regulation of epidermal growth factor receptor signaling in human cancer cells by MicroRNA-7," *The Journal of Biological Chemistry*, vol. 284, no. 9, pp. 5731–5741, 2009.

[45] L. Jiang, X. Liu, Z. Chen et al., "MicroRNA-7 targets IGF1R (insulin-like growth factor 1 receptor) in tongue squamous cell carcinoma cells," *Biochemical Journal*, vol. 432, no. 1, pp. 199–205, 2010.

[46] Y.-C. Yen, S.-G. Shiah, H.-C. Chu et al., "Reciprocal regulation of MicroRNA-99a and insulin-like growth factor I receptor signaling in oral squamous cell carcinoma cells," *Molecular Cancer*, vol. 13, no. 1, article 6, 2014.

[47] B. Yan, Q. Fu, L. Lai et al., "Downregulation of microRNA 99a in oral squamous cell carcinomas contributes to the growth and survival of oral cancer cells," *Molecular Medicine Reports*, vol. 6, no. 3, pp. 675–681, 2012.

[48] A. Uesugi, K.-I. Kozaki, T. Tsuruta et al., "The tumor suppressive microRNA miR-218 targets the mTOR component rictor and inhibits AKT phosphorylation in oral cancer," *Cancer Research*, vol. 71, no. 17, pp. 5765–5778, 2011.

[49] J. Minor, X. Wang, F. Zhang et al., "Methylation of microRNA-9 is a specific and sensitive biomarker for oral and oropharyngeal squamous cell carcinomas," *Oral Oncology*, vol. 48, no. 1, pp. 73–78, 2012.

[50] T. Yu, K. Liu, Y. Wu et al., "MicroRNA-9 inhibits the proliferation of oral squamous cell carcinoma cells by suppressing expression of CXCR4 via the Wnt/β-catenin signaling pathway," *Oncogene*, vol. 33, pp. 5017–5027, 2013.

[51] J. P. Their, "Epithelial-mesenchymal transitions in tumor progression," *Nature Reviews Cancer*, vol. 2, no. 6, pp. 442–454, 2002.

[52] Y. Jin, C. Wang, X. Liu et al., "Molecular characterization of the MicroRNA-138-Fos-like antigen 1 (FOSL1) regulatory module in squamous cell carcinoma," *The Journal of Biological Chemistry*, vol. 286, no. 46, pp. 40104–40109, 2011.

[53] X. Liu, C. Wang, Z. Chen et al., "MicroRNA-138 suppresses epithelial-mesenchymal transition in squamous cell carcinoma cell lines," *Biochemical Journal*, vol. 440, no. 1, pp. 23–31, 2011.

[54] L. Jiang, X. Liu, A. Kolokythas et al., "Downregulation of the Rho GTPase signaling pathway is involved in the microRNA-138-mediated inhibition of cell migration and invasion in tongue squamous cell carcinoma," *International Journal of Cancer*, vol. 127, no. 3, pp. 505–512, 2010.

[55] M. Islam, J. Datta, J. C. Lang, and T. N. Teknos, "Down regulation of RhoC by microRNA-138 results in de-activation of FAK, Src and $Erk^{1/2}$ signaling pathway in head and neck squamous cell carcinoma," *Oral Oncology*, vol. 50, no. 5, pp. 448–456, 2014.

[56] M. Liu, J. Wang, H. Huang, J. Hou, B. Zhang, and A. Wang, "MiR-181a-Twist1 pathway in the chemoresistance of tongue squamous cell carcinoma," *Biochemical and Biophysical Research Communications*, vol. 441, no. 2, pp. 364–370, 2013.

[57] L. Lu, X. Xue, J. Lan et al., "MicroRNA-29a upregulates MMP2 in oral squamous cell carcinoma to promote cancer invasion and anti-apoptosis," *Biomedicine and Pharmacotherapy*, vol. 68, no. 1, pp. 13–19, 2014.

[58] S. Hunt, A. V. Jones, E. E. Hinsley, S. A. Whawell, and D. W. Lambert, "MicroRNA-124 suppresses oral squamous cell carcinoma motility by targeting ITGB1," *FEBS Letters*, vol. 585, no. 1, pp. 187–192, 2011.

[59] W.-C. Huang, S.-H. Chan, T.-H. Jang et al., "MiRNA-491-5p and GIT1 serve as modulators and biomarkers for oral squamous cell carcinoma invasion and metastasis," *Cancer Research*, vol. 74, no. 3, pp. 751–764, 2014.

[60] C.-C. Chang, Y.-J. Yang, Y.-J. Li et al., "MicroRNA-17/20a functions to inhibit cell migration and can be used a prognostic marker in oral squamous cell carcinoma," *Oral Oncology*, vol. 49, no. 9, pp. 923–931, 2013.

[61] H. M. Jung, R. S. Patel, B. L. Phillips et al., "Tumor suppressor miR-375 regulates MYC expression via repression of CIP2A coding sequence through multiple miRNA-mRNA interactions," *Molecular Biology of the Cell*, vol. 24, no. 11, pp. 1638–1648, 2013.

[62] N. Nohata, T. Hanazawa, N. Kikkawa et al., "Tumor suppressive microRNA-375 regulates oncogene AEG-1/MTDH in head and neck squamous cell carcinoma (HNSCC)," *Journal of Human Genetics*, vol. 56, no. 8, pp. 595–601, 2011.

[63] J. Wang, H. Huang, C. Wang, X. Liu, F. Hu, and M. Liu, "MicroRNA-375 sensitizes tumour necrosis factor-alpha (TNF-α)-induced apoptosis in head and neck squamous cell carcinoma in vitro," *International Journal of Oral and Maxillofacial Surgery*, vol. 42, no. 8, pp. 949–955, 2013.

[64] B. Kumar, A. Yadav, J. Lang, T. N. Teknos, and P. Kumar, "Dysregulation of microRNA-34a expression in head and neck squamous cell carcinoma promotes tumor growth and tumor angiogenesis," *PLoS ONE*, vol. 7, no. 5, Article ID e37601, 2012.

[65] M. Shiiba, K. Shinozuka, K. Saito et al., "MicroRNA-125b regulates proliferation and radioresistance of oral squamous cell carcinoma," *British Journal of Cancer*, vol. 108, no. 9, pp. 1817–1821, 2013.

[66] L. Gao, W. Ren, S. Chang et al., "Downregulation of miR-145 expression in oral squamous cell carcinomas and its clinical significance," *Onkologie*, vol. 36, no. 4, pp. 194–199, 2013.

[67] Y. Shao, Y. Qu, S. Dang, B. Yao, and M. Ji, "MiR-145 inhibits oral squamous cell carcinoma (OSCC) cell growth by targeting c-Myc and Cdk6," *Cancer Cell International*, vol. 13, no. 1, article 51, 2013.

[68] N. J. Park, H. Zhou, D. Elashoff et al., "Salivary microRNA: discovery, characterization, and clinical utility for oral cancer detection," *Clinical Cancer Research*, vol. 15, no. 17, pp. 5473–5477, 2009.

[69] S. A. MacLellan, J. Lawson, J. Baik, M. Guillaud, C. F. Poh, and C. Garnis, "Differential expression of miRNAs in the serum of patients with high-risk oral lesions," *Cancer Medicine*, vol. 1, no. 2, pp. 268–274, 2012.

[70] S.-C. Lin, C.-J. Liu, J.-A. Lin, W.-F. Chiang, P.-S. Hung, and K.-W. Chang, "miR-24 up-regulation in oral carcinoma: positive association from clinical and in vitro analysis," *Oral Oncology*, vol. 46, no. 3, pp. 204–208, 2010.

[71] C.-M. Hsu, P.-M. Lin, Y.-M. Wang, Z.-J. Chen, S.-F. Lin, and M.-Y. Yang, "Circulating miRNA is a novel marker for head and neck squamous cell carcinoma," *Tumour Biology*, vol. 33, no. 6, pp. 1933–1942, 2012.

[72] C.-J. Liu, S.-C. Lin, C.-C. Yang, H.-W. Cheng, and K.-W. Chang, "Exploiting salivary miR-31 as a clinical biomarker of oral squamous cell carcinoma," *Head and Neck*, vol. 34, no. 2, pp. 219–224, 2012.

[73] F. Momen-Heravi, A. J. Trachtenberg, W. P. Kuo, and Y. S. Cheng, "Genomewide study of salivary microRNAs for detection of oral cancer," *Journal of Dental Research*, vol. 93, no. 7, supplement, pp. 86S–93S, 2014.

[74] W.-Y. Lo, H.-J. Wang, C.-W. Chiu, and S.-F. Chen, "miR-27b-regulated TCTP as a novel plasma biomarker for oral cancer: from quantitative proteomics to post-transcriptional study," *Journal of Proteomics*, vol. 77, pp. 154–166, 2012.

[75] J. Dang, Y.-Q. Bian, J. Y. Sun et al., "MicroRNA-137 promoter methylation in oral lichen planus and oral squamous cell carcinoma," *Journal of Oral Pathology & Medicine*, vol. 42, no. 4, pp. 315–321, 2013.

[76] Y. Yang, Y.-X. Li, X. Yang, L. Jiang, Z.-J. Zhou, and Y.-Q. Zhu, "Progress risk assessment of oral premalignant lesions with saliva miRNA analysis," *BMC Cancer*, vol. 13, article 129, 2013.

[77] C.-C. Yang, P.-S. Hung, P.-W. Wang et al., "miR-181 as a putative biomarker for lymph-node metastasis of oral squamous cell carcinoma," *Journal of Oral Pathology and Medicine*, vol. 40, no. 5, pp. 397–404, 2011.

[78] T. Harris, L. Jimenez, N. Kawachi et al., "Low-level expression of miR-375 correlates with poor outcome and metastasis while altering the invasive properties of head and neck squamous cell carcinomas," *The American Journal of Pathology*, vol. 180, no. 3, pp. 917–928, 2012.

[79] G. Childs, M. Fazzari, G. Kung et al., "Low-level expression of microRNAs let-7d and miR-205 are prognostic markers of head and neck squamous cell carcinoma," *The American Journal of Pathology*, vol. 174, no. 3, pp. 736–745, 2009.

[80] M. Avissar, M. D. McClean, K. T. Kelsey, and C. J. Marsit, "MicroRNA expression in head and neck cancer associates with alcohol consumption and survival," *Carcinogenesis*, vol. 30, no. 12, pp. 2059–2063, 2009.

[81] M. S. Ebert, J. R. Neilson, and P. A. Sharp, "MicroRNA sponges: competitive inhibitors of small RNAs in mammalian cells," *Nature Methods*, vol. 4, no. 9, pp. 721–726, 2007.

[82] R. Garzon, G. Marcucci, and C. M. Croce, "Targeting microRNAs in cancer: rationale, strategies and challenges," *Nature Reviews Drug Discovery*, vol. 9, no. 10, pp. 775–789, 2010.

[83] E. van Rooij and E. N. Olson, "MicroRNA therapeutics for cardiovascular disease: opportunities and obstacles," *Nature Reviews Drug Discovery*, vol. 11, no. 11, pp. 860–872, 2012.

[84] Y. Dai, C.-H. Xie, J. P. Neis, C.-Y. Fan, E. Vural, and P. M. Spring, "MicroRNA expression profiles of head and neck squamous cell carcinoma with docetaxel-induced multidrug resistance," *Head and Neck*, vol. 33, no. 6, pp. 786–791, 2011.

[85] L. Sun, Y. Yao, B. Liu et al., "MiR-200b and miR-15b regulate chemotherapy-induced epithelial-mesenchymal transition in human tongue cancer cells by targeting BMI1," *Oncogene*, vol. 31, no. 4, pp. 432–445, 2012.

[86] Y.-E. Suh, N. Raulf, J. Gäken et al., "microRNA-196a promotes an oncogenic effect in head and neck cancer cells by suppressing annexin A1 and enhancing radioresistance," *International Journal of Cancer*, 2015.

[87] W. Ren, X. Wang, L. Gao et al., "MiR-21 modulates chemosensitivity of tongue squamous cell carcinoma cells to cisplatin by targeting PDCD4," *Molecular and Cellular Biochemistry*, vol. 390, no. 1-2, pp. 253–262, 2014.

[88] L. Piao, M. Zhang, J. Datta et al., "Lipid-based nanoparticle delivery of pre-miR-107 inhibits the tumorigenicity of head and neck squamous cell carcinoma," *Molecular Therapy*, vol. 20, no. 6, pp. 1261–1269, 2012.

[89] K. Lefort, Y. Brooks, P. Ostano et al., "A miR-34a-SIRT6 axis in the squamous cell differentiation network," *The EMBO Journal*, vol. 32, no. 16, pp. 2248–2263, 2013.

[90] Y. Kai, W. Peng, W. Ling, H. Jiebing, and B. Zhuan, "Reciprocal effects between microRNA-140-5p and ADAM10 suppress migration and invasion of human tongue cancer cells," *Biochemical and Biophysical Research Communications*, vol. 448, no. 3, pp. 308–314, 2014.

[91] K.-H. Shin, S. D. Bae, H. S. Hong, R. H. Kim, M. K. Kang, and N.-H. Park, "miR-181a shows tumor suppressive effect against oral squamous cell carcinoma cells by downregulating K-ras," *Biochemical and Biophysical Research Communications*, vol. 404, no. 4, pp. 896–902, 2011.

[92] J.-S. Kim, S.-K. Yu, M.-H. Lee et al., "MicroRNA-205 directly regulates the tumor suppressor, interleukin-24, in human KB oral cancer cells," *Molecules and Cells*, vol. 35, no. 1, pp. 17–24, 2013.

[93] J.-S. Kim, S.-Y. Park, S. A. Lee et al., "MicroRNA-205 suppresses the oral carcinoma oncogenic activity via down-regulation of Axin-2 in KB human oral cancer cell," *Molecular and Cellular Biochemistry*, vol. 387, no. 1-2, pp. 71–79, 2014.

[94] T. Bertero, I. Bourget-Ponzio, A. Puissant et al., "Tumor suppressor function of miR-483-3p on squamous cell carcinomas due to its pro-apoptotic properties," *Cell Cycle*, vol. 12, no. 14, pp. 2183–2193, 2013.

[95] L. Darda, F. Hakami, R. Morgan et al., "The role of HOXB9 and miR-196a in head and neck squamous cell carcinoma," *PLOS ONE*, vol. 10, no. 4, Article ID e0122285, 2015.

[96] I. Fukumoto, T. Hanazawa, T. Kinoshita et al., "MicroRNA expression signature of oral squamous cell carcinoma: functional role of microRNA-26a/b in the modulation of novel cancer pathways," *British Journal of Cancer*, vol. 112, no. 5, pp. 891–900, 2015.

[97] F. Ganci, A. Sacconi, V. Manciocco et al., "microRNAs expression predicts local recurrence risk in oral squamous cell carcinoma," *Head & Neck*, 2014.

[98] C.-J. Liu, M.-M. Tsai, H.-F. Tu, M.-T. Lui, H.-W. Cheng, and S.-C. Lin, "MiR-196a overexpression and mir-196a2 gene polymorphism are prognostic predictors of oral carcinomas," *Annals of Surgical Oncology*, vol. 20, no. 3, pp. S406–S414, 2013.

[99] K.-W. Chang, C.-J. Liu, T.-H. Chu et al., "Association between high miR-211 microRNA expression and the poor prognosis of oral carcinoma," *Journal of Dental Research*, vol. 87, no. 11, pp. 1063–1068, 2008.